

The landscape of QCD axion models

Luca Di Luzio

Deutsches Elektronen-Synchrotron DESY, Notkestraße 85, D-22607 Hamburg, Germany

Maurizio Giannotti

Physical Sciences, Barry University, 11300 NE 2nd Ave., Miami Shores, FL 33161, USA

Enrico Nardi*

INFN, Laboratori Nazionali di Frascati, C.P. 13, I-00044 Frascati, Italy

Luca Visinelli

*Gravitation Astroparticle Physics Amsterdam (GRAPPA),
Institute for Theoretical Physics Amsterdam and Delta Institute for Theoretical Physics,
University of Amsterdam, Science Park 904, 1098 XH Amsterdam, The Netherlands*

Abstract

We review the landscape of QCD axion models. Theoretical constructions that extend the window for the axion mass and couplings beyond conventional regions are highlighted and classified. Bounds from cosmology, astrophysics and experimental searches are reexamined and updated.

Keywords: Axion phenomenology, axion cosmology and astrophysics, axion models

*Corresponding author

Email addresses: `luca.diluzio@desy.de` (Luca Di Luzio), `MGiannotti@barry.edu` (Maurizio Giannotti), `enrico.nardi@lnf.infn.it` (Enrico Nardi), `l.visinelli@uva.nl` (Luca Visinelli)

Contents

1	Introduction	4
2	From the strong CP problem to the QCD axion	7
2.1	QCD vacuum structure	7
2.2	Dependence of the QCD vacuum energy on θ	10
2.3	Neutron EDM and the strong CP problem	12
2.4	Musings on the strong CP problem	13
2.4.1	Solutions without axions	14
2.4.2	Peccei Quinn mechanism	14
2.5	Axion effective Lagrangian	15
2.5.1	Axion potential and axion mass	16
2.5.2	Axion-pion coupling	17
2.5.3	Axion-photon coupling	18
2.5.4	Axion-nucleon coupling	18
2.5.5	Axion-electron coupling	19
2.6	Origin of model-dependent axion couplings	19
2.7	Benchmark axion models	20
2.7.1	KSVZ axion	21
2.7.2	DFSZ axion	22
2.8	Summary of flavour and CP conserving axion couplings	25
2.9	Flavour violating axion couplings	26
2.10	CP-violating axion couplings	27
2.11	The dirty side of the axion	28
3	Axion cosmology	30
3.1	Basics of cosmology and thermodynamics in the early Universe	31
3.2	The axion potential and the axion mass at finite temperature	33
3.3	Axion misalignment mechanism	34
3.4	Topological defects and their contribution to axion cold dark matter	38
3.4.1	Cosmic axion strings	39
3.4.2	String populations	39
3.4.3	Spectrum of radiated axions	41
3.4.4	Cosmological domain walls	42
3.5	Axion isocurvature fluctuations	43
3.6	Cosmological bounds on the axion mass	45
3.7	Benchmark axion mass region for $\Omega_a \simeq \Omega_{\text{CDM}}$	46
3.7.1	Post-inflationary scenario	46
3.7.2	Pre-inflationary scenario	47
3.7.3	Summary of cosmological bounds	48
3.8	QCD axions as dark radiation	50
3.9	Axion miniclusters and axion stars	53
4	Astrophysical signatures and bounds	55
4.1	Axion-photon coupling	56
4.2	Axion-electron coupling	60
4.3	Axion-nucleon coupling	62
4.4	Axion coupling to the neutron EDM	65
4.5	Axion CP-odd couplings	66
4.6	Axion coupling to gravity and black hole superradiance	66
4.7	Summary of astrophysical bounds	67

5	Experimental Searches	70
5.1	Solar axions and helioscopes	70
5.2	Helioscopes sensitivity to $g_{a\gamma}$ and g_{ae}	71
5.3	Haloscopes and DM axions	74
5.4	Searches for axions produced in the laboratory	76
5.5	Summary of experimental constraints	77
6	The axion landscape beyond benchmarks	81
6.1	Enhancing/suppressing $g_{a\gamma}$	81
6.1.1	KSVZ-like scenarios	82
6.1.2	DFSZ-like scenarios	86
6.1.3	Enhancing $g_{a\gamma}$ above KSVZ- and DFSZ-like scenarios	88
6.2	Enhancing/suppressing g_{ae}	89
6.2.1	Enhancing g_{ae} in KSVZ-like scenarios	89
6.2.2	Enhancing g_{ae} in DFSZ-like scenarios	90
6.2.3	Suppressing g_{ae} in DFSZ-like scenarios: the electrophobic axion	90
6.3	Enhancing/suppressing g_{aN}	91
6.3.1	Enhancing g_{aN}	91
6.3.2	Suppressing g_{aN} : the nucleophobic axion	92
6.4	Enhanced axion couplings and astrophysics	94
6.5	Flavour violating axions	97
6.5.1	Generation dependent Peccei-Quinn symmetries	99
6.5.2	Constraints on flavour violating axion couplings	100
6.6	Extending the mass region region for dark matter axions	101
6.6.1	Non-standard cosmological evolution	103
6.6.2	Modifying the m_a - f_a relation or the axion mass function $m_a(T)$	104
6.6.3	Alternative mechanisms for axion dark matter production	107
6.7	Super-heavy axions	108
7	Axions and...	111
7.1	Axions and neutrino masses	111
7.2	Axions and the cosmological baryon asymmetry	112
7.3	Axions and inflation	113
7.4	Gravitational waves from the Peccei-Quinn phase transition	114
7.5	Solutions to the domain walls problem	114
7.6	Solutions to the Peccei-Quinn quality problem	116
7.7	Axions and composite dynamics	118
7.8	Axions and GUTs	118
7.9	Axions from superstrings	119
8	Concluding remarks and <i>desiderata</i>	121
	Acknowledgments	123
	Appendix: Tables of notations and of acronyms	124
	References	127

1. Introduction

At the dawn of the third decade of the third millennium, particle physics seems stranded in an awkward intrigue. The celebrated theoretical construction known as the Standard Model (SM) has been established as the correct description of fundamental phenomena down to scales of the order of 10^{-16} cm. However, a certain number of observations including dark matter (DM), neutrino masses m_ν , and the cosmological matter-antimatter asymmetry η_b , remain unaccounted within the SM, and constitute indisputable evidences that the present theory must be extended. Besides this, the SM discomfits particle physicists because of a certain number of theoretical distresses generically related with exceedingly small numbers, that are usually referred to as problems of naturalness, as for example the value of the cosmological constant (dark energy) in units of the Planck mass $\Lambda \sim 10^{-31} m_{\text{Pl}}$, the electroweak breaking vacuum expectation value (VEV) $v \sim 10^{-17} m_{\text{Pl}}$, the CP violating QCD angle $\theta \lesssim 10^{-10}$.¹

Theoretical constructions that extend the SM are clearly more appealing when they are able to solve more than one of the previous issues with the same amount of theoretical input. A well known case is supersymmetry equipped with an R -parity symmetry to forbid fast proton decay, which protects the value of v/m_{Pl} from quantum corrections, and at the same time predicts that a new stable particle, which shares all the properties of a good DM candidate, must exist. Another example is the type-I seesaw model for neutrino masses which, besides accounting for the suppression of the neutrino mass scale [6–9], can also yield quite naturally a cosmological baryon asymmetry of the correct size [10]. The serious drawbacks of these two theories are that supersymmetry has not been found at the LHC, while the experimental verification of type-I seesaw leptogenesis remains well outside the reach of all current experiments [11–15].

A third example of a ‘two birds with one stone’ theory is provided by the axion [16, 17]. In an effective field theory (EFT) description, the SM is extended by introducing a single new massless pseudo-scalar particle a , the axion, for which only one coupling is mandatory, namely an effective coupling to the CP violating topological gluon density $(a/f_a + \theta)G\tilde{G}$, where f_a is the scale suppressing the effective operator, $G = G_{\mu\nu}$ is the gluon field strength tensor, $\tilde{G}_{\mu\nu}$ its dual, and we have added to the axion-gluon operator the infamous CP violating θ term. Such a simple extension has astonishingly far reaching consequences: the strong CP problem is solved because the minimum of the vacuum energy occurs when the coefficient of $G\tilde{G}$ vanishes [18]. Thus, by acquiring a suitable VEV, the axion disposes of the perilous CP violating operator. In performing this task, the axion acquires a tiny mass, and in this process a cosmological population of zero momentum excitations, which nowadays still sums to the energy density of the Universe, is unavoidably produced. Hence axions definitely contribute to the DM. Whether they can wholly account for it remains, for the time being, an open question. Solving the strong CP problem and providing a natural DM candidate by no means exhausts the role of axions in fundamental physics. Axion phenomenology crosses boundaries between particle physics, astrophysics and cosmology, it is replete with interdisciplinary connections which have already provided fruitful insights into different domains of physics. Axions have unusually intriguing features, although deeply interwoven with QCD, they interact more feebly than all SM particles, and although their typical mass is much smaller than the mass of at least two types of neutrinos, they might dominate the matter content of our Universe. Moreover, differently from the case of supersymmetry, current experimental searches have so far only been able to cut out relatively small regions of the parameter space in which the QCD axion can naturally live, but differently from leptogenesis, the axion hypothesis is within the reach of experimental verification, and it is conceivable, for example, that the canonical axion DM mass window could be thoroughly explored within the next one or two decades. If ever discovered, there is little doubt that the existence of axions would reshape more than one branch of fundamental physics.

The axion has been so far introduced by postulating a non-renormalizable axion-gluon operator. In quantum field theory (QFT) there is a simple prescription for constructing a renormalizable completion

¹These small number problems do not stand on the same footing. For example a tiny value of θ is *technically natural*, in the sense that it does not get lifted by quantum corrections. On the other hand, while anthropic or environmental selection arguments can provide explanations for the values of Λ [1] and v [2, 3], a value of θ_{QCD} many orders of magnitude larger than the experimental limit would still leave our Universe basically unaffected [4, 5].

whose low-energy limit matches the required form of the effective action density. What is needed is a Lagrangian equipped with a global $U(1)_{\text{PQ}}$ symmetry, exact at the classical level but broken at the quantum level by a colour anomaly, that undergoes spontaneous breaking at some high energy scale. Such a symmetry is known as Peccei-Quinn (PQ) symmetry after its proposers [19, 20].² As we will see in the next sections, the pseudo-Nambu Goldstone Boson (pNGB) resulting from such a broken symmetry exhibits precisely the properties required for an axion.

The result of dressing the QFT prescription with a complete model is, however, far from being unique. For example, in many cases different realizations of the PQ symmetry give rise to axions that do not interact only with the gluons, but that couple also to other SM particles. This indeed enriches in many aspects the subject of axion phenomenology. In particular, it provides additional important channels for experimental axion searches. However, the continuous proliferation of new theoretical constructions, that has received a major boost especially in recent years, has brought to a state of affairs in which it is rather arduous for experimental and theoretical researchers to attain a sufficiently complete and reliable acquaintance with the vast literature on axion models. Hence, we believe that an updated account of new (and old) theoretical ideas in axion model building, which we feel is lacking in the literature, could be timely and useful.

The aim of this work is to review the landscape of QFT realizations of the PQ symmetry.³ A reasoned classification of the babel of axion models is accomplished by pinpointing theoretical constructions that predict unusual properties of the axion, especially in relation to the different experimental approaches that could be pursued for their detection, as for example enhanced or suppressed couplings to specific SM states, or unconventional mass regions where the axion could saturate the DM density. Although presently axion searches rely almost exclusively on axion couplings to photons, a number of novel detection concepts which exploit cutting-edge techniques has been recently put forth with the aim of searching for axions through their couplings to nucleons or electrons. Even if in most cases only pathfinder or demonstrative small-scale setups have been commissioned, which generally have projected sensitivities that hardly reach into the parameter space regions hinted by most popular axion models, other less known theoretical constructions could be probed, constrained or ruled out by these experiments, which can then effectively contribute to circumscribe the realm of viable axion models. We thus expect that the experimental community of axion hunters could benefit from the classification scheme that we have adopted.

This Review is self contained, it includes pedagogical, but at the same time sufficiently detailed introductions to axion theory, cosmology, astrophysics and experimental searches, that are intended to provide guidance to the neophyte, whether she is a young student planning to orient her researches towards axion physics, or an experienced colleague active in a different domain of physics, but willing to get insights in a field that is currently experiencing a blooming phase. Experts in the field can instead browse quickly through the most pedagogical parts, and focus directly on the sections of their interest.

We start in Section 2 with a description of the origin of the strong CP problem and of the PQ mechanism that solves it. We then review model-independent properties of the axion (mass and couplings) illustrating how they can be derived from a chiral Lagrangian formulation. Model-dependent features are addressed here only for two popular benchmark constructions, universally known as KSVZ and DFSZ axion models. An introduction to flavour violating axion couplings and a brief discussion of CP violating couplings are also included. We conclude this section with some remarks about possible sources of explicit breaking of the PQ symmetry and the way they could endanger the effectiveness of the PQ mechanism. Excellent reviews exist in the literature that address in more depth some of these topics. Coleman’s Erice lectures [21] contain an enlightening treatment of the QCD vacuum and of the strong CP problem. Early reviews on axion theory can be found in Refs. [22–24]. More recent accounts are given in Ref. [25] and in the review of Kim and Carosi [26].

²Historically, axion theory developed in the reverse order: the PQ symmetry was invented first, and only subsequently it was realized that the PQ mechanism implied the existence of a very light pseudo-scalar boson [16, 17].

³We will only target genuine QCD axion models, that is, models that generate an effective axion-gluon operator and that solve the strong CP problem. Other types of very light pseudo-scalar particles that share some of the properties of the QCD axion, but do not solve the strong CP problem, and that are commonly denoted as axion-like particles (ALPs), are not touched on in this Review.

Section 3 addresses axion cosmology. After a basic introduction to the physics of the early Universe, we recall the properties of the axion potential and of the axion mass at temperatures around the QCD phase transition. Then we describe the misalignment mechanism as a source of a relic density of axions. The issue of cosmic topological defects which arise during axion-related phase transitions is also briefly addressed, as well as the constraints from axion isocurvature fluctuations that apply when the PQ symmetry is broken before inflation. Next we discuss the canonical mass window within which axions can saturate the DM relic density. We conclude this section with a brief overview of axion miniclusters and axion stars. An excellent review on the theory and cosmology of axions can be found in Ref. [27]. Another review of the cosmological role of axions, which also addresses the cosmology of axions superpartners in supersymmetric models, is Ref. [28]. A more recent and rather complete account of axion cosmology is given in Ref. [29].

Section 4 is devoted to a thorough description of the role of axions in astrophysics. The layout of the discussion analyzes axion couplings to SM states one at the time, and describes in which particular stellar environment and for which reasons each coupling becomes particularly relevant. This section also contains an updated summary of astrophysical bounds on the different types of couplings. The astrophysics of axions has been the subject of thorough investigations since the time the axion was invented. An early compilation of astrophysical bounds from stars can be found in Ref. [30]. The early reviews of Turner [31] and Raffelt [32] are still actual as concerns many qualitative aspects of axion astrophysics, and remain important references. Two accounts of astrophysical axion bounds dating around year 2006 can be found in Refs. [33] and [34]. A recent review which also includes an assessment of the astrophysical hints for the existence of axions which can be inferred from some anomalies observed in specific phases of stellar evolution can be found in Ref. [35].

Section 5 contains an account of the status of axion experimental searches (helioscopes, haloscopes, light shining through wall) and a summary of existing experimental constraints and projected limits that, at the time of writing, is up to date. However, in view of the continuous and rapid evolution of the experimental landscape, this part will likely become outdated in the not too distant future. Early accounts of experimental searches for invisible axions have been presented in Refs. [36, 37] and later in Ref. [38]. A recent review, which is also remarkably complete, can be found in Ref. [39]. Simultaneously with the present work, Ref. [40] appeared which contains a review of proposed methods to search for the axion.

Section 6 is the central part of this Review. We begin with a systematic classification of models that predict sizable enhancements in the axion coupling to photons, electrons and nucleons. We describe the mechanisms at the basis of these enhancements, and we confront the resulting enlarged parameter space with current bounds. We then focus on models that predict flavour violating axion couplings to quarks and leptons, and we review the role played by existing limits on Flavour Changing Neutral Currents (FCNC) in constraining constructions of this type. Mechanisms that allow to extend the mass region in which axions can account for the whole of DM deserve particular attention, in view of the fact that the best experimental sensitivities to the axion-photon coupling are attained by haloscope experiments, which however can only probe rather narrow and pre-defined axion-DM mass intervals. We review models that implement the possibility of saturating the DM energy density for values of the axion mass both larger and smaller than the conventional values, and we explain through which mechanisms this result can be obtained. For completeness, we include at the end of this section a review of models in which the axions are ‘super-heavy’, namely with masses in excess of 100 keV.

In Section 7, we extend the discussion to a different set of axion-related topics. We first review constructions that attempt to connect axion physics to other unsolved SM issues, like neutrino masses, the cosmological baryon asymmetry, inflation, and the possibility of detecting gravitational waves originating from the PQ phase transition. Next we discuss available solutions to a couple of well know problems that can generally affect model realisations of the PQ symmetry, namely how to maintain under control dangerous sources of explicit PQ breaking, and how to ensure that axion-related domain walls will not represent cosmological threats. The possibility that axions are composite states arising from a new strong dynamics is an old idea that has been recently revived, hence we present a survey of the related literature. We include a brief account of attempts to embed axions in Grand Unified Theories (GUTs), and we quickly touch on a last topic, that by itself would deserve a dedicated review, that is, axion arising from string theory.

In the Appendix the reader can find a table with the symbols and notations that have been used in the mathematical expressions including an explanation of their meaning, a table containing the definition of the

acronyms used in the text, and a table containing a list of current and planned axion experiments, with the relevant reference where the experimental setup is described.

2. From the strong CP problem to the QCD axion

This Section is devoted to the physical foundations of the QCD axion as a solution of the strong CP problem. We start by reviewing the non-trivial vacuum structure of Yang-Mills theories in Section 2.1 and the θ dependence of the QCD vacuum energy in Section 2.2. Next, we discuss the θ contribution to the neutron electric dipole moment (EDM) in Section 2.3 and give a critical assessment of the strong CP problem and its possible solutions in Section 2.4, among which the axion solution via the PQ mechanism. The rest of the Section is devoted to the study of standard axion properties, starting from the axion effective Lagrangian in Section 2.5, including a general description of model-dependent axion couplings in Section 2.6, and continuing with a pedagogical derivation of the so-called benchmark axion models in Section 2.7. In Section 2.8 we provide a concise summary of standard axion properties, while Sections 2.9–2.10 are devoted to a basic introduction to flavour and CP violating axions. We conclude in Section 2.11 with the so-called PQ quality problem.

2.1. QCD vacuum structure

Until the mid of the 70's, when the formulation of Quantum Chromodynamics (QCD) was being developed, the so-called $U(1)$ problem [41] was thought to be one of its major difficulties, while the absence of strong CP violation was believed to be one of its main successes [42, 43]. Few years later, with the discovery of Yang Mills instantons [44] and the non-trivial QCD vacuum structure [45, 46], this point of view was unexpectedly turned around. The solution of the $U(1)$ problem brought as a gift the so-called strong CP problem. In order to present this story, which also provides the physical foundations of axion physics, let us start from the QCD Lagrangian⁴

$$\mathcal{L}_{\text{QCD}} = \sum_q \bar{q} (i\not{D} - m_q e^{i\theta_q}) q - \frac{1}{4} G^{a\mu\nu} G_{\mu\nu}^a + \theta \frac{g_s^2}{32\pi^2} G^{a\mu\nu} \tilde{G}_{\mu\nu}^a. \quad (1)$$

This Lagrangian contains two potential sources of CP violation: the phases of the quark masses θ_q , and the so-called topological term, proportional to θ (in short $G\tilde{G}$). In fact, both θ_q and θ violate P and T (and hence CP). On the other hand, the $G\tilde{G}$ operator can be written as a total derivative

$$G^{a\mu\nu} \tilde{G}_{\mu\nu}^a = \partial_\mu K^\mu = \partial_\mu \epsilon^{\mu\alpha\beta\gamma} \left(A_\alpha^a G_{\beta\gamma}^a - \frac{g_s}{3} f^{abc} A_\alpha^a A_\beta^b A_\gamma^c \right), \quad (2)$$

in terms of the Chern-Simons current, K^μ , and hence it bears no effects in perturbation theory. However, classical configurations do exist for which the effects of this term cannot be ignored. These configurations are topological in nature, and can be identified by going to Euclidean space and writing the volume integral of the $G\tilde{G}$ term as

$$\int d^4x G_{\mu\nu}^a \tilde{G}_{\mu\nu}^a = \int d^4x \partial_\mu K_\mu = \int_{S_3} d\sigma_\mu K_\mu, \quad (3)$$

where S_3 is the three-sphere at infinity and $d\sigma_\mu$ an element of its hypersurface. In order for these configurations to contribute to the path integral, we require that the gauge potentials are such that the field strength tensor $G_{\mu\nu}^a$ vanishes as $|x| \rightarrow \infty$ so that the action is finite. Besides $A_\mu^a|_{S_3} = 0$, other configurations that can be obtained from this by a gauge transformation also satisfy $G_{\mu\nu}^a = 0$ at the boundary. In terms of the Lie algebra valued potential $A_\mu = A_\mu^a T^a$ where T^a are the group generators, they read $A'_\mu = U^{-1} A_\mu U + i g_s^{-1} U^{-1} \partial_\mu U$, so that at the boundary $A'_\mu = i g_s^{-1} U^{-1} \partial_\mu U$. Configurations of this type are

⁴We adopt the following conventions: $D_\mu = \partial_\mu - i g_s T^a A_\mu^a$, $G_{\mu\nu}^a = \partial_\mu A_\nu^a - \partial_\nu A_\mu^a + g_s f^{abc} A_\mu^a A_\nu^b$ and $\tilde{G}_{\mu\nu}^a = \frac{1}{2} \epsilon_{\mu\nu\rho\sigma} G^{\rho\sigma a}$, with $\epsilon^{0123} = -1$. The latter convention is used in [47], while for instance Ref. [39] employs $\epsilon^{0123} = +1$.

called a *pure gauges*. We are interested in pure gauges for which U cannot be continuously deformed into the identity in group space. To argue that such configurations exist, let us consider an $SU(2)$ subgroup of $SU(3)$ and let us restrict the gauge potentials defining K_μ in the surface integral in Eq. (3) to this subgroup. Since $SU(2)$ has S_3 as group manifold, these potentials provide a mapping $S_3 \rightarrow S_3$. It can be shown that for mappings of non-trivial topology the integral in Eq. (3) counts the number of times the hypersphere at infinity is wrapped around the S_3 group manifold. More precisely $\int d^4x G_{\mu\nu}^a \tilde{G}_{\mu\nu}^a = \frac{32\pi^2}{g_s^2} \nu$, where $\nu \in \mathbb{Z}$ is called winding number or Pontryagin index. Thus, in Euclidean space $SU(2)$ field configurations of finite action fall in homotopy classes of different winding number. An important point is that it is not possible to deform a field configuration into another of different winding number while maintaining the action finite. As regards general $SU(3)$ gauge field configurations, they can be classified in the same $SU(2)$ homotopy classes, the reason being that any mapping from S_3 into any simple Lie group G can be deformed into a mapping to a $SU(2)$ subgroup of G in a continuous way [48], hence with no change of homotopy class. Configurations of unit winding number were explicitly constructed by Belavin, Polyakov, Schwartz and Tyupkin [44] who also showed that their finite action $S_1 = \frac{8\pi^2}{g_s^2}$ corresponds to a minimum, which implies that they are solutions of the classical equation of motion in Euclidean space. Being of finite action, these gauge configuration are localised in all the four dimensions, which justifies the name *instantons*.

To assess the relevance of instantons let us return to physical Minkowski space and let us consider a gauge field configuration of winding number ν . Choosing the temporal gauge $A_0^a = 0$ so that $K_i = 0$ allows to rewrite Eq. (3) as

$$\nu = \frac{g_s^2}{32\pi^2} \int d^4x G_{(\nu)\mu\rho}^a \tilde{G}_{(\nu)}^{a\mu\rho} \rightarrow \frac{g_s^2}{32\pi^2} \int d^4x \partial_0 K_{(\nu)}^0 = \frac{g_s^2}{32\pi^2} \int d^3x K_{(\nu)}^0(\mathbf{x}, t) \Big|_{t=-\infty}^{t=+\infty} = \nu. \quad (4)$$

This shows that $\int d^4x G_{(\nu)} \tilde{G}_{(\nu)}$ corresponds to an interpolation from a pure gauge with winding number n at $t = -\infty$, to a different pure gauge configuration at $t = +\infty$ with winding number $m = n + \nu$. More precisely, one can interpret (multi)instanton solutions as tunnelling from one $G_{\mu\nu}^a = 0$ vacuum state $|n\rangle$ to a gauge-rotated one with different winding number $|m\rangle$ [49, 50]. In the semiclassical approximation the tunnelling probability is given by the exponential of the (multi)instanton action e^{-S_ν} where $S_\nu = \frac{8\pi^2}{g_s^2} \nu$ [45, 46], so that the effects of solutions with higher winding number $\nu > 1$ [51, 52] are strongly suppressed with respect to instanton effects with action S_1 , and hence of little interest.

An important remark is now in order. While the integral in Eq. (4) is gauge invariant, and hence the difference $m - n = \nu$ is a physically meaningful number, the Chern-Simons current K^μ by itself is not gauge invariant, which means that n and m labelling the vacuum states have no real physical meaning. This is also evidenced by the fact that the action of a gauge transformation of non-trivial winding number amounts to a relabelling $U_{(1)}|n\rangle = |n+1\rangle$. Clearly a more consistent definition of the physical vacuum is called for. Let us consider the linear combination

$$|\theta\rangle = \sum_{n=-\infty}^{+\infty} e^{in\theta} |n\rangle, \quad (5)$$

where $\theta \in [0, 2\pi)$ is an angular parameter, which is known as the θ vacuum.⁵

This vacuum state has the important property of being an eigenstate of the unitary operator of the gauge transformation

$$U_{(1)}|\theta\rangle = \sum_{n=-\infty}^{+\infty} e^{in\theta} |n+1\rangle = e^{-i\theta} |\theta\rangle, \quad (6)$$

so that is physically well-defined. The introduction of the θ vacuum is also necessary to preserve locality and cluster decomposition [45, 54]. To see this, let us consider the expectation value of a local operator \mathcal{O}

⁵A less conventional and more intuitive way of introducing the θ vacuum that relies on general quantum-mechanical principles applied to a Yang-Mills theory can be found in Ref. [53].

within a large Euclidean volume Ω

$$\langle O \rangle_\Omega = \frac{\sum_\nu f(\nu) \int_\nu \mathcal{D}\phi e^{-S_\Omega[\phi]} \mathcal{O}[\phi]}{\sum_\nu f(\nu) \int_\nu \mathcal{D}\phi e^{-S_\Omega[\phi]}}, \quad (7)$$

where ϕ denotes all the fields of the theory, S_Ω is the integral of the Lagrangian restricted to the volume Ω and we have included the sum over all topological sectors ν , with a general weight factor $f(\nu)$. Suppose now the volume Ω is split into two large regions, $\Omega = \Omega_1 + \Omega_2$, with \mathcal{O} localized in Ω_1 . The integral in Eq. (7) can hence be split into

$$\langle O \rangle_\Omega = \frac{\sum_{\nu_1, \nu_2} f(\nu_1 + \nu_2) \int_{\nu_1} \mathcal{D}\phi e^{-S_{\Omega_1}[\phi]} \mathcal{O}[\phi] \int_{\nu_2} \mathcal{D}\phi e^{-S_{\Omega_2}[\phi]}}{\sum_{\nu_1, \nu_2} f(\nu_1 + \nu_2) \int_{\nu_1} \mathcal{D}\phi e^{-S_{\Omega_1}[\phi]} \int_{\nu_2} \mathcal{D}\phi e^{-S_{\Omega_2}[\phi]}}, \quad (8)$$

with the constraint $\nu = \nu_1 + \nu_2$. The principle of cluster decomposition (which states that distant enough experiments must yield uncorrelated results) requires that the physics in the volume Ω_2 cannot affect the average of an observable localized in Ω_1 . In order for this to be true one needs

$$f(\nu_1 + \nu_2) = f(\nu_1) f(\nu_2), \quad (9)$$

so that the volume Ω_2 cancels out in the ratio of Eq. (8). Remarkably, this fixes the form of $f(\nu)$ to be

$$f(\nu) = e^{i\theta\nu}, \quad (10)$$

where θ is a free parameter.

A notable property of θ is the fact that its value cannot be changed via the action of a gauge invariant operator. This can be seen by considering the time ordered product of a set of gauge invariant operators $\mathcal{O}_1 \mathcal{O}_2 \dots$ between two different vacuum states

$$\langle \theta' | T(\mathcal{O}_1 \mathcal{O}_2 \dots) | \theta \rangle = \sum_{m, n} e^{i(n\theta - m\theta')} \langle m | T(\mathcal{O}_1 \mathcal{O}_2 \dots) | n \rangle = \sum_{m, n} e^{i(n\theta - m\theta')} F(\nu), \quad (11)$$

where in the last step we have emphasized that the matrix element depends only on the difference $\nu = n - m$, because $\Omega_1 T(\mathcal{O}_1 \mathcal{O}_2 \dots) \Omega_1^{-1} = T(\mathcal{O}_1 \mathcal{O}_2 \dots)$ and hence both n and m are shifted by the same amount under a large gauge transformation. Then Eq. (11) becomes:

$$\langle \theta' | T(\mathcal{O}_1 \mathcal{O}_2 \dots) | \theta \rangle = \sum_n e^{in(\theta - \theta')} \sum_\nu e^{i\frac{\nu}{2}(\theta + \theta')} F(\nu) = 2\pi \delta(\theta - \theta') \sum_\nu e^{i\nu\theta} F(\nu), \quad (12)$$

which is zero for $\theta \neq \theta'$. This property is referred to as a super-selection rule: θ is a fundamental parameter that labels the Yang-Mills vacuum and each value of θ labels a different theory.

To see explicitly how the θ term enters the QCD Lagrangian, let us consider the vacuum-to-vacuum transition in the presence of an external source J

$$\langle \theta_+ | \theta_- \rangle_J = \sum_{m, n} e^{in\theta} e^{-im\theta} \langle m_+ | n_- \rangle_J = \sum_\nu e^{i\nu\theta} \sum_m \langle m_+ | (\nu + m)_- \rangle_J. \quad (13)$$

The vacuum amplitude is a sum over different vacuum transitions in which ν corresponds to the net change of winding number between $t = -\infty$ and $t = +\infty$, weighted by the factor $e^{i\nu\theta}$. The latter can be replaced, thanks to Eq. (4), by an effective contribution to the Yang-Mills Lagrangian

$$\langle \theta_+ | \theta_- \rangle_J = \sum_\nu \int \mathcal{D}A e^{-\int d^4x \frac{1}{4} G\tilde{G} + i\theta \frac{g_s^2}{32\pi^2} \int d^4x G\tilde{G} + J\text{-term}} \delta\left(\nu - \frac{g_s^2}{32\pi^2} \int d^4x G\tilde{G}\right), \quad (14)$$

where the transition amplitude $\sum_m \langle m_+ | (\nu + m)_- \rangle_J$ has been expressed in terms of a path integral over all gauge field configurations A with fixed ν (hence the delta function) and the phase factor $e^{i\nu\theta}$ has been replaced by a $G\tilde{G}$ term in the Euclidean action.

In summary, the non-trivial structure of the Yang-Mills vacuum requires that the path integral is extended to include gauge field configurations with non-trivial winding number, and in turn this requires that the CP-violating $G\tilde{G}$ term must be included in the effective action. A strong argument in support of the correctness of this picture comes from the fact that in the hadronic spectrum there are no signs of a light state that could correspond to the Goldstone boson of a $U(1)_A$ symmetry spontaneously broken by the quark condensates, a puzzle that was dubbed by Weinberg ‘the $U(1)_A$ problem’ [41]. The topologically non-trivial gauge configurations responsible for the non-vanishing of the surface integral in Eq. (3) provide the solution: the complex nature of the QCD vacuum makes $U(1)_A$ not a true symmetry of QCD [49, 50, 55], and this explains the heaviness of the η' meson compared to the other pseudo Goldstone bosons of the spontaneously broken chiral symmetry.

2.2. Dependence of the QCD vacuum energy on θ

We are interested in determining the θ dependence of the QCD vacuum energy density, $E(\theta)$. This is because the axion VEV can be treated as an effective θ parameter, so that some exact results that can be established for the QCD θ angle hold for the axion as well, and are especially important in the study of the axion potential. In the large 4-volume (V_4) limit, $E(\theta)$ this is related to the Euclidean functional generator, $Z(\theta)$, via (see e.g. [21])

$$Z(\theta) = \lim_{V_4 \rightarrow \infty} e^{-E(\theta)V_4}. \quad (15)$$

The latter also admits a path integral representation given by⁶

$$Z(\theta) = \int \mathcal{D}A e^{-\frac{1}{4} \int d^4x G G + i\theta \frac{g_s^2}{32\pi^2} \int d^4x G \tilde{G}} \sim e^{-\frac{8\pi^2}{g_s^2}} e^{i\theta}, \quad (16)$$

where in the last step we have taken the leading term in the semi-classical approximation $\hbar \rightarrow 0$, corresponding to the contribution of a $\nu = 1$ instanton. Since the instanton is translational invariant one still needs to integrate over its center. This can be done within the dilute-instanton-gas approximation, which corresponds to summing-up the contribution of approximate solutions consisting of n instantons and \bar{n} anti-instantons with $n - \bar{n} = 1$ and with their centers widely separated. Using this approximation one gets (see e.g. [21])

$$E(\theta) = -2K e^{-\frac{8\pi^2}{g_s^2}} \cos \theta, \quad (17)$$

where K is a positive constant encoding Jacobian factors due to the instanton zero modes (translations and dilatations) and a functional determinant originating from the gaussian integration over the quantum fluctuations on the instanton background. The latter are actually crucial for stabilizing the zero mode associated to dilatations, since the integration over the instanton size ρ formally diverges (at short distances) at the classical level, due to the classical scale invariance of QCD which is broken via radiative corrections. In practice, the breaking of scale invariance can be approximated by taking a running coupling $g_s(\mu = 1/\rho)$ in Eq. (17), with

$$g_s^2(\mu) = \frac{8\pi^2}{\beta_0 \log(\mu/\Lambda_{\text{QCD}})}, \quad (18)$$

in terms of the one-loop QCD beta-function $\beta_0 = 11 - 2n_f/3$ with n_f active flavours and the integration constant $\Lambda_{\text{QCD}} \approx 150$ MeV. Hence, the integration over the instanton sizes is dominated by values of ρ corresponding to an unsuppressed exponential factor

$$e^{-\frac{8\pi^2}{g_s^2(1/\rho)}} = (\rho \Lambda_{\text{QCD}})^{\beta_0}, \quad (19)$$

namely for $\rho \sim 1/\Lambda_{\text{QCD}}$, which corresponds to the so-called *large instantons*, in contrast to possible short-distance contributions which are exponentially suppressed due to the asymptotic freedom of the coupling

⁶In passing to the Euclidean, $t = -it_E$, the $G\tilde{G}$ operator picks up an imaginary part, which eventually leads to the periodic θ -dependence of the QCD vacuum energy.

g_s . It should be noted that the semi-classical approximation breaks down for $g_s(\mu = \Lambda_{\text{QCD}}) \rightarrow \infty$, so that instanton calculus cannot be used for accurate predictions in QCD.⁷

An alternative way to systematically deal with the θ dependence of the QCD vacuum is via chiral Lagrangian techniques, which will be reviewed in Section 2.5 for the case of the axion. Before that, however, one needs to include massive quarks. In order to understand the role of quark fields in the problem, let us perform a global chiral transformation on a single quark field

$$q \rightarrow e^{i\gamma_5 \alpha} q. \quad (20)$$

The associated axial current, $J_\mu^5 = \bar{\psi} \gamma_\mu \gamma_5 \psi$, is not conserved because of the quark mass term and the chiral anomaly (note that the latter has a structure similar to the topological term)

$$\partial^\mu J_\mu^5 = 2m_q \bar{q} i \gamma_5 q + \frac{g_s^2}{16\pi^2} G \tilde{G}. \quad (21)$$

Hence, we expect that both θ_q (see Eq. (1)) and θ are shifted upon the transformation in Eq. (20). One has $\theta_q \rightarrow \theta_q + 2\alpha$, while it is less trivial to show that $\theta \rightarrow \theta - 2\alpha$. This can be most easily understood in terms of the non-invariance of the path integral measure [57] under the transformation in Eq. (20)

$$\mathcal{D}q \mathcal{D}\bar{q} \rightarrow \left(e^{-i\alpha \frac{g_s^2}{16\pi^2} \int d^4x G \tilde{G}} \right) \mathcal{D}q \mathcal{D}\bar{q}. \quad (22)$$

Hence, only the linear combination

$$\bar{\theta} = \theta + \theta_q \quad (23)$$

is invariant under a quark chiral rotation, and hence physically observable. The generalization of the $\bar{\theta}$ parameter in the electroweak theory (invariant under a generic chiral transformation involving an arbitrary set of quark fields) reads

$$\bar{\theta} = \theta + \text{Arg Det } Y_U Y_D, \quad (24)$$

in terms of the up and down Yukawa matrices.

Some exact results regarding the θ dependence of the QCD vacuum energy density, $E(\theta)$, can be derived by using its path integral representation in the presence of fermions as well. Denoting collectively by $\mathcal{D}\phi \equiv \mathcal{D}A \mathcal{D}q \mathcal{D}\bar{q}$ the functional integration variables comprising gluons, quarks and anti-quarks fields, recalling the expression of the QCD vacuum energy density in terms of the functional $Z(\theta)$ defined in Eq. (15), and being ν the winding number defined in Eq. (4), one can show the following properties:

- $E(0) \leq E(\theta)$

This is a special case of the Vafa-Witten theorem [18], which states that parity cannot be spontaneously broken in QCD. To prove that, one exploits the following inequality

$$Z(\theta) = \int \mathcal{D}\phi e^{-S_{\theta=0} + i\theta\nu} = \left| \int \mathcal{D}\phi e^{-S_{\theta=0} + i\theta\nu} \right| \leq \int |\mathcal{D}\phi e^{-S_{\theta=0} + i\theta\nu}| = \int \mathcal{D}\phi e^{-S_{\theta=0}} = Z(0), \quad (25)$$

where we crucially exploited the fact that the path integral measure is positive definite, which is true for a vector-like theory like QCD [58]. This, however, does not hold in chiral gauge theories like the SM. The consequences of this fact will be discussed in Section 2.10.

- $E(\theta) = E(\theta + 2\pi)$

This simply follows from the fact that θ is a global phase and ν an integer.

⁷On the other hand, large instantons at finite temperature are suppressed by electric screening so that the semiclassical approximation is increasingly reliable at high $T \gg \Lambda_{\text{QCD}}$, which serves as an infrared cut-off (see e.g. [56]).

- $E(\theta) = E(-\theta)$

To show this let us perform a field redefinition $\phi \xrightarrow{\text{CP}} \phi'$ which leaves $\mathcal{D}\phi$ invariant. Hence, we have

$$Z(\theta) = \int \mathcal{D}\phi e^{-S(\phi)_{\theta=0} + i\theta\nu(\phi)} = \int \mathcal{D}\phi' e^{-S(\phi')_{\theta=0} + i\theta\nu(\phi')} = \int \mathcal{D}\phi e^{-S(\phi)_{\theta=0} - i\theta\nu(\phi)} = Z(-\theta), \quad (26)$$

where in the last but one step we used the fact that $S(\phi)_{\theta=0}$ is CP invariant, while the topological term is CP odd. Note, however, that $S(\phi')_{\theta=0} \neq S(\phi)_{\theta=0}$ in the SM, due to the CKM phase, so $E(\theta)$ picks up a small contribution odd in θ .

2.3. Neutron EDM and the strong CP problem

Among the CP violating observables induced by $\bar{\theta}$, the neutron EDM (nEDM) stands out as the most sensitive one. The latter is defined in terms of the non-relativistic Hamiltonian

$$H = -d_n \vec{E} \cdot \hat{S}, \quad (27)$$

and the current experimental limit is $|d_n^{\text{exp}}| < 3.0 \cdot 10^{-26} \text{ e cm} = 1.5 \cdot 10^{-12} \text{ e GeV}^{-1}$ (90% CL) [59].⁸ A new round of searches are actively underway with the goal of improving the sensitivity to CP violation by up to two orders of magnitude (see e.g. [61]). Eq. (27) can be written in terms of a Lorentz invariant Lagrangian operator as follows

$$\mathcal{L} = -d_n \frac{i}{2} \bar{n} \sigma_{\mu\nu} \gamma_5 n F^{\mu\nu}. \quad (28)$$

The calculation of the nEDM has been performed using different kind of techniques, such as chiral perturbation theory [62–64], QCD sum-rules [65], holography [66] and lattice QCD [67, 68] (for a review of the technical challenges involved see e.g. [69, 70]). These approaches show an overall agreement, albeit with uncertainties of $\mathcal{O}(50\%)$. Future inputs from the lattice could be crucial for reducing such error [68]. The natural size of the $\bar{\theta}$ contribution to the nEDM can be understood as follows. The operator in Eq. (28) is $d = 5$ so one would naively expect its Wilson coefficient to be of $\mathcal{O}(1/m_n)$ size. However, in order to contribute to the nEDM one needs to pick-up an imaginary part which can only originate from the phase of a light quark mass (working in the basis where the $G\bar{G}$ term is absent). Moreover, being a dipole, the operator must be generated via an EM loop. Hence, taking into account these two extra suppression factors, the effective contribution to d_n can be estimated as

$$\mathcal{L} \sim \frac{e}{16\pi^2} \frac{m_q}{m_n} \frac{e^{i\bar{\theta}}}{m_n} \frac{1}{m_n} \bar{n} \sigma_{\mu\nu} \gamma_5 n F^{\mu\nu}, \quad (29)$$

Expanding linearly in $\bar{\theta}$ one gets

$$|d_n| \sim \frac{1}{8\pi^2} \frac{m_q}{m_n} \frac{\bar{\theta} e}{m_n} \approx 10^{-4} \bar{\theta} \text{ e GeV}^{-1}. \quad (30)$$

In fact, this naive estimate yields a somewhat smaller value compared to a real calculation. For instance, one of the most precise ones, based on QCD sum-rules, yields [65]

$$d_n = 2.4 (1.0) \cdot 10^{-16} \bar{\theta} \text{ e cm} = 1.2 (0.5) \cdot 10^{-2} \bar{\theta} \text{ e GeV}^{-1}, \quad (31)$$

thus implying the bound⁹

$$|\bar{\theta}| \lesssim 10^{-10}. \quad (32)$$

Understanding the smallness of $\bar{\theta}$ consists in the so-called strong CP problem.

⁸In Feb 2020 the nEDM experiment at PSI has published a new improved limit $|d_n^{\text{exp}}| < 1.8 \cdot 10^{-26} \text{ e cm}$ (90% CL) [60].

⁹Experiments searching for the EDM of the electron in paramagnetic systems have recently achieved a remarkable sensitivity and they can be used to obtain novel independent constraints on the QCD theta term at the level of $|\bar{\theta}| \lesssim 3 \cdot 10^{-8}$ [71].

2.4. Musings on the strong CP problem

The strong CP problem turns out to be qualitatively different from other “small value” problems in the SM. One first observation concerns the radiative stability of $\bar{\theta}$. Since CP is violated in the SM, one expects $\bar{\theta}$ to receive an infinite renormalization due to the CKM phase [72, 73]. Based just on spurionic properties, the SM contribution to $\bar{\theta}$ must be proportional to the Jarlskog invariant [74], which is given in terms of the following CP-odd, flavour singlet (lowest order) combination of the quark Yukawas

$$\text{Im Det}[Y_U Y_U^\dagger, Y_D Y_D^\dagger] = \left(\frac{2^6}{v^{12}}\right) \prod_{i>j=u,c,t} (m_i^2 - m_j^2) \prod_{k>l=d,s,b} (m_k^2 - m_l^2) J_{\text{CKM}} \approx 10^{-20}, \quad (33)$$

where $v = 246$ GeV and $J_{\text{CKM}} = \text{Im } V_{ud} V_{cd}^* V_{cs} V_{us}^* \approx 3 \times 10^{-5}$.¹⁰ As shown in Ref. [72], this would correspond diagrammatically to the insertion of 12 Yukawas (connected pairwise via 6 Higgs propagators) in the propagator of a quark field and hence to a 6-loop diagram, whose imaginary part contributes to $\bar{\theta}$. On the other hand, the SM Yukawa Lagrangian features an accidental exchange symmetry: $H \leftrightarrow \tilde{H}$, $u_R \leftrightarrow d_R$, $Y_U \leftrightarrow Y_D$, under which $\text{Im Det}[Y_U Y_U^\dagger, Y_D Y_D^\dagger]$ is odd. Hence, the 6-loop contribution must vanish, and in order to get a non-zero contribution one has to insert e.g. a $U(1)_Y$ gauge boson which breaks the $u_R \leftrightarrow d_R$ symmetry. Then a typical 7-loop contribution to the radiatively induced $\bar{\theta}$ will look like

$$\delta\bar{\theta}_{\text{div.}} \sim \frac{g'^2 (y_{u_R}^2 - y_{d_R}^2) \text{Im Det}[Y_U Y_U^\dagger, Y_D Y_D^\dagger]}{(4\pi^2)^7} \log \Lambda_{\text{UV}} \approx 10^{-33} \log \Lambda_{\text{UV}}, \quad (34)$$

where y_{u_R, d_R} denotes the hypercharge of a given SM chiral quark and Λ_{UV} is an ultraviolet (UV) cut-off. Thus if we take the tree-level value of $\bar{\theta}$ to be small at some UV boundary (e.g. the Planck scale), it will remain radiatively small when run down to the QCD scale. This has to be contrasted instead with the hierarchy problem of the electroweak scale, for which the Higgs mass parameter is quadratically sensitive to threshold effects from UV physics, $\delta\mu^2 \sim (\text{loop}) \times \Lambda_{\text{UV}}^2$. Remarkably, the CP and flavour structure of the SM provides a non-trivial screening mechanism against radiative corrections to $\bar{\theta}$, which is not guaranteed in generic SM extensions.

Integrating out the heavy SM quarks can also lead to finite threshold corrections to $\bar{\theta}$, which arise at lower orders in perturbation theory. The size of the largest contribution were first estimated in [72] to be¹¹

$$\delta\bar{\theta}_{\text{fin.}} \sim \left(\frac{\alpha_s}{\pi}\right)^4 \left(\frac{\alpha_2}{\pi}\right)^2 \left(\frac{m_s^2 m_c^2}{m_W^4}\right) J_{\text{CKM}} \approx 10^{-18}, \quad (35)$$

where long-distance QCD effects are such that the strong structure constant is $\alpha_s(\text{GeV})/\pi \approx 1$ at the scale relevant for the calculation of the nEDM. A refined estimate [76], based on an actual 3-loop calculation, finds instead an $\mathcal{O}(\alpha_s G_F^2)$ contribution yielding $\delta\bar{\theta}_{\text{fin.}} \approx 4 \times 10^{-19}$ (using a somewhat smaller value $\alpha_s \approx 0.2$). Although in both cases the contribution is only of 2-loop order in the electroweak structure constant, α_2 , it is still well below the nEDM experimental sensitivity. Generic SM extensions might however spoil this conclusion (see e.g. [77]).

Another fact that renders the strong CP problem different from other small value problems of the SM such as that of the light Yukawas ($y_{u,d,e}$) or the cosmological constant, is the apparent lack of a possible anthropic explanation. In fact, as long as $\bar{\theta} \lesssim 1\%$, nuclear physics and Big Bang Nucleosynthesis are practically unaffected [4], so that a value $\bar{\theta} \lesssim 10^{-10}$ does not seem to be connected to any ‘catastrophic boundary’. A possible pathway to enforce explanations based on anthropic selection arguments might then be attempted by trying to correlate the value of $\bar{\theta}$ with the value of some other small parameter for which an anthropic explanation does exist, as for example the cosmological constant [78]. Attempts in this direction have been carried out for example in Refs. [79, 80]. However, the recent analysis of Ref. [5] found that anthropic requirements on the cosmological constant rather favour values of the CP violating angle of $\mathcal{O}(1)$, reinforcing the idea that $\bar{\theta} \ll 1$ is not related to anthropic selection.

¹⁰An alternative form of the Jarlskog invariant can be found in [75].

¹¹The different numerical value compared to Ref. [72] originates from employing up-to-date values for the SM parameters.

2.4.1. Solutions without axions

Before introducing the axion solution of the strong CP problem, we discuss for completeness three class of solutions which do not rely on the axion.¹²

- *Massless quark solution.* If one of the quark fields (say the up quark) were massless, the QCD Lagrangian would feature a global $U(1)_u$ axial symmetry, which could be used to rotate the θ term to zero (cf. the discussion below Eq. (20)). For some time this was believed to be a possible solution of the strong CP problem, due to the difficulty in extracting the value of m_u/m_d in chiral perturbation theory. Most notably, this was due to a second-order effect in the chiral Lagrangian, known as Kaplan-Manohar ambiguity [82] (see also [83–85]). Nowadays this possibility has been ruled out by the fit to light quark masses on the lattice [86], which yields $m_u^{\overline{\text{MS}}}(2 \text{ GeV}) = 2.32(10) \text{ MeV}$, that is more than 20σ away from zero. An independent strategy in order to disprove the massless up quark solution without simulating light quarks on the lattice was put forth in Refs. [87, 88] and recently implemented on the lattice [89], which confirmed the non-viability of the massless up-quark hypothesis.
- *Soft P (CP) breaking.* It is conceivable that either P or CP are symmetries of the high-energy theory, thus setting $\bar{\theta} = 0$ in the UV. Models of this type were first proposed in [90–92] and later on in [93, 94] in the context of grand-unified models. Eventually, P must be spontaneously broken in order to account for the SM chiral structure and similarly for CP in order to generate the CKM phase (and the extra CP violation that is needed for baryogenesis). In these setups the $\bar{\theta}$ term becomes calculable and the main challenge consists in generating the observed CP violation in the quark sector in such a way that threshold contributions to $\bar{\theta}$ are screened enough so that $\delta\bar{\theta} \lesssim 10^{-10}$. This can be done, however at the cost of some tuning or a somewhat exotic model building (for reviews, see e.g. [95, 96]).
- *QCD solutions.* It is conceivable, at least in principle, that the solution of the strong CP problem might be hidden in the infrared (IR) dynamics of QCD. Attempts in this direction, e.g. by ‘trivializing’ the QCD vacuum by changing the topology of spacetime [97–100] or by invoking screening effects due to confinement [101–103], often fail to provide a simultaneous solution to the η' problem.

It is fair to say that, while it is certainly worth looking for solutions of the strong CP problem within QCD, no convincing framework has emerged so far. As far as concerns the soft P (CP) breaking solutions instead, besides the model building complications involved, it is also unappealing the fact that the strong CP problem is solved by UV dynamics, without a clear experimental way to test the mechanism. From this point of view, the Peccei Quinn solution, which is reviewed in the next section, is crucially different, since it delivers a low-energy experimental handle in the form of the axion.

2.4.2. Peccei Quinn mechanism

From a modern perspective, the basic ingredient of the PQ solution [16, 17, 19, 20] of the strong CP problem consists in the introduction of a new spin zero field $a(x)$, hereby denoted as the axion field, whose effective Lagrangian

$$\mathcal{L}_a = \frac{1}{2}(\partial_\mu a)^2 + \mathcal{L}(\partial_\mu a, \psi) + \frac{g_s^2}{32\pi^2} \frac{a}{f_a} G\tilde{G} \quad (36)$$

is endowed with a quasi shift symmetry $a \rightarrow a + \kappa f_a$ (where f_a is an energy scale called the axion decay constant) that leaves the action invariant up to the term

$$\delta S = \frac{\kappa}{32\pi^2} \int d^4x G\tilde{G}. \quad (37)$$

¹²Besides the three possibilities outlined below, more speculative solutions that do not invoke an axion also exist, see for example [81].

The transformation parameter κ is arbitrary and can be chosen to remove the $\bar{\theta}$ term, while the Vafa-Witten theorem [18] (see Eq. (25) for the proof) ensures that $\langle a \rangle = 0$ in a vector-like theory like QCD,¹³ thus solving dynamically the strong CP problem. Alternatively, one can explicitly compute the axion potential $V(a)$ with chiral Lagrangian techniques (which will be done in Section 2.5.1) and show that the absolute minimum is in $\langle a \rangle = 0$.

Since the Lagrangian Eq. (36) is non-renormalizable, it requires a UV completion at energies of the order of f_a . Historically, the first renormalizable model incorporating the axion solution of the strong CP problem was due to Peccei and Quinn [19, 20], which postulated the existence of a $U(1)_{\text{PQ}}$ global symmetry, spontaneously broken and anomalous under QCD. The presence of a pseudo-Goldstone boson $a(x)$ (dubbed axion, since it washes out the strong CP problem) was soon realized by Weinberg and Wilczek [16, 17]. However, before considering explicit models we will first discuss some general properties of the axion effective Lagrangian in Eq. (36), which is already sufficient for characterizing some general aspects of axion physics.

2.5. Axion effective Lagrangian

The effective operator $aG\tilde{G}$ is the building block of the PQ solution of the strong CP problem, and provides some model-independent properties of the axion, which we discuss here with the help of the chiral Lagrangian [47, 104]. Let us consider for simplicity 2-flavor QCD, with $q^T = (u, d)$ and $M_q = \text{diag}(m_u, m_d)$. The axion effective Lagrangian reads

$$\mathcal{L}_a = \frac{1}{2}(\partial_\mu a)^2 + \frac{a}{f_a} \frac{g_s^2}{32\pi^2} G\tilde{G} + \frac{1}{4} g_{a\gamma}^0 a F\tilde{F} + \frac{\partial_\mu a}{2f_a} \bar{q} c_q^0 \gamma^\mu \gamma_5 q - \bar{q}_L M_q q_R + \text{h.c.} \quad (38)$$

For later purposes, we have extended Eq. (36) to include two model-dependent couplings: $g_{a\gamma}^0$ that couples the axion to $F\tilde{F}$ and violates the shift symmetry, and $c_q^0 = \text{diag}(c_u^0, c_d^0)$ that couples derivatively the axion to the quark axial current.¹⁴ Their origin will be clarified in Section 2.6. It is convenient to first eliminate the $aG\tilde{G}$ term via a field-dependent axial transformation of the quark fields:

$$q \rightarrow e^{i\gamma_5 \frac{a}{2f_a} Q_a} q, \quad (39)$$

where Q_a is a generic matrix acting on the quark fields. This transformation has the effect of generating a term $-g_s^2 \text{Tr} Q_a / (32\pi^2) \frac{a}{f_a} G\tilde{G}$ which, by requiring that $\text{Tr} Q_a = 1$, precisely cancels the axion-gluon term. Since in general this transformation is anomalous under QED, it will also affect the $F\tilde{F}$ term. Moreover, extra axion-dependent terms are generated by the quark mass operator and the quark kinetic term. Then Eq. (38) becomes

$$\mathcal{L}_a = \frac{1}{2}(\partial_\mu a)^2 + \frac{1}{4} g_{a\gamma} a F\tilde{F} + \frac{\partial_\mu a}{2f_a} \bar{q} c_q \gamma^\mu \gamma_5 q - \bar{q}_L M_a q_R + \text{h.c.}, \quad (40)$$

where we have defined axion-dressed parameters

$$g_{a\gamma} = g_{a\gamma}^0 - (2N_c) \frac{\alpha}{2\pi f_a} \text{Tr}(Q_a Q^2) \quad \text{with} \quad Q = \text{diag}(2/3, -1/3), \quad (41)$$

$$c_q = c_q^0 - Q_a, \quad (42)$$

$$M_a = e^{i\frac{a}{2f_a} Q_a} M_q e^{i\frac{a}{2f_a} Q_a}, \quad (43)$$

¹³A crucial step of the proof relies on the positive definiteness of the fermionic determinant in the background of the gauge fields, i.e. $\det(\not{D} + m) > 0$. This is not ensured for a chiral theory where $m = 0$, since it is not possible to write a bare mass term for fermions, and hence the Vafa-Witten theorem does not apply in such case. In fact, in the SM, which is chiral and contains an extra source of CP violation in the Yukawa sector, one expects an irreducible contribution to the axion VEV, as discussed in Section 2.10.

¹⁴While the anomalous dimension of conserved currents vanishes, that is not the case for anomalous currents. In fact, as shown in Refs. [105, 106] the iso-spin singlet axial current, $j_{\Sigma q}^\mu = \sum_q \bar{q} \gamma^\mu \gamma_5 q$, renormalizes multiplicatively. Taking this effect into account it is possible to connect the low-energy derivative axion couplings to quarks with their UV counterparts, which are understood to be the coefficients c_q^0 (for details see [47]).

where $\alpha = e^2/(4\pi)$ and $N_c = 3$ is the number of colours. The axial quark current can be conveniently decomposed into an iso-singlet and an iso-triplet component

$$\bar{q}c_q\gamma^\mu\gamma_5q = \frac{1}{2}\text{Tr}[c_q]\bar{q}\gamma^\mu\gamma_5q + \frac{1}{2}\text{Tr}[c_q\sigma^a]\bar{q}\gamma^\mu\gamma_5\sigma^aq, \quad (44)$$

where we have used the Fierz identity for Pauli matrices, $(\sigma^a)_{ij}(\sigma^a)_{kl} = 2\delta_{il}\delta_{kj} - \delta_{ij}\delta_{kl}$. Eq. (40) should be compared with the chiral axion Lagrangian, including for simplicity only pions and axions¹⁵

$$\mathcal{L}_a^{\chi\text{PT}} = \frac{f_\pi^2}{4} [\text{Tr}((D^\mu U)^\dagger D^\mu U) + 2B_0 \text{Tr}(UM_a^\dagger + M_a U^\dagger)] + \frac{\partial^\mu a}{2f_a} \frac{1}{2} \text{Tr}[c_q\sigma^a]J_\mu^a, \quad (45)$$

where we neglected the iso-singlet current since it is associated to the heavy η' .¹⁶ B_0 is related to the quark condensate and

$$J_\mu^a = \frac{i}{2}f_\pi^2 \text{Tr}[\sigma^a(UD_\mu U^\dagger - U^\dagger D_\mu U)], \quad (46)$$

is the pion iso-triplet axial-vector current (derived from the covariant derivative term in Eq. (45)) that has the same transformation properties under $SU(2)_L \otimes SU(2)_R$ as the corresponding quark current in Eq. (44), and we have employed the standard parametrization

$$U = e^{i\pi^a\sigma^a/f_\pi} = \mathbb{I} \cos \frac{\pi}{f_\pi} + i \frac{\sigma^a\pi^a}{\pi} \sin \frac{\pi}{f_\pi}, \quad (47)$$

with $\pi = \sqrt{(\pi^0)^2 + 2\pi^+\pi^-}$, $f_\pi = 92.3$ MeV and $D_\mu U = \partial_\mu U + ieA_\mu[Q, U]$. In the following, we discuss the various terms arising from the axion chiral Lagrangian.

2.5.1. Axion potential and axion mass

Expanding the non-derivative part of the axion chiral Lagrangian, one obtains

$$\begin{aligned} 2B_0 \frac{f_\pi^2}{4} \text{Tr}(UM_a^\dagger + M_a U^\dagger) &= B_0 f_\pi^2 (m_u + m_d) - \frac{1}{2} B_0 (m_u + m_d) \pi^2 \\ &\quad - \frac{i}{4} B_0 \frac{f_\pi^2}{f_a} a \text{Tr}(U\{Q_a, M_q\}) + \text{h.c.} + \dots \end{aligned} \quad (48)$$

It is customary to choose $Q_a = M_q^{-1}/\text{Tr} M_q^{-1}$. Note that any linear coupling of the axion to an arbitrary number of pion fields is set to zero: for an odd number of pions because $\text{Tr} \sigma^a = 0$, while for an even number there is a cancellation with the hermitian conjugate. In particular, this sets to zero a mass mixing term between a and π^0 (ignoring possible kinetic mixing between a and π^0 , cf. Section 2.5.2), while from the second term in Eq. (48) we obtain $m_\pi^2 = B_0(m_u + m_d)$ at the leading order (LO) in the chiral Lagrangian expansion. With the above choice of Q_a the axion-pion potential turns out to be

$$\begin{aligned} V(a, \pi^a) &= -2B_0 \frac{f_\pi^2}{4} \text{Tr}(UM_a^\dagger + M_a U^\dagger) \\ &= -\frac{m_\pi^2 f_\pi^2}{m_u + m_d} \left\{ \left[m_u \cos\left(\frac{m_d}{m_u + m_d} \frac{a}{f_a}\right) + m_d \cos\left(\frac{m_u}{m_u + m_d} \frac{a}{f_a}\right) \right] \cos\left(\frac{\pi}{f_\pi}\right) \right. \\ &\quad \left. + \frac{\pi^0}{\pi} \left[m_u \sin\left(\frac{m_d}{m_u + m_d} \frac{a}{f_a}\right) - m_d \sin\left(\frac{m_u}{m_u + m_d} \frac{a}{f_a}\right) \right] \sin\left(\frac{\pi}{f_\pi}\right) \right\}. \end{aligned} \quad (49)$$

¹⁵Nucleons can be included as well in chiral Lagrangian [104]. However, due to the lack of a mass gap between $\Lambda_\chi = 4\pi f_\pi$ and m_N , the convergence of the EFT is not good. For this reason we are going to discuss axion-nucleon couplings separately, in the context of a non-relativistic EFT for nucleons [47] (cf. Section 2.5.4).

¹⁶Interactions between the axion and the η' meson can be taken into account in the large N approximation by using the formalism of Refs. [107, 108].

Expanding for $a/f_a \ll 1$ we obtain

$$V(a, \pi^a) = -m_\pi^2 f_\pi^2 \cos\left(\frac{\pi}{f_\pi}\right) + \frac{1}{2} \frac{m_u m_d}{(m_u + m_d)^2} \frac{m_\pi^2 f_\pi^2}{f_a^2} a^2 \cos\left(\frac{\pi}{f_\pi}\right) + \mathcal{O}\left(\frac{a^3}{f_a^3}\right), \quad (50)$$

where linear terms in the axion field are absent by construction. The axion mass (squared) is then readily obtained by setting the pion on its ground state $\pi = 0$, which yields [16]

$$m_a^2 = \frac{m_u m_d}{(m_u + m_d)^2} \frac{m_\pi^2 f_\pi^2}{f_a^2} \implies m_a \simeq 5.7 \left(\frac{10^{12} \text{ GeV}}{f_a} \right) \mu\text{eV}. \quad (51)$$

An alternative expression for the axion-pion potential, corresponding to the choice $Q_a = \frac{1}{2} \text{diag}(1, 1)$, is given by [47, 108]

$$V(a, \pi^0) = -m_\pi^2 f_\pi^2 \sqrt{1 - \frac{4m_u m_d}{(m_u + m_d)^2} \sin^2\left(\frac{a}{2f_a}\right) \cos\left(\frac{\pi^0}{f_\pi} - \phi_a\right)}, \quad (52)$$

with

$$\tan \phi_a = \frac{m_u - m_d}{m_u + m_d} \tan\left(\frac{a}{2f_a}\right), \quad (53)$$

which clearly shows that the absolute minimum is in $(a, \pi^0) = (0, 0)$.¹⁷ In particular, on the pion ground state, $\pi^0 = \phi_a f_\pi$, the chiral perturbation theory (χ PT) axion potential takes the form

$$V(a) = -m_\pi^2 f_\pi^2 \sqrt{1 - \frac{4m_u m_d}{(m_u + m_d)^2} \sin^2\left(\frac{a}{2f_a}\right)}. \quad (54)$$

Note that while in an expansion around $a = 0$ at the leading order the chiral potential and the one instanton cosine potential of Eq. (17) coincide, for large field values, $a \sim f_a$ the two differ even qualitatively. This is because in the regime of confinement, where the estimate of the potential Eq. (54) based on chiral perturbation theory is reliable, the instanton semiclassical approximation breaks down, since in that regime fluctuations of topologically non-trivial gauge configurations away from the instanton solution that extremise the classical action also become important. On the other hand, the chiral potential cannot be used above the chiral phase transition, and the one-instanton potential becomes more reliable at $T \sim 1 \text{ GeV}$, which is the relevant regime for the calculation of the axion DM relic density (cf. Section 3).

2.5.2. Axion-pion coupling

Next we inspect the derivative part of the axion-pion Lagrangian. This is obtained by expanding the iso-triplet current term in Eq. (45):

$$\begin{aligned} \frac{\partial_\mu a}{2f_a} \frac{1}{2} \text{Tr}[c_q \sigma^a] J_a^\mu &\simeq -\frac{1}{2} \left(\frac{m_d - m_u}{m_u + m_d} + c_d^0 - c_u^0 \right) \frac{f_\pi}{f_a} \partial_\mu a \partial^\mu \pi^0 \\ &+ \frac{1}{3} \left(\frac{m_d - m_u}{m_u + m_d} + c_d^0 - c_u^0 \right) \frac{1}{f_a f_\pi} \partial_\mu a (2\partial^\mu \pi^0 \pi^+ \pi^- - \pi_0 \partial^\mu \pi^+ \pi^- - \pi_0 \pi^+ \partial^\mu \pi^-). \end{aligned} \quad (55)$$

Note that the first term in Eq. (55) represents a kinetic mixing between the axion and the pion fields, which needs to be diagonalized in order to define the canonical axion and pion fields. The quadratic part of the axion-pion Lagrangian reads

$$\mathcal{L}_a^{\text{quad.}} = \frac{1}{2} \begin{pmatrix} \partial_\mu a & \partial_\mu \pi^0 \end{pmatrix} \begin{pmatrix} 1 & \epsilon \\ \epsilon & 1 \end{pmatrix} \begin{pmatrix} \partial^\mu a \\ \partial^\mu \pi^0 \end{pmatrix} - \frac{1}{2} \begin{pmatrix} a & \pi^0 \end{pmatrix} \begin{pmatrix} m_a^2 & 0 \\ 0 & m_\pi^2 \end{pmatrix} \begin{pmatrix} a \\ \pi^0 \end{pmatrix}, \quad (56)$$

¹⁷QED corrections could in principle generate new minima [109]. However, this is prevented by the hierarchy $m_q/f_\pi \gg \alpha/\pi$, which makes the vacuum structure for the pion potential trivial.

with $\epsilon = -\frac{1}{2} \left(\frac{m_d - m_u}{m_u + m_d} + c_d^0 - c_u^0 \right) \frac{f_\pi}{f_a}$ and $m_a/m_\pi = \mathcal{O}(\epsilon)$. In order to work with canonical propagators one can perform: *i*) an orthogonal transformation to diagonalize the kinetic term, *ii*) a rescaling to make the kinetic term canonical and *iii*) an orthogonal transformation to re-diagonalize the mass term (which does not affect the canonical kinetic term). The net effect of these operations is to shift the current basis fields by $a \rightarrow a - \epsilon \pi^0$ and $\pi^0 \rightarrow \pi^0 + (m_a^2/m_\pi^2)\epsilon a$. Since the axion component into the current pion field is suppressed at the level of ϵ^3 , this redefinition has no practical consequences for experimental sensitivities and astrophysical bounds, which are sensitive at most to $\mathcal{O}(\epsilon^2)$ effects. This justifies the fact that the correction due to kinetic mixing is generally ignored in the literature.

The second addend in Eq. (55) gives instead the axion-pion coupling (see also [26, 110]), defined via the Lagrangian term

$$\mathcal{L}_a^{\text{int}} \supset \frac{C_{a\pi}}{f_a f_\pi} \partial_\mu a (2\partial^\mu \pi^0 \pi^+ \pi^- - \pi_0 \partial^\mu \pi^+ \pi^- - \pi_0 \pi^+ \partial^\mu \pi^-), \quad (57)$$

with

$$C_{a\pi} = -\frac{1}{3} \left(c_u^0 - c_d^0 - \frac{m_d - m_u}{m_u + m_d} \right). \quad (58)$$

Note that once the canonical axion and pion field are properly identified, the only linear coupling of the axion to the pions is the one in Eq. (57). The axion-pion coupling in Eq. (58) generalizes the expressions available in the literature in the case of KSVZ [110] and DFSZ [26] axions.

2.5.3. Axion-photon coupling

With the choice of $Q_a = M_q^{-1}/\text{Tr } M_q^{-1}$ to ensure no axion-pion mass mixing, the LO axion-photon coupling in Eq. (41) becomes

$$g_{a\gamma} = g_{a\gamma}^0 - \frac{\alpha}{2\pi f_a} \left(\frac{2}{3} \frac{4m_d + m_u}{m_u + m_d} \right). \quad (59)$$

The same result can be obtained via another choice of Q_a (e.g. the one leading to the χ PT potential in Eq. (54)), but requires the inclusion of a non-zero axion-pion mixing.

2.5.4. Axion-nucleon coupling

Following [47] we derive the axion coupling to nucleons (protons and neutrons), via an effective theory at energies $\ll \Lambda_{\text{QCD}}$, relevant for momentum exchanges of the order of the axion mass, where the nucleons are non-relativistic. This approach turns out to yield a more reliable approximation than current algebra techniques [111] or the chiral EFT for nucleons [104, 112]. Our goal is to match the quark current operator in Eq. (40) with a non-relativistic axion-nucleon Lagrangian. Using iso-spin as an active flavour symmetry and the axion as an external current, the LO effective axion-nucleon Lagrangian reads

$$\begin{aligned} \mathcal{L}_N &= \bar{N} v^\mu \partial_\mu N + 2g_A \frac{c_u - c_d}{2} \frac{\partial_\mu a}{2f_a} \bar{N} S^\mu \sigma^3 N + 2g_0^{ud} \frac{c_u + c_d}{2} \frac{\partial_\mu a}{2f_a} \bar{N} S^\mu N + \dots \\ &= \bar{N} v^\mu \partial_\mu N + 2g_A \frac{c_u - c_d}{2} \frac{\partial_\mu a}{2f_a} (\bar{p} S^\mu p - \bar{n} S^\mu n) + 2g_0^{ud} \frac{c_u + c_d}{2} \frac{\partial_\mu a}{2f_a} (\bar{p} S^\mu p + \bar{n} S^\mu n) + \dots, \end{aligned} \quad (60)$$

where $N = (p, n)^T$ is the iso-spin doublet field, v^μ is the four-velocity of the non-relativistic nucleon and S^μ the spin operator. The couplings g_A and g_0^{ud} correspond respectively to the axial iso-vector and axial iso-scalar combinations, while the dots in Eq. (60) denote higher order terms, including non-derivative axion couplings which for $\langle a \rangle = 0$ (no extra sources of CP violation) are at least quadratic in a . Matching the two effective Lagrangians over a single-nucleon matrix element, for example $\langle p | \mathcal{L}_a | p \rangle = \langle p | \mathcal{L}_N | p \rangle$, at the LO in the isospin breaking effects, we get

$$\frac{\partial_\mu a}{2f_a} c_u \underbrace{\langle p | \bar{u} \gamma^\mu \gamma_5 u | p \rangle}_{s^\mu \Delta u} + \frac{\partial_\mu a}{2f_a} c_d \underbrace{\langle p | \bar{d} \gamma^\mu \gamma_5 d | p \rangle}_{s^\mu \Delta d} = \frac{\partial_\mu a}{2f_a} g_A \frac{c_u - c_d}{2} \underbrace{2\langle p | \bar{p} S^\mu p | p \rangle}_{s^\mu} + \frac{\partial_\mu a}{2f_a} g_0^{ud} \frac{c_u + c_d}{2} \underbrace{2\langle p | \bar{p} S^\mu p | p \rangle}_{s^\mu}, \quad (61)$$

where we used the definition $2\bar{p}S^\mu p = \bar{p}\gamma^\mu\gamma_5 p$, and s^μ is the spin of the nucleon at rest. Reshuffling the previous equation

$$g_A = \Delta u - \Delta d, \quad (62)$$

$$g_0^{ud} = \Delta u + \Delta d. \quad (63)$$

and substituting back into Eq. (60), we get

$$\mathcal{L}_N \supset \frac{\partial_\mu a}{2f_a} \left\{ \frac{c_u - c_d}{2} (\Delta u - \Delta d) (\bar{p}\gamma^\mu\gamma_5 p - \bar{n}\gamma^\mu\gamma_5 n) + \frac{c_u + c_d}{2} (\Delta u + \Delta d) (\bar{p}\gamma^\mu\gamma_5 p + \bar{n}\gamma^\mu\gamma_5 n) \right\}. \quad (64)$$

The axion-nucleon coupling is defined in analogy to the axion-quark ones as

$$\frac{\partial_\mu a}{2f_a} \bar{N} C_{aN} \gamma^\mu \gamma_5 N, \quad (65)$$

with $C_{aN} = \text{diag}(C_{ap}, C_{an})$, for which we get (recall that $c_q = c_q^0 - Q_a$)

$$C_{ap} = - \left(\frac{m_d}{m_u + m_d} \Delta u + \frac{m_u}{m_u + m_d} \Delta d \right) + c_u^0 \Delta u + c_d^0 \Delta d, \quad (66)$$

$$C_{an} = - \left(\frac{m_u}{m_u + m_d} \Delta u + \frac{m_d}{m_u + m_d} \Delta d \right) + c_d^0 \Delta u + c_u^0 \Delta d, \quad (67)$$

where $\Delta u = 0.897(27)$, $\Delta d = -0.376(27)$ and $m_u^{\overline{\text{MS}}}(2 \text{ GeV})/m_d^{\overline{\text{MS}}}(2 \text{ GeV}) = 0.48(3)$ [47].

2.5.5. Axion-electron coupling

The axion-electron coupling is defined via the Lagrangian term

$$C_{ae} \frac{\partial_\mu a}{2f_a} \bar{e} \gamma^\mu \gamma_5 e, \quad (68)$$

where $C_{ae} = c_e^0 + \delta c_e$. In models where the tree-level contribution, c_e^0 , is zero, the axion-electron coupling can still be generated radiatively. The relevant one-loop diagram is logarithmically divergent, and can be understood as an RGE effect on the C_{ae} coefficient from the PQ scale down to the IR scale μ_{IR} [104]. One finds [110, 111]¹⁸

$$\delta c_e = \frac{3\alpha^2}{4\pi^2} \left[\frac{E}{N} \log \left(\frac{f_a}{\mu_{\text{IR}}} \right) - \frac{2}{3} \frac{4m_d + m_u}{m_u + m_d} \log \left(\frac{\Lambda_\chi}{\mu_{\text{IR}}} \right) \right]. \quad (69)$$

where E/N is related to $g_{a\gamma}^0$ via Eq. (74) as explained in the next Section. The part proportional to E/N corresponds to the running between f_a and $\mu_{\text{IR}} < \Lambda_\chi$, while the second term arises from axion-pion mixing and is cut-off at the chiral symmetry breaking scale, $\Lambda_\chi \simeq 1 \text{ GeV}$, since for loop momenta larger than Λ_χ the effect of the color anomaly is negligible. The IR parameter μ_{IR} should be taken of the order of the energy scale relevant to the physical process under consideration, typically $\mu_{\text{IR}} = m_e$.

2.6. Origin of model-dependent axion couplings

Before discussing explicit axion models, it is useful to describe in a general way how the ‘model-dependent’ axion couplings g_γ^0 and c_q^0 introduced in the axion effective Lagrangian Eq. (38) arise from the point of view of a spontaneously broken $U(1)_{\text{PQ}}$ symmetry. Let us denote by J_μ^{PQ} the associated PQ current, which is conserved up to anomalies

$$\partial^\mu J_\mu^{\text{PQ}} = \frac{g_s^2 N}{16\pi^2} G\tilde{G} + \frac{e^2 E}{16\pi^2} F\tilde{F}, \quad (70)$$

¹⁸As pointed out by [110], the original expression in Ref. [111] contains a typo.

where N and E are respectively the QCD and EM anomaly coefficients. From the Goldstone theorem $\langle 0 | J_\mu^{\text{PQ}} | a \rangle = i v_a p_\mu$, where the axion a is the pseudo Goldstone boson of $U(1)_{\text{PQ}}$ breaking and we introduced the order parameter v_a . The axion effective Lagrangian contains the terms

$$\mathcal{L}_a \supset \frac{a}{v_a} \frac{g_s^2 N}{16\pi^2} G\tilde{G} + \frac{a}{v_a} \frac{e^2 E}{16\pi^2} F\tilde{F} + \frac{\partial_\mu a}{v_a} J_\mu^{\text{PQ}}, \quad (71)$$

where the first two terms are required by anomaly matching and the PQ current depends on the global charges of the fields transforming under $U(1)_{\text{PQ}}$. E.g. for a chiral SM fermion f_L one has $J_\mu^{\text{PQ}}|_{f_L} = \bar{f}_L \mathcal{X}_{f_L} \gamma^\mu f_L$, where \mathcal{X}_{f_L} denotes its PQ charge. Using the standard normalization of the $G\tilde{G}$ term in terms of f_a as in Eq. (38) yields

$$f_a = \frac{v_a}{2N}. \quad (72)$$

Hence Eq. (71) can be rewritten as (taking for illustrative purposes just two chiral fermions f_L and f_R)

$$\begin{aligned} \mathcal{L}_a &\supset \frac{a}{f_a} \frac{g_s^2}{32\pi^2} G\tilde{G} + \frac{a}{f_a} \frac{e^2}{32\pi^2} \frac{E}{N} F\tilde{F} + \frac{\partial_\mu a}{2f_a} \frac{1}{N} [\bar{f}_L \mathcal{X}_{f_L} \gamma^\mu f_L + \bar{f}_R \mathcal{X}_{f_R} \gamma^\mu f_R], \\ &= \frac{a}{f_a} \frac{g_s^2}{32\pi^2} G\tilde{G} + \frac{1}{4} g_{a\gamma}^0 a F\tilde{F} + \frac{\partial_\mu a}{2f_a} \bar{f} c_f^0 \gamma^\mu \gamma_5 f, \end{aligned} \quad (73)$$

where in the second step we have dropped the coupling with the conserved vector current since the corresponding term vanishes upon integration by part. The axion-photon couplings is thus defined as

$$g_{a\gamma}^0 = \frac{\alpha}{2\pi f_a} \frac{E}{N}, \quad (74)$$

and the axion coupling to the fermion f as

$$c_f^0 = \frac{\mathcal{X}_{f_R} - \mathcal{X}_{f_L}}{2N} = -\frac{\mathcal{X}_{H_f}}{2N}, \quad (75)$$

where in the last step, assuming a Yukawa term $\bar{f}_L f_R H_f$, we have replaced the fermion PQ charges with the charge \mathcal{X}_{H_f} of the corresponding Higgs. While the expressions above have a general validity in terms of the defining properties of the $U(1)_{\text{PQ}}$ symmetry (i.e. its anomalous content and the global charge assignments), in the following we will illustrate how to derive them in the context of specific UV models.

2.7. Benchmark axion models

We now move to the discussion of explicit axion models, which provide a UV completion for the axion effective Lagrangian in Eq. (38). The simplest realization of the PQ mechanism is given by the Weinberg-Wilczek (WW) model [16, 17], in which the QCD anomaly of the $U(1)_{\text{PQ}}$ current is generated by SM quarks charged under the PQ symmetry, while the scalar sector is extended via an extra Higgs doublet in order to enforce the additional $U(1)_{\text{PQ}}$ symmetry. In the WW model the axion decay constant, $f_a = (v/6) \sin 2\beta$, with $\tan \beta = v_u/v_d$, is of the order of the electroweak scale $v \simeq 246$ GeV. Hence, being the axion coupling to SM fields not sufficiently suppressed, the WW model was soon ruled out by laboratory searches.¹⁹ This led to the so-called “invisible axion” models, in which the PQ symmetry breaking is decoupled from the electroweak scale via the introduction of a SM singlet scalar field, acquiring a VEV $v_a \sim f_a \gg v$. Axion’s interactions are then parametrically suppressed as $1/f_a \ll 1/v$.

¹⁹The original WW model was ruled out by a combination of beam dump experiments [113] and rare meson decays such as $K \rightarrow \pi a$ [114] and Quarkonia $\rightarrow \gamma a$ [115]. For a historical account see for instance Sect. 3 in Ref. [116]. However, this was under the assumption of universality of the PQ charges. Variant axion models of the WW type (i.e. with non-universal PQ charges and the PQ breaking connected to the electroweak scale), took instead almost a decade to be ruled out from rare π and K meson decays [117].

UV completions of the axion effective Lagrangian can be divided in two large classes, according to the way the QCD anomaly of the $U(1)_{\text{PQ}}$ current is realized. In models of the Dine-Fischler-Srednicki-Zhitnitsky (DFSZ) type [118, 119] the anomaly is carried by SM quarks (as in the WW model), while models of the Kim-Shifman-Vainshtein-Zakharov (KSVZ) type [120, 121] require new colored fermions. Since these two constructions provide the building blocks of most of the models considered in this report, we review them here in detail.

2.7.1. KSVZ axion

The KSVZ model [120, 121] extends the SM field content with a vector-like fermion $\mathcal{Q} = \mathcal{Q}_L + \mathcal{Q}_R$ in the fundamental of color, singlet under $SU(2)_L$, and neutral under hypercharge: $\mathcal{Q} \sim (3, 1, 0)$, and a SM-singlet complex scalar $\Phi \sim (1, 1, 0)$. In the absence of a bare mass term for \mathcal{Q} ,²⁰ the Lagrangian

$$\mathcal{L}_{\text{KSVZ}} = |\partial_\mu \Phi|^2 + \bar{\mathcal{Q}} i \not{D} \mathcal{Q} - (y_{\mathcal{Q}} \bar{\mathcal{Q}}_L \mathcal{Q}_R \Phi + \text{h.c.}) - V(\Phi), \quad (76)$$

features a $U(1)_{\text{PQ}}$ symmetry

$$\Phi \rightarrow e^{i\alpha} \Phi, \quad \mathcal{Q}_L \rightarrow e^{i\alpha/2} \mathcal{Q}_L, \quad \mathcal{Q}_R \rightarrow e^{-i\alpha/2} \mathcal{Q}_R. \quad (77)$$

The potential

$$V(\Phi) = \lambda_\Phi \left(|\Phi|^2 - \frac{v_a^2}{2} \right)^2, \quad (78)$$

is such that the $U(1)_{\text{PQ}}$ symmetry is spontaneously broken, with order parameter v_a . Decomposing the scalar field in polar coordinates

$$\Phi = \frac{1}{\sqrt{2}} (v_a + \varrho_a) e^{ia/v_a}, \quad (79)$$

the axion field a corresponds to the Goldstone mode (massless at tree level), while the radial mode ϱ_a picks up a mass $m_{\varrho_a} = \sqrt{2\lambda_\Phi} v_a$. In the PQ broken phase also the fermion \mathcal{Q} gets massive, with $m_{\mathcal{Q}} = y_{\mathcal{Q}} v_a / \sqrt{2}$.

The Lagrangian term (where we neglected the heavy scalar radial mode)

$$\mathcal{L}_{\text{KSVZ}} \supset -m_{\mathcal{Q}} \bar{\mathcal{Q}}_L \mathcal{Q}_R e^{ia/v_a} + \text{h.c.}, \quad (80)$$

is responsible for the generation of the $aG\tilde{G}$ operator in the effective theory below $m_{\mathcal{Q}}$. To see that, let us perform a field-dependent axial transformation:

$$\mathcal{Q} \rightarrow e^{-i\gamma_5 \frac{a}{2v_a}} \mathcal{Q}, \quad (81)$$

or, equivalently, $\mathcal{Q}_L \rightarrow e^{i\frac{a}{2v_a}} \mathcal{Q}_L$ and $\mathcal{Q}_R \rightarrow e^{-i\frac{a}{2v_a}} \mathcal{Q}_R$. In the transformed variables the field \mathcal{Q} is now disentangled from the axion, so we can safely integrate it out. Moreover, being the transformation in Eq. (81) anomalous under QCD, one gets (e.g. from the non-invariance of the path integral measure [57]):

$$\delta \mathcal{L}_{\text{KSVZ}} = \frac{g_s^2}{32\pi^2} \frac{a}{v_a} G\tilde{G}, \quad (82)$$

where we have used the fact that \mathcal{Q} is in the fundamental of color. In such a case one can identify $v_a = f_a$ (cf. Eq. (38)), and the only coupling of the axion with the SM fields is via the $aG\tilde{G}$ term (model-independent contribution) discussed in Section 2.5.

For later purposes (cf. Section 6.1.1) we discuss the KSVZ model in the more general setup in which the heavy fermions \mathcal{Q} reside in a generic reducible representation $\sum_{\mathcal{Q}} (\mathcal{C}_{\mathcal{Q}}, \mathcal{I}_{\mathcal{Q}}, \mathcal{Y}_{\mathcal{Q}})$ of the $SU(3)_c \times SU(2)_L \times U(1)_Y$ gauge group. The only requirement for the PQ mechanism to work, is that at least one $\mathcal{C}_{\mathcal{Q}}$ is a

²⁰In the spirit of having the PQ to arise as an accidental global symmetry (cf. Section 2.11), this can be enforced e.g. via the discrete gauge symmetry [120]: $\mathcal{Q}_L \rightarrow -\mathcal{Q}_L$, $\mathcal{Q}_R \rightarrow \mathcal{Q}_R$, $\Phi \rightarrow -\Phi$.

non-trivial representation. The PQ current will have in general both a QCD and EM anomaly, represented by the anomaly coefficients E and N (see definition in Eq. (70)) which read

$$N = \sum_{\mathcal{Q}} N_{\mathcal{Q}}, \quad E = \sum_{\mathcal{Q}} E_{\mathcal{Q}}, \quad (83)$$

with $N_{\mathcal{Q}}$ and $E_{\mathcal{Q}}$ denoting the contributions to the anomalies of each irreducible representation (all taken to be left-handed, so in particular $\mathcal{X}_{\mathcal{Q}_L^c} = -\mathcal{X}_{\mathcal{Q}_R}$)

$$N_{\mathcal{Q}} = \mathcal{X}_{\mathcal{Q}} d(\mathcal{I}_{\mathcal{Q}}) T(\mathcal{C}_{\mathcal{Q}}), \quad (84)$$

$$E_{\mathcal{Q}} = \mathcal{X}_{\mathcal{Q}} d(\mathcal{C}_{\mathcal{Q}}) \text{Tr } q_{\mathcal{Q}}^2 = \mathcal{X}_{\mathcal{Q}} d(\mathcal{C}_{\mathcal{Q}}) d(\mathcal{I}_{\mathcal{Q}}) \left(\frac{1}{12} (d(\mathcal{I}_{\mathcal{Q}})^2 - 1) + \mathcal{Y}_{\mathcal{Q}}^2 \right). \quad (85)$$

Here $d(\mathcal{C}_{\mathcal{Q}})$ and $d(\mathcal{I}_{\mathcal{Q}})$ denote the dimension of the colour and weak isospin representations, $T(\mathcal{C}_{\mathcal{Q}})$ is the color Dynkin index (with standard normalization $T(3) = 1/2$, $T(6) = 5/2$, $T(8) = 3$, $T(15) = 10$, etc.), $q_{\mathcal{Q}} = T_{\mathcal{Q}}^{(3)} + \mathcal{Y}_{\mathcal{Q}}$ denotes the $U(1)_{\text{EM}}$ charge generator, and $\mathcal{X}_{\mathcal{Q}_R} = -\mathcal{X}_{\mathcal{Q}_L} = \mp 1/2$ depending if in Eq. (76) the quark bilinear $\bar{\mathcal{Q}}_L \mathcal{Q}_R$ couples to Φ or Φ^\dagger . Hence, after removing the axion field from the Yukawa Lagrangian via the transformation in Eq. (81), one gets the effective anomalous interactions (with $\alpha_s = g_s^2/(4\pi)$, etc.)

$$\delta \mathcal{L}_{\text{KSVZ}} = \frac{\alpha_s N}{4\pi} \frac{a}{v_a} G \tilde{G} + \frac{\alpha E}{4\pi} \frac{a}{v_a} F \tilde{F}. \quad (86)$$

It is customary to normalize the first term as in the axion effective Lagrangian Eq. (38), so that

$$\delta \mathcal{L}_{\text{KSVZ}} = \frac{\alpha_s}{8\pi} \frac{a}{f_a} G \tilde{G} + \frac{\alpha}{8\pi} \frac{E}{N} \frac{a}{f_a} F \tilde{F}, \quad (87)$$

where the relation between the coefficient of the EM term and the effective coupling introduced in Eq. (38) is $g_{a\gamma}^0 = \frac{\alpha}{2\pi f_a} \frac{E}{N}$ with f_a defined in Eq. (72). From Eq. (79) we see that the axion is defined as an angular variable over the domain $[0, 2\pi v_a)$.²¹ On the other hand, the QCD induced axion potential is periodic in $[0, 2\pi f_a)$ (cf. Eq. (52) or Eq. (49)). We operatively define the domain wall (DW) number, will be important in cosmology, in terms of the QCD anomaly factor

$$N_{\text{DW}} \equiv 2N, \quad (88)$$

as the number of inequivalent degenerate minima of the axion potential, that correspond to $\theta = 2\pi n/N_{\text{DW}}$ with $n \in \{0, 1, \dots, N_{\text{DW}} - 1\}$. The consequences of DWs in cosmology will be discussed in Section 3.4, while the cosmological DW problem, which arises in models with $N_{\text{DW}} > 1$, is reviewed in Section 7.5, together with possible solutions. Here we just remark that the original KSVZ construction with one vector-like pair of heavy quarks, singlets under $SU(2)_L$ ($d(\mathcal{I}_{\mathcal{Q}}) = 1$), in the fundamental of $SU(3)$ ($T(\mathcal{C}_{\mathcal{Q}}) = 1/2$), and with PQ charges $\mathcal{X}_{\mathcal{Q}_L} = -\mathcal{X}_{\mathcal{Q}_R} = 1/2$ as follows from Eq. (77), belongs to the class of $N_{\text{DW}} = 1$ models.

2.7.2. DFSZ axion

The field content of the DFSZ model includes two Higgs doublets $H_u \sim (1, 2, -\frac{1}{2})$ and $H_d \sim (1, 2, +\frac{1}{2})$ and a SM-singlet complex scalar field, $\Phi \sim (1, 1, 0)$. The latter extends the WW model, allowing to decouple the PQ breaking scale from the electroweak scale. We write the renormalizable scalar potential as²²

$$V(H_u, H_d, \Phi) = \tilde{V}_{\text{moduli}}(|H_u|, |H_d|, |\Phi|, |H_u H_d|) + \lambda H_u H_d \Phi^{\dagger 2} + \text{h.c.} \quad (89)$$

²¹For $\mathcal{X}_{\Phi} \neq 1$ the axion domain would be instead $[0, 2\pi v_a/\mathcal{X}_{\Phi})$.

²²We couple the Higgs bilinear to Φ^\dagger rather than to Φ to ensure positive values of the anomaly coefficients (see below) while maintaining the convenient charge normalization $\mathcal{X}_{\Phi} = 1$, as in Eq. (96). A different possibility for the Higgs coupling to the PQ breaking field is to replace the quartic coupling with the super-renormalizable operator $H_u H_d \Phi^\dagger$. This is a physically distinct choice as it implies $N_{\text{DW}} = 3$, that is half of the one in standard DFSZ (cf. discussion below Eq. (102)). Note, however, that none of the previous two choices has effects on the axion couplings.

Eq. (89) contains all the moduli terms allowed by gauge invariance plus a non-hermitian operator which is responsible for the explicit breaking of the re-phasing symmetry of the three scalar fields into two linearly independent $U(1)$'s, to be identified with the hypercharge and the PQ symmetry

$$U(1)_{H_u} \times U(1)_{H_d} \times U(1)_\Phi \rightarrow U(1)_Y \times U(1)_{\text{PQ}}. \quad (90)$$

The action of the PQ symmetry on the fermion fields is taken to be the same for all the generations and, in the case of the DFSZ-I model, is determined by the following Yukawa Lagrangian

$$\mathcal{L}_{\text{DFSZ-I}}^Y = -Y_U \bar{q}_L u_R H_u - Y_D \bar{q}_L d_R H_d - Y_E \bar{\ell}_L e_R H_d + \text{h.c.} \quad (91)$$

Alternatively, one can couple $\tilde{H}_u = i\sigma_2 H_u^*$ in the lepton sector, which goes under the name of DFSZ-II variant,

$$\mathcal{L}_{\text{DFSZ-II}}^Y = -Y_U \bar{q}_L u_R H_u - Y_D \bar{q}_L d_R H_d - Y_E \bar{\ell}_L e_R \tilde{H}_u + \text{h.c.} \quad (92)$$

By means of a proper scalar potential in Eq. (89) one can ensure that all the three scalar fields pick up a VEV

$$H_u \supset \frac{v_u}{\sqrt{2}} e^{i\frac{a_u}{v_u}} \begin{pmatrix} 1 \\ 0 \end{pmatrix}, \quad H_d \supset \frac{v_d}{\sqrt{2}} e^{i\frac{a_d}{v_d}} \begin{pmatrix} 0 \\ 1 \end{pmatrix}, \quad \Phi \supset \frac{v_\Phi}{\sqrt{2}} e^{i\frac{a_\Phi}{v_\Phi}}, \quad (93)$$

where $v_\Phi \gg v_{u,d}$ and we have neglected EM-charged and radial modes that do not contain the axion. Note that the parametrisation of the singlet field Φ in the last relation differs from the one used in Eq. (79) in that $a \rightarrow a_\Phi$ and $v_a \rightarrow v_\Phi$. This distinction is necessary whenever, as in DFSZ models, besides the singlet angular mode a_Φ , Goldstone bosons of other scalar multiplets concur to define the physical axion a , and additional VEVs contribute to its dimensional normalization factor v_a . In order to identify the axion field a in terms of $a_{u,d,\Phi}$ let us write down the PQ current

$$J_\mu^{\text{PQ}} = -\mathcal{X}_\Phi \Phi^\dagger i \overleftrightarrow{\partial}_\mu \Phi - \mathcal{X}_{H_u} H_u^\dagger i \overleftrightarrow{\partial}_\mu H_u - \mathcal{X}_{H_d} H_d^\dagger i \overleftrightarrow{\partial}_\mu H_d + \dots \supset J_\mu^{\text{PQ}}|_a = \sum_{i=\Phi,u,d} \mathcal{X}_i v_i \partial_\mu a_i, \quad (94)$$

where the dots stand for the fermion contribution to the current, while in $J_\mu^{\text{PQ}}|_a$ we have retained only the $a_{u,d,\Phi}$ fields and defined $\mathcal{X}_{u,d} = \mathcal{X}_{H_u,H_d}$ to compactify the result. The axion field is now defined as [111]

$$a = \frac{1}{v_a} \sum_i \mathcal{X}_i v_i a_i, \quad v_a^2 = \sum_i \mathcal{X}_i^2 v_i^2, \quad (95)$$

so that $J_\mu^{\text{PQ}}|_a = v_a \partial_\mu a$ and, compatibly with Goldstone theorem, $\langle 0 | J_\mu^{\text{PQ}} | a \rangle = i v_a p_\mu$. Note, also, that under a PQ transformation $a_i \rightarrow a_i + \kappa \mathcal{X}_i v_i$ the axion field transforms as $a \rightarrow a + \kappa v_a$. The PQ charges in the scalar sector can be determined by requiring: *i*) PQ invariance of the operator $H_u H_d \Phi^{\dagger 2}$, which implies $\mathcal{X}_{H_u} + \mathcal{X}_{H_d} - 2\mathcal{X}_\Phi = 0$, and *ii*) orthogonality between $J_\mu^{\text{PQ}}|_a$ in Eq. (94) and the corresponding contribution to the hypercharge current $J_\mu^Y|_a = \sum_i Y_i v_i \partial_\mu a_i$, which implies $\sum_i 2Y_i \mathcal{X}_i v_i^2 = -\mathcal{X}_{H_u} v_u^2 + \mathcal{X}_{H_d} v_d^2 = 0$. The latter condition ensures that there is no kinetic mixing between the physical axion and the Z boson.²³ All charges are hence fixed up to an overall normalisation²⁴ that can be fixed by choosing a conventional value for \mathcal{X}_Φ :

$$\mathcal{X}_\Phi = 1, \quad \mathcal{X}_{H_u} = 2 \cos^2 \beta, \quad \mathcal{X}_{H_d} = 2 \sin^2 \beta, \quad (96)$$

where we have defined $v_u/v = \sin \beta$, $v_d/v = \cos \beta$, with $v \simeq 246$ GeV. Substituting these expressions into Eq. (95) we obtain:

$$v_a^2 = v_\Phi^2 + v^2 (\sin 2\beta)^2, \quad (97)$$

²³This canonical form is required in order to formally integrate out the Z boson, via a gaussian integration in the path-integral, when defining the axion EFT.

²⁴Physical quantities such as axion couplings and the DW number do not depend from this normalization, as it can be readily verified by repeating all the steps above for a generic \mathcal{X}_Φ .

and given that $v_\Phi \gg v$ we have $v_a \simeq v_\Phi$. The axion coupling to SM fermions can be derived by inverting the first relation in Eq. (95) to express $a_{u,d}$ in terms of a and select the a dependent terms. This boils down to replace $a_u/v_u \rightarrow \mathcal{X}_{H_u} a/v_a$, $a_d/v_d \rightarrow \mathcal{X}_{H_d} a/v_a$ and yields

$$\mathcal{L}_{\text{DFSZ-I}} \supset -m_U \bar{u}_L u_R e^{i\mathcal{X}_{H_u} \frac{a}{v_a}} - m_D \bar{d}_L d_R e^{i\mathcal{X}_{H_d} \frac{a}{v_a}} - m_E \bar{e}_L e_R e^{i\mathcal{X}_{H_d} \frac{a}{v_a}} + \text{h.c.} . \quad (98)$$

The axion field can be now removed from the mass terms by redefining the fermion fields according to the field-dependent axial transformations:

$$u \rightarrow e^{-i\gamma_5 \mathcal{X}_{H_u} \frac{a}{2v_a}} u, \quad d \rightarrow e^{-i\gamma_5 \mathcal{X}_{H_d} \frac{a}{2v_a}} d, \quad e \rightarrow e^{-i\gamma_5 \mathcal{X}_{H_d} \frac{a}{2v_a}} e, \quad (99)$$

which, because of the QCD and EM anomalies, induce an axion coupling to both $G\tilde{G}$ and $F\tilde{F}$. Let us note in passing that since the fermion charges satisfy the relations $\mathcal{X}_{u_L} - \mathcal{X}_{u_R} = \mathcal{X}_{H_u}$, $\mathcal{X}_{d_L} - \mathcal{X}_{d_R} = \mathcal{X}_{H_d}$, $\mathcal{X}_{e_L} - \mathcal{X}_{e_R} = \mathcal{X}_{H_d}$ as dictated by PQ invariance of the Yukawa couplings, the transformations Eq. (99) are equivalent to redefine the LR chiral fields with a phase transformation proportional to their PQ charges. Specifying now Eqs. (84)–(85) to the DFSZ-I case, one obtains

$$N = n_g \left(\frac{1}{2} \mathcal{X}_{H_u} + \frac{1}{2} \mathcal{X}_{H_d} \right) = 3, \quad (100)$$

$$E = n_g \left(3 \left(\frac{2}{3} \right)^2 \mathcal{X}_{H_u} + 3 \left(-\frac{1}{3} \right)^2 \mathcal{X}_{H_d} + (-1)^2 \mathcal{X}_{H_d} \right) = 8, \quad (101)$$

where $n_g = 3$ is the number of SM fermion generations while $\mathcal{X}_{H_{u,d}}$ are given in Eq. (96). The anomalous part of the axion effective Lagrangian then reads

$$\delta \mathcal{L}_{\text{DFSZ-I}} = \frac{\alpha_s}{8\pi} \frac{a}{f_a} G\tilde{G} + \frac{\alpha}{8\pi} \left(\frac{E}{N} \right) \frac{a}{f_a} F\tilde{F}, \quad (102)$$

with $f_a = v_a/(2N) = v_a/6$ (hence the DW number is $N_{\text{DW}} = 6$) and $E/N = 8/3$. The transformations in Eq. (99), however, do not leave the fermion kinetic terms invariant, and their variation corresponds to derivative couplings of the axion to the SM fermion fields:

$$\delta(\bar{u}i\cancel{\partial}u) = \mathcal{X}_{H_u} \frac{\partial_\mu a}{2v_a} \bar{u} \gamma^\mu \gamma_5 u = \left(\frac{1}{3} \cos^2 \beta \right) \frac{\partial_\mu a}{2f_a} \bar{u} \gamma^\mu \gamma_5 u, \quad (103)$$

$$\delta(\bar{d}i\cancel{\partial}d) = \mathcal{X}_{H_d} \frac{\partial_\mu a}{2v_a} \bar{d} \gamma^\mu \gamma_5 d = \left(\frac{1}{3} \sin^2 \beta \right) \frac{\partial_\mu a}{2f_a} \bar{d} \gamma^\mu \gamma_5 d, \quad (104)$$

$$\delta(\bar{e}i\cancel{\partial}e) = \mathcal{X}_{H_d} \frac{\partial_\mu a}{2v_a} \bar{e} \gamma^\mu \gamma_5 e = \left(\frac{1}{3} \sin^2 \beta \right) \frac{\partial_\mu a}{2f_a} \bar{e} \gamma^\mu \gamma_5 e, \quad (105)$$

from which we can read out the effective axion-fermion couplings for DFSZ-I (cf. the definition of the axion effective Lagrangian Eq. (38) with an obvious extension to include the leptons):

$$c_{u_i}^0 = \frac{1}{3} \cos^2 \beta, \quad c_{d_i}^0 = \frac{1}{3} \sin^2 \beta, \quad c_{e_i}^0 = \frac{1}{3} \sin^2 \beta, \quad (106)$$

where $i = 1, 2, 3$ is a generation index. In the DFSZ-II model, the leptons couple to the complex conjugate up-type Higgs \tilde{H}_u instead than to H_d . This implies changing $\mathcal{X}_{H_d} \rightarrow -\mathcal{X}_{H_u}$ in the last (leptonic) term in equations (98), (99) and (101) which yields $E = 2$, $E/N = 2/3$ and $c_{e_i}^0 = -\frac{1}{3} \cos^2 \beta$.

For DFSZ phenomenological studies it is important to determine the allowed range for $\tan \beta = v_u/v_d$, which is set by the perturbative range of the top and bottom Yukawa couplings. A conservative limit is obtained by imposing a (tree-level) unitarity bound on Yukawa-mediated $2 \rightarrow 2$ fermion scattering amplitudes at $\sqrt{s} \gg M_{H_{u,d}}$: $|\text{Re } a_{J=0}| < 1/2$, where $a_{J=0}$ is the $J = 0$ partial wave. Ignoring running effects, which would make the bound even stronger, and taking into account group theory factors [122, 123], one

gets [124]: $y_{t,b}^{\text{DFSZ}} < \sqrt{16\pi/3}$ (the strongest bound comes from the channel $Q_L u_R(d_R) \rightarrow Q_L u_R(d_R)$, with the initial and final states prepared into $SU(3)_c$ singlets). These translate into a lower and upper bound on $\tan\beta$, that can be obtained via the relations $y_t^{\text{SM}} = \sqrt{2}m_t/v = y_t^{\text{DFSZ}} \sin\beta$, $y_b^{\text{SM}} = \sqrt{2}m_b/v = y_b^{\text{DFSZ}} \cos\beta$. Using $m_t = 173.1$ GeV, $m_b = 4.18$ GeV and $v = 246$ GeV yields the range

$$\tan\beta \in [0.25, 170] . \quad (107)$$

Note that the range in Eq. (107) holds both for DFSZ-I and DFSZ-II, since the τ Yukawa plays a sub-leading role for perturbativity.

2.8. Summary of flavour and CP conserving axion couplings

Focussing on the most relevant axion couplings from the point of view of astrophysical constraints (see Section 4) and experimental sensitivities (see Section 5), we collect here their numerical values including available higher-order corrections. Flavour and CP violating axion couplings will be discussed instead in the next two Sections.

The relation between the axion mass and the axion decay constant (see Eq. (51) for a LO expression), has been computed including QED and NNLO corrections in the chiral expansion [125] and reads

$$m_a = 5.691(51) \left(\frac{10^{12} \text{ GeV}}{f_a} \right) \mu\text{eV} . \quad (108)$$

A direct calculation of the topological susceptibility (see Eqs. (131) and (132) below) via QCD lattice techniques finds a similar central value, with an error five time larger [126].

The axion interaction Lagrangian with photons, matter fields $f = p, n, e$, pions and the nEDM operator can be written as

$$\mathcal{L}_a^{\text{int}} \supset \frac{\alpha}{8\pi} \frac{C_{a\gamma}}{f_a} a F \tilde{F} + C_{af} \frac{\partial_\mu a}{2f_a} \bar{f} \gamma^\mu \gamma_5 f + \frac{C_{a\pi}}{f_a f_\pi} \partial_\mu a [\partial\pi\pi\pi]^\mu - \frac{i}{2} \frac{C_{an\gamma}}{m_n} \frac{a}{f_a} \bar{n} \sigma_{\mu\nu} \gamma_5 n F^{\mu\nu} , \quad (109)$$

where we have schematically defined $[\partial\pi\pi\pi]^\mu = 2\partial^\mu \pi^0 \pi^+ \pi^- - \pi_0 \partial^\mu \pi^+ \pi^- - \pi_0 \pi^+ \partial^\mu \pi^-$. The LO values of the C_{ax} coefficients have been derived in Section 2.5. Taking into account Next-to-LO (NLO) chiral corrections for the axion-photon coupling and a LO non-relativistic effective Lagrangian approach for axion-nucleon couplings,²⁵ and including as well running effects, Ref. [47] finds

$$C_{a\gamma} = \frac{E}{N} - 1.92(4) , \quad (110)$$

$$C_{ap} = -0.47(3) + 0.88(3) c_u^0 - 0.39(2) c_d^0 - C_{a,\text{sea}} , \quad (111)$$

$$C_{an} = -0.02(3) + 0.88(3) c_d^0 - 0.39(2) c_u^0 - C_{a,\text{sea}} , \quad (112)$$

$$C_{a,\text{sea}} = 0.038(5) c_s^0 + 0.012(5) c_c^0 + 0.009(2) c_b^0 + 0.0035(4) c_t^0 , \quad (113)$$

$$C_{ae} = c_e^0 + \frac{3\alpha^2}{4\pi^2} \left[\frac{E}{N} \log \left(\frac{f_a}{m_e} \right) - 1.92(4) \log \left(\frac{\text{GeV}}{m_e} \right) \right] , \quad (114)$$

$$C_{a\pi} = 0.12(1) + \frac{1}{3} (c_d^0 - c_u^0) , \quad (115)$$

$$C_{an\gamma} = 0.011(5) e , \quad (116)$$

where we have added to the list of [47] also C_{ae} , $C_{a\pi}$ (at the LO in the chiral expansion) and $C_{an\gamma}$ (from the static nEDM result in Eq. (31)).

Sometimes the axion coupling to photons and matter field (first two terms in Eq. (109)) is written as

$$\mathcal{L}_a^{\text{int}} \supset \frac{1}{4} g_{a\gamma} a F \tilde{F} - i g_{af} a \bar{f} \gamma_5 f - \frac{i}{2} g_d a \bar{n} \sigma_{\mu\nu} \gamma_5 n F^{\mu\nu} , \quad (117)$$

²⁵ Axion-nucleon couplings in the framework of the NNLO chiral Lagrangian have been recently considered in [127].

where in the second term we have integrated by parts, applied the equations of motion (which is only valid for on-shell fermion states) and defined

$$g_{a\gamma} = \frac{\alpha}{2\pi} \frac{C_{a\gamma}}{f_a}, \quad g_{af} = C_{af} \frac{m_f}{f_a}, \quad g_d = \frac{C_{an\gamma}}{m_n f_a}. \quad (118)$$

The ‘model-independent’ predictions for the axion couplings (namely those exclusively due to the $aG\tilde{G}$ operator) are obtained by setting $E/N \rightarrow 0$ and $c_i^0 \rightarrow 0$ in Eqs. (110)–(116). The latter also correspond to the predictions of the simplest KSVZ model discussed in Section 2.7.1, while the two DFSZ variants of Section 2.7.2 yield

$$\text{DFSZ-I: } E/N = 8/3 \quad c_{u_i}^0 = \frac{1}{3} \cos^2 \beta, \quad c_{d_i}^0 = \frac{1}{3} \sin^2 \beta, \quad c_{e_i}^0 = \frac{1}{3} \sin^2 \beta, \quad (119)$$

$$\text{DFSZ-II: } E/N = 2/3 \quad c_{u_i}^0 = \frac{1}{3} \cos^2 \beta, \quad c_{d_i}^0 = \frac{1}{3} \sin^2 \beta, \quad c_{e_i}^0 = -\frac{1}{3} \cos^2 \beta, \quad (120)$$

with the index $i = 1, 2, 3$ denoting generations and the perturbative unitarity domain $\tan \beta \in [0.25, 170]$. In Section 6 we will explore in depth how these ‘model-dependent’ coefficients can be modified compared to the standard KSVZ/DFSZ benchmarks.

For completeness, in the next two Sections we are going to discuss two other classes of model-dependent axion couplings which can be of phenomenological interest, although they do not arise to a sizeable level in the standard KSVZ/DFSZ benchmarks. These are namely flavour violating axion couplings (Section 2.9) and CP-violating ones (Section 2.10).

2.9. Flavour violating axion couplings

Relaxing the hypothesis of the universality of the PQ current in DFSZ-like constructions leads to flavour violating axion couplings to quarks and leptons. This option will be explored in detail in Section 6.5. Here, we preliminary show how such couplings arise in a generalized DFSZ setup with non-universal PQ charges. Let us assume that quarks with the same EM charge but of different generations couple to different Higgs doublets, for definiteness H_1 or H_2 , to which we assign the same hypercharge $Y_{H_1} = Y_{H_2} = -\frac{1}{2}$ but different PQ charges $\mathcal{X}_1 \neq \mathcal{X}_2$. Let us start by considering the following Yukawa terms for the up-type quarks

$$\mathcal{L}_{12}^{Y_U} = -(Y_U)_{11} \bar{q}_{1L} u_{1R} H_1 - (Y_U)_{22} \bar{q}_{2L} u_{2R} H_2 - (Y_U)_{12} \bar{q}_{1L} u_{2R} H_1 + \dots \quad (121)$$

The quark bilinear $\bar{q}_{1L} u_{2R}$ in the last term (or alternatively a similar term in the down-quark sector) is needed to generate the CKM mixing, and for the present discussion it is irrelevant whether it couples to H_1 or H_2 . Note, also, that from PQ charge consistency $\mathcal{X}(\bar{q}_{2L} u_{1R}) = \mathcal{X}(\bar{q}_{2L} u_{2R}) - \mathcal{X}(\bar{q}_{1L} u_{2R}) + \mathcal{X}(\bar{q}_{1L} u_{1R}) = -\mathcal{X}_2$ it follows that the term $\bar{q}_{2L} u_{1R} H_2$ is also allowed. However, being its structure determined by the first three terms we do not need to consider it explicitly. Projecting out from the Higgs doublets the neutral Goldstone bosons, as was done in Eq. (93), and identifying the axion field, we obtain the analogous of Eq. (98) in the form

$$\mathcal{L}_{12}^{m_U} = -(m_u)_{11} \bar{u}_{1L} u_{1R} e^{i\mathcal{X}_1 \frac{a}{v_a}} - (m_u)_{22} \bar{u}_{2L} u_{2R} e^{i\mathcal{X}_2 \frac{a}{v_a}} - (m_u)_{12} \bar{u}_{1L} u_{2R} e^{i\mathcal{X}_1 \frac{a}{v_a}} + \dots \quad (122)$$

Because of the presence of the mixing term, in this case it is not possible to remove the axion field from the mass terms with a pure axial redefinition of the quark fields as in Eq. (99), but it is necessary to introduce also a vectorial part in the field redefinition:

$$u_1 \rightarrow e^{-i(\gamma_5 \mathcal{X}_1 + \mathcal{X}_2) \frac{a}{2v_a}} u_1, \quad u_2 \rightarrow e^{-i(\gamma_5 \mathcal{X}_2 + \mathcal{X}_1) \frac{a}{2v_a}} u_2. \quad (123)$$

By introducing a vector of the two quark flavours $u = (u_1, u_2)^T$ and the two matrices of charges $\mathcal{X}_{12} = \text{diag}(\mathcal{X}_1, \mathcal{X}_2)$ and $\mathcal{X}_{21} = \text{diag}(\mathcal{X}_2, \mathcal{X}_1)$ the variation of the fermion kinetic terms due to the redefinitions in Eq. (123) can be written as

$$\delta(\bar{u} i \not{\partial} u) = \frac{\partial_\mu a}{2v_a} \{ \bar{u} \mathcal{X}_{12} \gamma_\mu \gamma_5 u + \bar{u} \mathcal{X}_{21} \gamma_\mu u \} = \frac{\partial_\mu a}{2v_a} \{ \bar{u}_L \mathcal{X}_L \gamma_\mu u_L + \bar{u}_R \mathcal{X}_R \gamma_\mu u_R \}, \quad (124)$$

where $\mathcal{X}_R = \mathcal{X}_{21} + \mathcal{X}_{12} = (\mathcal{X}_1 + \mathcal{X}_2) \begin{pmatrix} 1 & \\ & -1 \end{pmatrix}$ and $\mathcal{X}_L = \mathcal{X}_{21} - \mathcal{X}_{12} = (\mathcal{X}_2 - \mathcal{X}_1) \begin{pmatrix} 1 & \\ & -1 \end{pmatrix}$. The matrix of charges for the RH fields is proportional to the identity, and hence rotation to the mass eigenstates has no effects (this could have been argued already from Eq. (121) since the first and third Yukawa terms imply $\mathcal{X}(u_{1R}) = \mathcal{X}(u_{2R}) = -\mathcal{X}(\bar{q}_{1L}H_1)$). However, since \mathcal{X}_L is not proportional to the identity, once the LH interaction states are rotated into the mass eigenstates $u'_L = U_L^u u_L$ flavour violating couplings, controlled by the matrix $(\mathcal{X}_2 - \mathcal{X}_1)U_L^u \begin{pmatrix} 1 & \\ & -1 \end{pmatrix} U_L^{u\dagger}$ unavoidably appear. Clearly, had we coupled the third term in Eq. (121) to H_2 rather than to H_1 , flavour violating couplings would have instead appeared in the RH sector, while by extending the scheme to three generations of up-type quarks, both the RH and LH sectors can be simultaneously affected. We will see in Section 6.5 that interesting models which necessarily involve generation dependent PQ charges are indeed characterised by flavour changing axion couplings of this type.

2.10. CP-violating axion couplings

Under some circumstances, discussed below, the axion field can develop CP-violating (scalar) couplings to matter fields, which can be parametrized via the following Lagrangian term

$$\mathcal{L}_a^{\text{CPV}} = -g_{af}^S a \bar{f} f. \quad (125)$$

In particular, CP-violating (scalar) axion couplings to nucleons $N = p, n$, mediate new forces in the form of scalar–scalar (monopole–monopole) or scalar–pseudo-scalar (monopole–dipole) interactions [128]. This terminology comes from the fact that in the non-relativistic limit the scalar coupling is spin-independent, contrary to the case of the pseudo-scalar density. Let us consider, for instance, the monopole-monopole interaction. The non-relativistic potential between two nucleons N_1 and N_2 can be calculated in the inverse Born approximation (with \vec{q} denoting the moment transferred)

$$V(r) = \int \frac{d^3q}{(2\pi)^3} \frac{g_{N_1}^S g_{N_2}^S e^{i\vec{q}\cdot\vec{r}}}{\vec{q}^2 + m_a^2} = -\frac{g_{N_1}^S g_{N_2}^S e^{-m_a r}}{4\pi r}, \quad (126)$$

which for $m_a \lesssim 1$ eV is subject to strong limits from e.g. precision tests of Newton’s inverse square law. Instead monopole-dipole interaction are at the base of new experimental setups sensitive to either $g_{aN}^S g_{an}$ or $g_{aN}^S g_{ae}$, that could eventually target the QCD axion, as discussed in Section 5.4.

CP-violating scalar axion couplings to nucleons are generated whenever the axion potential does not exactly relax the axion VEV to zero.²⁶ In the presence of extra sources of CP violation in the UV it is expected that $\theta_{\text{eff}} = \langle a \rangle / f_a \neq 0$ and one finds [128]

$$g_{aN}^S = \frac{\theta_{\text{eff}}}{f_a} \frac{m_u m_d}{m_u + m_d} \langle N | (\bar{u}u + \bar{d}d) | N \rangle \approx \theta_{\text{eff}} \left(\frac{17 \text{ MeV}}{f_a} \right), \quad (127)$$

where we used the lattice matrix element $(m_u + m_d) \langle N | (\bar{u}u + \bar{d}d) | N \rangle / 2 \approx 38$ MeV from [129]. Higher-order corrections to Eq. (127) were recently computed in Ref. [130] by using different approximation methods. Regarding instead the possible values of θ_{eff} , for instance, in the SM it is expected to be (based naive dimensional analysis [131])

$$\theta_{\text{eff}}^{\text{SM}} \sim G_F^2 f_\pi^4 J_{\text{CKM}} \approx 10^{-18}, \quad (128)$$

(note that $J_{\text{CKM}} = \text{Im } V_{ud} V_{cd}^* V_{cs} V_{us}^*$ has the same spurionic properties of θ , being a CP-violating flavour singlet) which leads, however, to axion scalar couplings that are far from being experimentally accessible. New physics above the electroweak scale might provide extra sources of CP violation and be responsible for a sizeable θ_{eff} which could bear some phenomenological consequences. Consider for definiteness the CP-violating operator (colour EDM)

$$\mathcal{O}_{\text{CPV}} = \frac{i}{2} \bar{d}_q g_s \bar{q} T^a G_{\mu\nu}^a \sigma^{\mu\nu} \gamma_5 q, \quad (129)$$

²⁶Since electrons always couple derivatively to the axion, the VEV of the latter does not generate a scalar axion coupling to electrons. Hence, only scalar axion couplings to nucleons are relevant for the QCD axion.

for any light quark flavour $q = u, d, s$, together with the QCD-dressed 1-point and 2-point axion functions, defined as

$$\chi' = i \int d^4x \langle 0 | T \frac{\alpha_s}{8\pi} G \tilde{G}(x) \mathcal{O}_{\text{CPV}}(0) | 0 \rangle, \quad (130)$$

$$\chi = i \int d^4x \langle 0 | T \frac{\alpha_s}{8\pi} G \tilde{G}(x) \frac{\alpha_s}{8\pi} G \tilde{G}(0) | 0 \rangle. \quad (131)$$

The latter is known as topological susceptibility (sometimes also denoted as K [121]) and can be also written as the second derivative of the QCD generating functional Eq. (16) (see also the QCD action density in Minkowski Eq. (1)) with respect to θ . A comparison with the effective axion Lagrangian in Eq. (36) and the replacement $\frac{\partial^2}{\partial \theta^2} \big|_{\theta=0} \rightarrow f_a^2 \frac{\delta^2}{\delta a^2} \big|_{a=0}$ highlights its relation with the axion mass:

$$\chi = f_a^2 m_a^2. \quad (132)$$

A detailed computation that exploits chiral Lagrangian techniques, chiral fits and lattice QCD results gives the value $\chi = (75.5(5) \text{ MeV})^2$ [47]. The two quantities χ' and χ enter the axion potential as

$$V(a) \approx \chi' \left(\frac{a}{f_a} \right) + \frac{1}{2} \chi \left(\frac{a}{f_a} \right)^2, \quad (133)$$

where we neglected higher orders in $a/f_a \ll 1$. Hence, the induced axion VEV is obtained by solving the tadpole equation

$$\theta_{\text{eff}} = - \frac{\chi'}{|\chi|}. \quad (134)$$

Using standard current algebra techniques one finds [132]

$$\theta_{\text{eff}} = - \frac{m_0^2}{2} \frac{\tilde{d}_q}{m_q}, \quad (135)$$

with $m_0^2 = \langle 0 | g_s \bar{q} (T^a G_{\mu\nu}^a \sigma^{\mu\nu}) q | 0 \rangle / \langle 0 | \bar{q} q | 0 \rangle \approx 0.8 \text{ GeV}^2$. This shows that it is possible to generate values of θ_{eff} which saturate the nEDM bound $|\theta_{\text{eff}}| \lesssim 10^{-10}$, e.g. for $\tilde{d}_q \sim 1/(10^{12} \text{ GeV})$. In terms of a SM gauge invariant effective operator above the electroweak scale, the scale of new physics is given by $v/\Lambda_{\text{NP}}^2 = \tilde{d}_q$, which yields $\Lambda_{\text{NP}} \sim 10^4 \text{ TeV}$.

2.11. The dirty side of the axion

One of the most delicate aspects of the PQ mechanism is the fact that it relies on a global $U(1)_{\text{PQ}}$ symmetry, which has to be preserved to a great degree of accuracy in order for the axion VEV to be relaxed to zero, a precision compatible with the non-observation of the neutron EDM. This issue is known as the *PQ quality problem* [133–138], and it is reviewed below.

Global symmetries are generally considered not to be fundamental features in a QFT, and this is particularly well justified in the case of anomalous symmetries which do not survive at the quantum level. However, in some cases the field content of the theory together with the requirement of Lorentz and local gauge invariance restricts the allowed renormalizable operators to a set which remains invariant under some global redefinition of the fields. These symmetries are thus *accidental* in the sense that they result from other first principle requirements. However, given that they are not imposed on the theory, in general are not respected by higher-order non-renormalizable operators. A well known example of an accidental global symmetry is baryon number (B) in the SM: operators carrying nonzero baryon number must have at least three quark fields to be colour singlets, and then at least four fermion fields to form a Lorentz scalar. Thus their minimal dimension is $d = 6$, whence the renormalizable Lagrangian conserves B . The high level of accuracy of baryon number conservation required to comply with proton decay bounds implies that B -violating effective operators must be suppressed by a rather large scale $\Lambda_B \gtrsim 10^{15} \text{ GeV}$ which, however, can be considered natural when understood in terms of some GUT dynamics.

It would certainly be desirable to generate also the PQ symmetry as an accidental symmetry. The benchmark KSVZ and DFSZ constructions discussed in the previous sections do not address this issue and, in particular, there is no first principle reason that impedes writing in $\mathcal{L}_{\text{KSVZ}}$ in Eq. (76) a quark mass term $\mu_Q \bar{Q}_L Q_R$ or in $\mathcal{L}_{\text{DFSZ}}$ in Eq. (89) a direct coupling $\mu_H^2 H_u H_d$, both of which would destroy PQ invariance of the renormalizable Lagrangians. The problem becomes even more serious once, after assuming that an accidental PQ symmetry can be enforced in some way, one proceeds to estimate at which operator dimension the symmetry can be first broken in order not to spoil the solution to the strong CP problem for a given value of the suppression scale. Let us consider the following set of effective operators of dimension $d = 2m + n$ that violate the PQ symmetry by n units, and let us assume for definiteness that they are suppressed by the largest scale that can consistently appear in a QFT, the Planck scale m_{Pl} :

$$\begin{aligned} -V_{\text{PQ-break}}^n &= \frac{\lambda_n |\Phi|^{2m} (e^{-i\delta_n} \Phi^n + e^{i\delta_n} \Phi^{\dagger n})}{m_{\text{Pl}}^{d-4}} \supset \frac{\lambda_n f_a^4}{2} \left(\frac{f_a}{\sqrt{2} m_{\text{Pl}}} \right)^{d-4} \cos \left(\frac{na}{f_a} - \delta_n \right) \\ &\approx m_*^2 f_a^2 \left(\frac{\theta^2}{2} - \frac{\theta}{n} \tan \delta_n \right), \end{aligned} \quad (136)$$

with λ_n real and δ_n the phase of the coupling,²⁷ and we have taken for simplicity a colour anomaly factor $2N = 1$ so that $\Phi = \frac{1}{\sqrt{2}}(f_a + \varrho_a) e^{ia/f_a}$. In the last relation we have expanded for $\theta = \frac{a}{f_a} \ll 1$ neglecting an irrelevant constant, and we have defined $m_*^2 = \frac{\lambda_n f_a^2}{2} (f_a/(\sqrt{2} m_{\text{Pl}}))^{d-4} \cos \delta_n$. The effect of the explicit breaking $V_{\text{PQ-break}}^n$ is to move the minimum of the axion potential away from the CP conserving minimum $\langle \theta \rangle = 0$ of the QCD induced potential $V(\theta) = \frac{1}{2} m_a^2 f_a^2 \theta^2$ (see Eq. (50)) and shift it to

$$\langle \theta \rangle = \frac{m_*^2 \tan \delta_n}{n(m_a^2 + m_*^2)}. \quad (137)$$

Taking for example operators that violate PQ by one unit ($n = 1$) and assuming $\lambda_1 \sim \tan \delta_1 \sim 1$, implies that to satisfy $m_*^2/m_a^2 \lesssim 10^{-10}$ the dimension of these operators should be uncomfortably large: $d \geq 8, 10, 21$ respectively for $f_a \sim 10^8, 10^{10}, 10^{15}$ GeV.

Of course, in QFT it is always possible to assume that there are no heavy states mediating PQ-violating interactions, so that operators of the type Eq. (136) do not arise. However, there is a general consensus that quantum gravity effects violate all global symmetries at some level. The standard argument is that particles carrying global charges can be swallowed by black holes, which subsequently may evaporate by emitting Hawking radiation [139].²⁸ One can then speculate that non-perturbative quantum gravity formation of “virtual” black holes would eventually result in an effective theory containing all types of operators compatible with the local gauge symmetries of the theory, but violating global charge conservation, with suppression factors provided by appropriate powers of the cutoff scale m_{Pl} . This latter feature is often justified from the requirement that quantum gravity effects should disappear when sending $m_{\text{Pl}} \rightarrow \infty$. However, while this is indeed reasonable for perturbative quantum gravity corrections, global charge violation is intrinsically a non-perturbative phenomenon, and the assumption that the corresponding effects could be described only in terms of operators suppressed by powers of m_{Pl} is at least questionable. After all, non-perturbative QCD effects in the axion potential are approximately described by a cosine term $V(a) \approx -\Lambda_{\text{QCD}}^4 \cos(a/f_a)$ with a positive power of Λ_{QCD} , rather than by effective operators suppressed by inverse powers of Λ_{QCD} . Similarly, one cannot exclude that gravity could give rise to operators like $m_{\text{Pl}}^3 (\Phi + \Phi^\dagger)$ or to other operators not containing m_{Pl} in the denominator [140–142].

In the absence of reliable ways to assess the validity of Eq. (136) for describing quantum gravity effects, other approaches have been pursued. Most noticeably, in scenarios in which Einstein gravity is minimally

²⁷Precisely because these operators are not PQ invariant, the PQ transformation required to remove $\bar{\theta}$ from the QCD Lagrangian will in any case give a contribution $n\bar{\theta}$ to δ_n .

²⁸Local charges, such as the electric charge, cannot disappear because Gauss law ensures that the electric field flux remains preserved when the charged particle falls into the black hole. Hence, charged black holes cannot evaporate entirely, but instead get stabilised as extremal black holes.

coupled to the axion field, non-conservation of global charges arises from non-perturbative effects related to wormholes that can absorb the global charge and consequently break the symmetry. These effects are to some extent computable and have been studied for example in Refs. [140–142] and, more recently, also in Ref. [143]. These studies indicate that in this setup global symmetries remain intact at any finite order in a perturbative expansion in $1/m_{\text{Pl}}$ so that power-suppressed operators are not generated [143]. However, non-perturbative wormhole effects do generate additional cosine terms $\sim \cos(a/f - \delta_1)$ similar to the last term in Eq. (136). However, they come with an exponential suppression factor $e^{-S_{\text{wh}}}$ of the wormhole action. Then, if S_{wh} is sufficiently large, as it appears possible in many cases [142, 143], the axion solution to the strong CP problem would not be endangered.

The conclusion of this discussion is that, in a complete model, it would be highly desirable that the PQ symmetry could arise as an accidental symmetry as a consequence of fundamental principles, like for example gauge and Lorentz invariance. These principles should not only guarantee that the symmetry remains perturbatively unbroken at the renormalizable level, but they should also impede writing down PQ violating effective operators of dimension $d \leq 10$. This, unless some other mechanism can guarantee an appropriate strong suppression of the coefficients of any such higher dimensional operator. In this respect, in order to guarantee the quality of the PQ symmetry different mechanisms have been put forth. They can be conceptually divided in three different classes:

- *Low f_a .* For $f_a \lesssim 10^3$ GeV, only $d > 5$ is required in order not to generate a too large $\langle \theta \rangle$ from Eq. (137). From this point of view the original WW axion model would have been perfectly natural, since in absence of SM-singlet fields the first gauge invariant PQ breaking operator that one can write in the scalar potential is $(H_u H_d)^3$, which is $d = 6$. Over the years, the increasing lower bounds on f_a let the PQ quality problem to emerge. In ‘super-heavy’ axion models, reviewed in Section 6.7, one can evade the astrophysical constraints on $f_a \gtrsim 10^8$ GeV, e.g. by modifying the QCD relation between m_a and f_a . These models feature an axion decay constant of the order of $10^{4\div 5}$ GeV, thus improving a lot on the PQ quality problem.
- *Gauge protection.* New local symmetries can lead to an accidental PQ symmetry protected from higher-order PQ breaking operators, up to some fixed order. Various mechanisms have been proposed, based on discrete gauge symmetries [144–148], Abelian [135, 137, 149–151] and non-Abelian [152, 153] gauge symmetries, composite dynamics [154–158] as well as extra-dimensional setups [159, 160].
- *Small coupling.* There is the possibility that the overall coupling λ_n in Eq. (136) is extremely tiny, even though effective operators are generated at relatively low-dimension [161]. Another possibility that was already mentioned above, is that PQ breaking terms generated by quantum gravity come with a suppression factor $e^{-S_{\text{wh}}}$ which is exponentially small for a sizeable wormhole action.

A more detailed account of all these mechanisms will be given in Section 7.6. All in all, we believe that theoretical efforts to search for a compelling mechanism to generate accidentally a PQ symmetry of the required high quality keep being of primary importance. Meanwhile, this ‘incompleteness’ of a theory, that is otherwise quite elegant and particularly rich of phenomenological implications, should not discourage in any way experimental axion searches. Although theoretical UV completions of axion models and PQ protection mechanisms, for their very nature, tend to remain confined at high energy, thus challenging experimental tests, with the large number of ongoing and planned axion search experiments we are now entering a data driven era. If the axion will be discovered, probing its fine properties with good accuracy could hopefully provide the clues needed to unveil the fundamental origin of the PQ symmetry.

3. Axion cosmology

The main goal of this Section is to review the mechanisms through which axions contribute to the present DM energy density. In Section 3.1 we briefly recall some basic equations for cosmology and for early Universe thermodynamics, and we establish the notations. The temperature dependence of the axion potential and axion mass is reviewed in Section 3.2. In Section 3.3 we describe the mechanism of cold axions production

from the misalignment mechanism. The contribution to the axion relic density from the decay of topological defects is reviewed in Section 3.4. Section 3.5 addresses the issue of isocurvature fluctuations in the axion field and of the related bounds that can be derived on the scale of inflation. Section 3.6 collects some bounds on the axion mass that can be obtained (mainly) from cosmological considerations. In Section 3.7, we consider the important problem of identifying for which mass range the axion can account for the totality of the DM. In Section 3.8 we address some issues related with the existence of a thermal population of relativistic axions. Finally, the role of axion-related substructures, in the form of axion miniclusters and axion stars, is reviewed in Section 3.9.

3.1. Basics of cosmology and thermodynamics in the early Universe

Observations at scales larger than 100 Mpc support the evidence that the Universe is spatially homogeneous and isotropic. Our starting point is the description of such a Universe in terms of Einstein equations

$$\mathcal{G}^{\mu\nu} = 8\pi G_N \mathcal{T}^{\mu\nu}, \quad (138)$$

where the Einstein tensor $\mathcal{G}^{\mu\nu}$ describes the geometry of the space-time and is defined in terms of (derivatives) of the metric tensor $g_{\mu\nu}$ through the affine connection and its derivatives. The stress-energy tensor $\mathcal{T}^{\mu\nu}$ describes the energy content of the Universe, and G_N is Newton constant. In the following we rewrite it as $G_N = 1/m_{\text{Pl}}^2$ that defines the Planck mass with a value $m_{\text{Pl}} = 1.221 \times 10^{19}$ GeV. The indices μ, ν run over the four space-time dimensions (t, x, y, z) where t is *cosmic* time (i.e. the time measured by a physical clock at rest in the comoving frame) which, for any given value, slices space-time into a three-dimensional homogeneous and isotropic space manifold \mathcal{M}_3 with a constant curvature that can be positive, negative or zero, corresponding respectively to an open, closed or flat Universe. Observations and theoretical considerations support the last possibility (flat Universe) for which the line element is

$$ds^2 \equiv g^{\mu\nu} dx_\mu dx_\nu = dt^2 - R^2(t) (dx^2 + dy^2 + dz^2), \quad (139)$$

where $R = R(t)$ is the cosmic scale factor. Eq. (139) defines the Friedmann-Lemaître-Robertson-Walker (FLRW) metric. Consistency with the symmetries of the metric (homogeneity and isotropy) requires $\mathcal{T}_{\mu\nu}$ to be diagonal and with equal spatial components. A simple realisation is a perfect fluid at rest in the comoving frame with time dependent energy density $\rho = \rho(t)$ and pressure $P = P(t)$ for which the stress-energy tensor is $\mathcal{T}_\nu^\mu = \text{diag}(\rho, -P, -P, -P)$. The stress energy in the Universe is conveniently described by the simple equation of state $P = w\rho$ so that a FLRW Universe remains completely characterised by the total energy density and by the fractional size and w -values of its components.

From the FLRW metric Eq. (139) the affine connection is computed, then the Einstein tensor, and inserting it into Einstein's field equations (138) with the stress-energy tensor for the perfect fluid on the right-hand-side, yields

$$H^2 \equiv \left(\frac{\dot{R}}{R} \right)^2 = \frac{8\pi}{3m_{\text{Pl}}^2} \rho, \quad (140)$$

$$\dot{H} + H^2 = \frac{\ddot{R}}{R} = -\frac{4\pi}{3m_{\text{Pl}}^2} (\rho + 3P), \quad (141)$$

where the first equation is obtained from the 0-0 component and the second from the spatial j - j component after making use of Eq. (140) while, due to the symmetries of the system, all the other components vanish. $H \equiv \dot{R}/R$ with the dot meaning derivation with respect to cosmic time, expresses the rate of the change in the scale factor, and is called the Hubble rate. Combining the two Friedmann equations leads to the conservation law in an expanding Universe:

$$\dot{\rho} + 3H(P + \rho) = 0, \quad \text{or equivalently} \quad \frac{\partial}{\partial t}(\rho R^3) = -P \frac{\partial}{\partial t}(R^3). \quad (142)$$

The second form, whose physical meaning is that the change in energy in a comoving volume is equal to minus the pressure times the change in volume, is the first law of thermodynamics. This form is particularly

useful for deducing the scaling of the energy density in matter and radiation with the expansion. Matter is pressureless ($w = 0$) and immediately we obtain $\rho_m \propto R^{-3}$. For radiation $P_{\text{rad}} = \rho_{\text{rad}}/3$ ($w = -1/3$) and Eq. (142) can be recast as $\partial(\rho_{\text{rad}} R^4)/\partial t = 0$. Hence $\rho_{\text{rad}} \propto R^{-4}$ where the additional factor of R^{-1} accounts for the redshift of radiation wavelength. Finally, from Eq. (141) we see that an accelerated expansion ($\ddot{R}/R > 0$) requires $\rho + 3P < 0$ that is, given that the energy density is always positive, acceleration requires a negative pressure $P < -\rho/3$. The simplest possibility is $P_\Lambda = -\rho_\Lambda$ ($w = -1$) in which case from the first relation in Eq. (142) we immediately obtain $\rho_\Lambda = \text{const.}$ which corresponds to a Universe dominated by vacuum energy.

The FLRW metric Eq. (139) together with the Friedmann equation (140) and Eq. (142) provides the framework in which the so-called standard cosmological, or Λ CDM, model is defined. According to this model, the present Universe is dominantly filled with a mysterious vacuum energy component ρ_Λ which accounts for about 2/3 of the total energy density. The remaining 1/3 corresponds to a matter component, which is again dominated by an unknown type of DM. Known particle species as baryons, electrons and (depending on their masses) neutrinos, contribute a subleading amount $\rho_b \sim 0.2 \rho_{\text{DM}}$ while the photon contribution is even smaller $\rho_{\text{rad}} \ll \rho_\Lambda, \rho_{\text{DM}}, \rho_b$. However, in the early Universe, at temperatures above ~ 1 eV, the Universe was dominated by radiation, $\rho \simeq \rho_{\text{rad}}$. The regime of radiation domination is the most relevant one for the topics that will be developed in the forthcoming Sections.

Let us now review some basic notions of thermodynamics in an expanding Universe. For particles in kinetic equilibrium with a thermal bath at temperature T , the phase space occupancy is given by the distributions $f(E) = [\exp((E - \mu)/T) \pm 1]^{-1}$ with $+1$ for fermions and -1 for bosons, while μ is the chemical potential of the particle species. If a certain number of species $p = 1, 2, 3, \dots$ are in *chemical equilibrium*, then $\sum_p \mu_p = 0$. In the relativistic limit ($T \gg m$) the contribution to the energy density of the thermal bath of a particle p with g_p internal degrees of freedom is

$$\rho_p = \frac{\pi^2}{30} \eta_p g_p T_p^4, \quad (143)$$

where the statistical factor $\eta_p = 1$ (7/8) for bosons (fermions), and T_p is the temperature that characterises the p -particle distribution. If a species is kinetically decoupled from the thermal bath, then T_p might differ from T .²⁹ In the early Universe, a very important fiducial quantity is the total entropy in a comoving volume $S = R^3(\rho + P)/T$, and this is because entropy it is conserved, or approximately conserved, in most phases of the cosmological evolution.³⁰ For relativistic species $P_p = \rho_p/3$ so that the contribution to the entropy density $s = S/R^3$ of a relativistic particle is

$$s_p = \frac{2\pi^2}{45} \eta_p g_p T_p^3. \quad (144)$$

It is customary to write the energy and entropy densities of relativistic species in a compact form as

$$\rho_{\text{rad}} = \frac{\pi^2}{30} g_*(T) T^4, \quad s_{\text{rad}} = \frac{2\pi^2}{45} g_S(T) T^3, \quad (145)$$

where the effective number of energy (g_*) and entropy (g_S) relativistic degrees of freedom are defined as

$$g_*(T) = \sum_p \eta_p g_p \left(\frac{T_p}{T} \right)^4, \quad g_S(T) = \sum_p \eta_p g_p \left(\frac{T_p}{T} \right)^3. \quad (146)$$

These expressions account for the possibility that for some species $T_p \neq T$, in which case $g_S \neq g_*$, while they are otherwise equal. Since we will mainly deal with the Universe history during the radiation dominated era

²⁹In the SM this occurs only for the neutrinos, and below $T \sim 1$ MeV.

³⁰This expression for S holds whenever all the particle chemical potentials are negligible $|\mu| \ll T$, which is generally true to an excellent approximation.

($\rho \simeq \rho_{\text{rad}}$) in the following we will drop the subscript $_{\text{rad}}$ and simply use ρ and s . When g_S remains constant during the Universe evolution, entropy conservation $dS \sim d(T^3 R^3) = 0$ implies $T \propto 1/R \propto t^{-1/2}$. Finally, from the Friedmann equation (140) and from the expression for the total energy density in the radiation dominated era Eq. (145), one obtains the following expression for the Hubble parameter:

$$H(T) = \left(\frac{4\pi^3 g_*(T)}{45} \right)^{1/2} \frac{T^2}{m_{\text{Pl}}} \simeq 1.66 g_*^{1/2} \frac{T^2}{m_{\text{Pl}}}. \quad (147)$$

In the early Universe, for $T > m_t$ all the SM degrees of freedom are in the relativistic regime, and $g_* = 106.75$. Other relevant values are $g_*(m_b > T > m_c) = 75.75$, $g_*(T > T_C) = 61.75$ (T_C is the QCD critical temperature), $g_*(T > m_\pi) = 17.25$, $g_*(T > m_e) = 10.75$. At temperatures below the electron mass g_* and g_S differ, because neutrinos are kinetically decoupled from the thermal bath and are not reheated by e^+e^- annihilation. The neutrino temperature is in fact lower by a factor $T_\nu/T_\gamma = (4/11)^{1/3}$ so that from Eq. (146) we obtain $g_*(T < m_e) \simeq 3.36$ and $g_S(T < m_e) \simeq 3.91$.

3.2. The axion potential and the axion mass at finite temperature

The dependence of the axion potential and mass on the temperature of the early Universe thermal bath is very important because it concurs to determine the present relic abundance of the axions generated through the misalignment mechanism. Although this is not the only mechanism of production of cold relic axions, it is the most model independent and possibly a quite relevant one. However, deriving a reliable expression for $V(a, T)$ is not an easy task. The chiral Lagrangian approach that in Section 2.5 proved to be a powerful tool to determine axion properties at zero temperature cannot be used, because convergence of the perturbative expansion deteriorates as the temperature approaches the critical temperature $T_C \simeq 160$ MeV where QCD starts deconfining, and for $T \simeq T_C$ the chiral approach is clearly inadequate to describe QCD. However, it is expected that at larger temperatures $T \gg T_C$ QCD becomes perturbative, in which case other computational approaches, as for example those based on the so-called dilute instanton gas approximation (DIGA) [162] can represent a sensible approach. The result of computing the axion potential around the background of a dilute instanton gas [56] gives a potential of the form

$$V(a, T)|_{T > T_C} = \chi(T) \left[1 - \cos\left(\frac{a}{f_a}\right) \right]. \quad (148)$$

The finite temperature QCD topological susceptibility $\chi(T)$ is related to the temperature dependent axion mass as

$$\chi(T) = f_a^2 m_a^2(T). \quad (149)$$

The DIGA predicts a power-law dependence of the topological susceptibility on temperature with a rather large exponent $\chi(T) \propto \chi(0) T^{-8}$. However, the reliability of the DIGA estimate has been questioned because $\chi(T)$ exhibits an exponential dependence on quantum corrections that are difficult to estimate perturbatively.³¹ To tackle this problem different techniques have been used, as for example a semi-analytical approach based on the interacting instanton liquid model [165, 166] or non-perturbative QCD lattice methods. In particular several groups have carried out dedicated QCD simulations on the lattice in ranges of temperature relevant for the axion mass [126, 164, 167–169]. Above some threshold temperature of the order of several 100 MeV, a power-law dependence close to the DIGA prediction is found, however, sizeable deviations in general appear at lower temperatures. For definiteness we will assume in the following that well above T_C the temperature dependence of the axion mass can be parametrised as

$$m_a(T) \simeq \beta m_a \left(\frac{T_C}{T} \right)^\gamma, \quad (150)$$

³¹The range of validity of the DIGA and the corresponding theoretical uncertainty on $\chi(T)$ and on the axion relic abundance was given in Ref. [163]. However, some lattice simulations (see e.g. [164]) indicate that for temperatures in the range $[T_C, 4T_C]$ $\chi(T)$ differs strongly from the DIGA both in the size and in the temperature dependence. Further lattice studies are needed in order to settle this issue.

where m_a is the zero-temperature axion mass, the exponent has a value $\gamma \approx 4$, $T_C \approx 160$ MeV (see e.g. [170]) while the parameter β , that depends on the number of quark flavours active at the temperature T and on other details of QCD physics, is found in the DIGA to be of the order of a few $\times 10^{-2}$ [56]. Expanding Eq. (148) around $a/f_a = 0$ gives

$$V(a, T)|_{T > T_C} \approx \frac{1}{2} m_a^2(T) a^2 \left[1 + b_2(T) \frac{a^2}{f_a^2} + \dots \right], \quad (151)$$

where the coefficient of the quadratic term in the expansion is identified with the square of the axion mass, while terms higher than quadratic, that correspond to higher momenta of the topological charge distribution $(\alpha_s/8\pi)G\tilde{G}$, describe self-interactions of the axion field. In particular, it is found in lattice simulations that the fourth order coefficient has a value $b_2 \approx -\frac{1}{12}$, as it would be expected from the cosine potential (that is from the DIGA). Being this coefficient negative, the interaction between axions is attractive.

3.3. Axion misalignment mechanism

The effective periodic potential $V(a, T)$ in Eq. (148) is responsible for the generation of a cosmological population of cold axions, whose abundance was first computed in Refs. [171–173]. In the so-called *misalignment mechanism*, the present energy density stored in the zero modes³² of the axion field can be obtained by solving the equation of motion in an expanding Universe

$$\ddot{a} + 3H\dot{a} - \frac{1}{R^2(t)} \nabla^2 a + V'(a, T) = 0, \quad (152)$$

where the Hubble rate H has been defined in Eq. (140), ∇^2 is the spatial Laplacian operator and V' is the first derivative of the potential with respect to the axion field a . Although a proper treatment would consist in solving Eq. (152) numerically for a given effective potential, for illustrative purposes and to better understand the physics involved let us consider the expansion given in Eq. (151) truncated to the quadratic term. In terms of the axion angle $\theta(x) = a(x)/f_a$ Eq. (152) then reads

$$\ddot{\theta} + 3H\dot{\theta} - \frac{1}{R^2(t)} \nabla^2 \theta + m_a^2(t) \theta = 0, \quad (153)$$

where $m_a(t) \equiv m_a(T(t))$. In this approximation, the Fourier transform of the axion field follows a similar expression as in Eq. (152), with the replacement $\nabla^2 \rightarrow -k^2$ in terms of the mode $k^2 \equiv \mathbf{k} \cdot \mathbf{k}$ for each field decomposition. Hubble expansion implies that the wavelength of each mode k gets stretched as $\lambda(t) = \frac{2\pi}{k} R(t)$. There are two qualitatively different regimes in the evolution of a mode, depending on whether at a given time its wavelength is larger than the horizon $\lambda(t) > t$, or is inside the horizon $\lambda(t) < t$. Recalling that $t = 1/(2H)$ super-horizon modes are then defined by the condition $k \lesssim R(t)H(t)$, while for $k \gtrsim R(t)H(t)$ the mode is inside the horizon. For super-horizon modes the contribution from the spatial gradient in Eq. (153) can be neglected. If the mass term is also negligible, the solution for the mode goes to a constant as $t^{-1/2}$ (see Eq. (155) below). For modes well inside the horizon, and for an adiabatic expansion, the solution to Eq. (153) conserves the number of axions in each mode. The number density of these higher frequency modes is suppressed with respect to the contribution from super-horizon modes so we neglect it. Additional details on higher modes can be found in Refs. [174–180].

When analysing Eq. (153), we see that the Hubble drag effectively damps the evolution of the axion field as long as the Hubble rate is significantly larger than the mass term. As the Universe cools and the expansion rate slows down, the mass term eventually begins to contribute to the evolution of the axion field once the condition

$$m_a(t_{\text{osc}}) \approx 3H(t_{\text{osc}}), \quad (154)$$

³²The axion field can be expanded in terms of a linear superposition of eigenmodes with definite co-moving wavevector \mathbf{k} $a(\mathbf{x}, t) = \int d^3k a(\mathbf{k}, t) e^{i\mathbf{k} \cdot \mathbf{x}}$, and the axion zero mode refers to the component $a(\mathbf{k} = 0, t)$.

has been fulfilled.³³ Eq. (154) defines implicitly the time t_{osc} at which the axion mass becomes important, and from this moment on, the axion field begins to oscillate in the quadratic potential with oscillations that are damped by the expansion rate.³⁴

For super-horizon modes $k \lesssim RH$ ($\nabla^2 \theta \simeq 0$) and as long as $t \ll t_{\text{osc}}$ ($m_a(t) \simeq 0$), Eq. (153) reduces to $\ddot{\theta} + (3/2t)\dot{\theta} = 0$. Defining the initial conditions at the PQ symmetry breaking time as $\theta(t_{\text{PQ}}) \equiv \theta_{\text{PQ}}$ and $\dot{\theta}(t_{\text{PQ}}) \equiv \dot{\theta}_{\text{PQ}}$ ³⁵ the solution to Eq. (153) reads

$$\theta(t) = \theta_{\text{PQ}} + \frac{\dot{\theta}_{\text{PQ}}}{H_{\text{PQ}}} \left(1 - \frac{R_{\text{PQ}}}{R(t)} \right), \quad (155)$$

$$\dot{\theta}(t) = \dot{\theta}_{\text{PQ}} \left(\frac{R_{\text{PQ}}}{R(t)} \right)^3, \quad (156)$$

where $H_{\text{PQ}} = H(t_{\text{PQ}})$ and $R_{\text{PQ}} = R(t_{\text{PQ}})$. At the time when the axion mass becomes relevant, defined by Eq. (154) as t_{osc} , we have

$$\frac{R_{\text{PQ}}}{R(t_{\text{osc}})} = \frac{T_{\text{osc}}}{T_{\text{PQ}}} \approx \frac{T_{\text{osc}}}{f_a} \lesssim 10^{-8}, \quad (157)$$

where we have used $T_{\text{osc}} \equiv T(t_{\text{osc}}) \approx 1 \text{ GeV}$ and $T_{\text{PQ}} \equiv T(t_{\text{PQ}}) \simeq f_a \gtrsim 10^8 \text{ GeV}$. The ratio of the scale factors in parenthesis in Eq. (155) is thus a transient that rapidly decays after the PQ phase transition. We define the initial conditions at the onset of oscillations $\theta_i \equiv \theta(t_{\text{osc}})$ and $\dot{\theta}_i \equiv \dot{\theta}(t_{\text{osc}})$ as

$$\theta_i = \theta_{\text{PQ}} + \frac{\dot{\theta}_{\text{PQ}}}{H_{\text{PQ}}}, \quad (158)$$

$$\dot{\theta}_i = \dot{\theta}_{\text{PQ}} \left(\frac{H(t_{\text{osc}})}{H_{\text{PQ}}} \right)^{3/2}, \quad (159)$$

where in the second equation we have used $R \propto 1/T$ and $H \propto T^2/m_{\text{Pl}}$. θ_i in Eq. (158) is known in the literature as the *initial misalignment angle*. The effects of the initial velocity $\dot{\theta}_i$ would be important if at t_{osc} the kinetic energy stored in the axion field $\dot{a}^2/2$ exceeds the potential barrier $2m_a^2 f_a^2$, see Eq. (148), that is if $\dot{\theta}_i > 2m_a(t_{\text{osc}})$. Using Eq. (154) we can rewrite Eq. (159) as

$$\dot{\theta}_i = m_a(t_{\text{osc}}) \frac{\dot{\theta}_{\text{PQ}}}{H_{\text{PQ}}} \frac{T_{\text{osc}}}{3T_{\text{PQ}}}, \quad (160)$$

so that we obtain the condition

$$\frac{\dot{\theta}_{\text{PQ}}}{H_{\text{PQ}}} > \frac{6}{T_{\text{osc}}} \frac{T_{\text{PQ}}}{3} \gtrsim 10^8. \quad (161)$$

where for the numerical value we have used Eq. (157). We can conclude that unless the axion velocity at the PQ breaking scale is at least eight orders of magnitude larger than the expansion rate of the Universe, the results for axion DM are indistinguishable from what is obtained by setting, as it is usually done, $\dot{\theta}_i = 0$. Some models that assume that at t_{osc} the axion kinetic energy dominates the potential energy are reviewed in Section 6.6.3.

Regarding the misalignment angle θ_i , the possible initial values depend on the cosmological history of the axion field. To better see this, let us consider the following two conditions:

³³The factor three appearing in Eq. (154) serves as a crude approximation to estimate the value of t_{osc} . In general, this factor should be matched to a numerical solution.

³⁴The intuitive meaning of the condition Eq. (154) is the following: in radiation domination $H(t) = 1/(2t)$, hence the condition can be rewritten as $m_a(t_{\text{osc}})t_{\text{osc}} \approx 1$. In this regime, the angular frequency of the oscillations is $\omega \approx m_a(t)$. Therefore, requiring that the condition is satisfied, amounts to require that the Universe is sufficiently old to host a sizeable fraction of one oscillation period.

³⁵As we will see below, the PQ symmetry can get broken before or after inflation. Only in the latter case the label PQ can consistently refer to quantities like temperature, Hubble rate, etc. at the PQ breaking time. We will leave understood that in the case the symmetry is broken during inflation, the same label PQ rather refers to a suitable early time after the end of inflation.

- a) The PQ symmetry is spontaneously broken during inflation;
- b) The PQ symmetry is never restored after its spontaneous breaking occurs.

Condition **a)** is realised whenever the axion energy scale is larger than the Hubble rate at the end of inflation, $f_a > H_I$, while condition **b)** is realised whenever the PQ scale is larger than the maximum temperature reached in the post-inflationary Universe. Broadly speaking, one of these two possible scenarios occurs:

- *Pre-inflationary* scenario. If both **a)** and **b)** are satisfied, inflation selects one patch of the Universe within which the spontaneous breaking of the PQ symmetry leads to a homogeneous value of the initial misalignment angle θ_i . In this scenario, topological defects are inflated away and do not contribute to the axion energy density. However, other bounds that come from isocurvature modes [181–183] severely constrain this scenario, which require a relatively low-energy scale of inflation to be viable.
- *Post-inflationary* scenario. If at least one of the conditions **a)** or **b)** is violated, the PQ symmetry breaks with θ_i taking different values in patches that are initially out of causal contact, but that today populate the volume enclosed by our Hubble horizon. In this scenario, isocurvature fluctuations in the PQ field randomise θ , with no preferred value in the power spectrum. Moreover, modes with $k \gtrsim RH$ decay because of the gradient term in the equation of motion. The proper treatment in this scenario is to solve numerically the equation of motion of the PQ field in an expanding Universe, in order to capture all features coming from the misalignment mechanism, including the contribution from topological defects, see Section 3.4. Here, we discuss how to approximate the computation of the relic density of cold axions, neglecting for the moment the important contribution from axionic strings and domain walls. In this scenario, the initial misalignment angle θ_i within a Hubble patch takes all possible values on the unit circle. The strategy to compute the present abundance relies on computing Eq. (153) many times, each time drawing the initial value θ_i from a uniform distribution over the unit circle. For a quadratic potential, this is the same as assuming for the initial condition the value

$$\theta_i \equiv \sqrt{\langle \theta_i^2 \rangle} = \frac{\pi}{\sqrt{3}} \simeq 1.81, \quad (162)$$

where the angle brackets represent the value of the initial condition averaged over $[-\pi, \pi]$. For the periodic potential that defines the QCD axion this result is modified due to the presence of non-harmonic terms [179, 184–188] which can be parametrised in terms of a function $F(\theta_i)$ [185] that accounts for the anharmonic corrections in the axion potential, so that

$$\langle \theta_i^2 \rangle = \frac{1}{2\pi} \int_{-\pi}^{\pi} d\theta_i F(\theta_i) \theta_i^2, \quad (163)$$

where $F(\theta_i) \rightarrow 1$ for small θ_i and increases monotonically with θ_i . Including anharmonicities, numerically one obtains $\theta_i \approx 2.15$ [47], which is slightly larger than the value in Eq. (162). Thus, in this scenario the initial condition is fixed by the averaging of θ_i over the Hubble patch, which leaves the zero temperature value of the axion mass as the sole unknown for estimating the contribution to axion cold DM (CDM) from the misalignment mechanism. (It should be kept in mind, however, that in this case topological defects form after inflation and remain within the horizon, contributing to the axion energy density, and that this contribution still has to be assessed with sufficient confidence and precision, see the discussion in Section 3.4 below.)

The evolution of the axion field can be described in terms of its effective equation of state w_a given by

$$w_a \equiv \left\langle \frac{\frac{1}{2}\dot{a}^2 - V(a, T)}{\frac{1}{2}\dot{a}^2 + V(a, T)} \right\rangle, \quad (164)$$

where the angle brackets stand for a temporal average over times larger than the oscillation period. The dependence of the axion energy density on the scale factor ranges from a dark energy-like solution, $w_a = -1$,

valid at $t \lesssim t_{\text{osc}}$ (corresponding to the axion field frozen) to a CDM-like solution, $w_a = 0$, for $t \gtrsim t_{\text{osc}}$ when, due to the oscillating behaviour, the average potential energy equals the average kinetic energy. The number of axions in a comoving volume is then frozen from about T_{osc} on, with a number density of axions at the onset of oscillations given by

$$n_a(T_{\text{osc}}) = \frac{b}{2} m_a(T_{\text{osc}}) f_a^2 \langle \theta_i^2 \rangle. \quad (165)$$

Here, b is a factor of order one [184] that captures the uncertainties derived from using the approximation in Eq. (154) to estimate the number density $n_a(T_{\text{osc}})$, instead of numerically solving Eq. (152). Assuming that entropy remains conserved within a comoving volume since the axion field starts oscillating, the ratio of the axion number density to the entropy density is then conserved to any temperature $T < T_{\text{osc}}$,

$$n_a(T) = n_a(T_{\text{osc}}) \frac{s(T)}{s(T_{\text{osc}})}, \quad (166)$$

where $s(T) \propto T^3$ is given in Eq. (146). Neglecting the contribution from the topological defects the energy density of axions as a function of the temperature, at $T \ll T_C$, then is

$$\rho_a^{\text{mis}}(T) = m_a n_a(T_{\text{osc}}) \frac{g_S(T)}{g_S(T_{\text{osc}})} \left(\frac{T}{T_{\text{osc}}} \right)^3 = \frac{b\beta}{2} m_a^2 f_a^2 \langle \theta_i^2 \rangle \frac{g_S(T)}{g_S(T_{\text{osc}})} \frac{T^3 T_C^\gamma}{T_{\text{osc}}^{3+\gamma}}, \quad (167)$$

where in the second equality we have used Eq. (165) and Eq. (150). T_{osc} appearing in this equation can be evaluated using the condition for the start of oscillations Eq. (154) together with the mass-temperature relation in Eq. (150) and the Hubble-temperature relation $H(T) = 1.66 g_*^{1/2} T^2 / m_{\text{Pl}}$ in Eq. (147), obtaining

$$T_{\text{osc}}^{2+\gamma} \simeq \left(\frac{\beta T_C^\gamma m_{\text{Pl}}}{4.98 g_*(T_{\text{osc}})^{1/2}} \right) m_a. \quad (168)$$

As a reference, with $g_*(T > T_C) = 61.75$, $\gamma = 4$, $T_C = 160 \text{ MeV}$ and $\beta \approx 0.026$ [184] one obtains $T_{\text{osc}} \approx 800 \left(\frac{m_a}{1 \mu\text{eV}} \right)^{1/6} \text{ MeV}$. Plugging now Eq. (168) into Eq. (167) we obtain

$$\rho_a^{\text{mis}}(T) = \frac{b\beta}{2} m_a^2 f_a^2 \langle \theta_i^2 \rangle \frac{g_S(T)}{g_S(T_{\text{osc}})} \left(\frac{4.98 g_*(T_{\text{osc}})^{1/2}}{\beta m_{\text{Pl}} m_a} \right)^{\frac{3+\gamma}{2+\gamma}} T_C^{-\frac{\gamma}{2+\gamma}} T^3. \quad (169)$$

In Fig. 1 we show the evolution of $\theta(T)$ (blue solid line) and of the energy density of cold axions in units of the present CDM energy density $\rho_a^{\text{mis}}(T)/\rho_{\text{CDM}}$ (red dashed line) as a function of the inverse plasma temperature T_{osc}/T . To draw the picture, we have set the initial misalignment angle $\theta_i = 1$, a vanishing initial axion energy density when the axion field is frozen to the configuration $\theta = \theta_i$ at $T \gtrsim T_{\text{osc}}$, and the value of the axion mass has been chosen so that the present value of ρ_a^{mis} saturates the measured CDM energy density. Finally, the present axion energy density from the misalignment mechanism normalised to the critical energy density $\rho_{\text{crit}} = 3m_{\text{Pl}}^2 H_0^2 / (8\pi) \approx 8.06 \times 10^{-11} h^2 \text{ eV}^4$, where h is defined in terms of the Hubble constant as $H_0 = 100 h \text{ km/s/Mpc}$, can be obtained from Eq. (169) as:

$$\Omega_a^{\text{mis}} h^2 \approx 0.12 \left(\frac{28 \mu\text{eV}}{m_a} \right)^{\frac{7}{6}} = 0.12 \left(\frac{f_a}{2.0 \times 10^{11} \text{ GeV}} \right)^{\frac{7}{6}}, \quad (170)$$

where we have used $\langle \theta_i^2 \rangle = (2.15)^2$, $T_0 = 2.73 \text{ K} \simeq 2.35 \times 10^{-4} \text{ eV}$ and $g_S(T_0) = 3.91$ for the present photon temperature and effective number of entropic degrees of freedom, $m_a f_a \simeq 5.7 \times 10^{15} \text{ eV}^2$ from Eq. (108), $g_S(T \gtrsim T_C) = g_*(T \gtrsim T_C) = 61.75$, $\gamma = 4$, $T_C = 160 \text{ MeV}$, $\beta = 0.026$ and $b = 1$, and we have put in evidence a factor of the measured CDM abundance $\Omega_{\text{CDM}} \approx 0.12$. Although the value of the axion mass that saturates the CDM density obtained via this simple analytical estimate falls in the ballpark of the results of dedicated numerical studies, the derivation outlined above neglects several effects, and thus the simple form of Eq. (170) should be taken only as an illustrative approximation. More reliable estimates

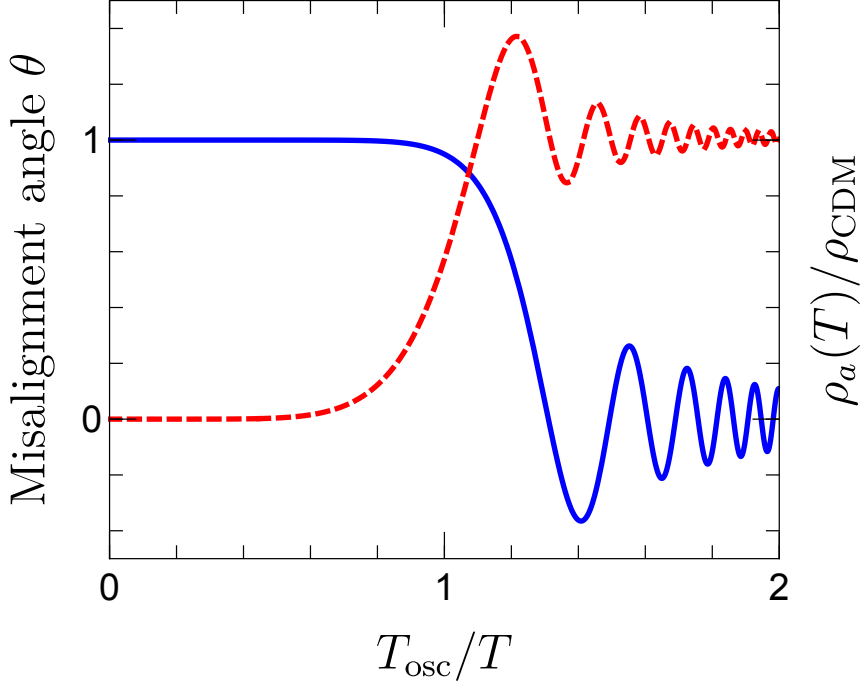


Figure 1: The axion angle θ (blue solid line) and the energy density of axions in units of the present CDM energy density (red dashed line), as a function of the inverse plasma temperature T_{osc}/T . We set the initial misalignment angle $\theta_i = 1$.

require describing with a better accuracy the dependence of the axion mass on the temperature, including the effects of the axion potential anharmonic terms, and taking properly into account the details of the quark-hadron phase transition [187, 189, 190]. Finally, Eq. (170) has been obtained assuming a standard cosmology and canonical properties for the axion. In Section 6.6.1 we will challenge some of these assumptions, and we will argue that in non-standard scenarios different ranges of mass values for CDM axions are possible.

3.4. Topological defects and their contribution to axion cold dark matter

In post-inflationary scenarios the production of cold axions from misalignment discussed in the previous section is not the only CDM production mechanism. Additional contributions are possible because of the existence of topological defects, specifically strings and domain walls (DW) associated with the axion field (for a review on topological defects of cosmological relevance see Ref. [191]). If the PQ symmetry is broken before inflation, topological defects related to the breaking of the PQ symmetry (axionic strings) are inflated away, while those related to $N_{\text{DW}} > 1$ do not form. Topological defects are therefore relevant only in the post inflationary scenario, a condition that will be assumed throughout this section.

Axion strings are formed through the Kibble mechanism [192, 193] at the time of the spontaneous breaking of the $U(1)$ PQ symmetry. At the end of the phase transition, the phase $a(x)/v_a$ of the PQ field acquires uncorrelated values between 0 and 2π in different causally disconnected Hubble patches. Therefore, when these patches reenter the horizon, the value of the axion field will have random fluctuations within every Hubble patch, and unavoidably there will be loops around which $a(x)$ wraps all the values in the domain $[0, 2\pi v_a]$. Any closed loop over which the phase changes by $2\pi v_a$ must necessarily contain a point in which the axion field assumes all the values between 0 and $2\pi v_a$, i.e. it is singular. To avoid that the loop

could be contracted in a topologically trivial manner, such points should form an infinite or a closed string, called axion string, where the axion is singular, while along any path encircling the string its value changes by $2\pi v_a$. Single string configurations are stable, however strings within string networks are not, because in this case strings can interact among each other, crossing strings can form loops that decay, radiating low momentum axions. Estimating the contribution of the string decay to the abundance of cold axions is a complex problem, not yet completely solved, that will be briefly address in Section 3.4.1.

As the Universe expands, once the temperature lowers to ~ 1 GeV non perturbative QCD effects become important and the axion acquires a potential which provides an explicit breaking of the PQ symmetry. This potential has periodicity $2\pi f_a$ with $f_a = v_a/N_{\text{DW}}$, see Eq. (88), and hence it is characterised by N_{DW} equivalent minima, which are related by a $\mathbb{Z}_{N_{\text{DW}}}$ discrete symmetry. The axion relaxes to one of these minima thus breaking spontaneously $\mathbb{Z}_{N_{\text{DW}}}$. In each casually disconnected Hubble patch a different minimum is randomly chosen, so that after a few Hubble times, when several patches will have reentered the horizon, DWs form as field configurations that interpolate in space between neighbouring vacua. The DW tension (energy per unit area) for a QCD cosine potential is $\sigma = 8m_a f_a^2$, and the contribution to the Universe energy density from the energy stored in such configurations largely exceeds the critical energy density. This constitutes a serious issue, known as the axion DW problem, which is briefly addressed in Section 3.4.4. Here we anticipate that the problem does not subsist in the case of $N_{\text{DW}} = 1$, since in this case the network of strings and DWs is unstable. Also for the case $N_{\text{DW}} > 1$ there are ways to circumvent the DW problem, which are revied in Section 7.5.

3.4.1. Cosmic axion strings

As predicted by the Kibble mechanism [192–194], a network of global strings originates whenever a global $U(1)$ symmetry is spontaneously broken. In the case of the PQ symmetry, the Kibble mechanism produces *axionic* strings, which are vortex-like defects that form as soon as the symmetry is spontaneously broken. As we shall see below, the string population consists in long strings and in string loops. The last, formed by the continuous intersection of long intercommuting strings, contribute to the majority of the radiated axions. As was mentioned above, in models with $N_{\text{DW}} = 1$ the network of axionic topological defects is unstable. This is because in this case each string is attached to a single DW. This DW forms because, wrapping in space around the string, at some point the value of the axion field must change abruptly by $2\pi v_a$. Since the system evolves to minimize the energy stored in the DW, two strings attached to the same wall are pulled together until they eventually annihilate, so that the string and DW energy is released in radiation of low-momentum axions [195, 196]. For $N_{\text{DW}} > 1$ instead, each string is attached to more than one DW that pull in different directions, reaching a stable equilibrium that prevents annihilation. Let us focus on the $N_{\text{DW}} = 1$ case. The spontaneous decay of the axionic string network contributes to the present abundance of cold axions [195–201]. Although all numerical simulations [202–216] agree in confirming this qualitative result, no quantitative agreement has been reached yet regarding the efficiency of cold axion production from topological defects. The main challenge being the limitations in numerical simulations of the evolution of the string-DW network, which requires that final results are extrapolated through several orders of magnitude in the ratio of relevant dimensional quantities. The uncertainty in estimating the overall cosmological abundance of cold axions has an obvious impact on axion DM searches, and indeed it constitutes one of the most important open problems in axion physics.

3.4.2. String populations

The population of strings can be divided into two subgroups: *long strings* and *string loops*.

Long strings are string-like defects of size comparable to the horizon scale [195–197, 217–219]. The string energy per unit length, called string tension μ , of an isolated string gets contributions from the string core where the divergence related to the singularity is cutoff by the heavy degree of freedom, that is by the radial mode ϱ_a sitting on the top of its potential. For a standard potential as $V(\Phi)$ in Eq. (78) one has $\varrho_a^2 \sim f_a^2$ at the potential maximum, and the string core can be defined as a region of size $r_c \sim f_a^{-1}$ from the center. Thus, in integrating the volume energy density r_c provides a short-distance cutoff. There is, however, also a large-distance logarithmic divergence, that is cutoff by a length of the order of the Hubble size $t \sim H^{-1}$.

For an single string configuration the string tension then is

$$\mu(t) \simeq \pi f_a^2 \log(\eta f_a t) \quad (171)$$

where η is an $\mathcal{O}(1)$ factor, possibly dependent on time, which takes into account the fact that the string can have non-trivial shape features on length scales smaller than the Hubble length.

In the real case one has to consider a full system of axion strings that can interact. Already in earlier studies it was claimed that a system of interacting strings should evolve towards a particular configuration that is independent of the initial conditions at early times [192, 194, 195]. This represents a crucial property to allow model-independent estimates of the cold axion contribution from topological defects. The existence of a unique asymptotic configuration can be justified qualitatively in a simple way. To minimize the energy, bended strings tend to straighten emitting radiation, closed strings of size smaller than the Hubble radius tend to shrink further, long strings crossing each other recombine in new configurations of reduced length. The rate of these processes depends on the overall length of strings within the Hubble volume $\ell_{\text{tot}}(t)$. When this quantity is large the rate of the length reducing processes is also large. However, when $\ell_{\text{tot}}(t)$ falls below some critical value, these processes become inefficient, and $\ell_{\text{tot}}(t)$ tends to grow because new strings enter the horizon. Thus equilibrium should be reached for a particular value of the density of strings. The results of different simulations agree in confirming such a behaviour and, in particular, it is found that, regardless of the initial conditions, at late times the number of strings for Hubble patch $\xi(t \rightarrow \infty)$ converges towards a value of order of a few [204, 206, 210, 211, 220]. Quite noticeably, other properties of the network, including the spectrum of axions emitted, also converge.

Given an overall length of strings $\ell_{\text{tot}}(L)$ within a large volume L^3 , the average number of strings of length $t \sim H^{-1}$ per Hubble volume $\sim t^3$ is given in terms of the length density $\ell_{\text{tot}}(L)/L^3$ as

$$\xi(t) = \frac{\ell_{\text{tot}}(L)}{L^3} t^2. \quad (172)$$

For a string network, the average separation between strings is then $t/\sqrt{\xi}$, and this distance provides a cutoff for the large distance log divergence. One can then define an effective string tension as

$$\mu_{\text{eff}}(t) = \gamma(t) \pi f_a^2 \log \left(\frac{\eta f_a t}{\sqrt{\xi(t)}} \right) \quad (173)$$

where $\gamma(t)$ is an effective boost factor, typically of $\mathcal{O}(1)$, that accounts for the kinetic energy associated with the string network configuration. In terms of the effective string tension the energy density in strings then is:

$$\rho_{\text{long}} = \xi(t) \frac{\mu_{\text{eff}}(t)}{t^2}. \quad (174)$$

Hence, to the extent the theoretical expectation for the effective string tension Eq. (173) is a good approximation (and numerical simulations indicate that this is the case) the energy density of the string network at a particular time, once the equilibrium regime is reached, remains basically determined from the density of strings. Various levels of sophistications have been used to describe the dynamics of string networks. In the original formulation of the so-called one-scale model [221, 222], the evolution of the network of strings does not depend on the string velocity. A more accurate description is obtained by accounting for the effects of the velocity of the centre of mass of the string [223–225]. More sophisticated treatments also include the effects of friction due to the interaction of the strings with the surrounding matter and radiation [226, 227]. The mean-squared velocity of the long string gas $\langle v^2 \rangle$ enters the equation of state w_{str} that describes the evolution of the energy density, namely [228]

$$w_{\text{str}} = \frac{2\langle v^2 \rangle - 1}{3}. \quad (175)$$

For ultra-relativistic strings $\langle v^2 \rangle \approx 1$, and a free network of long strings evolves as radiation, while in the case of slow-moving strings $\langle v^2 \rangle \approx 0$ and $w_{\text{str}} = -1/3$. In general, we expect the equation of state for

the string gas to vary within the range $-1/3 \leq w_{\text{str}} \leq 1/3$. Numerical simulations of string networks in a radiation-dominated cosmology hint to a mean velocity $\langle v^2 \rangle^{1/2} \approx 0.5$, see for example Table 1 in Ref. [229].

String loops. A population of closed loops of sub-Hubble size ℓ and energy density ρ_{loop} forms from the continuous intersection of long strings. Segments of high curvature in long strings can also split off forming isolated loops. Loops vibrate and shrink while releasing energy into a spectrum of radiated axions. The power loss of the network into radiation can be described through the dissipation of the energy $E_{\text{loop}} = \mu_{\text{eff}}(t)\ell$ of a closed loop of length ℓ into axions as [202, 227, 230],

$$\frac{dE_{\text{loop}}}{dt} = \kappa_s \mu_{\text{eff}}(t), \quad (176)$$

where $\kappa_s \approx 0.15$ is a dimensionless quantity [228, 231, 232] computed at a fixed value of the string velocity $\langle v^2 \rangle^{1/2} \approx 0.5$. Although in principle the length of the loops formed could be ranging at any size, numerical simulations [203, 233–238] show that the initial length of the large loop at its formation tracks the time of formation as

$$\ell(t_I) = \alpha_{\text{loop}} t_I, \quad (177)$$

where α_{loop} is an approximately constant loop size parameter which gives the fraction of the horizon size at which loops predominantly form. The loop spectrum is described in terms of a loop formation rate $r_\ell(\ell_I, t_I)$, which is related to the rate of the energy density dissipated into axions by [239, 240]

$$\frac{d\rho_{\text{loop}}}{dt} = \int_0^\infty d\ell \mu_{\text{eff}}(t) \ell r_\ell(\ell, t). \quad (178)$$

Eventually, a loop of initial size ℓ_I shrinks and disappears by a time t_F defined implicitly as $\ell(t_F, \ell_I) = 0$.

The total energy density of the string network receives contributions from both string populations $\rho_{\text{str}} = \rho_{\text{long}} + \rho_{\text{loop}}$. Numerical simulations indicate that roughly 80% of the string length per Hubble patch is contained in long strings, while the remaining 20% is equally distributed in sub-Hubble loops of different lengths, ranging from the horizon scale $\sim H^{-1}$ to the size of the string core $\sim f_a^{-1}$ [213]. Note that the ratio 4:1 in favour of long strings justifies the approximation of using the effective tension defined for the long string in Eq. (173) also for the string loops.

3.4.3. Spectrum of radiated axions

In order to extract the energy density of the radiated axions from the simulation of the evolution of an axionic string network, the evolution of the energy density in the strings ρ_{str} is compared to what is obtained for a gas of free strings of energy density ρ_{free} that do not radiate [213]. The evolution of a free, non-intercommuting string gas is described by the kinetic equation

$$\frac{d\rho_{\text{free}}}{dt} + 3H(1 + w_{\text{str}})\rho_{\text{free}} = 0, \quad (179)$$

where w_{str} is given in Eq. (175). The solution to Eq. (179) is $\rho_{\text{free}} \propto a^{-3(1+w_{\text{str}})}$ which, in the case of a radiation-dominated cosmology and fixing the proportionality constant to match the initial energy density of the string network in Eq. (174), gives

$$\rho_{\text{free}}(t) = \xi \frac{\mu_{\text{eff}}(t)}{t_{\text{PQ}}^2} \left(\frac{t}{t_{\text{PQ}}} \right)^{-\frac{3}{2}(1+w_{\text{str}})}. \quad (180)$$

When the axion emission is included, Eq. (179) is modified to include the effective energy lost in the emission of axions per unit time $\Gamma_{\text{str} \rightarrow a}$, defined as the difference in the rates at which the energy densities in the free string gas and the string network change,

$$\Gamma_{\text{str} \rightarrow a}(t) \equiv \dot{\rho}_{\text{free}}(t) - \dot{\rho}_{\text{str}}(t) = H(1 - 3w_{\text{str}})\rho_{\text{str}} - \frac{\rho_{\text{str}}}{\mu_{\text{eff}}} \frac{d\mu_{\text{eff}}}{dt}. \quad (181)$$

Once the power radiated by the string network $\Gamma_{\text{str} \rightarrow a}$ has been obtained, the energy density of the radiated axions follows the evolution $\rho_a^{\text{str}} + 4H\rho_a^{\text{str}} = \Gamma_{\text{str} \rightarrow a}$; the axion energy density from the decay of the string network contributes to an additional source on top of the abundance expressed in Eq. (167) obtained from the misalignment mechanism. The number density of axions associated to this process is [213]

$$n_a^{\text{str}} = \int^t dt' \frac{\Gamma_{\text{str} \rightarrow a}(t')}{H(t')} \left(\frac{R(t')}{R(t)} \right)^3 \int \frac{dk}{k} F(k) = \frac{(1 - 3w_{\text{str}}) \pi f_a^2}{t^{3/2}} \int^t dt' \frac{\ln(f_a t')}{(t')^{1/2}} \int \frac{dk}{k} F(k), \quad (182)$$

where the spectral energy density $F(k) \propto k^{-q}$ has been explored in different regimes in the literature depending on the value of the spectral index q . A choice $q > 1$ assumes that axions are radiated away on a timescale comparable to the Hubble time, and describes a power spectrum ranging over all modes from $k \approx 1/\ell(t_I) \approx H(t_I)/\alpha_{\text{loop}}$ to infinity [202, 230]. On the other hand, assuming that strings efficiently shrink emitting all of their energy at once leads to a flat power spectrum per logarithmic interval with an infrared cutoff at the wave mode $k \approx H$ and an ultraviolet cutoff at $k = f_a$, with a harder spectral index $q = 1$ [199, 241, 242]. Demanding that the spectrum is normalised over the given interval results in

$$F(k) = \begin{cases} \frac{q-1}{\alpha_{\text{loop}}^{q-1}} \left(\frac{k}{H} \right)^{-q}, & \text{for } q > 1, \\ \frac{1}{\ln(f_a/H)} \frac{H}{k}, & \text{for } q = 1. \end{cases} \quad (183)$$

The integration of Eq. (182) with the spectrum in Eq. (183) and $q > 1$ finally leads to

$$n_a^{\text{str}} \approx \frac{(1 - 3w_{\text{str}}) \pi f_a^2}{2t_{\text{osc}}} \times \begin{cases} \alpha_{\text{loop}} \frac{q-1}{q} \ln(f_a t_{\text{osc}}), & \text{for } q > 1, \\ 1, & \text{for } q = 1. \end{cases} \quad (184)$$

This expression shows that most of the axions are radiated by loops right before t_{osc} , when DWs dissipate the network. The computation matches the estimation for the decay of the string network at the time of DW formation [196, 202]. The number density of axions at time t_{osc} from Eq. (184) results from a steeply falling integrand function of t , so that the dominant contribution comes from loops originating nearly instantaneously at values $t_I \sim t_{\text{osc}}$ [196, 202, 203]. The use of the harder spectrum with $q = 1$ generically leads to results for the string contributions which are smaller by a factor $\log(f_a t_{\text{osc}}) \approx 70$.

3.4.4. Cosmological domain walls

Cosmological DWs emerge with the spontaneous breaking of discrete symmetries [191, 197, 226]. When the PQ symmetry is explicitly broken by nonperturbative QCD effects, the axion acquires a periodic potential with N_{DW} equivalent minima. Thus, the original $U(1)$ symmetry, which guaranties the equivalence of all values of θ , is broken into a discrete $\mathbb{Z}_{N_{\text{DW}}}$ symmetry. Uncorrelated patches will choose different ground states randomly selecting one of the N_{DW} equivalent vacua. Axion DWs appear at the boundaries of physical regions that are in different minima, providing a smooth interpolation between the two vacua. Such configurations have a thickness $\delta_{\text{wall}} \approx 1/m_a(t_{\text{osc}})$ and an energy per unit area $\sigma_{\text{wall}} \approx 8m_a^2(t_{\text{osc}})v_a$ for the cosine potential [47]. Notice that there are axion DWs even in the case of $N_{\text{DW}} = 1$, which have an interpolating field configuration starting and ending in the same vacuum, but winding around the bottom of the Mexican hat potential once [27]. At the time when the axion acquires a mass, axion strings become the edge of DWs, forming a string-wall network [191, 226] whose dynamics depends on the value of N_{DW} . In the case of $N_{\text{DW}} = 1$, strings disrupt the DWs soon after their formation by separating them into smaller pieces [197, 243] and dissipating the network whose decay produces a spectrum of radiated axions which also includes a cold axion component that adds up to the axion CDM produced by misalignment [209, 213–215].

In contrast, in theories with $N_{\text{DW}} > 1$ the DWs are generally stable, and eventually come to dominate the energy density of the Universe, largely overshooting any acceptable value. However, some solutions to this problem also exist, and are discussed in Section 7.5.

3.5. Axion isocurvature fluctuations

This topic is relevant in the pre-inflationary scenario. We consider an early inflationary period described by the quasi-de Sitter space-time metric, with a nearly-constant Hubble rate H_I . In this setting, the axion field is a massless spectator. Inflationary models generically predict the appearance of primordial scalar and tensor fluctuations, which redshift to super-horizon scales to later evolve into primordial curvature perturbations as well as primordial gravitational waves, leaving an imprint in the CMB radiation anisotropy and on the large-scale structure [244–249]. CMB features distinct peaks both in its angular power spectrum of temperature (TT) as well as in the temperature-polarisation cross-power spectrum (TE), with the first peak in TT located at $\ell = 220.6 \pm 0.6$ at 68% CL by the *Planck* collaboration survey [250]. Other information extracted from the CMB include the polarisation angular power spectrum (EE).

Adiabatic curvature perturbations generated during inflation show a nearly scale-invariant dimensionless power spectrum of primordial curvature perturbations with amplitude $\Delta_{\mathcal{R}}^2(k_0)$, with a mild dependence on the co-moving wavenumber k which is parametrised by a scalar spectral index n_S around an arbitrary reference scale k_0 ³⁶ as [253–255]

$$\Delta_{\mathcal{R}}^2(k) \equiv \Delta_{\mathcal{R}}^2(k_0) \left(\frac{k}{k_0} \right)^{n_S-1}. \quad (185)$$

If the axion field a originates during inflation, it also inherits quantum fluctuations with the typical standard deviation σ_a of a massless scalar field in the accelerated expansion, see e.g. Ref. [256],

$$\sigma_a = \sqrt{\langle a^2 \rangle} \simeq \frac{H_I}{2\pi}, \quad (186)$$

and with a corresponding standard deviation for the distribution of the axion angle $\sigma_\theta = \sigma_a/f_a$. Since these fluctuations are independent of the quantum fluctuations of the inflaton field, they are of the isocurvature type. More in detail, the fluctuations in the axion field do not perturb the total energy density during inflation, but change the value of the axion number density with respect to entropy density, $\delta(n_a/s) \neq 0$. Axion isocurvature fluctuations convert into curvature perturbations at the time at which the axion mass becomes relevant, around the QCD phase transition [181–183], due to the feedback of isocurvature into curvature modes [257, 258]. Since the axion field behaves as CDM at recombination, these axion perturbations imprint into the temperature and polarisation fluctuations in the CMB and, because of their isocurvature nature, they are completely uncorrelated with the adiabatic curvature perturbations.

The magnitude of the axion isocurvature perturbations $\Delta_a^2(k) = \Delta^2(k_0)(k/k_0)^{n_I-1}$ where n_I the isocurvature spectral index, is given by the relative fluctuation in the axion energy density [259]. In terms of the initial angle θ_i the amplitude can be written as

$$\Delta_a(k) = \frac{\delta\Omega_{\text{CDM}}}{\Omega_{\text{CDM}}} = \mathcal{F}_{\text{CDM}}^a \frac{\delta \ln \Omega_a}{\delta \theta_i} \sigma_\theta \simeq \mathcal{F}_{\text{CDM}}^a \frac{H_I}{\pi \theta_i f_a}, \quad (187)$$

where $\mathcal{F}_{\text{CDM}}^a = \Omega_a/\Omega_{\text{CDM}}$ is the relative contribution of axions to CDM, we have assumed $\delta\Omega_{\text{CDM}} = \delta\Omega_a$ and the last step holds in the small θ_i regime in which anharmonic corrections can be neglected and $\Omega_a \propto \theta_i^2$ (see for example Eq. (169)). Measurements of the anisotropies in the CMB can be used to constrain $\Delta_a^2(k)$, since data show that primordial fluctuations are predominantly adiabatic with little space left for fluctuations of the isocurvature type. The *Planck* mission constrains the fraction of uncorrelated isocurvature fluctuations by placing an upper bound on the quantity

$$\beta(k) \equiv \frac{\Delta_a^2(k)}{\Delta_{\mathcal{R}}^2(k) + \Delta_a^2(k)}, \quad (188)$$

³⁶The reference scale k_0 is also called the “pivot” scale in cosmology, and refers to the comoving scale at which measurements are taken. For example, the *Planck* mission often refers to the pivotal scale $k_0 = 0.05 \text{ Mpc}^{-1}$ [251]. For isocurvature and tensor modes, the constraints are quoted at three different scales: $k_{\text{low}} = 0.002 \text{ Mpc}^{-1}$, $k_{\text{mid}} = 0.050 \text{ Mpc}^{-1}$, and $k_{\text{high}} = 0.100 \text{ Mpc}^{-1}$ [252].

Parameter	Prior	Reference
$\Omega_{\text{CDM}} h^2$	0.1200 ± 0.0012	Base Λ CDM, <i>Planck</i> TT, TE, EE + lowE + lensing [251]
$\ln(10^{10} \Delta_{\mathcal{R}}^2)$	3.044 ± 0.014	Base Λ CDM, <i>Planck</i> TT, TE, EE + lowE + lensing [251]
β	< 0.038 at 95% CL	CDI $n_{\text{II}} = 1$, <i>Planck</i> TT, TE, EE + lowE + lensing [252].
n_S	0.9649 ± 0.0042	Λ CDM+r, <i>Planck</i> TT, TE, EE + lowE + lensing [251]
r	< 0.056 at 95% CL	Λ CDM+r, <i>Planck</i> TT, TE, EE + lowE + lensing+BK15 [252]

Table 1: Cosmological parameters from the joint *Planck* and BICEP2/Keck Array (BK15) analysis of the combined TT, TE, EE + lowE + lensing + BK15 dataset, from Refs. [251, 252]. The value of $\Delta_{\mathcal{R}}^2$ and the constraint on the primordial isocurvature fraction β defined in Eq. (188) are at the default pivot scale $k_0 = 0.05 \text{ Mpc}^{-1}$. The limit on the tensor to scalar ratio r is at the pivot scale $k_0 = 0.002 \text{ Mpc}^{-1}$.

where the spectra are computed at a pivot scale k . Here, we have used the measurements of the CMB temperature and polarisation anisotropies from the *Planck* satellite, jointly with the BICEP2/Keck Array (BK15) for the combined TT, TE, EE + lowE + lensing + BK15 dataset at 68% CL [251, 252, 260–265]. We list the values used in this Review in Table 1, where data in the form $A \pm B$ are reported at 68% CL, while upper limits are reported at 95% CL. Isocurvature bounds place a stringent constraint on the scale of inflation, so that models of axion DM in the pre-inflationary scenario require a relatively low Hubble rate H_I compared to the scale $H_I \lesssim 10^{13} \text{ GeV}$ which has currently been probed using CMB tensor modes. Using the results in Table 1, from Eqs. (187) and (188) the following constraint on the inflationary scale can be derived:

$$H_I \lesssim \frac{0.9 \times 10^7}{\mathcal{F}_{\text{CDM}}^a} \left(\frac{\theta_i}{\pi} \frac{f_a}{10^{11} \text{ GeV}} \right) \text{ GeV}. \quad (189)$$

The bound from isocurvature perturbations can, however, be evaded in many ways. The simplest one is to appeal to the post-inflationary scenario, since in this case there is no massless Goldstone boson during inflation, although, for $N_{\text{DW}} > 1$, one then has to deal with the DW problem, see Section 3.4.4. However, other possibilities are viable also within scenarios in which the PQ symmetry is already broken during inflation. For example, in Ref. [266] it was argued that the isocurvature bound holds only under the assumption that f_a does not change during the last stages of inflation or after it, and it was argued that this assumption is not valid in general. Axion models embedded into a *hybrid inflation* scenario in which the background value of the axion field slowly decreases, rolling down to its equilibrium value $\langle |\Phi| \rangle = v_a / \sqrt{2} \propto f_a$ were in fact shown to be compatible with an inflationary scale several orders of magnitude larger than the reference value in Eq. (189), while still keeping $f_a \sim 10^{11} \text{ GeV}$ ($m_a \sim 6 \cdot 10^{-5} \text{ eV}$) and without the need to tune θ_i to particularly small values. Ref. [267] considered instead the possibility of a non-minimal derivative coupling of the axion field to gravity. While the new coupling does not affect the density of axion CDM, it can effectively suppress the isocurvature perturbations during inflation. Another solution studied in Ref. [268] relies on the observation that if the axion acquires a sufficiently large mass already during inflation, its quantum fluctuations at super-horizon scales would become significantly suppressed, thereby relaxing the constraint on the inflation scale. This can be achieved by assuming a phase in the early Universe in which QCD becomes strong thus rendering the axion massive. Such a scenario was in fact first proposed in Refs. [269, 270] in the attempt of suppressing the cosmological abundance of axions from the misalignment mechanism, a task that, as is outlined in Section 3.7.2 below, eventually turned out to be rather difficult to accomplish. However, an early strong QCD phase yielding an axion mass larger than the Hubble scale over a certain period of inflation was reconfirmed in Ref. [271] as a viable mechanism to suppress isocurvature axion fluctuations. Finally, the issue would of course disappear within inflationary models that could naturally respect the isocurvature constraint on the inflationary Hubble scale in Eq. (189), and indeed this was shown to be possible in low-scale models of hybrid inflation [272].

3.6. Cosmological bounds on the axion mass

Before addressing the upper bounds that can be set on the axion mass from early Universe and cosmological consideration, let us mention a generic (non cosmological) argument that is sometimes invoked to claim a *lower* limit on the axion mass. This argument is based on the belief that an axion decay constant f_a above the Planck scale is incompatible with an effective QFT description so that, according to Eq. (108), $f_a \lesssim m_{\text{Pl}}$ would yield $m_a \gtrsim 5 \times 10^{-13}$ eV. Note, however, that even this seemingly model-independent bound can be circumvented in a particular axion construction that exploits the Kim-Nilles-Peloso mechanism [273]. This mechanism requires the existence of at least two axions, and can produce an effective super-Planckian axion scale, although the original fundamental scale is sub-Planckian [273]. In any case this lower limit would not compete with the lower limit on the axion mass $m_a \gtrsim 2 \times 10^{-11}$ eV that can be obtained from considerations of the super-radiance phenomenon (a topic that will be touched on in Section 4.6) and that as long as axion self interactions are sufficiently feeble, is truly model independent.

Moving now to review the cosmological arguments that allow to constrain from above the value of the axion mass, it should be mentioned from the start that altogether these bounds are much less constraining than the limits that can be inferred from astrophysical processes (discussed in Section 4), by translating the bounds on the different axion couplings $g_{a\gamma}, g_{ae}, g_{aN}$ into lower bounds on the axion decay constant f_a and in turn on upper limits on m_a . Although the upper limits derived in this way are admittedly model dependent, and a precise number cannot be given without specifying the theoretical setup, the indication that $m_a \lesssim 0.1$ eV is rather solid. In spite of this, the cosmological bounds are well worth mentioning because they rely on completely independent arguments.

Hot dark matter. As will be discussed in more detail in Section 3.8, at temperatures below the QCD phase transition axions interact with pions ($a\pi \leftrightarrow \pi\pi$) and nucleons ($aN \leftrightarrow \pi N$) with a strength that increases as m_a is increased. Then, for sufficiently large values of m_a a thermal population of axions arises, which would constitute a Hot DM (HDM) component. However, HDM abundance is severely constrained by data from cosmological surveys. Using 7-year data from the Wilkinson Microwave Anisotropy Probe (WMAP-7) together with Sloan Digital Sky Survey (SDSS) observations and the Hubble constant from Hubble Space Telescope (HST) Ref. [274] set the bound $m_a \lesssim 0.72$ eV. A bound on m_a using only CMB data was reported in [275]. More recently, using Planck 2015 results the bound was strengthened to $m_a \lesssim 0.53$ eV [276]. A study of the potential of future cosmological surveys for further constraining the axion mass has been presented in Ref. [277].

Baryon to photon ratio from Big Bang Nucleosynthesis (BBN) and from CMB. Axions decay to two photons with a lifetime inversely proportional to the fifth power of the mass,

$$\tau_a = \frac{64\pi}{g_{a\gamma}^2 m_a^3} \sim 10^{24} \left(\frac{\text{eV}}{m_a} \right)^5 \text{ s}. \quad (190)$$

For $m_a \gtrsim 20$ eV the axion lifetime drops below the age of the Universe, hence, for a sufficiently large mass, the decay happens early enough and the HDM bound no longer applies. However, if axions decay not too early, non-thermal photons injected in the bath would produce a spectral distortion in the CMB, and this can be used to derive restrictive constraints [278]. However, if decays occur early enough, photons will have the time to thermalise and the CMB would not be affected. Nevertheless, the additional entropy injected into the bath increases the number of photons relative to that of baryons, decreasing the ratio $\eta_b = n_b/n_\gamma$. Nowadays we know with good precision the value of η_b , which is inferred independently from BBN and from CMB data, and there is a beautiful agreement between the two results. Since the relevant physics processes responsible for the primordial abundances of light elements and for the CMB occur in different cosmological eras that are characterised by temperatures that differ by about six orders of magnitude, the amount of entropy that can be injected in the thermal bath between $T_{\text{BBN}} \lesssim 1$ MeV and $T_{\text{CMB}} \lesssim 1$ eV is tightly constrained. This argument was used in Ref. [279] to exclude $m_a \lesssim 300$ keV. A later study that used Planck data, together with new inferences of primordial element abundances, pushed the limit up to $m_a \gtrsim 1$ MeV [280], while an assessment of the robustness of the bounds with respect to possible deviations

in the standard cosmology was recently presented in Ref. [281]. These bounds are nicely complemented by constraints from beam dump and reactor experiments which exclude axion (and ALP) masses from MeV up to several GeVs [282–293]. Altogether, these considerations allow to identify $m_a \lesssim 0.53$ eV as the cosmologically allowed axion mass window.

3.7. Benchmark axion mass region for $\Omega_a \simeq \Omega_{\text{CDM}}$

The present axion relic abundance Ω_a depends on multiple production mechanisms that have been reviewed in the previous sections. Here, we discuss the benchmark axion DM mass regions both in the post- and pre-inflationary PQ breaking scenarios, including also the constraints coming from various cosmological considerations.

3.7.1. Post-inflationary scenario

In post inflationary scenarios we would expect that the contribution to CDM from axions could be assessed with particular precision, given that estimates of the density of axions produced from the misalignment mechanism do not suffer from uncertainties related to particular choices of the initial conditions. Unfortunately this is not completely true. Other important sources of uncertainties are in fact present and hamper, for example, precise determinations of the value of m_a for which axions can account for the whole of CDM, a quantity to which we will refer as *the DM axion mass*. These uncertainties are primarily related to the serious difficulties that one encounters in trying to assess the contribution to the population of cold axions from the decay of topological defects, but additional uncertainties are also associated with evaluations of the dependence on temperature of the topological susceptibility $\chi(T)$, see Eq. (149). As a consequence, although it is not uncommon to find in the literature values of the DM axion mass with relatively small errors, differences between different estimates can easily be several times larger than the quoted errors. This is simply due to the fact that the theoretical uncertainties mentioned above are not accounted for. To be conservative, one can take as a reasonable range for the DM axion mass $m_a \approx (10 - 100) \mu\text{eV}$, and likely with an even larger upper value if $N_{\text{DW}} > 1$. It is clear, however, that to guide experimental searches for axion DM any improvement in controlling the major sources of uncertainties is highly desirable. To this aim, several groups are carrying out extended simulations of the network of axionic strings in order to improve in the understanding of their effect. In this respect, models with $N_{\text{DW}} = 1$ are more promising because they do not require additional assumptions about the dissipation of the domain wall network, and for this reason most studies focus on this case. Hiramatsu *et al.* [206] simulate the evolution of the axionic string network using an efficient identification scheme of global strings in order to assess the energy spectrum and the axion decay constant, which is found to be $f_a \lesssim 3 \times 10^{11}$ GeV or $m_a \gtrsim 20 \mu\text{eV}$, while the string stretching parameter appearing in Eq. (174) is found to be $\xi = 0.87 \pm 0.14$. Klaer and Moore [211] have used the expertise in Refs. [210, 294] and developed a numerical scheme to handle on the lattice the large hierarchy $\log(f_a t_{\text{osc}}) \sim 70$ between the scale of the string core $f_a \sim r_c^{-1}$ and the string separation scale at the time when the axion acquires a mass of order $t_{\text{osc}} \sim H_{\text{osc}}^{-1}$. Using their technique along with the QCD susceptibility obtained in Ref. [126], Klaer and Moore find that the total axion production when strings are included is somewhat less efficient than in the angle-averaged misalignment case. They quote a value of the axion mass $m_a = (26.2 \pm 3.4) \mu\text{eV}$ [212]. Gorghetto *et al.* [213, 216] find an axion spectrum peaked at the energy of the order of the string core scale that, when extrapolated to the physical parameter region, would lead to a negligible number density of relic axions from strings. However, they also showed that the presence of small logarithmic corrections to the spectrum shape could completely alter such a conclusion, and their ongoing studies in this direction indicate that this might indeed be the case.³⁷ Buschmann *et al.* [215] have performed high-resolution simulations of the evolution of the PQ field starting at the epoch before the PQ phase transition and ending at matter-radiation equality, about the time at which axion miniclusters collapse. The value of the axion mass obtained from the simulations is $m_a = (25.2 \pm 11.0) \mu\text{eV}$. Both results in Refs. [213, 215] find a logarithmic deviation to the number of strings per Hubble patch from

³⁷G. Villadoro, private communication.

the scaling regime. Kawasaki *et al.* [295] estimate the abundance of CDM axions both from the misalignment mechanism and the decay of topological defects, obtaining the mass range $m_a = (115 \pm 25) \mu\text{eV}$ for the models with the domain wall number $N_{\text{DW}} = 1$. The results for the present axion energy density as a function of the axion mass obtained in Refs. [212, 215] are consistent with each other, while the results in Ref. [295] are larger by a factor of order ten. Such a discrepancy could be partially due to the explicit separation of the misalignment and string decay production mechanisms enforced in Ref. [295], which leads to an over-counting of the axion energy density [212]. The simulation by Vaquero *et al.* [214] differs from that in Ref. [215] for a number of details, including the use of the “fat” string scheme [296], initial condition, the measurement of the CDM energy density, the length and the details of the evolution to the matter-radiation equality. These results strongly depend on the choice of the temperature dependence of the QCD topological susceptibility. Refs. [206, 215, 295] have derived their results using a susceptibility with an index corresponding to $2\gamma = 6.68$ in Eq. (150), using the parametrisation in the Interacting Instanton Liquid Model [166]. This exponent is milder than what obtained in Ref. [126] for which, at temperatures $T \gg T_C$, $2\gamma = 8.2$. The bottom line is that, although the misalignment is the most model independent and best understood of all the axion CDM production mechanisms, no consensus has been achieved yet about the share of axion CDM ascribable to the misalignment mechanism with respect to the much less understood contributions from topological defects. This reflects in a large uncertainty in determining the real value for the axion mass that can fully saturate the DM density.

3.7.2. Pre-inflationary scenario

This scenario is realised whenever the PQ symmetry is spontaneously broken during inflation, $H_I < f_a$, and it is not restored afterwards [172]. In this scenario, the axion field is homogeneous through various Hubble patches, with a unique value of θ_i characterising the whole observable Universe. As shown in Fig. 2, each value of θ_i is related to a unique value of the DM axion mass. A global fit of this scenario [297] performed using the DarkBit module [298] of the GAMBIT numerical code [299] yields the DM axion mass range $0.12 \mu\text{eV} \leq m_a \leq 0.15 \text{ meV}$ at the 95% equal-tailed confidence interval of the marginalised posterior distribution accounting for the QCD axion (both the KSVZ and the DFSZ models) and taking into account results from various observations and experiments in the likelihood including the light-shining-through-wall experiments, helioscopes, cavity searches, distortions of gamma-ray spectra, supernovae, horizontal branch stars and the hint from the cooling of white dwarfs. An important assumption that impacts on the result is the choice for the prior on θ_i , which in Ref. [297] is assumed to be uniform over the interval $[-\pi, \pi)$.

Small initial values of θ_i might also occur naturally, i.e. without any fine tuning, in low-scale inflation models in which inflation lasts sufficiently long [300, 301]. If $H_I \lesssim \Lambda_{\text{QCD}}$ the axion acquires a mass already during inflation, the θ_i -distribution flows towards the CP conserving minimum and, for long durations of inflation, stabilises around sufficiently small θ_i values. As a result the QCD axion can naturally give the DM abundance for axion masses well below the classical window, down to $m_a \approx 10^{-12} \text{ eV}$ [300, 301].

Another way to suppress the value of the axion misalignment angle is by assuming a period in the early Universe during which the QCD coupling constant takes a value larger than the present one, allowing the color group to become strong for a certain period, during which therefore $m_a \gtrsim H$ [269] (see also [270]). The axion field is then dynamically driven to its minimum at early times. Attempts to realise this scenario have generally relied on supersymmetric models in which the gauge coupling constant is related to the expectation value of some moduli field, like the dilaton, that initially sits away from its true minimum and later adjusts to its present value. Ref. [302] questioned this possibility and concluded that, under generic conditions, an early phase of stronger QCD is not useful for raising the cosmological upper bound of the axion scale, although, as was mentioned in Section 3.5, it can still be effective for suppressing axion isocurvature fluctuations [268, 271]. The negative conclusion of Ref. [302] can however be circumvented, and a viable realisation in which $f_a \sim \mathcal{O}(10^{16} - 10^{17}) \text{ GeV}$ can be obtained has been recently given in Ref. [303].

Going in the opposite direction, values of the initial misalignment angle that are close to the hilltop of the potential $\theta_i \simeq \pi$ could drive the axion energy scale to values $f_a \lesssim 10^{12} \text{ GeV}$ ($m_a \gtrsim 10 \mu\text{eV}$), because of the relevance of the non-harmonic terms in the axion potential. With the choice $\pi - \theta_i \simeq 10^{-3}$, one obtains $f_a \approx 10^{10} \text{ GeV}$. It is possible that the axion field has been driven to such a value of θ_i during inflation.

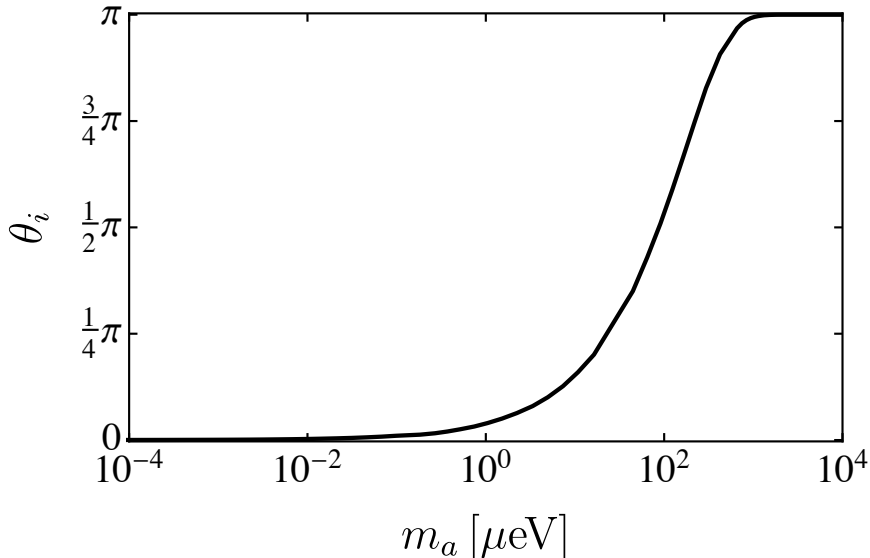


Figure 2: The relation between the DM axion mass and the initial misalignment angle in the pre-inflationary scenario.

This can be again obtained by enhancing the QCD confinement scale so that the axion acquires a potential during inflation [304], or by assuming that the inflation scale is below the QCD scale [305].

3.7.3. Summary of cosmological bounds

The various constraints on the parameter space of the QCD axion can be summarised as in Fig. 3, in which we focus on the KSVZ model (with $E/N = 0$ and $N_{\text{DW}} = 1$), and we show the axion energy scale f_a (left Y axis) as a function of the Hubble rate at the end of inflation H_I (bottom X axis). The parameter space of the DM axion depends on four quantities, namely the axion energy scale f_a , the initial misalignment angle θ_i , the Hubble rate during inflation H_I , and the contribution from topological defects to the total axion energy density $\alpha_{\text{tot}} \equiv \rho_a/\rho_a^{\text{mis}}$. For the QCD axion, the axion mass m_a is related to f_a as in Eq. (108), see the different grids used on the Y axes. For single-field inflation, the tensor-to-scalar ratio r is proportional to H_I^2 , as expressed in the top X axis. The parameter space is bound to the right by the non-detection of primordial gravitational waves by the *Planck*-BICEP2 joint analysis [263], which set an upper limit on the scale of inflation H_I . The axion energy scale f_a is bound from below by various astrophysical considerations, for example the duration of the neutrino burst from the supernova (SN) 1987A, see Fig. 11 and Section 4.4. This translates into an upper bound on the mass of the QCD axion. The phenomenon of superradiance excludes the portion of the axion mass given in Eq. (236) (see Section 4.6). The solid red line marks the watershed $f_a = H_I$ and separates the region where the axion is present during inflation (top-left region, pre-inflationary scenario) from the region where the axion field originates after inflation (bottom-right region, post-inflationary scenario). This line has to be thought as a qualitative bound between the two scenarios considered, since the exact details depend on the inflationary model, the preheating-reheating scenarios, and axion particle physics.

For $f_a \gtrsim H_I$ (pre-inflationary scenario), we show the values $\theta_i \in \{1, 10^{-1}, 10^{-2}, 10^{-3}\}$. The parameter space in this scenario is bound to the right by the non-observation of axion isocurvature fluctuations in the CMB by the *Planck* mission [251, 252, 310], subject to the requirement that axions constitute the DM. The change in the slope corresponds to the effect of the non-harmonic terms in the axion potential when $\theta_i \gtrsim \mathcal{O}(1)$ [188]. The possible presence of axion isocurvatures in the spectrum of the CMB relies on the fact that the PQ symmetry has never been restored after the end of inflation. For example, in the unified Standard Model–Axion–seesaw–Higgs portal inflation (SMASH) model of Refs. [311–313], although the axion

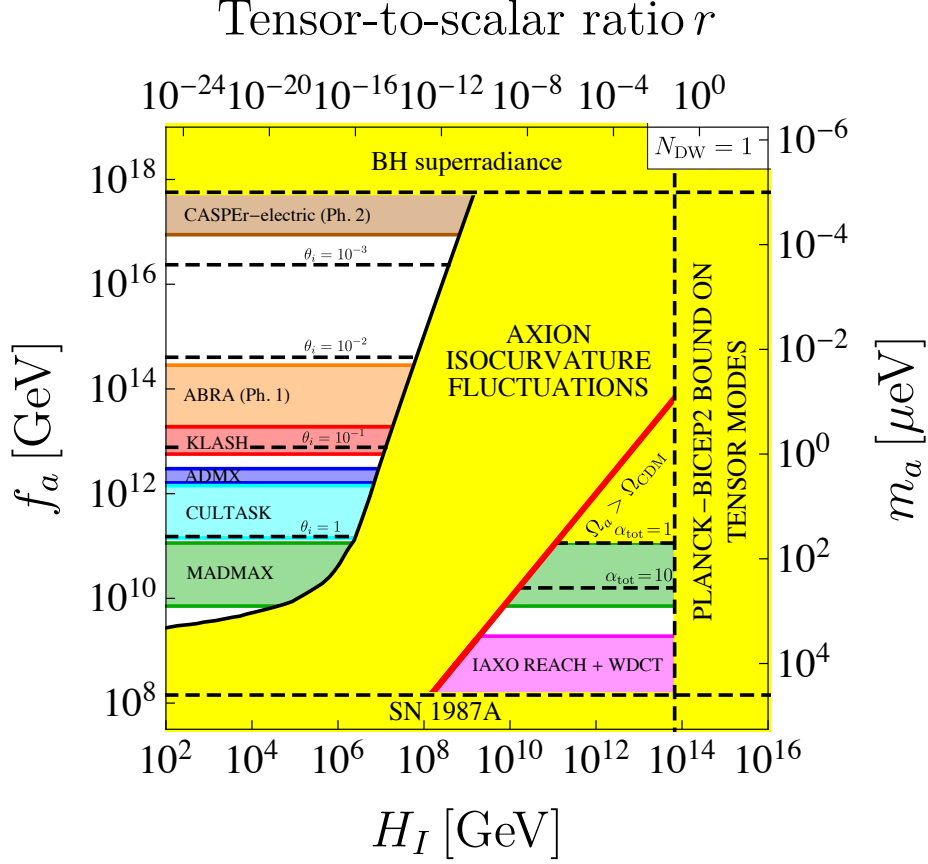


Figure 3: Region of axion parameter space where the axion constitutes the totality of the DM observed. The axion mass scale on the right corresponds to Eq. (51) for the case $N_{\text{DW}} = 1$. If the PQ symmetry breaks during inflation and the axion spectates inflation ($f_a \gtrsim H_I$, pre-inflationary scenario), axion isocurvature perturbations constrain the parameter space to the region on the top left, which is marked by the values of θ_i necessary to achieve the observed CDM density for a given value of f_a . If the PQ symmetry breaks after inflation ($f_a < H_I$, post-inflationary scenario), the axion is the CDM particle only for a specific value of f_a , which takes into account the contributions from the decay of topological defects α_{tot} . The lower bound on f_a results from astrophysical considerations [33, 35, 306, 307], the upper bound on f_a relies on the non-detection in LIGO of gravitational waves associated with the super-radiance phenomenon from stellar-mass black holes [308, 309], the upper bound on H_I comes from the non-observation of tensor modes in the CMB [251, 252, 310]. The coloured transparent bands indicate future reaches of planned or ongoing experiments covering the allowed regions of the parameter space: CASPER-Electric Phase 2 (bronze), ABRACADABRA (ABRA Ph.1, orange), KLASH (red), ADMX (blue), CULTASK (Cyan), MADMAX (green), and IAXO (magenta).

energy scale can be as large as $f_a \sim 4 \times 10^{16}$ GeV, the PQ symmetry is restored immediately after the end of inflation and isocurvature modes are absent. Caveats that allow to evade the bound from isocurvature fluctuations include the presence of more than one axion [314], or the identification of the inflaton with the radial component of the PQ field [315], see Section 7.3.

Note, that in single-field inflation models in which the axion constitutes the DM, the pre-inflationary scenario requires a value of the tensor-to-scalar ratio r which is well below the projected sensitivity of forthcoming cosmological surveys, $r \sim 10^{-3}$, which is forecast for example by the next-generation ground-based cosmic microwave background experiment CMB-S4 [316].³⁸ For example, an explicit realisation of an inflation model with an extremely low value of the tensor-to-scalar ratio $r \sim 10^{-13}$ such that the axion is

³⁸If the DM is in the form of QCD axions, a joint analysis of axion direct detection experiments and future CMB-S4

the DM has been recently presented in Ref. [317].

For $f_a \lesssim H_I$ (post-inflationary scenario), the axion is present during inflation as the Goldstone boson of the PQ field. The initial value of the misalignment angle is averaged out over many Hubble patches. We have used $\langle \theta_i^2 \rangle \approx (2.15)^2$ as in Ref. [47], and we show results for two cases: 1) $\alpha_{\text{tot}} = 1$ (no contribution from the decay of topological defects), and 2) $\alpha_{\text{tot}} = 10$, where the parameter $\alpha_{\text{tot}} \equiv \rho_a / \rho_a^{\text{mis}}$ parametrises the ratio of the present energy density in axions ρ_a to that coming from misalignment only ρ_a^{mis} . We have also reported the forecasts for the sensitivities of various experiments, either planned or already running, including the Cosmic Axion Spin Precession Experiment (CASPER) in its Phase 2 [318], A Broadband/Resonant Approach to Cosmic Axion Detection with an Amplifying B-field Ring Apparatus (ABRACADABRA) in its Phase 1 ($B_{\text{max}} = 5\text{ T}$ and Volume = 1 m^3) and in the resonant configuration [319, 320], the KLoe magnet for Axion Search (KLASH) [321, 322], the Axion Dark Matter Experiment (ADMX) [323–327], the region labeled CULTASK which combines the expected sensitivity of the Center for Axion and Precision Physics (CAPP) haloscope in both configurations CAPP-12TB and CAPP-25T [328, 329] (see also Ref. [330]), the Magnetized Disc and Mirror Axion eXperiment (MADMAX) [331], and the International Axion Observatory (IAXO) [332–334]. Notice that we have chosen the bounds from laboratory searches by setting the ratio $E/N = 0$ as in the original KSVZ model. Additional details on the experimental setups for axion helioscopes are given in Section 5.1, for axion haloscopes in Section 5.3, and for laboratory searches in Section 5.4.

3.8. QCD axions as dark radiation

So far, we have discussed the population of non-thermal axions that stems from the classical evolution of the axion field, which can represent an important contribution to the total amount of CDM. A thermal population of axion is also expected from more conventional production mechanisms like particle scatterings, and for the typical sub-eV range of axion masses it will represent a dark radiation component.

The energy density in relativistic particles at the epoch of matter-radiation decoupling is conventionally described in terms of an effective number of neutrino species N_{eff} as

$$\rho_{\text{rad}} \equiv \left[1 + \frac{7}{8} \left(\frac{T_\nu}{T_\gamma} \right)^4 N_{\text{eff}} \right] \rho_\gamma, \quad (191)$$

where ρ_γ is the energy density of the CMB photons, and $T_\nu/T_\gamma = (4/11)^{1/3}$ is the ratio of neutrino to photon temperature. If there are no new relativistic particles besides the three SM neutrinos the prediction is $N_{\text{eff}} = N_{\text{eff}}^{\text{SM}} = 3.045$ [335].³⁹ A new relativistic particle species, such as thermal axions, would then appear as a modification in the number of effective neutrinos N_{eff} :

$$\rho_{\text{rad}} = \rho_\gamma + \rho_\nu + \rho_a = \left[1 + \frac{7}{8} \left(\frac{T_\nu}{T_\gamma} \right)^4 N_{\text{eff}}^{\text{SM}} + \frac{1}{2} \left(\frac{T_a}{T_\gamma} \right)^4 \right] \rho_\gamma, \quad (192)$$

where ρ_ν and ρ_a are respectively the energy density of neutrinos and axions and T_a is the temperature of the thermal population of axions, characterised by one bosonic degree of freedom. Confronting Eq. (191) and Eq. (192) we see that the contribution of thermal axions would appear as an excess in effective number of neutrinos

$$\Delta N_{\text{eff}} \equiv N_{\text{eff}} - N_{\text{eff}}^{\text{SM}} = \frac{4}{7} \left(\frac{T_a}{T_\nu} \right)^4. \quad (193)$$

Several groups have provided estimates of N_{eff} by using cosmological data (see e.g. Refs. [274, 340, 341] and Refs. [274–276, 342–345] in particular for the contribution of thermal axions). The current best-fit value $N_{\text{eff}} = 2.99 \pm 0.17$ at 68% CL comes from combining *Planck* 2018 TT, TE, EE+lowE+lensing datasets plus

experiments is able to probe the range $2.5 \times 10^6 \lesssim H_I/\text{GeV} \lesssim 4 \times 10^9$ [316], which is otherwise not accessible through CMB tensor modes alone.

³⁹See also Ref. [336] where the value $N_{\text{eff}}^{\text{SM}} = 3.046$ was obtained, and Refs. [337–339] for earlier works.

Baryon Acoustic Oscillations (BAO) data [251]. This determination is fully consistent with the SM value, hence it constrains any additional contribution from dark radiation.

To evaluate quantitatively the possible effects of a thermal axion population on N_{eff} we need to estimate the ratio T_a/T_ν . Let us denote with Γ_a the rate of reactions that keep the axions in thermal equilibrium

$$\Gamma_a = \sum_i n_i \langle v \sigma_i \rangle, \quad (194)$$

where for simplicity we consider only two-body processes with cross sections $\sigma_i = \sigma(p_i a \leftrightarrow p_j p_k)$ with p_i, p_j, p_k particle species in thermal equilibrium, n_i the number density of p_i , $v \approx 1$ the velocity of scatterers assumed to be relativistic, and the brackets denote a thermal average. Axions decouple from the thermal bath when the reaction rate Γ_a falls below the Hubble expansion rate, and after decoupling they maintain a thermal distribution which remains unaffected by other phenomena occurring in the plasma. Let us consider a decoupling temperature T_d for which the number of entropy degrees of freedom, including the axion, is $g_S(T_d) + 1$ and all the particles share the same temperature. At a temperature T_2 well below 1 MeV only the photon ($g_\gamma = 2$), the three SM neutrinos ($\sum_i g_{\nu_i} = 6$) and the axion ($g_a = 1$) are relativistic, with respective temperatures $T_\gamma = T_2$, $T_\nu = \left(\frac{4}{11}\right)^{1/3} T_\gamma$ and T_a . Including statistical factors, entropy conservation gives

$$[g_S(T_d) + 1] (T_d a_d)^3 = \left[2 \left(\frac{T_\gamma}{T_a} \right)^3 + \frac{7}{8} 6 \left(\frac{T_\nu}{T_a} \right)^3 + 1 \right] (T_a a_2)^3, \quad (195)$$

where a_d and a_2 are the cosmological scale factors at the respective temperatures T_d and T_2 . Since axions do not get reheated by subsequent particle annihilation, their temperature simply scales as $T \propto a^{-1}$ so that $T_1 a_1 = T_a a_2$. Eq. (195) then gives

$$\frac{T_a}{T_\nu} = \left\{ \frac{2}{g_S(T_d)} \left[\left(\frac{T_\gamma}{T_\nu} \right)^3 + \frac{21}{8} \right] \right\}^{1/3} = \left(\frac{43}{4 g_S(T_d)} \right)^{1/3}, \quad \Delta N_{\text{eff}} \simeq 0.027 \left(\frac{106.75}{g_S(T_d)} \right)^{4/3}, \quad (196)$$

where in the second equation we have normalised g_S to the total number of SM degrees of freedom $g_S(T > m_t) = 106.75$. Finally, in terms of the present number density of CMB photons $n_\gamma \simeq 411 \text{ cm}^{-3}$ the number density of thermal axions is easily obtained as $n_a \simeq (43/22) n_\gamma / g_S(T_d)$.

In the early Universe, there are various processes involving different types of particles which can produce a thermal population of axions [346–349]. Interactions with the gluons exist for any type of axion and are model independent. Coloured fermions interacting with the axion are also a necessary ingredient of any axion model, but in this case there is a difference if these states are exotic and heavy, as in KSVZ models ($m_Q \propto v_a$) or if they are instead SM quarks and much lighter, as in DFSZ models ($m_q \propto v \ll v_a$). Also, the axion mixes with the neutral pion and this gives rise to an axion-pion interaction (see the discussion in Section 2.5.2). This interaction can be particularly important when, at temperatures $m_\pi \lesssim T \lesssim T_C$, the abundance of pions in the plasma is of the order of the photon abundance. Let us discuss these thermalization channels in more detail.

Axion-gluon coupling. The relevant processes for axion thermalization involving the axion coupling to the gluons are (i) $a q \leftrightarrow g q$ and $a \bar{q} \leftrightarrow g \bar{q}$, (ii) $a g \leftrightarrow q \bar{q}$, (iii) $a g \leftrightarrow g g$, all of which have a cross section of order

$$\sigma_{ag} \simeq \frac{\alpha_s^3}{8\pi^2} \frac{1}{f_a^2}. \quad (197)$$

At temperature well above m_t all the six quark flavours populate the thermal bath, then, including the statistical factor 3/4 for the fermion number densities, for reaction (i) with quark and antiquarks we have $n_q + n_{\bar{q}} = 54 n_{\text{eq}}$, while (ii) and (iii) contribute a factor $2n_g = 32 n_{\text{eq}}$, where $n_{\text{eq}} = \frac{\xi(3)}{\pi^2} T^3$ is the equilibrium distribution for one bosonic degree of freedom, ξ is the Riemann zeta function and $\xi(3) \approx 1.2$. From this

and by using the cross section Eq. (197) we can estimate the total scattering rate Γ_a Eq. (194). Recalling the expression for H given in Eq. (147) the decoupling condition $\Gamma_a \lesssim H$ yields

$$T_d \simeq 12.5 \frac{\sqrt{g_*(T)}}{\alpha_s^3} \frac{f_a^2}{m_{\text{Pl}}} \simeq 4.0 \cdot 10^{11} \left(\frac{f_a}{10^{12} \text{ GeV}} \right)^2 \text{ GeV}, \quad (198)$$

where in the second relation we have used $g_*(T) = 106.75 + 1$ and $\alpha_s(T) \simeq 0.03$ which are the values appropriate for temperatures of the order $10^{11} \div 10^{12}$ GeV. From Eq. (198) we obtain $\Delta N_{\text{eff}} \simeq 0.027$ and $n_a \simeq 7.5 \text{ cm}^{-3}$ for the present abundance of thermal axions. Let us note, however, that since above the PQ breaking scale there is no axion, this result is only valid for $T_d < v_a = 2Nf_a$, that is for $f_a \lesssim 4N \cdot 10^{12}$ GeV. Also, if the scale of inflation and the reheating temperature are below T_d , this thermal population gets inflated away. It is then important to consider other processes that can be effective for producing a thermal axion population at lower temperatures.

Axion-quark coupling. The Compton-like scattering process $qg \leftrightarrow qa$ and its CP conjugate, which involve the axion coupling to coloured states, can be important as long as $T \gtrsim m_q$ when the coloured fermions are relativistic (for $T < m_q$, Γ_a is Boltzmann suppressed by n_q). Since the axion coupling to the KSVZ quarks is parametrically larger than the coupling to SM quarks by a factor $\sim v_a/v$ we concentrate on this case. The cross section is

$$\sigma_{aQ} \simeq \alpha_s \left(\frac{m_Q}{v_a} \right)^2 \frac{1}{T^2}, \quad (199)$$

and using $n_Q + n_{\bar{Q}} = 9 n_{\text{eq}}$ the decoupling condition yields

$$T_d \simeq 3 \cdot 10^8 \left(\frac{m_Q}{10^8 \text{ GeV}} \right)^2 \left(\frac{10^{12} \text{ GeV}}{v_a} \right)^2 \text{ GeV}, \quad (200)$$

where we have used $\alpha_s \approx 0.05$ valid for temperatures around $T \approx 10^8$ GeV. The resulting values of ΔN_{eff} and n_a are only slightly smaller than in the previous case if entropy injection from Q decays into SM particles is taken into account (see Section 6.1.1 for a discussion on this point). Note however, that the requirement $T_d > m_Q$ implies that this result holds only for $m_Q \gtrsim 3 \cdot 10^7 \left(\frac{v_a}{10^{12} \text{ GeV}} \right)^2$.

Axion-pion and axion-nucleon couplings. There are also processes that can keep axions in thermal equilibrium after the quark-hadron phase transition, and that could be important because in this case it is unlikely that the corresponding population of thermal axions could be wiped out by inflation. The most model independent mechanisms are pion-axion conversion $\pi\pi \leftrightarrow \pi a$, whose interaction term is described by Eq. (57), and scatterings involving nucleons $N\pi \leftrightarrow Na$, with $N = n, p$. The corresponding cross sections were computed in Ref. [110]. The rates of these two processes have a different behaviour with the temperature, and in particular scattering off nucleons becomes subdominant below $T \lesssim 200$ MeV because of the exponential suppression in the number density of protons and neutrons. For the pion channel Ref. [342] gives the following expression based on dimensional considerations and with numerically fitted coefficients:

$$\Gamma_{a\pi} \simeq 0.215 C_{a\pi}^2 \frac{T^5}{f_a^2 f_\pi^2} h\left(\frac{m_\pi}{T}\right), \quad (201)$$

with $C_{a\pi}$ given in Eq. (58), and $h(x)$, normalised as $h(0) = 1$ a rapidly decreasing function of its argument. To give an example of the values of f_a for which axion thermalisation can occur after the QCD phase transition, let us fix $T_d = T_C \simeq 160$ MeV, in which case we have $g_* = 17.25$ and $h\left(\frac{m_\pi}{T_C}\right) \simeq 0.8$, and let us consider the hadronic axion with $C_{a\pi} \simeq 0.12$, see Eq. (115). This decoupling temperature is obtained for $f_a \simeq 3 \times 10^7$ GeV which, as we will see in Section 4, is in conflict with various astrophysical bounds. Phenomenologically acceptable values of f_a would imply higher decoupling temperatures $T_d \gg T_C$ for which, however, nucleons and pions are deconfined into the fundamental QCD degrees of freedom and the previous

analysis breaks down.

We have seen that when axion thermalization occurs above the electroweak phase transition, one can expect a contribution $\Delta N_{\text{eff}} \sim 0.027$. Other processes not considered here, as the Primakoff process $\gamma q \leftrightarrow a q$ that could be enhanced by a large value of the axion-photon coupling, or reactions involving the SM quarks [345, 349] or leptons [350], for which large enhancements of the model-dependent couplings can be obtained within some type of construction (see Section 6), could contribute to thermalize the axions at lower temperatures, implying larger contributions to N_{eff} . In particular, the sensitivity of future cosmological measurements to axion couplings to all the SM degrees of freedom has been assessed in [351]. A hot axion component generated in this way has been also invoked [350] to alleviate the existing discrepancies between early and the late Universe determination of the Hubble constant H_0 (see Ref. [352] for a recent review). Projected sensitivities of forthcoming experimental determinations of N_{eff} suggest that axion contributions to the radiation density at the level of a few percent might still be detectable. In particular, conservative configurations of the next generation of ground-based CMB experiments, CMB-S4 [316], can reach a sufficient accuracy in the measurement of N_{eff} to test the minimal contribution of axions (or of any other light particle with zero spin thermalised above the electroweak phase transition) at the 1σ level. N_{eff} is indeed a unique measurement in cosmology. The overall importance of precise determinations of this observable cannot be understated and, as we have seen, it can provide fundamental information also on axion phenomenology.

3.9. Axion miniclusters and axion stars

An important feature of the post-inflationary scenario is that at the time when the axion acquires a mass, around $T \sim T_{\text{osc}}$ (see Section 3.3) the value of the initial misalignment angle θ_i changes by $\mathcal{O}(1)$ from one causal patch to the next. Accordingly, the density of cold axions produced by the misalignment mechanism is characterised by sizeable inhomogeneities $\delta\rho_a/\rho_a \sim \mathcal{O}(1)$. The free streaming length of the misalignment population of cold axions is too short to erase these inhomogeneities before the time t_{eq} of matter-radiation equality, so that at $T \sim T_{\text{eq}}$ the density perturbations decouple from the Hubble expansion and start growing by gravitational instability, rapidly forming gravitationally bound objects, called axion miniclusters [353–356]. The scale of minicluster masses is set by the total mass in axions within one Hubble volume of radius $2R_{\text{osc}} \sim H_{\text{osc}}^{-1} = \sqrt{\frac{3m_{\text{Pl}}^2}{8\pi\rho_{\text{osc}}}}$ at the time when the axion mass becomes relevant, since after the onset of oscillations the number of cold axions per comoving volume remains conserved. At T_{osc} the Universe energy density is radiation dominated so that $\rho_{\text{osc}} \simeq \rho_{\text{rad}} = \frac{\pi^2}{30}g_*T_{\text{osc}}^4$. The energy enclosed in a Hubble volume then is

$$M_{\text{rad}}(T_{\text{osc}}) = \frac{4\pi R_{\text{osc}}^3}{3} \rho_{\text{rad}} = \frac{3}{32\pi} \sqrt{\frac{5}{\pi g_*}} \frac{m_{\text{Pl}}^3}{T_{\text{osc}}^2}. \quad (202)$$

As the Universe expands, the energy in radiation gets redshifted, and at the matter-radiation equality temperature T_{eq} it provides an estimate of the gravitationally bound minicluster mass $M_{\text{MC}} \approx M_{\text{rad}}(T_{\text{eq}})$, that is

$$M_{\text{MC}} \approx M_{\text{rad}}(T_{\text{osc}}) \frac{T_{\text{eq}}}{T_{\text{osc}}} \simeq 1.3 \times 10^{46} \left(\frac{800 \text{ MeV}}{T_{\text{osc}}} \right)^3 \frac{T_{\text{eq}}}{0.8 \text{ eV}} \text{ GeV} \approx 10^{-11} M_{\odot}, \quad (203)$$

where we have used $g_*(T_{\text{osc}}) = 61.75$, and $M_{\odot} \approx 2 \cdot 10^{30} \text{ kg} = 1.3 \cdot 10^{57} \text{ GeV}$ represents one solar mass. The typical radius of the overdensities when they decouple from the Hubble flow at T_{eq} is also easily estimated. From $R_{\text{osc}} \approx 0.1 \text{ km}$ as is obtained from the expression given above Eq. (202) and using entropy conservation $(R_{\text{eq}}T_{\text{eq}})^3 g_S(T_{\text{eq}}) = (R_{\text{osc}}T_{\text{osc}})^3 g_S(T_{\text{osc}})$ gives

$$R_{\text{MC}} \approx R_{\text{eq}} = R_{\text{osc}} \frac{T_{\text{osc}}}{T_{\text{eq}}} \left(\frac{g_S(T_{\text{osc}})}{g_S(T_{\text{eq}})} \right)^{1/3} \approx 2.5 \cdot 10^8 \text{ km}, \quad (204)$$

where we have used $g_S(T_{\text{eq}}) \simeq 3.91$. The numbers in Eqs. (203) and (204) are of course indicative and can easily vary by a couple of orders of magnitude. For example it was recently argued in Ref. [357] that the characteristic size of the density fluctuations is smaller than the Hubble horizon at T_{osc} , implying that

typical miniclusters are both lighter and smaller with respect to the quoted numbers.⁴⁰ The dynamics of the collapse of non-linear density fluctuations that leads to the formation of axion miniclusters has been recently assessed through a semi-analytical Press-Schechter approach [357, 360, 361] or by numerical simulations [214, 215, 362].

Axion miniclusters would lead to important detection features. First, their typical density $\rho_{\text{MC}} \simeq 3M_{\text{MC}}/(4\pi R_{\text{MC}}^3) \approx 0.2 \times 10^6 \text{ GeV cm}^{-3}$ is about a factor 10^6 larger than the local DM density, so that in an encounter with the Earth the rate of conversion of axions into photons in dedicated resonant cavities or haloscopes (see Section 5.3), would be accordingly temporarily enhanced [27]. The expected signal would be time-dependent due to the revolution and rotation motions of the Earth, which leads to a detectable annual modulation [363] and possibly even to a detectable diurnal modulation [364]. Since the cavity would have to be tuned to the correct frequency in order to capture the signal, a broadband axion cavity resonator has been proposed to exploit this possibility, see Ref. [39]. Second, the presence of axion miniclusters could be assessed through picolensing of individual clusters [365], or microlensing of a halo formed of axion miniclusters that hierarchically merge [360, 361]. This latter possibility could also be used to assess the fraction of cold axions that are bound into clumped objects, a fraction that can also be accessed through numerical simulations. Third, axion minicluster could be disrupted by the gravitational field of a nearby star encounter, or by the mean galactic gravitational field, leading to tidal streams of axions that would enhance the local CDM density by about one order of magnitude [366].

As we have seen in Section 3.3 when $m(t_{\text{osc}}) \simeq 3H(t_{\text{osc}})$ a non-relativistic and cold population of axions ($\langle p_a \rangle \ll m_a \ll T_{\text{osc}}$) is created. Using as reference values $T_{\text{osc}} \sim 1 \text{ GeV}$ and $f_a \sim 10^{12} \text{ GeV}$ their number density can be estimated as $n_a(T) = m_a(T_{\text{osc}}) f_a^2 \frac{s(T)}{s(T_{\text{osc}})} \simeq \frac{3 f_a^2}{m_{\text{Pl}} T_{\text{osc}}} T^3 \sim 10^5 T^3$. This corresponds to a huge value of the initial phase-space density $\mathcal{N}_a \sim n_a / \langle p_a \rangle^3 \gg 10^5 (T_{\text{osc}}/m_a)^3 \approx 10^{47}$ which, given that effects of collisions are completely negligible, remains enormous at all subsequent times during the Universe expansion. Around the time of matter radiation equality gravitational instabilities grow and bound systems can form. As we have seen in Section 3.2 axions have an attractive self-interaction and, although extremely tiny $\sim (m_a/f_a)^4$, it can still produce significant effects due to the large phase space density, causing in particular a relaxation of gravitationally bound axions clouds. If the relaxation is efficient, an *axion star* could form within a time scale compatible with the age of the Universe. The possibility of formation of axion stars was first studied in Ref. [367]. Axion stars can be modelled as oscillaton-like solutions of the Klein-Gordon equation associated with the axion potential in Eq. (50) and coupled to the Einstein or Poisson equation to account for the feedback into the gravitational field. Contrarily to axion miniclusters, the mass of the axion star is not fixed once setting the mass of the QCD axion. The typical mass of the axion star is fixed once a formation mechanism is imposed [368, 369]. Axion stars are described by a real pseudo-scalar field that oscillates with time, with a frequency that is related to the mass of the axion. This configuration is different from what is obtained from a self-gravitating condensate made of a *complex* boson field, which is known in the literature as a ‘boson star’ [370, 371]. Both configurations possess black hole-like solutions for a null field and, in the case of the complex scalar field of mass m_ϕ , the boson star cannot grow to masses larger than the critical mass $M_* = 0.633/(Gm_\phi)$ [372]. If the axion potential were quadratic as in Eq. (151), the axion star would also possess a slightly smaller critical mass $M_* = 0.607/(Gm_a)$ [373], see also Ref. [374].

The formation of axion stars might proceed either by gravitational cooling out of the virialised minicluster or during a process of violent relaxation [369, 375–377], leading to a solution in the weak gravity regime [378, 379], with the mass and the radius of the axion star being related by [371, 379, 380]

$$R_{\text{as}} = \frac{9.9}{Gm_a^2 M_{\text{as}}} . \quad (205)$$

This solution is known in the literature as the “dilute” regime, since the average energy density inside the axion star is much smaller than the energy scale $(m_\pi^2 f_\pi^2)^{1/4}$ at which the axion potential saturates. As the

⁴⁰Even larger variations in mass and size are obtained when considering non standard cosmological scenarios, as was done for example in Refs. [358, 359].

density of the star increases, self-interactions become more relevant and destabilise the equilibrium when the mass of the star approaches the critical value [374, 381, 382]

$$M_{\text{as,crit}} \approx 18.4 m_{\text{Pl}} \frac{f_a}{m_a}. \quad (206)$$

This result is valid for an axion field moving in the potential described in Eq. (54) with $m_u/m_d = 0.48$.

4. Astrophysical signatures and bounds

Astrophysics, and stellar evolution in particular, offer powerful methods to probe the axion couplings to SM fields [32, 33, 383]. The observational properties of stars are conveniently shown in the Hertzsprung Russell (HR) or Color Magnitude Diagram (CMD), which shows the stellar luminosity (or magnitude) versus the surface temperature (expressed through the colour index).

No matter their initial mass, stars spend most of their life burning H into He in their core (main sequence). The post main sequence evolution depends on the stellar initial mass. A schematic picture of this evolution is shown in the left panel of Fig. 4. After the hydrogen in the core is exhausted, stars of roughly the same mass as our Sun enter the subgiant phase, burning hydrogen in a thick shell. It follows the Red Giant Branch (RGB) stage, with hydrogen burning in a thin shell surrounding an inert He core. The evolution in the RGB continues until the temperature in the core is high enough to ignite the He in the core (He-flash). Afterwards, the star moves to the Horizontal Branch (HB) region of the diagram. Such low mass stars never reach the conditions (temperature and density) required to ignite heavier elements and end up as carbon-oxygen White Dwarfs (WDs).

Stars a few times the mass of the Sun do not undergo a He-flash and ignite helium soon after the end of the main sequence stage, transitioning to the cold (red) region of the HR diagram. The evolution during

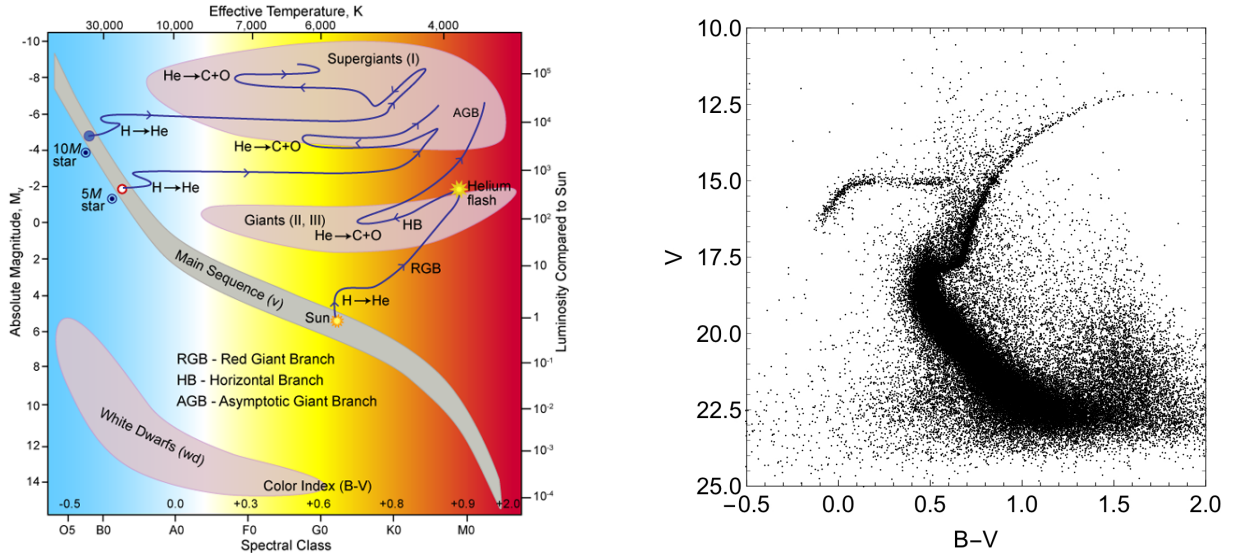


Figure 4: In the left panel, the theoretical Hertzsprung Russell (HR) or Color Magnitude Diagram (CMD), showing the evolution of luminosity and surface temperature of stars with different initial masses. To the right, the observational CMD of the M5 globular cluster, which shows the luminosity and surface temperature of stars at a fixed time (isochrones). More massive stars evolve more rapidly and are found in more advanced stages. The density of stars in different regions of the observational CMD reflects the duration of the corresponding evolutionary stage. The luminosity (energy emitted per unit time) is conventionally measured in magnitude. In the figures we show the magnitude in the visual (V) band. The surface temperature is shown as the B-V color, that is the difference between the blue (B) and visible (V) brightness. Note that, for historical reasons, the temperature increases toward the left of the diagram. So, stars with higher surface temperature (blue) are found to the left. See text for more details. The figure to the left is reproduced (with permission) from <https://physics.aps.org/articles/v2/69>.

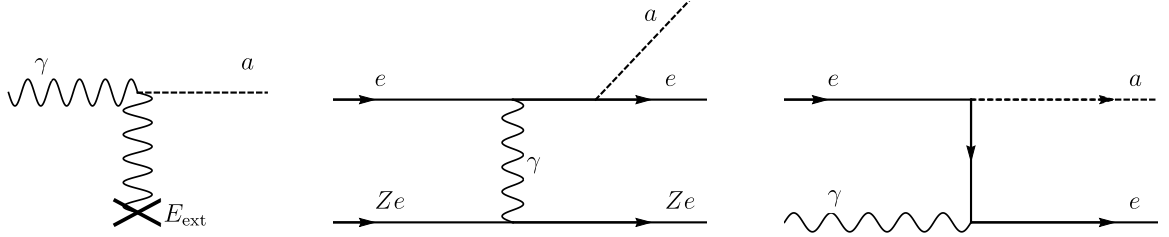


Figure 5: From left to right: axion Primakoff processes in an external electric field; axion bremsstrahlung process; and Compton processes. In the case of the bremsstrahlung process, Ze represents either an ion or an electron.

the He-burning stage may show a peculiar journey to the bluer region of the diagram and back, called the blue loop (see, e.g., the $5 M_{\odot}$ track in the left panel of Fig. 4). Stars with an initial mass larger than about $8 M_{\odot}$ do not become WD but undergo a core collapse, giving rise to a type II Supernova (SN) explosion and leaving a compact Neutro Star (NS) or, if very massive, a black hole.

The diagram in Fig. 4 is theoretical. It shows the evolutionary tracks of individual stars. Observationally, one extracts colour and magnitude of individual stars (at a fixed time) and shows the results in a diagram similar to the one shown in the right panel of Fig. 4. From the stellar population it is possible to reconstruct the evolutionary times of each stage (the longer the evolutionary time, the larger the stellar population corresponding to that phase), which can then be compared with the theoretical predictions extracted from numerical stellar evolution codes.

The method presents evident difficulties related to statistics (particularly for fast evolutionary stages), stellar contamination, interstellar absorption of the stellar light, etc. Nevertheless, numerical simulations reproduce with a remarkable level of agreement the observed CMD of particular stellar populations and allow to set stringent bounds on new physics. The emission of axions (or other light particles) from stars might, in fact, impact their expected evolution and spoil the agreement with observations.

The aim of this section is to provide an updated summary of the bounds on axions derived from stellar astrophysics considerations. In addition, we will briefly present the results of the axion interpretation of some observations of anomalous stellar evolution that have been reported in the last two decades (see, e.g., references [35, 297, 384] for more detailed discussions). Our general approach will be to present first all the results in a model independent way. The impact on the axion benchmark models (KSVZ and DFSZ-type) will also be discussed at the end of the section.

4.1. Axion-photon coupling

In the contest of stellar evolution, the most relevant process induced by the axion-photon coupling, $g_{a\gamma}$ (Section 2.5.3) is the Primakoff process (Fig. 5), consisting in the conversion of thermal photons in the electrostatic field of electrons and nuclei

$$\gamma + Ze \rightarrow a + Ze. \quad (207)$$

Neglecting degeneracy effects and the plasma frequency (a good assumption in plasma conditions when the Primakoff process is the dominating axion production mechanism), it is possible to provide a semi-analytical expression for the energy-loss rate per unit mass in axions [385]:

$$\varepsilon_P \simeq 2.8 \times 10^{-31} Z(\xi^2) \left(\frac{g_{a\gamma}}{\text{GeV}^{-1}} \right)^2 \frac{T^7}{\rho} \text{ erg g}^{-1} \text{ s}^{-1}, \quad (208)$$

where T and ρ are in K and in g cm^{-3} respectively. The coefficient $Z(\xi^2)$ is a function of $\xi^2 \equiv (\kappa_S/2T)^2$, with κ_S being the Debye-Huckel screening wavenumber. It can be explicitly expressed as an integral over the photon distribution (see Eq. (4.79) in Ref. [32]). Ref. [385] proposed the analytical parametrization

$$Z(\xi^2) \simeq \left(\frac{1.037\xi^2}{1.01+\xi^2/5.4} + \frac{1.037\xi^2}{44+0.628\xi^2} \right) \ln \left(3.85 + \frac{3.99}{\xi^2} \right), \quad (209)$$

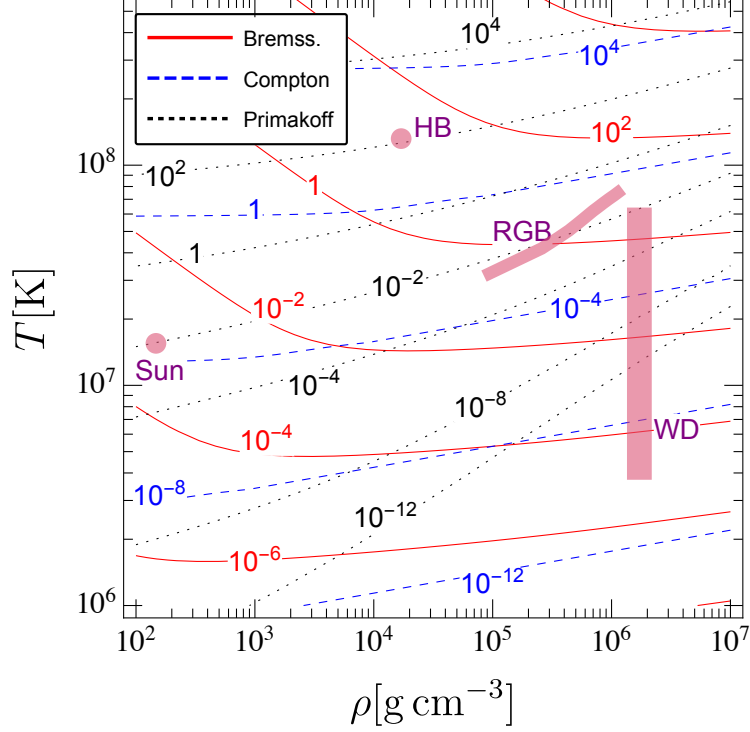


Figure 6: Contours of the axion energy-loss rates per unit mass, ϵ_a , in $\text{erg g}^{-1} \text{s}^{-1}$, for a pure He plasma. Different lines represent different channels, as shown in the legend. The Primakoff process is calculated for $g_{a\gamma} = 0.65 \times 10^{-10} \text{GeV}^{-1}$, corresponding to the bound from HB stars [386, 387]. The Bremsstrahlung and Compton processes are calculated for $g_{ae} = 4.3 \times 10^{-12}$, corresponding to the RGB bound from M5 [307]. The onset of the degeneracy region is visible in the bending of the bremsstrahlung contours. The central temperature and density of the Sun [388], RGB stars, HB stars and WDs are also shown, for reference. In the case of HB and RGB, these are the result of a numerical simulation of a $0.8 M_{\odot}$ model as obtained with the FuNS code [389]. The WD region is estimated using a polytropic model of WDs with mass from 0.6 to $0.7 M_{\odot}$, as discussed in Ref. [383], and spans luminosities in the range between 0.5×10^{-4} and $0.5 L_{\odot}$. Except for the WD case, the thickness of the lines has no significance.

which is better than 2% over the entire range of ξ . In general, $Z(\xi^2)$ is $\mathcal{O}(1)$ for relevant stellar conditions. For example, in the core of the Sun, $\xi^2 \sim 12$ and $Z \sim 6$ and in the core of a low-mass He burning star, $\xi^2 \sim 2.5$ and $Z \sim 3$ [32], while in a $10 M_{\odot}$ He burning star, $\xi^2 \sim 0.1$ and $Z \sim 0.4$ [385].

As shown in Fig. 6, the Primakoff process has a steep dependence on the stellar temperature, which controls the number of thermal photons, but is suppressed at high density because of the effects of a large plasma frequency and of the reduction of electron targets [390] (in such conditions, Eq. (208) ceases to be valid). Hence, this process is strongly suppressed in the degenerate core of WDs and RGB stars. Indeed, the strongest bounds on the axion-photon coupling are derived from the analysis of stars with a low density and high temperature core. In the following, we present the relevant stellar arguments used to constrain this coupling.

The Sun. Given its low density and, more importantly, its proximity, the Sun provides a good environment to test the axion-photon coupling. Moreover, as we shall see, the Sun is an important source for axions to be detected in terrestrial experiments (see Section 5.1). The (number) spectrum of axions produced in the Sun is shown in the left panel in Fig. 7. Interestingly, the axion spectra produced by processes induced by the axion-photon and the axion-electron couplings are similar, if we consider couplings of the order of the

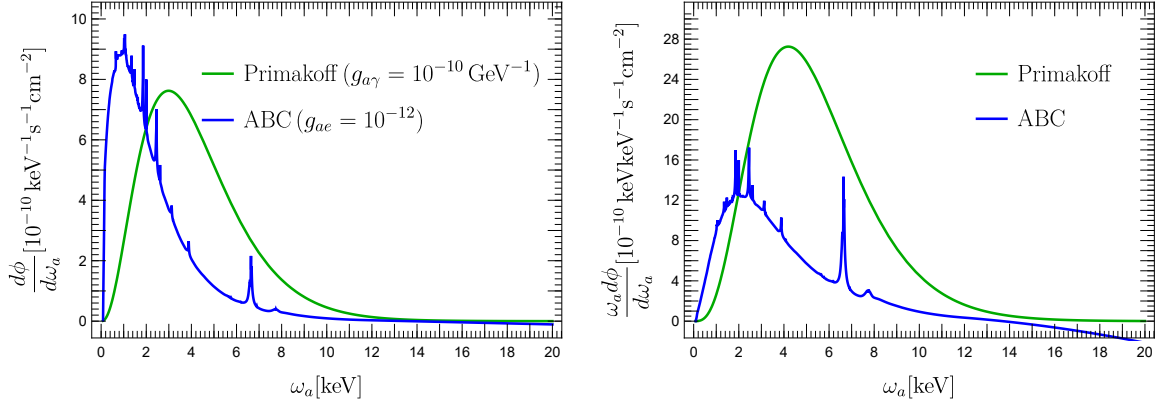


Figure 7: Solar axion spectrum. To the left shows the axion number and to the right the axion energy. The couplings are the same in both graphs.

current bounds (cf. Section 4.2 for the astrophysical bounds on the axion-electron coupling). This is a very impactful result for experimental searches, as we discuss in Section 5.1. For considerations about stellar cooling, however, the relevant quantity is the axion luminosity, not the axion number, and this is dominated by Primakoff axions since they are, in average, more energetic (cf. right panel of Fig. 7).

Strong bounds on exotic cooling processes in the Sun can be set from helioseismological considerations [391, 392]. The current bound is $g_{a\gamma} \leq 4.1 \times 10^{-10} \text{ GeV}^{-1}$ at 3σ [392], which corresponds to $g_{a\gamma} \leq 2.7 \times 10^{-10} \text{ GeV}^{-1}$ at 2σ . A somewhat weaker bound, $g_{a\gamma} \leq 7 \times 10^{-10} \text{ GeV}^{-1}$, was inferred in Ref. [393] from the axion impact on solar neutrinos.

R-parameter and HB stars. The major problem with the Sun as a source for axions is the relatively low temperature of its core. This limits strongly the Primakoff emission rate. Stars in the HB stage, which follows the RGB phase, have a low core density of about 10^4 g cm^{-3} and a high temperature (see Fig. 6), providing excellent conditions to produce axions through the Primakoff process.

To assess the effects of axions on the evolution of HB stars, it is convenient to introduce the R -parameter, defined as the ratio of the number of stars in the HB and in the upper portion of the RGB: $\mathcal{R} = N_{\text{HB}}/N_{\text{RGB}}$. In the presence of axions, this parameter is expected to be

$$\mathcal{R} = \mathcal{R}_0(Y) - F_{a\gamma} \left(\frac{g_{a\gamma}}{10^{-10} \text{ GeV}^{-1}} \right) - F_{ae} \left(\frac{g_{ae}}{10^{-12}} \right), \quad (210)$$

where $\mathcal{R}_0(Y)$ is a function of the helium abundance (Y) in the GC and the F are some positive-defined functions of the axion couplings.⁴¹ For completeness, we are including the contribution from processes induced by the axion coupling to photons, $g_{a\gamma}$, as well as the axion coupling to electrons, g_{ae} , which will be reviewed in more detail in Section 4.1. The positivity condition of the F insures that the axion emission can only lower the value of the R -parameter and that there could be a degeneracy between the effects of the axion couplings to electrons and photons. Although at the present a full numerical study that includes

⁴¹It is easy to infer that $F_{a\gamma}$ must be positive. A finite axion-photon coupling would contribute to the stellar energy-loss, particularly in the HB stage, since Primakoff is suppressed in the degenerate plasma typical of the RGB core. Thus, a large $g_{a\gamma}$ would shorten the life of HB stars and, consequently, their expected numbers in a cluster. The argument for the positivity of F_{ae} goes as follows. An efficient energy-loss channel, such as the one induced by a large coupling of axions to electrons, would delay the He-ignition in the RGB core (He-flash), allowing the core to grow more, and ultimately increasing the luminosity of the RGB tip and the number of RGB stars. The impact of a finite g_{ae} on the energy-loss in HB star is considerably less significant.

axions coupled to both electrons and photons does not exist, reference [394] provided approximate analytical expressions for the F in Eq. (210):

$$\mathcal{R}_0(Y) = 0.02 + 7.33 Y; \quad (211)$$

$$F_{a\gamma}(x) = 0.095\sqrt{21.86 + 21.08 x}; \quad (212)$$

$$F_{ae}(x) = 0.53 x^2 + 0.039 \left(\sqrt{1.23^2 + 100 x^2} - 1.23 - 4.36 x^{3/2} \right). \quad (213)$$

Neglecting the axion-electron coupling and adopting the value $Y = 0.2535$ for the helium abundance [395], reference [386] derived the upper bound on the axion-photon coupling

$$g_{a\gamma} < 0.66 \times 10^{-10} \text{ GeV}^{-1} \quad (95\% \text{ CL}) . \quad (214)$$

This is known as the HB bound,⁴² since by neglecting the axion-electron coupling we are essentially ignoring the RGB evolution. In addition to the result in Eq. (214), the analysis in [386] inferred an R parameter somewhat larger than observed, indicating a 2σ preference for a small, non-vanishing axion-photon coupling, later confirmed in [387] using an updated value of the He abundance [396, 397]. The result,

$$g_{a\gamma} = (0.29 \pm 0.18) \times 10^{-10} \text{ GeV}^{-1} \quad (68\% \text{ CL}), \quad (215)$$

is known as the HB hint.

Massive Stars. Further insights on the axion-photon coupling can be extracted from the analysis of intermediate mass stars, $M \sim 8 - 12M_\odot$ [385, 398]. As discussed at the beginning of this section, the (core) He burning stage of these stars is characterized by a migration toward the blue (hotter) region of the CMD and back. This journey is known as the *blue loop*. The existence of the loop is corroborated by many astronomical observations. In particular, this stage is essential to account for the observed Cepheid stars (see, e.g., [399]). The disappearance of the blue loop stage in the luminosity ranges where Cepheid stars are observed is forbidden [398]. A nonvanishing axion-photon coupling would reduce the time a star spends in the blue loop stage and, consequently, the number of *blue* versus *red* stars of a given luminosity. According to the analysis in [385], based on numerical simulations of solar metallicity stars in the $8 - 12M_\odot$ mass range, a coupling larger than $\approx 0.8 \times 10^{-10} \text{ GeV}^{-1}$ would cause the complete disappearance of the blue loop. The result is comparable to the globular cluster bound. Somewhat lower values of $g_{a\gamma}$ might help explaining the observed deficiency of blue with respect to red supergiants discussed, e.g., in [400]. The numerous uncertainties in the microphysics and in the numerical description of the blue loop stage have not permitted a more quantitative assessment of this possibility [401].

More recently, the analysis of SN progenitors has also indicated a preference for additional cooling, in the form of axions or, possibly, other light particles [389]. Surveys show that in many cases the SN type II progenitors are red supergiants with a certain maximal (surface) luminosity. To stay below this luminosity, stars would need to be relatively light, contrary to observations. Standard modifications to the stellar codes, e.g., adding rotations, overshooting, etc., do not help but rather worsen the agreement with the observations. The addition of a novel cooling channel, however, might help reconciling the simulations with the observations. Because of the more efficient cooling, the development of the envelop would freeze at lower luminosities, allowing for more massive stars to end up with the required surface luminosity [389]. In the case of axions, the hint is to rather large couplings to both electrons and photons, close to the current HB and RGB bounds. However, the data sample is still too sparse to draw definitive conclusions and the identification of reliable axion couplings is prohibitive. The situation will largely improve with the data from the Large Synoptic Survey Telescope (LSST) [402, 403], which will likely identify a large number of SN progenitors (see Section 3 in Ref. [403]).

⁴²This bound was slightly updated in reference [387] to $g_{a\gamma} < 0.66 \times 10^{-10} \text{ GeV}^{-1} \text{ (95\% CL)}$.

4.2. Axion-electron coupling

The axion-electron coupling, g_{ae} (Section 2.5.5), induces several processes relevant for stellar evolution (see Ref. [383] for a comprehensive presentation). The most important are the Atomic recombination and de-excitation, the electron and ion Bremsstrahlung, and the Compton process, collectively known as the ABC processes.⁴³ The atomic recombination and deexcitation processes are an important contribution to the solar axion spectrum [405] (see Section 5.1) but can be ignored in numerical simulations of stellar evolution.

At high densities, particularly in electron degeneracy conditions, the most efficient axion production mechanism is the electron/ion bremsstrahlung process

$$e + Ze \rightarrow e + Ze + a, \quad (216)$$

shown in the central panel of Fig. 5. The axion energy-loss rates per unit mass for the case of a pure He plasma is shown in Fig. 6. As clear from the figure, at high density and relatively low temperature, when electrons become degenerate, the bremsstrahlung rate has a very mild dependence on the density. On the other hand, in nondegenerate conditions the rate depends linearly on the density. In both cases, there is also a dependence on the stellar chemical composition. Explicit expressions for the energy-loss rates per unit mass in the degenerate (d) and nondegenerate (nd) limits are provided in Ref. [406]. Approximately,

$$\varepsilon_{\text{ND}} \simeq 47 g_{ae}^2 T^{2.5} \frac{\rho}{\mu_e} \sum \frac{X_j Z_j}{A_j} \left(Z_j + \frac{1}{\sqrt{2}} \right) \text{erg g}^{-1} \text{s}^{-1}, \quad (217)$$

$$\varepsilon_{\text{D}} \simeq 8.6 \times 10^{-7} F g_{ae}^2 T^4 \left(\sum \frac{X_j Z_j^2}{A_j} \right) \text{erg g}^{-1} \text{s}^{-1}, \quad (218)$$

where T and ρ are in K and in g cm^{-3} respectively, $\mu_e = (\sum X_j Z_j / A_j)^{-1}$ is the mean molecular weight per electron, X_j is the relative mass density of the j -th ion, and Z_j , A_j its charge and mass number respectively.⁴⁴ The mild density dependence of the degenerate rate is accounted for by the dimensionless function F . An explicit expression for this function can be found in [406] (see also section 3.5 of Ref. [383] for a pedagogical presentation). Numerically, it is of order 1 for the stellar plasma conditions, $\rho \sim 10^5 - 10^6$ and $T \sim 10^7 - 10^8$, of interest for our discussion here, when the degenerate bremsstrahlung process dominates. The intermediate regime between degenerate and nondegenerate conditions in Fig. 6 is calculated as $\varepsilon_B = (1/\varepsilon_B^{(\text{d})} + 1/\varepsilon_B^{(\text{nd})})^{-1}$, following the prescription in Ref. [406].

The Compton process

$$\gamma + e \rightarrow \gamma + a \quad (219)$$

(right panel of Fig. 5) accounts for the production of axions from the scattering of thermal photons on electrons. The Compton axion emission rate is a steep function of the temperature

$$\varepsilon_{\text{C}} \simeq 2.7 \times 10^{-22} g_{ae}^2 \frac{1}{\mu_e} \left(\frac{n_e^{\text{eff}}}{n_e} \right) T^6 \text{erg g}^{-1} \text{s}^{-1}, \quad (220)$$

where n_e is the number density of electrons while n_e^{eff} is the effective number density of electron targets. At high densities, degeneracy effects reduce n_e^{eff} , suppressing the Compton rate (cf. Fig. 6). The Compton process can effectively dominate over the bremsstrahlung only at low density and high temperature.

Below, we review the bounds on the axion-electron coupling derived by the most relevant stellar systems.

⁴³Another astrophysical process discussed in the literature is the electron-positron annihilation, $e^+e^- \rightarrow \gamma + a$ [404], which plays, however, a less significant role in stellar evolution.

⁴⁴In the typical plasma conditions where the bremsstrahlung is relevant, one finds $Z_j/A_j \approx 1/2$. So, the rate has a dependence on the chemical composition of the plasma and increases in the case of high Z . In particular, the rate is larger in a CO WD core than in the core of a RGB star, composed mostly of He.

Star	$P(\text{s})$	$\dot{P}_{\text{obs}}(\text{s/s})$	$\dot{P}_{\text{th}}(\text{s/s})$	$g_{ae}^{(\text{best})}$	$g_{ae}^{(\text{max})}(2\sigma)$
G117 - B15A	215	$(4.2 \pm 0.7) \times 10^{-15}$	$(1.25 \pm 0.09) \times 10^{-15}$	4.9×10^{-13}	6.0×10^{-13}
R548	213	$(3.3 \pm 1.1) \times 10^{-15}$	$(1.1 \pm 0.09) \times 10^{-15}$	4.8×10^{-13}	6.8×10^{-13}
PG 1351+489	489	$(2.0 \pm 0.9) \times 10^{-13}$	$(0.81 \pm 0.5) \times 10^{-13}$	2.1×10^{-13}	3.8×10^{-13}
L 19-2 (113)	113	$(3.0 \pm 0.6) \times 10^{-15}$	$(1.42 \pm 0.85) \times 10^{-15}$	5.1×10^{-13}	7.7×10^{-13}
L 19-2 (192)	192	$(3.0 \pm 0.6) \times 10^{-15}$	$(2.41 \pm 1.45) \times 10^{-15}$	2.5×10^{-13}	6.1×10^{-13}

Table 2: Hints, $g_{ae}^{(\text{best})}$, and bounds, $g_{ae}^{(\text{max})}$, on the axion-electron coupling from WD variable stars [407, 408]. P is the period of the variable star and \dot{P} its time derivative. We report the measured (observed) values and the theoretical predictions.

White Dwarfs. The strongest bounds on the axion-electron coupling are inferred from observations of stars with a dense core, where the bremsstrahlung is very effective. These conditions are realized in WD and RGB stars. As discussed above, the WD phase is the last stage of the evolution of a low mass star, after the nuclear energy sources are exhausted. Hence, the evolution of a WD is essentially a cooling process, governed by photon radiation and neutrino emission, with the possible addition of novel energy-loss channels, e.g. in axions.

There are at least two ways to test the cooling of WDs and, consequently, exotic cooling theories. First, one may study the WD Luminosity Function (WDLF), representing the distribution of WDs versus luminosity. While cooling, the WD luminosity decreases. Thus, the efficiency of the cooling reflects in the shape of the WDLF. Additionally, one can measure the secular drift of the oscillation period, \dot{P}/P , of WD variables, which is practically proportional to the cooling rate \dot{T}/T .

Let us begin with the WDLF. Current numerical analyses suggest the bound $g_{ae} \lesssim 2.8 \times 10^{-13}$ [408]. However, this result does not come with a credible confidence level because of the large theoretical and observational uncertainties (see, e.g., discussion in [409]). Moreover, the analyses show, fairly consistently (though not universally) an anomalously large energy-loss. In particular [409], using data from the Sloan Digital Sky Survey (SDSS) and the SuperCOSMOS Sky Survey (SCSS), showed that the axion coupling $g_{ae} \simeq 1.4 \times 10^{-13}$ is favored with respect to the standard model case at about 2σ confidence level.⁴⁵ A more recent analysis of the data in Ref. [409], found [35]

$$g_{ae} = 1.5_{-0.9}^{+0.6} \times 10^{-13} \quad (95\% \text{ CL}). \quad (221)$$

These results were confirmed in a later study [412], which attempted to reduce some systematic uncertainties, particularly those due to the star formation rate, by studying the WDLF of the thin and thick disk, and of the halo. A considerable improvement is expected from the next generation of astrophysical observations. Data from the GAIA satellite have already increased the catalog of WDs by an order of magnitude with respect to SDSS [413, 414]. The Large Synoptic Survey Telescope (LSST) is expected to detect even fainter WDs, ultimately increasing the census of WDs to tens of millions [402, 403].

An independent method to study the cooling of WDs is the analysis of the period change of the WD variables. Unfortunately, the period changes very slowly, $\dot{P}/P \approx 10^{-18} \text{ s}^{-1}$ in most measured cases (see Table 2), and an accurate assessment of this change requires decades of accurate data taking. Therefore, although there are many known WD variables, \dot{P}/P has been measured only for a handful of them (see Ref. [408] for an update review of this subject). Interestingly, in all cases the observed period change rate is always larger than the expected one, $\dot{P}_{\text{obs}} > \dot{P}_{\text{th}}$, hinting at an unexpected cooling channel. Such result could be attributed to an axion coupled to electrons with the couplings shown in Table 2. The highest level of discrepancy is observed in G117 - B15A but that may be due to some assumptions about the trapping mode and should perhaps be reconsidered [409]. The combined analysis of all other WD variables in the table gives a fairly good fit, $\chi^2_{\text{min}}/\text{d.o.f.} = 1.1$, for $g_{ae} = 2.9 \times 10^{-13}$ and favors the axion (or ALP) interpretation

⁴⁵The additional energy can also be accounted for by hidden photons [394, 410] but not by anomalous neutrino electromagnetic form factors [411].

at 2σ .

Red Giants. Another strong bound on the axion-electron coupling is inferred from the luminosity of the tip of the RGB in Globular Clusters (GC). After the hydrogen in the core of a main sequence star is exhausted, the stellar core contracts and the star enters the RGB phase. During the RGB evolutions, the star expands, its surface cools down, and its luminosity increases (see Fig. 4). For sufficiently low mass stars, as those populating a GC, the electrons in the stellar core eventually become degenerate. Meanwhile, the core continues to contract and heat up, while its mass grows by the H-shell burn. The process continues until the core reaches the conditions necessary to ignite He. At this time, known as the He-flash, the star reaches the point of highest luminosity in the CMD, known as the RGB tip. The luminosity of the RGB tip is an excellent observable to probe the cooling of the star during the RGB phase, being the He ignition extremely sensitive to the temperature. Thus, any additional cooling, in the form of axions or other light, weakly interacting particles, can be effectively constrained by observations of the luminosity of the RGB tip. In the case of axions, the most efficient production mechanisms during the RGB production are the electron bremsstrahlung and the Compton processes. The two clusters studied so far,⁴⁶ M5 [307] and M3 [416], indicate fairly consistent, though not identical, results for the axion-electron coupling.⁴⁷ The combined analysis indicates the bound

$$g_{ae}^{(\text{best})} = 1.4 \times 10^{-13}, \quad (223a)$$

$$g_{ae} \leq 3.1 \times 10^{-13}, \quad \text{at 95\% CL} \quad (223b)$$

Several uncertainties, including the cluster morphology and distance as well as uncertainties in the nuclear reaction rates, affect the exact determination of the RGB bound on the axion-electron coupling [307, 416, 418]. The use of multi-band photometry of multiple globular clusters would provide a substantial improvement (see, e.g., [415, 416]). The error in the globular cluster distance, currently the largest observational uncertainty, will be reduced considerably (perhaps by as much as a factor of 10) with the release of the GAIA data relevant for GCs, expected in 2022 [419].

The combination of hints from the WDLF, the WD pulsation, and RGB stars gives the 1σ preferred interval

$$g_{ae} = 1.6^{+0.29}_{-0.34} \times 10^{-13}, \quad (224)$$

with $\chi^2_{\text{min}}/\text{d.o.f.} = 14.9/15 = 1.0$, and favors the axion (or ALP) solution at slightly more than 3σ [35].

Combining the results from the WDLF, the WD pulsation, and RGB stars, discussed in this section, with the analysis of the R parameter (Section 4.1), one finds the hinted regions presented in Fig. 8 [384]. The analysis shows a preference for an axion coupling to electrons at the level of 3σ . On the other hand, the coupling to photons is compatible with zero at 1σ . Notice, however, that the last conclusion cannot be drawn in the case of specific axion models, such as DFSZ I and II, which predict well-defined relations among couplings.

4.3. Axion-nucleon coupling

Finite axion-nuclei interactions allow for further ways axions may impact the evolution of stars. Non-thermal processes, such as nuclear transitions in stars (particularly, the Sun) with the emission of axions,

⁴⁶We point out, however, that very recently, Ref. [415] considered 50 GC to find the upper bound $g_{ae} = 2.5 \times 10^{-13}$ on the axion-electron coupling. The result is slightly more stringent than the one we discuss in this sections.

⁴⁷In particular, the analysis of M5 [307] suggests a stronger hint to a non-vanishing axion-electron coupling

$$\begin{aligned} g_{ae} &= 1.88^{+1.19}_{-1.17} \times 10^{-13}, & \text{at 68\% CL} \\ g_{ae} &\leq 4.3 \times 10^{-13}, & \text{at 95\% CL,} \end{aligned} \quad (222)$$

while the observations of M3 are rather consistent with expectations ($g_{ae}^{\text{best}} = 0.05 \times 10^{-13}$) and suggest a somewhat stronger bound $g_{ae} \leq 2.6 \times 10^{-13}$ at 95% CL [416]. Reference [417] attributes the disagreement between theory and observations in [307], at least partially, to the convention used for the screening of the nuclear reaction rates.

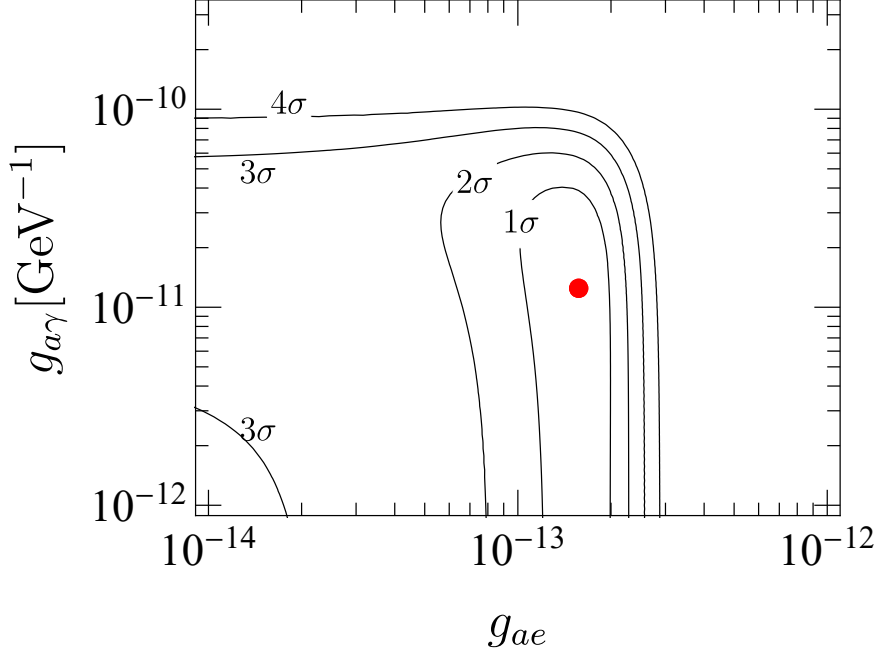


Figure 8: Stellar hints on general Axion Like Particles interacting with electrons and photons [384]. The hints are derived from the global analysis of WD pulsation, the WD luminosity function, RGB and HB stars. The best fit parameters are indicated with the red dot.

provide an interesting channel to produce a possibly detectable axion flux. However, their impact on stellar evolution is minimal. Thermal processes turn out to be quite more relevant, in this respect.

The most relevant thermal process involving the axion-nucleon coupling is the nucleon bremsstrahlung

$$N + N' \rightarrow N + N' + a, \quad (225)$$

with $N, N' = n, p$, where n represents a neutron and p a proton. The Feynman diagram for these processes is shown in Fig. 9. One of the major difficulties in dealing with the nucleon bremsstrahlung is the description

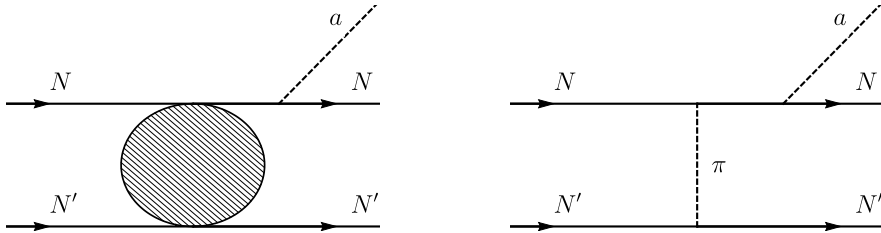


Figure 9: Axion nuclear bremsstrahlung (one of the possible diagrams). N, N' represent either a proton or a neutron. To the right is the Feynman diagram corresponding to the OPE approximation.

of the nuclear interaction, shown as a blob in figure 9. A substantial simplification, known as the One Pion Exchange (OPE) approximation, is to assume that the interaction is mediated by the exchange of a single pion, as shown in the right panel in figure 9. The OPE framework is not always justified (see, e.g., Ref. [32, 420]) but it does provide a starting point for more accurate computations (cf. Ref. [421] for a recent

review of the role of OPE and its corrections). Nevertheless, it is evident from the figure that the pion mass in the propagator is going to suppress the emission rate unless the temperature is such that the typical momentum exchanged in the collision, which is of the order of the nucleon momentum $q_N \sim (3m_N T)^{1/2}$, is larger than the pion mass. This demands $T \gtrsim 10\text{MeV}$, a temperature typical of the core of Supernovae (SNe) and NS. Therefore, only SNe and NS may (and, indeed, do) provide an environment to test the axion nucleon bremsstrahlung.

Approximate emission rates for the nn scattering (the pp scattering is similar) in the limit of nondegenerate and degenerate nuclei are given below [383]

$$\varepsilon_{\text{ND}} \approx 2.0 \times 10^{38} g_{an}^2 \rho_{14} T_{30}^{3.5} \text{ erg g}^{-1} \text{ s}^{-1}, \quad (226a)$$

$$\varepsilon_{\text{D}} \approx 4.7 \times 10^{39} g_{an}^2 \rho_{14}^{-2/3} T_{30}^6 \text{ erg g}^{-1} \text{ s}^{-1}, \quad (226b)$$

where $T_{30} = T/30\text{MeV}$ and $\rho_{14} = \rho/10^{14}\text{g cm}^{-3}$. Notice that eqs. (226) are only a crude approximation of the emission rate, calculated in the OPE approximation and ignoring the pion mass and medium effects. However, they do show the steeper temperature dependence of the degenerate emission rate and the stronger density dependence in the nondegenerate limit.

Below we report the recent bounds on the axion couplings to nuclei from SN and NS. However, we emphasize that, at the time of writing, there is an intense effort to provide a more reliable description of the nuclear processes that produce axions at very high density,⁴⁸ and such bounds are often reconsidered and reassessed.

SN 1987A. The most well known argument to constraint the axion interaction with protons and neutrons is the one based on the observed neutrino signal from SN 1987A [32, 424–426]. The signal duration depends on the efficiency of the cooling and is compatible with the assumption that SN neutrinos carry about 99% of the energy released in the explosion. For a light, weakly interacting particle, a bound can be extracted from the requirement that it does not contribute more than neutrinos, about $2 \times 10^{52} \text{ erg s}^{-1}$, to the cooling of the young SN, with a typical core conditions of $T \sim 30 \text{ MeV}$ and $\rho \sim 10^{14}\text{g cm}^{-3}$. The most recent analysis for the axion case [421] derived the bound⁴⁹

$$g_{an}^2 + 0.29 g_{ap}^2 + 0.27 g_{an} g_{ap} \lesssim 3.25 \times 10^{-18}, \quad (227)$$

shown in Fig. 10.

Strongly interacting axions may be trapped in the SN core. In this case the emission is reduced, as they thermalize and are effectively emitted from an *axiosphere*, similarly to what happens to neutrinos. The most recent analysis found that this condition is satisfied for $g_{an} = g_{ap} \gtrsim 10^{-7}$. However, even trapped axions may extract more energy than neutrinos from the young SN and couplings all the way to $g_{an} = g_{ap} \approx 10^{-4}$ should be probably excluded [421].

Neutron Stars. Observations of the cooling of NS also provides information about the axion-nucleon coupling [427–431]. In particular, the unexpectedly rapid cooling of the NS in CAS A was attributed to the presence of axions with coupling to neutrons [432]

$$g_{an} \simeq 4 \times 10^{-10}. \quad (228)$$

However, the anomalous rapid cooling may also be originated in the phase transition of the neutron condensate into a multicomponent state [433]. More recently, the data have been explained assuming a neutron

⁴⁸Many-body effects can be quite large in a high density medium. The inclusion of such effects in the description of axion production processes in SN and NS has a long history. Discussions can be found in Ref. [32, 421, 422]. Very recently, Ref. [423] reevaluated such medium effects, showing a significant dependence of the axion couplings to nucleons upon the environment density. These latest effects are not included in the results presented in this review, which reports the latest bounds on the axion-nucleon couplings available in the literature at the time of writing.

⁴⁹Eq. (227) shows a surprisingly subdominant contribution of the proton scattering to the emission rate, quite more accentuated than what reported in previous analyses [32, 35]. The reason is that, besides being less abundant than neutrons, protons are nondegenerate while neutrons are partially degenerate and the emission rate in SN conditions is more efficient for degenerate nuclei, as evident from Eqs. (226).

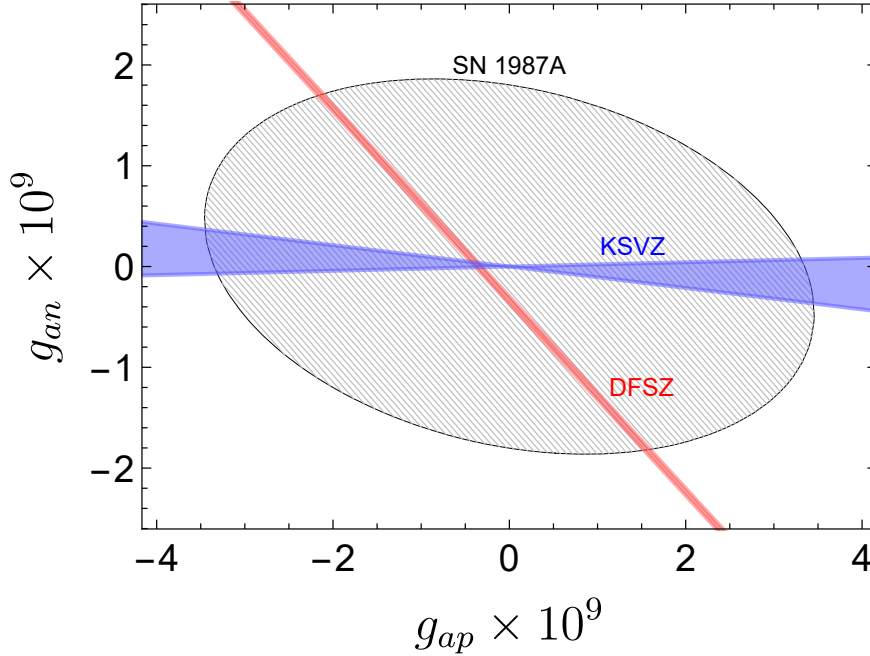


Figure 10: SN 1987A bound on the axion-nucleon couplings. In hatched gray, the region allowed by the SN 1987A bound derived in [421]. The parameter space for KSVZ and DFSZ axions is superimposed. The width of the lines represent the current uncertainties according to [47].

triplet superfluid transition occurring at the present time, $t \sim 320$ years, and that proton superconductivity is operating at $t \ll 320$ years [429]. The neutron triplet superfluid transition accelerates the neutrino emission through the breaking and reformation of neutron Cooper pairs. Under these assumptions the data can be fitted well, leaving little room for additional axion cooling. Quantitatively,

$$g_{ap}^2 + 1.6 g_{an}^2 \leq 1.1 \times 10^{-18}. \quad (229)$$

An even stronger bound, though only on the axion-neutron coupling,

$$g_{an} \leq 2.8 \times 10^{-10}, \quad (230)$$

was inferred from observations of the NS in HESS J1731-347 [430]. A considerable less stringent result,

$$g_{an} \lesssim (2.5 - 3.2) \times 10^{-9}, \quad (231)$$

was derived more recently in Ref. [431], the range depending on the adopted value for $\tan \beta$.⁵⁰ Interestingly, this latest analysis accounted also for a possible axion emission by electron bremsstrahlung in the neutron star crust, which cannot *a priori* be ignored for non-hadronic axion models, such as the DFSZ. The resulting rate is, however, in most cases subdominant with respect to the processes induced by nuclear couplings and becomes relevant only when the axion-neutron coupling is very small.

4.4. Axion coupling to the neutron EDM

As discussed in Section 2.8 a fundamental consequence of QCD axion models is that axions couple to the neutron EDM, effectively driving it to zero and solving the strong CP problem. The axion-neutron EDM

⁵⁰Notice that Ref. [431] uses the opposite for $\tan \beta$ and so what they call $\cos \beta$ is our $\sin \beta$ and viceversa.

vertex can be parameterized with the coupling g_d defined through the Lagrangian term (cf. Eq. (109))

$$\mathcal{L}_d = -\frac{i}{2} g_d a \bar{n} \sigma_{\mu\nu} \gamma_5 n F^{\mu\nu}. \quad (232)$$

This coupling induces the process $n + \gamma \rightarrow n + a$, allowing the production of axions that, in turn, contribute to the SN cooling. As discussed, observations of the SN 1987A neutrino burst limit the amount of possible exotic cooling rate to be less than the neutrino's. A rough estimate gives [434]

$$g_d \leq 4 \times 10^{-9} \text{ GeV}^{-2}. \quad (233)$$

We emphasize that the interaction in (232) is generic to any QCD axion model and does not demand any other assumption besides the solution of the strong CP problem. Therefore, the bound (233) is, effectively, a bound on the PQ constant or, equivalently, on the axion mass.⁵¹ If we express the coupling in terms of the axion mass, $g_d \approx 6 \times 10^{-10} (m_a/\text{eV}) \text{ GeV}^{-2}$, the SN bound implies $f_a \gtrsim 9 \times 10^5 \text{ GeV}$ or, equivalently, $m_a \lesssim 7 \text{ eV}$.

4.5. Axion CP-odd couplings

Stellar evolution provides also strong bounds on the axion CP odd couplings, discussed in Section 2.10. The axion scalar couplings to electrons g_{ae}^S can be constrained in globular cluster stars, where such particles can be produced through Compton scattering or bremsstrahlung [435]. The strongest bound is derived by the luminosity of the tip of the RGB. A semiquantitative argument, based on the assumption that any novel emission rate would spoil observations unless $\varepsilon \lesssim 10 \text{ erg s}^{-1} \text{ g}^{-1}$, gives the rather restrictive bound [436]

$$g_{ae}^S \leq 0.7 \times 10^{-15}. \quad (234)$$

HB stars provide a slightly less restrictive bound, $g_{ae}^S \leq 3 \times 10^{-15}$.

The scalar coupling to nuclei is likewise constrained in RGB stars [436]

$$g_{aN}^S \leq 1.1 \times 10^{-12}, \quad (235)$$

while HB stars provide the less restrictive bound $g_{aN}^S \leq 6 \times 10^{-12}$.

These astrophysical bounds are the dominant constraints on the coupling to nuclei for masses above 1 eV or so. However, for lower masses the experimental bounds on 5th force are much stronger (see Fig. 1 in Ref. [435]).

4.6. Axion coupling to gravity and black hole superradiance

In some cases, astrophysical considerations can provide insights on the couplings of axions to gravity, without assuming any interaction with standard model fields. Such considerations are, therefore, completely model-independent. The case of black holes (BH) discussed below is particularly interesting since, just like in the case of the other bounds discussed in this section, there is no assumption that axions are initially present, i.e. there is no requirement for axions to be the DM.

Axions form gravitational bound states around black holes whenever their Compton length is of the order of the black holes radii. The phenomenon of *superradiance* [437] then guarantees that the axion occupation numbers grow exponentially, providing a way to extract very efficiently energy and angular momentum from the black hole [308, 309]. The rate at which the angular momentum is extracted depends on the black hole mass and so the presence of axions could be inferred by observations of black hole masses and spins. Current observations exclude the region [309, 438]

$$6 \times 10^{17} \text{ GeV} \leq f_a \leq 10^{19} \text{ GeV}, \quad (236)$$

⁵¹Here, we are assuming the standard relation, Eq. (51), between axion mass and decay constant. We discuss mechanisms to modify this relation in Section 6.7.

Star	Hint (1σ)	Bound (2σ)
Sun	–	$g_{a\gamma} \leq 2.7 \times 10^{-10} \text{ GeV}^{-1}$
WDLF	$g_{ae} = 1.5_{-0.5}^{+0.3} \times 10^{-13}$	$g_{ae} \leq 2.1 \times 10^{-13}$
WDV	$g_{ae} = 2.9_{-0.9}^{+0.6} \times 10^{-13}$	$g_{ae} \leq 4.1 \times 10^{-13}$
RGB Tip	$g_{ae} = 1.4_{-1.3}^{+0.9} \times 10^{-13}$ (M3+M5)	$g_{ae} \leq 3.1 \times 10^{-13}$ (M3+M5)
HB	–	$g_{ae}^S \leq 0.7 \times 10^{-15}; \quad g_{aN}^S \leq 1.1 \times 10^{-12}$
	$g_{a\gamma} = (0.3 \pm 0.2) \times 10^{-10} \text{ GeV}^{-1}$	$g_{a\gamma} \leq 0.65 \times 10^{-10} \text{ GeV}^{-1}$
	–	$g_{ae}^S \leq 3 \times 10^{-15}; \quad g_{aN}^S \leq 6 \times 10^{-12}$
SN 1987A	–	$g_{an}^2 + 0.29 g_{ap}^2 + 0.27 g_{an} g_{ap} \lesssim 3.25 \times 10^{-18}$
	–	$g_d \lesssim 4 \times 10^{-9} \text{ GeV}^{-2} (\Rightarrow f_a \gtrsim 9 \times 10^5 \text{ GeV})$
NS in CAS A	–	$g_{ap}^2 + 1.6 g_{an}^2 \lesssim 1.1 \times 10^{-18}$
NS in HESS J1731-347	–	$g_{an} \leq 2.8 \times 10^{-10}$
Black Holes	–	$f_a \leq 6 \times 10^{17} \text{ GeV}$ or $f_a \geq 10^{19} \text{ GeV}$

Table 3: Summary of stellar hints and bounds on axions. The hints are all at 1σ and the bounds at 2σ , except for the case of SN 1987A and NS in CAS A, for which a confidence level was not provided. We have not reported the hint from the NS in CAS A [432] since it is in tension with the more recent bound in [429].

corresponding to the mass region (Cf. footnote 51) $6 \times 10^{-13} \text{ eV} \leq m_a \leq 10^{-11} \text{ eV}$.⁵² We underline that superradiance can start from a quantum mechanical fluctuation and does not require the prior existence of an axion population.

The condition for the BH superradiance relies on the assumption that the axion self interaction is small, which is why the bounds concern such large values of f_a . For sufficiently large couplings, the axion cloud could collapse in what is known as a *bosenova*,⁵³ producing periodic bursts which should be observable by Advanced LIGO and VIRGO [309].

Other observational signatures of BH superradiance are the gravitational waves produced in the transition of axions between gravitational levels or from axions annihilation to gravitons [309, 439].

4.7. Summary of astrophysical bounds

A summary of all bounds on the axion couplings from stellar evolution is shown in Table 3 where, whenever possible, we have reported the bounds at 2σ and the hints at 1σ . The bounds were derived without assuming any model dependence and are therefore quite general.

Particularly interesting among the astrophysical considerations are the bounds from BH superradiance and the SN 1987A bound on the neutron EDM, since they are the only ones that provide a bound on the axion mass rather than on the couplings.⁵⁴ Combined, they constrain the axion mass in the range $2 \times 10^{-11} \text{ eV} \leq m_a \leq 7 \text{ eV}$.

⁵²The results reported are the ones in the most recent analysis, Ref. [438].

⁵³Axion couplings to other fields, e.g. photons, would also induce an effective axion self-interaction. However, such couplings would need to be too large to have any significant effect. For example, the value of $g_{a\gamma}$ required to induce a self-coupling as large as what expected from the axion potential in Eq. (50), for masses $\sim 10^{-12} \text{ eV}$, is several orders of magnitude larger than the value excluded by the HB bound. This justifies plotting E/N up to very large values, as we do in Section 5.

⁵⁴Astrophysical considerations are, of course, affected by many uncertainties. In particular, the bound on the neutron EDM is based on a simple estimate and should be probably revised. Additionally, we are assuming a standard relation between the axion mass and decay constant (Cf. footnote 51).

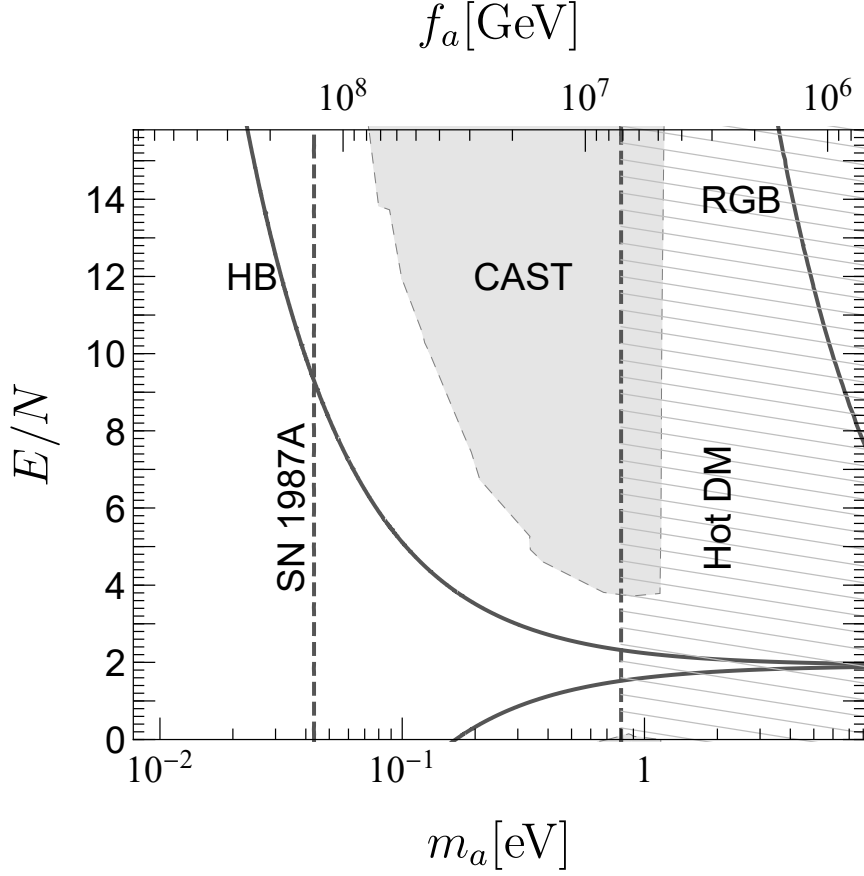


Figure 11: Astrophysical bounds on the hadronic axions (at 2σ). The region to the left of the curves are excluded. The bound from SN 1987A is shown with dashed lines since the bound is less robust than the others [421, 440] and its statistical significance is not well defined. The area probed by CAST is shown in light gray. The lightly hatched region is excluded by the hot DM bound [275] (see Section 3.8).

In the case of the other bounds, specific model-dependent relations connect the different couplings, as well as the axion mass. The astrophysical bounds for hadronic axion models are shown in Fig. 11. The models are parameterized in terms of the axion mass and E/N . We superimpose also the region excluded by the CERN Axion Solar Telescope (CAST) for reference. The astrophysical hinted region is not shown since hadronic axions cannot fit very well the required parameters [35].

Hadronic axions are naturally electrophobic. For axion masses between 10^{-9} and 1 eV, and with E/N between 0 and 15, the parameter C_{ae} , defined in Eq. (118), which parameterize the interaction with electrons, is always confined in the range $\approx 5 - 15 \times 10^{-3}$. Consequently, the RGB bound is always suppressed with respect to the HB and the hot DM bounds for such axions.

The analogous plot for DFSZ axions is shown in Fig. 12. Again, we superimpose the region experimentally excluded, in this case by the Large Underground Xenon (LUX) experiment (CAST does not probe these models). In this case, the stellar anomalous observations can be fitted quite well [35]. The hinted region is, however, quite difficult to explore experimentally and probably only the International AXion Observatory (IAXO) will be able to access parts of it in the near future [334].

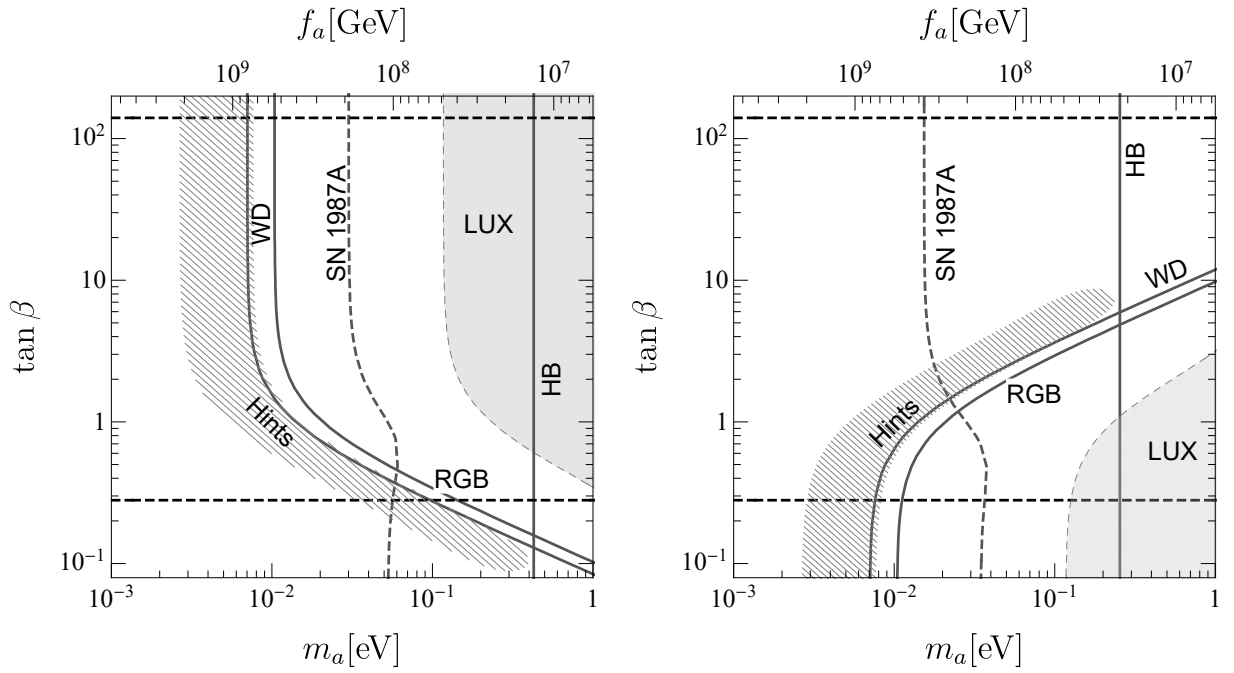


Figure 12: Astrophysical bounds on the DFSZ axions. The left panel represents the DFSZ I model. The right panel the DFSZ II. The region to the left of the curves are excluded by astrophysical considerations. The WD curve refers to the WD luminosity function bound (refer to the text for more information). The hatched region refers to the combined hints from the WD luminosity function, the WD pulsation, HB and RGB stars. The bound from SN 1987A is shown with dashed lines since the bound is less robust than the others [421].

5. Experimental Searches

In the interest of keeping this review self-consistent, we briefly describe the status of the axion experimental searches. More complete reviews can be found in Refs. [26, 38–40].

5.1. Solar axions and helioscopes

The Sun is a natural source of axions. These are produced through Primakoff (Section 4.1) and ABC (Section 4.2) processes:

$$\frac{dN_a}{dtd\omega} = \left(\frac{g_{a\gamma}}{\text{GeV}^{-1}} \right)^2 n_{a\gamma}(\omega) + g_{ae}^2 n_{ae}(\omega), \quad (237)$$

where $n_{a\gamma}$ represents the Primakoff contributions while n_{ae} gets contribution from atomic recombination and deexcitation, bremsstrahlung, and Compton processes, $n_{ae} = n_{ae}^A + n_{ae}^B + n_{ae}^C$. Good analytical approximations for these coefficients exist for all but the atomic recombination and deexcitation processes (see, e.g., Ref. [441] and [442]):

$$n_{a\gamma}(\omega) \approx 1.69 \times 10^{58} e^{-0.829\omega} \omega^{2.45} \text{ keV}^{-1} \text{ s}^{-1}; \quad (238a)$$

$$n_{ae}^B \approx 7.4 \times 10^{62} \frac{\omega e^{-0.77\omega}}{1 + 0.667\omega^{1.278}} \text{ keV}^{-1} \text{ s}^{-1}; \quad (238b)$$

$$n_{ae}^C \approx 3.7 \times 10^{60} \omega^{2.987} e^{-0.776\omega} \text{ keV}^{-1} \text{ s}^{-1}. \quad (238c)$$

The total number of axions emitted by the Sun per second is,

$$\frac{dN_a}{dt} = 1.1 \times 10^{39} \left[\left(\frac{g_{a\gamma}}{10^{-10} \text{ GeV}^{-1}} \right)^2 + 0.7 \left(\frac{g_{ae}}{10^{-12}} \right)^2 \right] \text{ s}^{-1}. \quad (239)$$

Evidently, the axion flux gets a similar contribution from Primakoff and ABC axions for couplings of phenomenological interest (cf. Fig. 7). Notice, however, that the ABC flux is peaked at slightly lower energies than the Primakoff, a fact that allows to distinguish between the two fluxes (and so infer some information about the underlying axion model) if enough data is collected in an helioscope experiment [443].⁵⁵

The weight of the two contributions in Eq. (239) depends on the specific axion model. In terms of $g_{e12} = g_{ae}/10^{-12}$ and $g_{\gamma10} = g_{a\gamma}/10^{-10} \text{ GeV}^{-1}$, we have

$$\text{KSVZ : } g_{e12}/g_{\gamma10} \approx 0; \quad (240a)$$

$$\text{DFSZ I : } g_{e12}/g_{\gamma10} = 20 \sin^2 \beta; \quad (240b)$$

$$\text{DFSZ II : } g_{e12}/g_{\gamma10} = 12 \cos^2 \beta. \quad (240c)$$

Experiments that aim at detecting the solar axion flux are known as axion helioscopes. The most notable example is the Sikivie helioscope [444], or simply helioscope, which adopts a strong laboratory magnetic field for the coherent conversion of solar axions into X-ray photons. However, the solar axion flux may be detected through other means, for example through the Primakoff-Bragg conversion [445] or the axio-electric effect [446, 447].

The Sikivie helioscope makes use of the axion coherent conversion in a transverse magnetic field B . The conversion probability is

$$P_{a \rightarrow \gamma} = \left(\frac{g_{a\gamma} B L}{2} \right)^2 \frac{\sin^2(qL/2)}{(qL/2)^2}, \quad (241)$$

⁵⁵For example, the number of axions produced in the energy bin $1 \leq \omega/\text{keV} \leq 2$ is 12.5% of the total, in the case of hadronic axions (no coupling with electrons) but it moves quickly to $\sim 30\%$ if $g_{ae}/g_{a\gamma} > 5 \times 10^{-2} \text{ GeV}$, which is typical for DFSZ axions.

where $q = q_\gamma - q_a$ is the momentum transfer provided by the magnetic field and L is the length of the magnet. Coherence is ensured whenever $qL \ll 1$. In this condition, the probability does not depend on the axion mass and energy. In vacuum, the relativistic approximation ($\omega_a \gg m_a$) gives $q \simeq m_a^2/2\omega$. A small mass, therefore, ensures coherence on macroscopic scales.

Whenever the coherence condition is verified, the conversion probability scales as $(g_{a\gamma}BL)^2$, rapidly increasing with the magnetic field and the size of the magnet. When coherence is lost, the sensitivity is reduced proportionally to m_a^{-2} .⁵⁶ Since for QCD axion models $g_{a\gamma}^2 \propto m_a^2$ the sensitivity line follows exactly the axion model line in the $g_{a\gamma} - m_a$ plane once coherence is lost at large masses.

To regain sensitivity, the coherence can be restored using a buffer gas in the magnet beam pipes [449]. In this case the momentum transfer is $q \simeq (m_a^2 - m_\gamma^2)/2\omega$, where m_γ is the effective photon mass in the gas. Tuning the effective photon mass to the axion mass allows to effectively regain coherence.

The CERN Solar Axion Experiment (CAST) [450], a 3-rd generation and currently the most advanced running axion helioscope,⁵⁷ reported the bound $g_{a\gamma} \leq 0.66 \times 10^{-10} \text{ GeV}^{-1}$ for masses $m_a \leq 20 \text{ meV}$, while reaching the $m_a \sim \text{eV}$ range at high masses [451]. Going beyond that mass may be less interesting because of the hot DM bound [275, 342] (see Section 3.8).

The proposed International Axion Observatory (IAXO), a 4-th generation axion helioscope [452], is expected to increase the sensitivity by a factor of $\gtrsim 10^4$, probing the axion-photon coupling down to $g_{a\gamma} \sim$ a few $10^{-12} \text{ GeV}^{-1}$ at low mass and exploring significant regions of the KSVZ and DFSZ axion models [334]. A scaled down (and significantly less expensive) version of IAXO, called BabyIAXO, will likely start operations in the mid of the current decade, in DESY. Though considerably less powerful than its brother IAXO, BabyIAXO [334] will still be sensitive to DFSZ axion models, unique in this respect among the experiments probing the axion mass region above a few meV. The sensitivity of IAXO and BabyIAXO to hadronic and DFSZ axion models is shown in Figs. 13, 14, and 15.

There are other technologies to detect solar axions. One explored option is to exploit the coherent enhancement of the axion conversion into photons, via Primakoff effect, when the solar axion beam satisfies the Bragg condition of scattering with a crystal plane [453]. However, the sensitivity of these experiments is not competitive with the Sikivie helioscope or with the astrophysical bounds.

Large Weakly Interacting Massive Particle (WIMP) detectors such as LUX and XENON100 have the capability to detect solar axions through the axio-electric effect and do, in fact, provide bounds on the axion-electron coupling. Specifically, the XENON100 collaboration [454] reported $g_{ae} < 7.7 \times 10^{-12}$ (90 % CL), LUX [455], $g_{ae} < 3.5 \times 10^{-12}$, and PandaX-II [456], $g_{ae} < 4 \times 10^{-12}$. These searches are particularly interesting since they permit the exploration of the axion-electron coupling in a very wide mass region. However, probing the parameter space allowed by the cooling of WDs and RGB may prove extremely challenging even for axio-electric helioscopes of the next generation [39].

5.2. Helioscopes sensitivity to $g_{a\gamma}$ and g_{ae}

Here we provide simple, approximate expressions to extract the helioscope sensitivity to general axion models, accounting for the fact that axions can be produced in the Sun through processes induced by their couplings to electrons and to photons. By helioscope here we mean any instrument that can detect solar axions. In particular, we consider the standard Sikivie helioscope, which uses an external magnetic field to convert axions into photons, and the axionelectric helioscope, which operates through the axion interaction with electrons.

In the Sikivie helioscope, solar axions are converted into photons in a transverse magnetic field B . The conversion probability is given in Eq. (241), where we remind that q is the momentum transfer provided by the magnetic field. In vacuum, $q \simeq m_a^2/2\omega$. Whenever $qL \ll 1$, the probability does not depend on the energy.

⁵⁶Given enough data (and a large enough axion mass), the spectral distortion induced by the loss of coherence may allow to pin down the axion mass [448].

⁵⁷CAST is expected to stop operating in 2020.

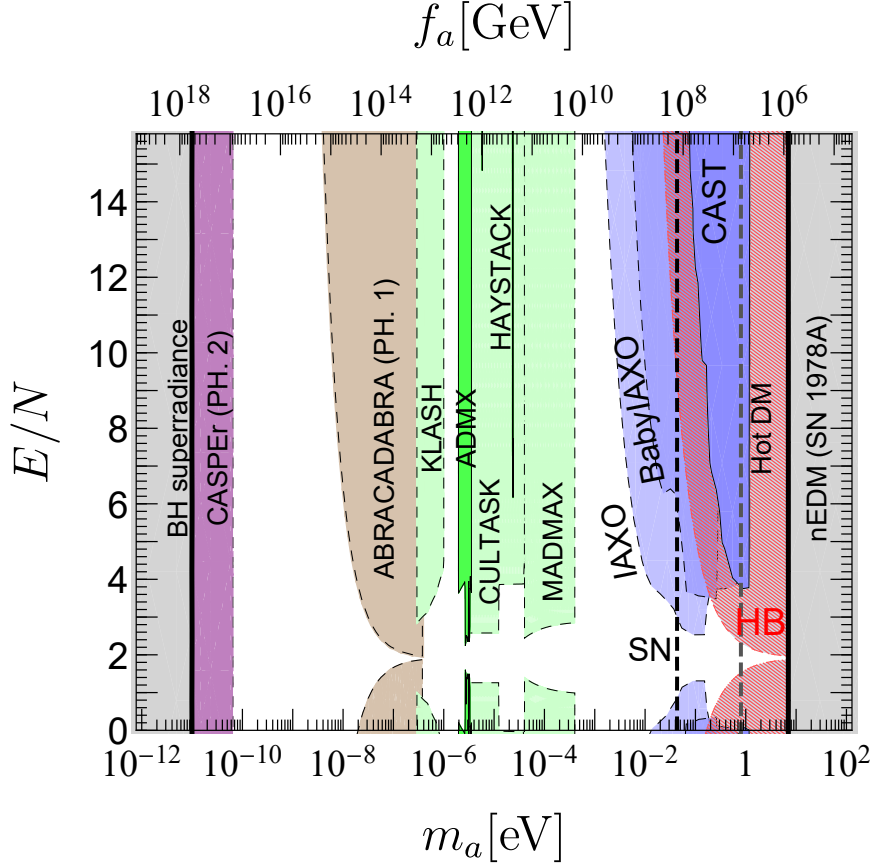


Figure 13: Hadronic axion parameter space. Interactions with electrons are neglected. Experimental bounds are shown with solid lines while projected sensitivities with dashed lines. The Helioscope lines refer to the latest results from CAST [451] and to the expected sensitivity of BabyIAXO and IAXO [334]. The sensitivity of the haloscope experiments is calculated assuming that axions comprise the totality of the cold dark matter in the Universe. In green are the cavity experiments. Darker colour corresponds to actual data while in lighter colour we show the sensitivity of proposed experiments. The region labeled CULTASK shows the combined expected sensitivity of CAPP-12TB and CAPP-25T (Cf. Table 4). The sensitivity of ABRACADABRA refers to phase 1 ($B_{\max} = 5\text{T}$ and Volume= 1 m^3 [319]) for the resonant case. CASPER refers to CASPER electric, phase 2, and indicates the most optimistic scenario compatible with the QCD uncertainty in the calculation of the nEDM (Cf. Eq. (116)).

The expected number of events in the Sikivie helioscope is

$$N_\gamma - N_b = \frac{S\Delta t}{4\pi D_\odot^2} \int \frac{dN_a}{dt d\omega} P_{a\gamma} \epsilon d\omega \quad (242)$$

where N_b is the total background, $D_\odot \simeq 1.5 \times 10^{11}\text{ m}$ is the distance to the Sun, S is the detector total area, Δt the exposure time, and ϵ a parameter that measures the detection efficiency. In general, the integral should be restricted to some ω region. We assume that these threshold values are accounted for by ϵ .

Be $\bar{g}_{a\gamma}$ the bound on the axion-photon coupling in the case of $g_{ae} = 0$. In the general case, we find

$$g_{a\gamma}^2 \int (g_{a\gamma}^2 n_\gamma + g_{ae}^2 n_e) \tilde{P}_{a\gamma} \epsilon d\omega \leq \bar{g}_{a\gamma}^4 \int n_\gamma \tilde{P}_{a\gamma} \epsilon d\omega \quad (243)$$

where $g_{a\gamma}$ is given in units of GeV^{-1} and $\tilde{P}_{a\gamma}$ is the oscillation probability divided by $g_{a\gamma}$. In the case of small axion mass, the factor qL in the expression for the probability is small and $P_{a\gamma}$ does not depend on

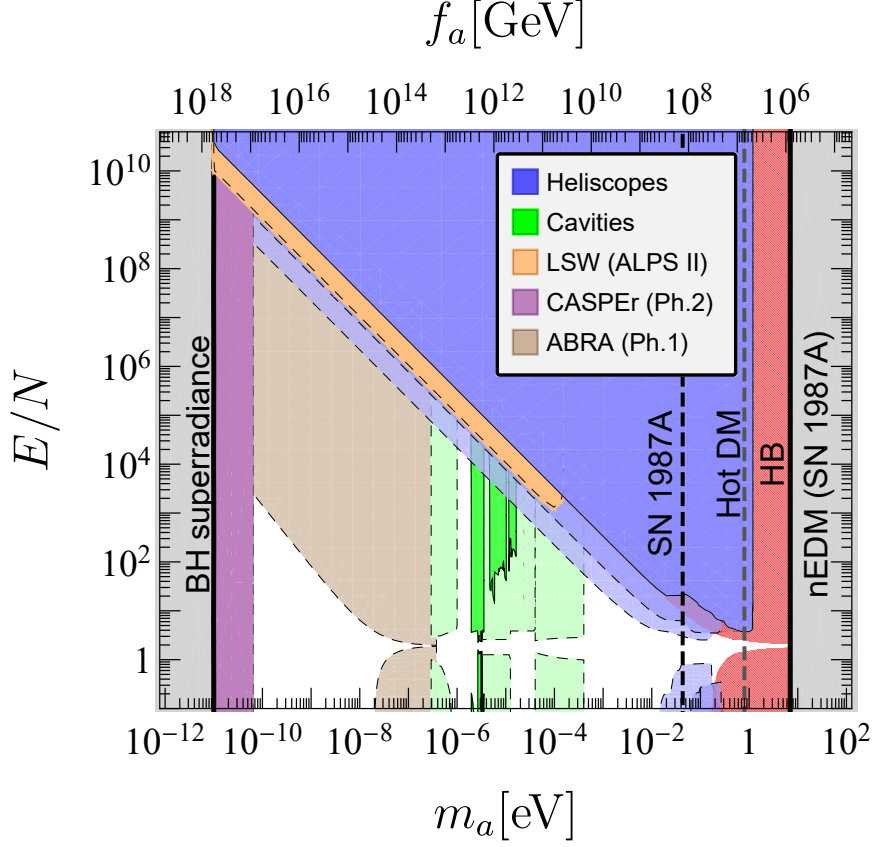


Figure 14: Phenomenological and experimental status for the hadronic axion. See caption of Fig. 13 for details.

the axion energy. We can assume that the factor ϵ is also roughly constant in the energy interval relevant for solar axions, if the experimental cuts in ω are performed far from the regions where the two fluxes are large.⁵⁸ In this case, the integrals can be performed⁵⁹ and one finds the very simple relation

$$g_{\gamma 10}^2 (g_{\gamma 10}^2 + 0.7 g_{e 12}^2) \lesssim \bar{g}_{\gamma 10}^4, \quad (244)$$

where, we remind, $g_{\gamma 10} = g_{a\gamma}/10^{-10}\text{GeV}^{-1}$ and $g_{e 12} = g_{ae}/10^{-12}$. At large masses, when coherence is lost, one cannot assume $P_{a\gamma}$ constant anymore. Assuming a ω^2 dependence for $P_{a\gamma}\epsilon$ we find that the coefficient 0.7 should be replaced with 0.3. Indeed, in this case Primakoff has a greater weight since it is peaked at higher energy. In this case, however, a gas can be used to restore coherence.

We now turn to the helioscopes based on the axio-electric effect. For nonrelativistic electrons and ultrarelativistic axions, the cross section for the axio-electric effect is proportional to the photoelectric cross section [457–459]

$$\sigma_{ae}(\omega) = \frac{g_{ae}^2}{8\pi\alpha} \left(\frac{\omega}{m_e} \right)^2 \sigma_{ph}(\omega) \simeq 2.1 \times 10^{-29} g_{e 12}^2 \omega_{\text{keV}}^2 \sigma_{ph}(\omega), \quad (245)$$

where $\omega_{\text{keV}} = \omega/\text{keV}$. The pronounced peak at low energy ($\omega_a \sim 1 \text{ keV}$), characteristic of the photoelectric cross section, which would favor the ABC over the Primakoff flux, is compensated by the ω^2 term in

⁵⁸This is not always the case. For example, in [442] the analysis is restricted to the energy range between 0.8 and 6.8 keV.

⁵⁹We integrate between $\omega = 100\text{eV}$ and $\omega = 12 \text{ keV}$. Below 100 eV the emission rate is less clear and unaccounted processes may contribute [39].

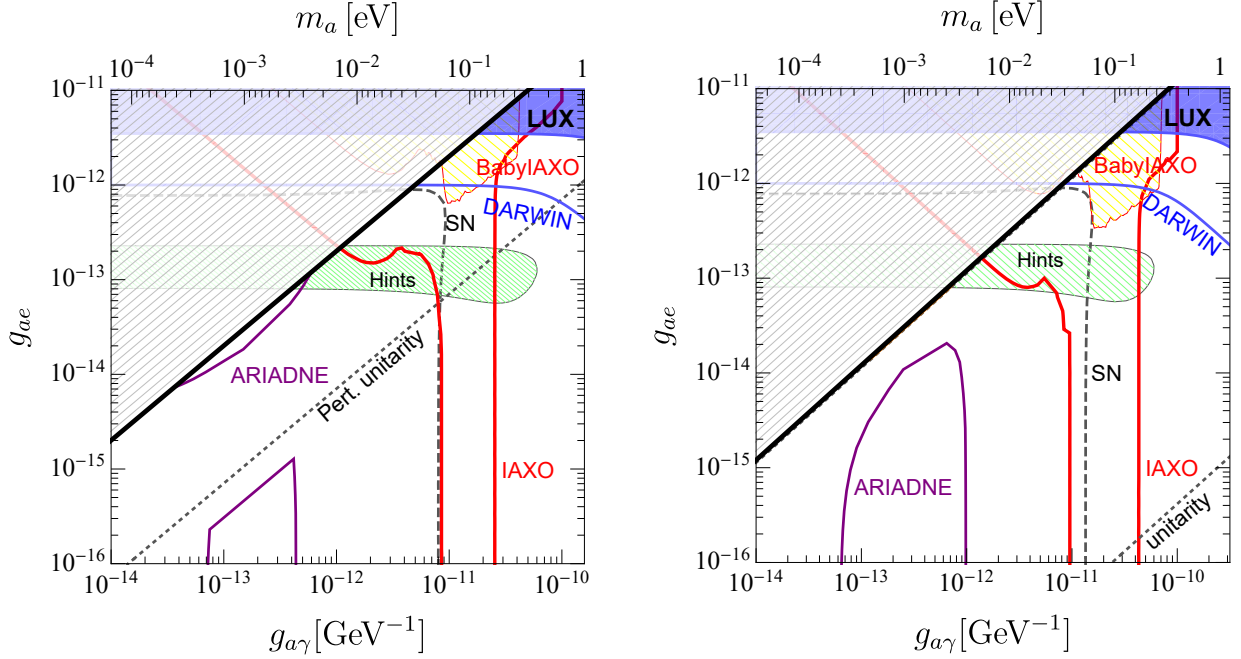


Figure 15: DFSZ axion I (left) and II (right) parameter space. The hatched region in the upper left corner is not accessible to such axions models. The green region represents the stellar evolution hints from HB, RGB and WD stars, as discussed in the text. The SN 1987A bound is shown with a dashed line to reflect the higher level of uncertainty with respect to other stellar bounds.

the case of the axio-electric cross section. Therefore, in general the Primakoff flux is not negligible and should be included in the estimates of the experimental potential. For example, setting $g_{ae} = 10^{-12}$ and $g_{a\gamma} = 10^{-10} \text{ GeV}^{-1}$, we find $g_{a\gamma}^2 \int \sigma_{ae} n_\gamma d\omega \simeq 2g_{ae}^2 \int \sigma_{ae} n_e d\omega$. Proceeding similarly to what done in the case of the Sikivie helioscopes, we set \bar{g}_{ae} to the experimental bound for a purely ABC spectrum and find the very simple relation for the axion couplings:

$$g_{ae}^2 \int (g_{a\gamma}^2 n_\gamma + g_{ae}^2 n_e) \tilde{\sigma}_{ae} \epsilon d\omega \leq \bar{g}_{ae}^4 \int n_\gamma \tilde{\sigma}_{ae} \epsilon d\omega, \quad (246)$$

where $\tilde{\sigma}_{ae}$ is the axio-electric cross section for $g_{ae} = 1$. If we assume that ϵ does not have a strong dependence on ω , the integrals can be performed analytically and we find:

$$g_{e12}^2 (2g_{\gamma10}^2 + g_{e12}^2) \lesssim \bar{g}_{e12}^4. \quad (247)$$

5.3. Haloscopes and DM axions

The local DM density is estimated to be about 0.45 GeV/cm^3 . If the axion paradigm is correct and axions do make up the totality of the DM matter, we should expect (locally) about $4.5 \times 10^{14} (\mu\text{eV}/m_a) \text{ cm}^{-3}$ non-relativistic axions, with energy $\omega_a \sim m_a(1 + O(10^{-6}))$, where the correction to the energy derives from the estimated axion velocity distribution ($v \sim 10^{-3}$). Several experimental techniques have been developed to detect such a huge number of nonrelativistic axions. Collectively, such experiments are known as *axion haloscopes*. As discussed in Section 3, the exact axion mass required for the axion to account for the totality of the DM in the Universe is unknown. Although, historically, there has been a preference for the mass region around a few μeV , theoretical uncertainties about the initial conditions (Section 3.3) and the production mechanisms, particularly the contribution from cosmological defects (Section 3.4), make the pinning of the exact mass very uncertain. Moreover, in Section 6.6 we present mechanisms that can shift the relevant mass region from $\lesssim \text{neV}$ all the way up to 10 meV or so, in the region accessible to the next generation of axion

helioscopes (see Section 5.1). Designing experiments that can probe this entire mass region is, therefore, extraordinary important to detect axions, if they really are a significant DM component.

The conventional haloscope technique is the resonant cavity haloscope [444], which employs the Primakoff conversion of DM axions in a strong magnetic field that permeates a resonant microwave cavity. The conversion is resonant if the axion energy $\omega_a = m_a(1 + O(10^{-6}))$ matches a cavity mode. Cavity experiments are well suited to search for axions in the μeV mass range, where they have reached extremely high sensitivities. In particular, the Axion Dark Matter eXperiment (ADMX), which is the most mature axion haloscope, has already reached into the KSVZ and DFSZ parameter space (under the assumption that axions are the totality of the DM) for masses $m_a \sim 3\mu\text{eV}$ [327, 460]. A drawback is the slow mass-scanning time, which scales quadratically with the desired signal to noise level, $\Delta t \propto (S/N)^2$.⁶⁰ Furthermore, the cavity size has to match with great accuracy the axion Compton wavelength. Therefore, scanning higher masses requires smaller cavities with the consequent loss of sensitivity at fixed scanning time (the power of the signal scales linearly with the volume).⁶¹

Nevertheless, an intense program to probe the higher mass range is currently in place. A series of ultra low temperature cavity experiments at IBS/CAPP (CULTASK) promise the exploration of the mass region between ADMX and MADMAX (see below) [328]. CAPP-8TB is designed to search for axions with mass 6.62 to 7.04 μeV , with enough sensitivity to detect DFSZ or KSVZ axions [463]. Operations of the more ambitious CAPP-12TB and CAPP-25T could begin in the early 2020s [328]. Combined, they are expected to explore the axion mass region from ~ 3 to $\sim 40\mu\text{eV}$, down to the KSVZ model ($E/N = 0$), with sensitivity to DFSZ I couplings for masses up to $\sim 10\mu\text{eV}$ (Cf. Fig. 16 and Table 4). Meanwhile, the HAYSTACK experiment is probing masses about an order of magnitude larger than ADMX. It recently reported the first results for a scan in the mass range 23.5 – 24 μeV , with sensitivity down to $g_{a\gamma} = 2 \times 10^{14} \text{ GeV}^{-1}$ [464]. At considerably higher masses, ORGAN [465] plans to probe the mass region $\sim 60 - 210\mu\text{eV}$.

A quite different haloscope concept, MADMAX [466] uses movable booster dielectric disks to enhance the photon signal and, as shown in Fig. 13 and 14, the projected sensitivity ranges from ~ 50 to a few 100 μeV [331]. A similar range of masses could be probed with tunable axion plasma haloscopes [467], which employ the axion coupling to plasmons. The resonance condition is induced by the matching of the axion mass with the plasma frequency and is, therefore, completely uncorrelated with the size of the experiment. Finally, the meV mass range might also become accessible using topological antiferromagnets [468]. The current study predicts enough sensitivity to probe, perhaps in its second stage, DFSZ axions in the 1 – 3 meV mass range.

Differently from the above experiments, the QUAX (QUaerere AXion) experiment [469] aims at detecting axion DM via the axion coupling to electrons. While the Earth moves through the cold axion halo, the coupling to the electron spins would induce spin flips in a magnetized material placed inside a static magnetic field. This effect can be detected using Nuclear Magnetic Resonance (NMR) techniques. The experiment aims at the mass range $m_a \sim 100\mu\text{eV}$, similar to the range of MADMAX. Recent experimental data [470] excluded the range of couplings $g_{ae} > 4.9 \times 10^{-10}$ at 95% CL, for an axion mass of 58 μeV . This first bound is not yet comparable with the stellar constraints discussed in Section 4.2, and is still several orders of magnitude larger than what predicted in DFSZ axion models.

An intriguing proposal to test the axion DM paradigm in a wide mass range, $m_a \sim 0.2 - 40\mu\text{eV}$, is through the detection of radio signals from the axion conversion into photons in NS magnetospheres [471–473]. The NS magnetosphere hosts a very intense magnetic field and a variable plasma frequency. If DM axions do exist, they would convert in such field at the radial distance where the plasma frequency matches the axion mass, and produce an observable flux. The detection potential of current and future radiotelescopes

⁶⁰The rate at which a mass range can be scanned is controlled by the Dicke radiometer equation [461]:

$$S/N = \frac{P_a}{P_N} \sqrt{\Delta\nu t} = \frac{P_a}{T_S} \sqrt{\frac{t}{\Delta\nu}}, \quad (248)$$

where $P_N = \Delta\nu T_S$ is the thermal noise power, $\Delta\nu$ is the bandwidth and T_S is the system noise temperature (physical + receiver noise) (cf. e.g. [39, 398]).

⁶¹A recent promising way-out consists in exploring higher order resonant modes [462].

is discussed in [471] and expected to reach enough sensitivity to probe the DFSZ axion parameter region. Another suggestion for probing cold dark matter axions with forthcoming radio telescopes such as the Square Kilometer Array (SKA) [474] was put forth in [475] and further elaborated in [476]. The proposed strategy is that of detecting axion decay into photons at radio frequencies monitoring astrophysical targets such as dwarf spheroidal galaxies, the Galactic Center and halo, and galaxy clusters. Depending on the environment and on the mass of the axion, a stimulated enhancement of the decay rate may amplify the photon flux by several orders of magnitude, bringing the signal within the reach of next-generation radio telescopes.

Probing lower masses is also quite challenging, requiring larger cavities and magnets. The KLASH (KLoe magnet for Axion SearchH) experiment aims at the mass region $\simeq 0.3 - 1 \mu\text{eV}$, just below the ADMX range. According to the preliminary study, KLASH has the potential to probe axion-photon couplings close to the DFSZ benchmarks in the given mass range [322]. Experiments that aim at exploring even lower masses adopt different techniques to avoid the problem, inherent in all cavity searches, of matching the axion wavelength with extremely large cavity sizes. ABRACADABRA (A Broadband/Resonant Approach to Cosmic Axion Detection with an Amplifying B-field Ring Apparatus) uses a toroidal magnet and a pickup loop to detect the variable magnetic flux induced by the oscillating current produced by DM axions in the static (lab) magnetic field. The experiment can operate as a broadband or as a resonant experiment by using an untuned or a tuned magnetometer respectively. The aim is to probe a wide mass region below 10^{-8} eV , with sensitivity to DFSZ axions for masses in the range $0.1 - 10 \text{ neV}$ (cf. Figs. 13 and 14). In the first data release, masses between $3.1 \times 10^{-10} \text{ eV}$ and $8.3 \times 10^{-9} \text{ eV}$ were explored, with slightly less sensitivity to the axion-photon coupling than CAST [320].

Another ingenious idea to probe low masses is to exploit the axion coupling to the neutron EDM, Eq. (232) [434]. The oscillating axion field generates an oscillating nEDM that can be detected using NMR techniques. The Cosmic Axion Spin Precession Experiment (CASPER), in its Electric version (CASPER-Electric), employs a ferroelectric crystal which possesses a large, permanent internal electric field with which the axion field interacts. In phase 2, this experiment is expected to reach the sensitivity necessary to probe QCD axions [477], as shown in purple in Fig. 13 and 14.

CASPER Electric is particularly interesting from the modeling point of view, since it would effectively probe the axion-gluon coupling which, differently to the other couplings, is model independent. A consequence is that, in the case of a signal induced by a QCD axion, it may be possible to infer the (local) axion DM fraction. In fact, the value of g_d can be inferred, within the QCD uncertainties, from the value of the axion mass (identifiable since it sets the oscillation frequency) and the signal strength is a function only of g_d and of the (local) axion abundance. This possibility is unique among the axion haloscope experiments.

5.4. Searches for axions produced in the laboratory

Pure laboratory searches are also emerging as powerful options to search for axions. Such methods avoid uncertainties related to the use of natural sources for the axion flux. However, the sensitivities of pure laboratory experiments are currently far from the benchmark QCD axion regions and aim at testing, more generically, the ALPs parameter space.

One of the most mature experimental strategies to search for ALPs is the Light Shining Through a Wall (LSW) [478]. A powerful photon source, e.g. a laser beam, is used to produce axions, which are then reconverted into photons after crossing a *wall* opaque to light but not to axions. In both cases, the conversion is induced by a strong laboratory magnetic field. The Any Light Particle Search (ALPS) experiment has probed the mass region $m_a \lesssim 100 \mu\text{eV}$, yet only for couplings not competitive with CAST. Its updated version ALPS II (data-taking expected starting from 2021) will surpass CAST and probe unexplored parameter space. However, the sensitivity is expected to be still far from the DFSZ and KSVZ regions and may be of interest for QCD axions only in the case of very photophilic models (see Fig. 14). Currently, the strongest existing limit on the axion-photon coupling using this technique is $g_{a\gamma} < 3.5 \times 10^{-8} \text{ GeV}^{-1}$ (95% CL), for $m_a \leq 0.3 \text{ meV}$, achieved by the OSQAR experiment [479]. Similarly, polarization experiments use a laser beam in a strong magnetic field to search for axions or other light particles coupled to photons. The PVLAS experiment has been exploring this possibility for over a decade. The most recent reported constraints on the axion-photon coupling are comparable to the OSQAR bound but extend to slightly higher mass [480]. Some improvement is expected with the Vacuum Magnetic Birefringence experiment (VMB@CERN) [481].

Long range monopole-monopole and dipole-monopole interactions (cf. Section 2.10), induced by CP-odd couplings, provide other possibilities to search for axions [128]. The CP-odd axion couplings expected in the SM are tiny, as evident from Eq. (128). However, additional contributions are allowed in theories beyond the SM and the current experimental bounds allow for considerably larger values. Long range forces are severely constrained by precision measurements of Newton's law and tests of the equivalence principle (see, e.g., [39] and references therein). A better strategy for axion detection consists in using NMR techniques to detect the axion field sourced by a macroscopic object. This program will be carried out by the ARIADNE experiment [482]. Interestingly, in the most optimistic scenario (largest allowed CP odd couplings), ARIADNE is expected to have enough sensitivity to probe the $g_{aN}^S g_{an}$ combination of couplings down to values expected for the DFSZ axion [482, 483]. The forecasted sensitivity under these assumptions is shown in Fig. 15. Standard KSVZ axions are not accessible to ARIADNE, since in that case the coupling to neutrons is vanishingly small.

Somewhat similarly, QUAX- $g_p g_s$ probes the $g_{aN}^S g_{ae}$ combination. However, even in the most optimistic case, the expected sensitivity is still far from the coupling region expected in the case of KSVZ or DFSZ axions [484].

5.5. Summary of experimental constraints

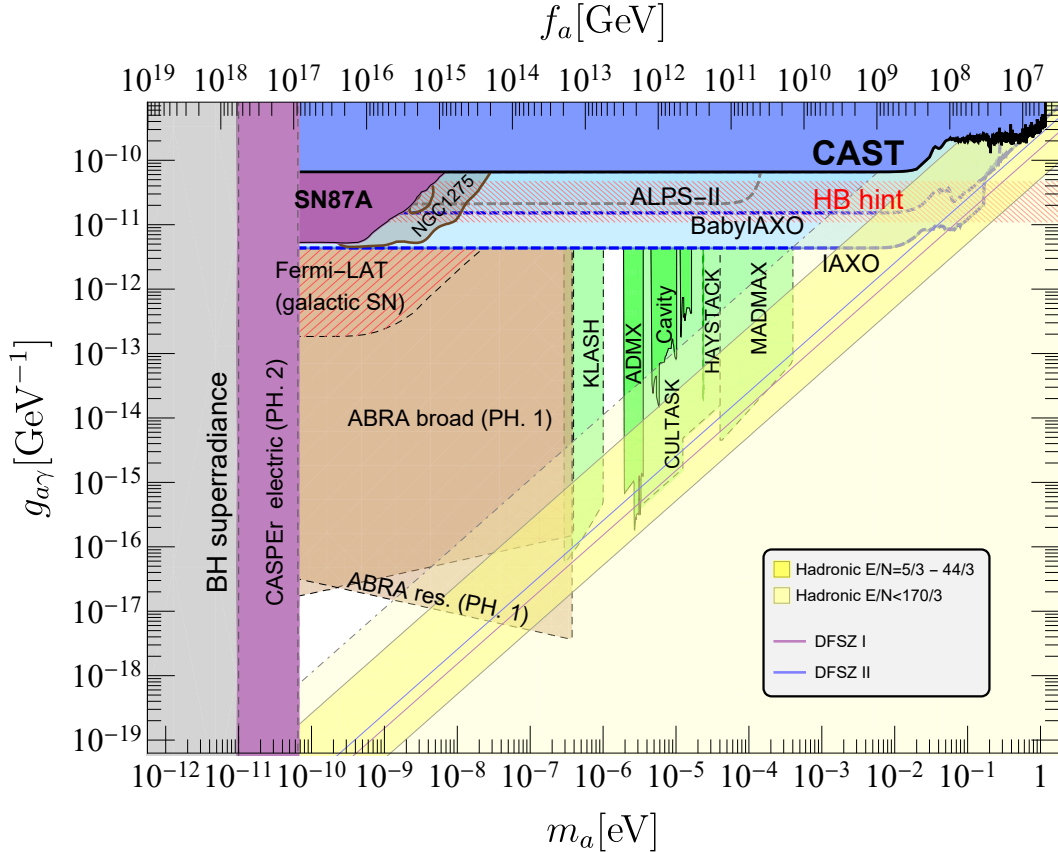


Figure 16: Phenomenological summary of the axion-photon interactions. We show also the region accessible to CASPER electric in phase II, when it will be able to probe the model independent axion coupling to gluons. The region presents the most optimistic scenario compatible with the QCD uncertainty in the calculation of the nEDM (Cf. Eq. (116)). The region expected for hadronic axions for certain ranges of E/N is shown in yellow. The relevance of these particular ranges for E/N is discussed in Section 6. For completeness, we also show the position of the DFSZ I and DFSZ II axions. However, in the case of the helioscopes the figure does not take into account the possible contribution of g_{ae} to the axion production. Refer to Fig. 15 for a more comprehensive analysis of the DFSZ axion models.

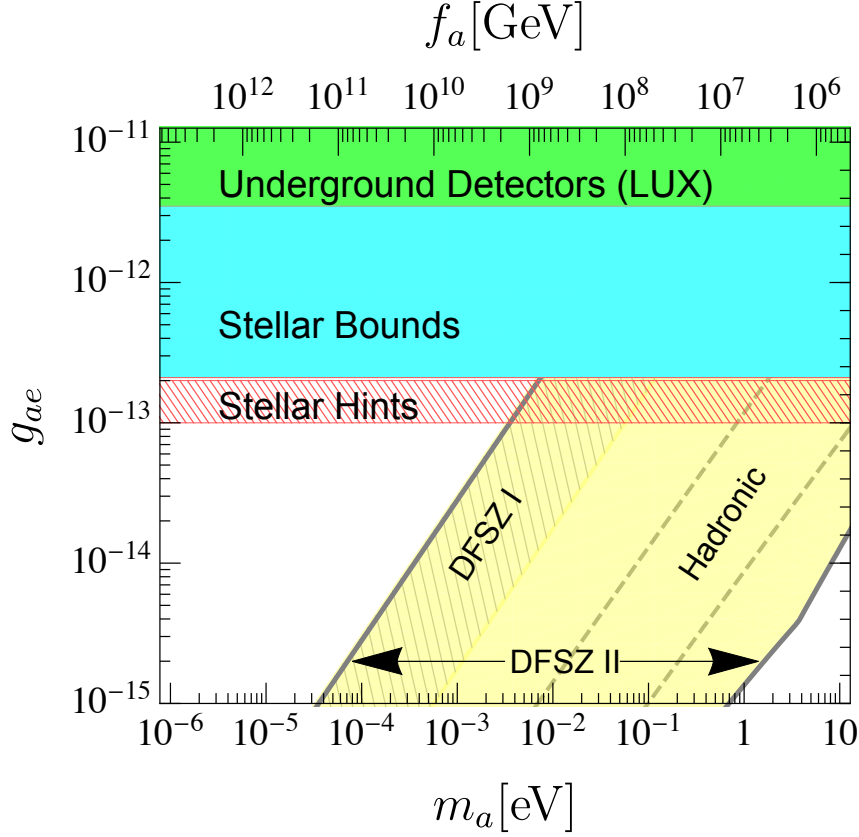


Figure 17: Phenomenological summary of the axion-electron interactions. The hadronic region is estimated for E/N between $5/3$ and $44/3$ (see Section 6). Notice the changing in the slope of the DFSZ II line at high mass. This happens when $\tan \beta$ is such that the tree level coupling of the DFSZ II axion to electrons is subdominant with respect to the 1-loop contribution.

In this section we summarize the experimental and astrophysical bounds on the individual axion couplings. Table 4 provides a quick reference to the major probes for each coupling. More details can be found in Fig. 16, for what concerns the axion-photon coupling, Fig. 17 for the axion-electron coupling, and Fig. 18 for the axion couplings to protons and neutrons. Notice that, in all cases, we are assuming that the axion solves the strong CP problem. Hence, we show the CASPERr electric potential in all cases since the experiment probes the model independent coupling to QCD gluons. However, we are not assuming any specific model and, hence, we are allowing for the couplings to be uncorrelated from the mass.

In the figures, we are showing the parameter space for DFSZ axions (I and II) and for hadronic axions within a specific range of E/N (cf. Section 6.1.1 and, in particular, Fig. 19). The reader should refer to Section 6 for a discussion of axion models beyond these benchmarks.

As evident from the figures, the axion-photon coupling is by far the most studied. Besides the experiments and bounds discussed in this section, we have added to the figure also the bound from the search for spectral irregularities in the gamma ray spectrum of NGC 1275 [485], from the non-observation of gamma rays from SN 1987A [486] and the Fermi Lat potential in the case of a future galactic SN [487]. Of course, such considerations apply to axions coupled to photons much more strongly than what expected in the benchmark axion models.

The axion-electron coupling is quite more difficult to probe, experimentally. The most efficient way is through helioscopes based on the axio-electric effect, discussed in Section 5.3. However, such experiments are still quite inefficient in the region below the astrophysical bounds. Given the very weak dependence of their potential on volume and observation time, this situation is not likely to change in the near future [39].

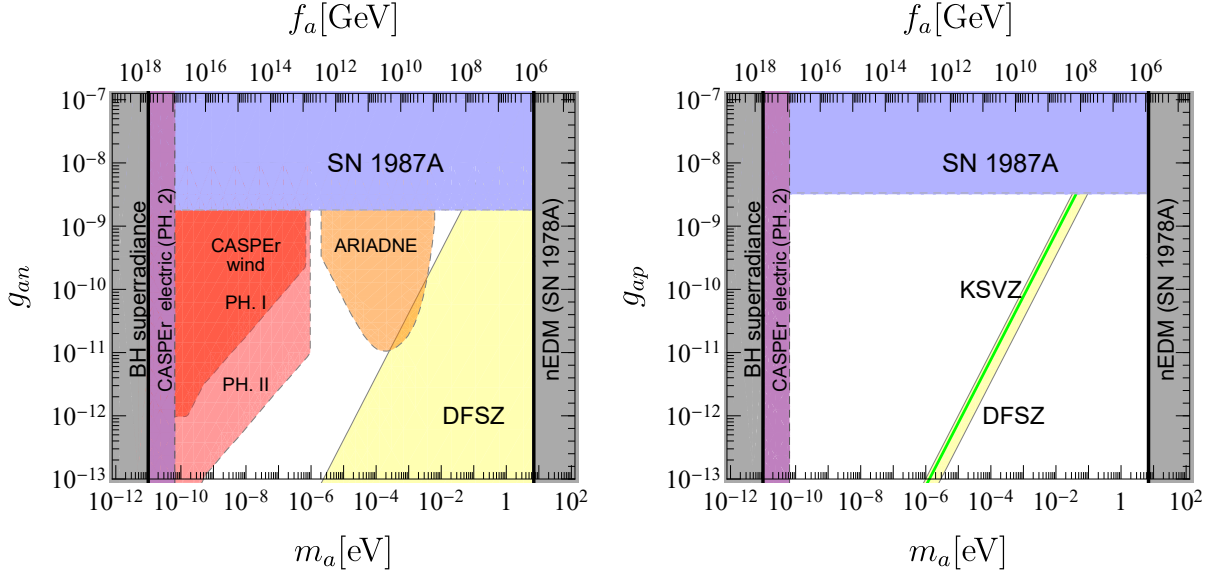


Figure 18: Phenomenological summary of the axion-nucleons interactions. In the case of the ARIADNE experiment, which measures the product $g_{aN}^S g_{an}$, the sensitivity is estimated for the most optimistic case of the scalar coupling, $g_{aN}^S = 10^{-12} \text{GeV}/f_a$ (see Ref. [482]). Notice that the axion-proton coupling remains largely unexplored. The hadronic axion coupling to neutrons is zero, within the errors [47]. Hence the absence of a KSVZ axion line in the left panel.

The strongest astrophysical constraints on the axion-nucleon coupling are derived from the cooling of NS and from SN 1987A (cf. Section 4.3). Experimentally, the couplings can be probed with NMR techniques. The experimental potential depends on the spin content of the nuclei adopted in the experiment. Our estimates for Fig. 18 are based on the single-particle Schmidt model [488], which predicts that only neutrons contribute to the nuclear spin of ^3He (adopted in ARIADNE) and ^{129}Xe (adopted in CASPER wind).⁶² Thus, assuming the Schmidt model, neither ARIADNE nor CASPER wind can probe the axion-proton coupling, implying that they would be blind to, e.g., KSVZ axions. This result is not completely correct. The single-particle Schmidt model does not always reproduce the experimental results well [489]. In particular, in the case of ^3He there is evidence of a small proton contribution to the nuclear spin [489]. Moreover, recently CASPER-ZULF-Comagnetometer used a mixture of ^{13}C and ^1H [490], which allows to access the axion-proton coupling. At any rate, the axion-proton coupling is significantly less probed experimentally and the current bounds on g_{ap} are not competitive with the astrophysical constraints.

In this section, we have focussed the attention to a subset of well known laboratory axion experiments, and more in general on experimental axion probes that either have already produced data, or that have passed some crucial step towards their realization, as for example having published a conceptual design report or having obtained funding to develop a R&D phase. In no way we have aimed at a complete review (a more comprehensive account of the experimental panorama can be found in Ref. [39, 40]). For example, recent results obtained by using superconducting LC circuit techniques at ADMX [491] or from the pathfinding run at the Western Australia haloscope ORGAN [465] have not been included. Most importantly, let us stress that the panorama of different proposals, that in many cases put forth originally new detection techniques, is much wider than what can be guessed from our brief review. To give a taste of the number of existing experimental projects and ideas, and to highlight the intellectual dynamism that permeates the community interested in axion searches, let us mention proposals for new helioscopes (TASTE) [492], or for variant haloscopes (ORPHEUS) [493], (RADES) [494, 495], also including multilayers optical techniques [496] or the possibility of broadband axion searches (BEAST) [497], new LSW based experiments (STAX/NEXT) [498–500], detection techniques based on laser spectroscopy (AXIOMA) [501, 502], methods based on precision

⁶²cf. Table 1 and 4 of Ref. [489].

Coupling	Source	Probes	Notes
$g_{a\gamma}$	Astro	Sun HB-stars SN 1987A	$g_{a\gamma} \leq 2.7 \times 10^{-10} \text{GeV}^{-1}$ for m_a up to a few keV $g_{a\gamma} \leq 0.65 \times 10^{-10} \text{GeV}^{-1}$ for m_a up to a few 10 keV $g_{a\gamma} \lesssim 6 \times 10^{-9} \text{GeV}^{-1}$ for $m_a \lesssim 100 \text{ MeV}$ $g_{a\gamma} \lesssim 5.3 \times 10^{-12} \text{GeV}^{-1}$ for $m_a \lesssim 4.4 \times 10^{-10} \text{ eV}$ $m_a \sim 2 - 3.5 \mu\text{eV}$. DFSZ for $m_a \sim 3 \mu\text{eV}$
	Cosmo	ADMX HAYSTACK MADMAX CULTASK KLASH ABRACADABRA Radio astronomy	$g_{a\gamma} \sim (2 - 3) \times 10^{-10} \text{GeV}^{-1}$ for $m_a \sim (23 - 24) \mu\text{eV}$ DFSZ for $m_a \sim 0.04 - 0.4 \text{meV}$ (<i>expected</i>) DFSZ for $m_a \sim 3 - 12 \mu\text{eV}$ (<i>expected</i> , CAPP 12-TB) KSVZ ($E/N = 0$) for $m_a \sim 3 - 40 \mu\text{eV}$ (<i>expected</i> , CAPP 25-T) $g_{a\gamma} \sim 3 \times 10^{-16} \text{GeV}^{-1}$ for $m_a \sim 0.3 - 1 \mu\text{eV}$ (<i>expected</i> , Ph. 3) $m_a \sim 2.5 \times 10^{-15} - 4 \times 10^{-7} \text{eV}$ (<i>expected</i>). DFSZ for $m_a \sim 40 - 400 \text{neV}$ (<i>expected</i> , ABRA res, Ph. 1) DFSZ for $m_a \sim 0.2 - 20 \mu\text{eV}$ (<i>expected</i>)
	Sun	CAST BabyIAXO IAXO	$g_{a\gamma} = 0.66 \times 10^{-10} \text{GeV}^{-1}$ for $m_a \lesssim 20 \text{meV}$ $g_{a\gamma} = 0.15 \times 10^{-10} \text{GeV}^{-1}$ for $m_a \lesssim 10 \text{meV}$ (<i>expected</i>) DFSZ for $m_a \sim 60 - 200 \text{meV}$ (<i>expected</i>) $g_{a\gamma} = 4.35 \times 10^{-12} \text{GeV}^{-1}$ for $m_a \lesssim 10 \text{meV}$ (<i>expected</i>) DFSZ for $m_a \gtrsim 8 \text{meV}$ (<i>expected</i>)
	Lab	PVLAS OSQAR ALPS II	$10^{-7} \text{GeV}^{-1} \lesssim g_{a\gamma} \lesssim 10^{-6} \text{GeV}^{-1}$ for $m_a \sim 0.5 - 10 \text{meV}$ $g_{a\gamma} \simeq 4 \times 10^{-8} \text{GeV}^{-1}$ for $m_a \lesssim 0.4 \text{meV}$ $g_{a\gamma} \simeq 2 \times 10^{-11} \text{GeV}^{-1}$ for $m_a \lesssim 60 \mu\text{eV}$ (<i>expected</i>)
g_{ae}	Astro	RGB-stars WDs	$g_{ae} \leq 3.1 \times 10^{-13}$ for m_a up to a few 10 keV $g_{ae} \leq 2.1 \times 10^{-13}$ for m_a up to a few keV
	Sun	LUX XENON100 PandaX-II LZ DARWIN	$g_{ae} \leq 3.5 \times 10^{-12}$ $g_{ae} \leq 7.7 \times 10^{-12}$ $g_{ae} \leq 4 \times 10^{-12}$ $g_{ae} \leq 1.5 \times 10^{-12}$ $g_{ae} \leq 1 \times 10^{-12}$
$g_{a\gamma}g_{ae}$	Sun	helioscopes (CAST, LUX,...)	Depends on explicit values of $g_{a\gamma}$ and g_{ae} . Can be extracted from Eq. (244) and Eq. (247)
g_{an}	Astro	SN 1987A, NS	$g_{an} \leq 2.8 \times 10^{-10}$ (from NS in HESS J1731-347)
	Lab	ARIADNE CASPEr wind	measures $g_{aN}^S g_{an}$ down to DFSZ for $m_a \sim 0.25 - 4 \text{meV}$ (<i>expected for most optimistic choice</i> $g_{aN}^S = 10^{-12} \text{GeV}/f_a$ [482]). From $m_a \simeq 3.6 \times 10^{-12} \text{eV}$ ($g_{an} \simeq 1.1 \times 10^{-14}$) and $m_a \simeq 9.5 \times 10^{-7} \text{eV}$ ($g_{an} \simeq 5.1 \times 10^{-12}$) (<i>expected</i> , Ph. 2).
g_{ap}	Astro	SN 1987A	$g_{ap} \lesssim 3.3 \times 10^{-9}$ for $g_{an} = 0$ (hadronic axions).
g_d	Astro	SN 1987A	$g_d \leq 3 \times 10^{-9} \text{GeV}^{-2}$
	Lab	CASPEr electric	QCD axion for $\log(\frac{m_a}{\text{eV}}) \simeq -11_{-0.9}^{+0.8}$ (<i>expected</i> , Ph. 2)

Table 4: Summary of astrophysical and experimental probes on the axion couplings. For proposed experiments, in the notes column we indicate the expected mass range and potential, as extracted from the original literature. Whenever necessary, we also indicate the phase (Ph.) during which such results are expected. The haloscope potential reported assumes that the totality of the DM component in the Universe is made of axions. Whenever an experiment can probe DFSZ axions, we have indicated the mass range using the sentence “DFSZ for $m_a \dots$ ”. In the case of CASPEr electric, we indicate the mass range in which the experiment may be sensitive to QCD axions. The error indicates the QCD uncertainty.

magnetometry [482], and on antiferromagnetically doped topological insulators (TOORAD) [468], or even more exotic ideas, like that of a global network of optical magnetometers sensitive to nuclear- and electron-spin couplings, that could reveal transient astrophysical events as the passage trough Earth of axion stars (GNOME) [503].

6. The axion landscape beyond benchmarks

Shortly after the KSVZ [120, 121] and DFSZ [118, 119] invisible axion models had been constructed, several variants started to appear in the literature. They were often motivated by the attempt of making more natural the preferred values of the axion decay constant $10^9 \text{ GeV} \lesssim f_a \lesssim 10^{12} \text{ GeV}$ which does not match neither the electroweak nor the GUT scale, by constructing the axion as a composite state of a new non-abelian gauge interaction [112, 154, 504, 505] that becomes strong at the required scale.⁶³ At the same time, these constructions implied different properties for the axion, as for example sizeable differences in the strength of the axion coupling to the photon with respect to the KSVZ and DFSZ models. Thus, the idea that the *axion window*, i.e. the region in the $(m_a, g_{a\gamma})$ plane predicted by QCD axion models, could be sizeably larger than what suggested by canonical KSVZ/DFSZ constructions, was already contemplated as a likely possibility by some early phenomenological studies [112, 154, 506]. Recent years have witnessed a proliferation of proposals for axion experiments [38, 39] (see also Section 5) and, although at present all ongoing attempts to detect the axion rely on the axion-photon coupling, a certain number of new proposals, often based on cutting-edge experimental techniques, are also sensitive to the axion couplings to nucleons and electrons. In many cases the projected sensitivity of new proposals does not reach the level required to test the KSVZ and DFSZ models, and this is especially true for first generation experiments which, at least in their initial operational stages, mainly represent a proof-of-concept for the effectiveness of new axion search techniques. For these experiments it is often understood that the explorable regions would at best test the possible existence of ALPs, that is particles that share some of the properties of the QCD axion, but that are not requested to solve the strong CP problem and, as a consequence, can exist within a much wider parameter space region.

The aim of this section is to carry out a thorough review of past and recent axion models, focussing on their predictions for the axion couplings to photons $g_{a\gamma}$ (Section 6.1), to electrons g_{ae} (Section 6.2), to protons g_{ap} and neutrons g_{an} (Section 6.3), and their constraints from astrophysics and direct searches (Section 6.4). The highlight of this section is to specify under which conditions the values of these couplings can be either enhanced or suppressed with respect to their canonical values, and in which cases new features, like for example flavour changing axion couplings, can emerge (Section 6.5). To classify the large number of possibilities, it turns out to be convenient to maintain a distinction between KSVZ-like and DFSZ-like scenarios. KSVZ-like refers to the class of models in which the SM fermions and the electroweak Higgs fields do not carry PQ charges, the axion-electron coupling vanishes at leading order, and the leading contribution to the axion-nucleon and axion-pion couplings only depends on the anomalous QCD term $(a/f_a)G\tilde{G}$. DFSZ-like instead broadly refers to the class of models in which the SM particles are charged under the PQ symmetry so that the couplings between the axion and the SM fermions acquire a contribution proportional to the quarks and leptons PQ charges.

In Section 6.6 we will address the issue of the range of axion masses m_a for which the axion can account for the whole cosmological density of DM. We will identify different variants in both the particle physics and cosmological models that allow to extend the canonical mass range towards smaller or larger values of m_a .

Finally, in Section 6.7, we will consider mechanisms that allow to modify drastically the m_a - f_a relation while maintaining the solution of the strong CP problem, yielding $m_a \gtrsim 100 \text{ keV}$ axions which, due to their large mass, can avoid most astrophysical constraints.

6.1. Enhancing/suppressing $g_{a\gamma}$

In Eq. (59) we have given the general expression for the axion coupling to photons. Including NLO corrections, which were computed in Ref. [47], and using $m_u/m_d \simeq 0.48(3)$, one obtains the expression given in Eq. (110) that we repeat below for convenience:

$$g_{a\gamma} = \frac{\alpha}{2\pi f_a} \left[\frac{E}{N} - 1.92(4) \right]. \quad (249)$$

⁶³Composite axions will be the subject of Section 7.7.

We recall that E and N are respectively the coefficients of the PQ electromagnetic and colour anomalies whose general expression is given in Eq. (83). The original KSVZ model discussed in Section 2.7.1 adopted the simplest choice in which the QCD anomaly is induced by heavy exotic colored fermions \mathcal{Q} , singlets under $SU(2)_L \times U(1)_Y$, so that $E/N = 0$ and $g_{a\gamma}$ is then determined solely by the model-independent numerical factor “ -1.92 ” originating from the $a/f_a G\tilde{G}$ term. This, however, implies that \mathcal{Q} -baryon number, associated with the non-anomalous $U(1)$ symmetry $\mathcal{Q} \rightarrow e^{i\beta} \mathcal{Q}$, is exactly conserved (being protected by the gauge symmetry). Hence, after confinement, the \mathcal{Q} ’s would give rise to stable fractionally charged hadrons which have not been observed [507]. Thus, charged \mathcal{Q} ’s that could mix with the light quarks and decay, and that would give rise to $E/N \neq 0$, should be considered phenomenologically preferred. For the DFSZ models discussed in Section 2.7.2 the SM quarks and leptons charges imply either $E/N = 8/3$ or $2/3$, depending on whether the leptons are coupled to the d -type (DFSZ-I) or to the u -type (DFSZ-II) Higgs. From Eq. (249) we see that large enhancements of the axion-photon coupling require $E/N \gg 2$, while the axion would approximately decouple from the photon if $E/N \approx 2$. Below we discuss several cases in which these possibilities can be realised.

6.1.1. KSVZ-like scenarios

The model dependence of the axion-photon coupling and the possibilities to arrange for large enhancements or for approximate decoupling, was first discussed by Kaplan in Ref. [112], where a variant of Kim’s composite axion model [505] (see also [508]) was put forth. Since composite axions will be the subject of Section 7.7, here we only provide the essential ingredients to explain the main features of Kaplan’s model. A gauge group factor $SU(\mathcal{N})$ of metacolor (or axicolor) that becomes strongly interacting at a large scale $\Lambda \sim f_a$ is added to the SM gauge group $SU(3)_c \times SU(2)_L \times U(1)_Y$, together with two multiplets of exotic Dirac fermions ψ and ξ that are $SU(2)_L$ singlets and transform under $SU(\mathcal{N}) \times SU(3)_c \times U(1)_Y$ as

$$\psi \sim (\mathcal{N}, 3)_{y_1}, \quad \xi \sim (\mathcal{N}, 1)_{y_2}, \quad (250)$$

where y_1, y_2 denote hypercharges. The exotic quarks have no mass term so that there is a $U(1)^4$ global symmetry for the kinetic term corresponding to $U(1)_{B_\psi} \times U(1)_{B_\xi} \times U(1)_{\bar{A}} \times U(1)_A$. The first two factors are vector-like and ensure ψ and ξ baryon number conservation. The remaining two axial symmetries get spontaneously broken by the condensates $\langle \bar{\psi}_L \psi_R \rangle = \langle \bar{\xi}_L \xi_R \rangle \neq 0$ resulting in two NGBs that acquire masses due to the anomaly of the corresponding currents with the strongly interacting gauge groups. The current $\tilde{J}_\mu^5 = \frac{1}{2} (\bar{\psi} \gamma_\mu \gamma_5 \psi + \bar{\xi} \gamma_\mu \gamma_5 \xi)$ has an anomaly with $SU(\mathcal{N})$ hence the corresponding NGB acquires a large mass of order f_a . In contrast, the current $J_\mu^5 = \frac{1}{\sqrt{24}} (\bar{\psi} \gamma_\mu \gamma_5 \psi - 3 \bar{\xi} \gamma_\mu \gamma_5 \xi)$ has only colour and electromagnetic anomalies:

$$\partial^\mu J_\mu^5 = \frac{g_s^2}{16\pi^2} \frac{\mathcal{N}}{2\sqrt{24}} G_{\mu\nu}^a \tilde{G}^{a\mu\nu} + \frac{e^2}{16\pi^2} \frac{3\mathcal{N}(y_2^2 - y_1^2)}{\sqrt{24}} F_{\mu\nu} \tilde{F}^{\mu\nu}, \quad (251)$$

so that the corresponding NGB, which is identified with the axion, acquires a tiny mass $m_a \sim m_\pi f_\pi (N/f_a)$. The axion coupling to photons involves the anomaly coefficient ratio $E/N = 6(y_1^2 - y_2^2)$ and is thus proportional to $g_{a\gamma} \propto 6(y_1^2 - y_2^2) - 1.92$. As remarked in Ref. [112], by choosing $(y_1, y_2) = (0, 1)$ one obtains an enhancement in $g_{a\gamma}$ of a factor of ten with respect to the DFSZ model with $E/N = 8/3$, while $(y_1, y_2) = (2/3, 1/3)$ give $E/N - 1.92 = 0.08$ which amounts to a suppression of a factor of ten. Although this composite axion model clearly relies on a different construction with respect to KSVZ models with fundamental scalars, it can still be classified as being of the KSVZ-type since the SM states do not carry PQ charges and at the leading order $g_{ae} = 0$. Models in which the axion does not couple directly to the leptons are also known as *hadronic* axion models. Note that similar constructions for composite axions always require at least two sets of massless exotic fermions in order to be able to generate a light axion that can solve the QCD θ problem, since a single set would give rise to just one heavy axion for which the dominant potential term would drive $\theta_N \rightarrow 0$ leaving θ at a generic $O(1)$ value (unless an accurate alignment between the two angles is arranged for, see Section 6.7). Taken as a mechanism to enhance or suppress $g_{a\gamma}$, composite axion models are not particularly economical since, as we will see, KSVZ models involving two sets of exotic fermions allow for much larger enhancements of $g_{a\gamma}$ as well as for more accurate cancellations between the two contributions to the coupling. Clearly in the first KSVZ construction the choice of a $SU(2)_L \times U(1)_Y$

singlet representation for the heavy vector-like quarks Q represented the simplest possibility. Colour representations with nontrivial electroweak quantum numbers, as in the Kaplan model, would work as well, with the difference that at least some of the heavy quarks would be electrically charged yielding $E/N \neq 0$. While in principle any electroweak representation is equally good for implementing the PQ solution, not all are phenomenologically allowed, and only a few are in fact phenomenologically preferred. A systematic attempt of classifying the viable representations $R_Q = (\mathcal{C}_Q, \mathcal{I}_Q, \mathcal{Y}_Q)$ under the $SU(3)_c \times SU(2)_L \times U(1)_Y$ gauge group was carried out in Refs. [507, 509]. Four possible phenomenological criteria to classify the representations as *phenomenologically preferred* were identified:

- (i) R_Q should not induce Landau poles (LP) below a scale Λ_{LP} of the order of the Planck scale;
- (ii) R_Q should not give rise to cosmologically dangerous strongly interacting relics;
- (iii) R_Q 's yielding domain wall number $N_{DW} = 1$ are preferred by cosmology;
- (iv) Improving gauge coupling unification can be an added value.

These four criteria have rather different discriminating power. Gauge coupling unification (iv) is a desirable feature for any particle physics model. However, improved unification for some R_Q might simply occur as an accident because of the many different representations that one can consider, as well as from the freedom in choosing the relevant mass scale m_Q between a few TeV (from exotic quark searches at the LHC) and Λ_{GUT} . Besides this, from the theoretical point of view envisaging a GUT completion of KSVZ axion models in which only a fragment R_Q of a complete GUT multiplet receives a mass $m_Q \lesssim v_a \ll \Lambda_{GUT}$, as is necessary to assist gauge coupling unification, while all the other fragments acquire GUT-scale masses, is not straightforward, and it appears especially challenging in all the cases in which the PQ symmetry commutes with the GUT gauge group (see Section 7.8 and in particular footnote 83). Difficulties in constructing explicit realisations of R_Q assisted unification thus suggest that discriminating the R_Q on the basis of the last property (iv) might be less meaningful than what one would initially guess. Axion models with $N_{DW} > 1$ face the so called cosmological DW problem [510] (see Section 3.4.4) while models with $N_{DW} = 1$ are cosmologically safe [197, 243], hence motivating the criterium (iii) above. However, one can envisage various solutions of the DW problem based either on cosmology or model-building (see Section 7.5). Due to these considerations, in Refs. [507, 509] criteria (iii) ($N_{DW} = 1$) and (iv) (improved gauge coupling unification) were only considered as desirable features of a KSVZ axion model, but not sufficiently discriminating to be used as criteria for identifying possibly pathological R_Q . The first two conditions are instead quite selective for discriminating among different representations, as it will be reviewed in the following.

(i) *Landau poles.* Large representations can often induce LP in the hypercharge, weak, or strong gauge couplings g_1, g_2, g_3 at some uncomfortably low-energy scale $\Lambda_{LP} < m_{Pl}$. In Refs. [507, 509], rather than $\Lambda_{LP} \sim m_{Pl}$ a more conservative choice $\Lambda_{LP} \sim 10^{18}$ GeV was made. This was justified by the fact that at energy scales approaching m_{Pl} , gravitational corrections to the running of the gauge couplings can become relevant, and explicit computations show that they go in the direction of delaying the emergence of LP [511]. Therefore a value of Λ_{LP} for which gravitational corrections are presumably negligible was chosen. The scale at which the LP arises was evaluated by using two-loops gauge beta functions⁶⁴ and by setting the threshold for including the R_Q representations in the running of the gauge couplings at $m_Q = 5 \cdot 10^{11}$ GeV. By recalling that $m_Q = y_Q N_{DW} f_a / \sqrt{2}$ (see Section 2.7.1), this value can be justified in post-inflationary scenarios in terms of the cosmological limit on f_a that follows from the requirement $\Omega_a \lesssim \Omega_{DM}$, and in pre-inflationary scenarios by demanding additionally that the initial value of the axion field is not tuned to be much smaller than f_a .

To see what is the maximum value of the $g_{a\gamma}$ coupling allowed by the LP condition, one can start by considering a single representation $R_Q = (\mathcal{C}_Q, \mathcal{I}_Q, \mathcal{Y}_Q)$ and look for the maximum allowed values of the E_Q/N_Q coupling factor. From Eq. (84) this factor can be written as

$$\frac{E}{N} = \frac{E_Q}{N_Q} = \frac{d(\mathcal{C}_Q)}{T(\mathcal{C}_Q)} \left[\frac{1}{12} (d(\mathcal{I}_Q)^2 - 1) + \mathcal{Y}_Q^2 \right]. \quad (252)$$

⁶⁴Accidental cancellations in the one-loop gauge beta function for higher-dimensional multiplets can lead indeed to erroneous estimates of the LP (see e.g. [512]).

The minimum value of the denominator is $T(\mathcal{C}_Q) = \frac{1}{2}$ which corresponds to colour triplets. For a hyperchargeless representation the LP condition in g_2 is saturated with a fermion quadruplet $R_Q(\mathcal{I}_Q^{\max}) = (3, 4, 0)$ while for an $SU(2)_L$ singlet the LP condition in g_1 is saturated by $R_Q(\mathcal{Y}_Q^{\max}) = (3, 1, 5/2)$, where the rational value $5/2$ is a simple approximation to the real valued result. The maximum allowed hypercharge value $\mathcal{Y}_Q = \frac{5}{2}$ in turn implies the condition $\mathcal{Y}_Q \sqrt{d(\mathcal{I}_Q)} \leq \frac{5}{2}$. E/N is then maximal for the value of $d(\mathcal{I}_Q)$ that, within the allowed range $1 \leq d(\mathcal{I}_Q) \leq 4$, maximises the expression in square brackets in Eq. (252) subject to this condition, that is, it maximises the function $d(\mathcal{I}_Q)^2 - 1 + 75/d(\mathcal{I}_Q)$. The maximum is found for [509]

$$R_Q(\mathcal{Y}_Q^{\max}) = (3, 1, 5/2) \Rightarrow E/N = 75/2. \quad (253)$$

Larger values can be obtained by adding the two representations $R_Q(\mathcal{Y}_Q^{\max}) \oplus R_Q(\mathcal{I}_Q^{\max})$ to maximise the numerator in Eq. (252) (this saturates the LP limits for g_1 and g_2) while the minimal possible value of the denominator $\sum_Q \mathcal{X}_Q d(\mathcal{I}_Q) T(\mathcal{C}_Q) = \pm 1/2$ can be retained by adding a $SU(2)_L \times U(1)_Y$ singlet in the adjoint of colour (with index $T(8) = 3$) and with opposite sign of the PQ charge: $(1 + 4) \times T(3) - T(8) = -1/2$. In this way one obtains the maximum value of E/N compatible with the LP condition:

$$(3, 1, 5/2) \oplus (3, 4, 0) \ominus (8, 1, 0) \Rightarrow E/N = -135/2. \quad (254)$$

(Here and below the symbol \ominus will refer to an irreducible fragment of a reducible representation that has opposite sign of the PQ charge with respect to the other fragments, that is it couples to the Hermitian conjugate of the PQ field as $y_Q \bar{Q}_L Q_R \Phi^\dagger$ rather than as in Eq. (76).) Equivalent possibilities can be obtained with different representations $(3, 1, \mathcal{Y}_Q) \oplus (3, 4, \mathcal{Y}_{Q'})$ satisfying $\mathcal{Y}_Q^2 + 4\mathcal{Y}_{Q'}^2 = (5/2)^2$, as for example $(3, 1, 3/2) \oplus (3, 4, 1)$, etc.

(ii) *Cosmologically dangerous relics.* The transformation properties of R_Q under the SM gauge group constrain the type of couplings of the Q 's with SM particles, and in several cases this might result in stable or long-lived anomalously heavy ‘hadrons’. In post-inflationary scenarios this can represent a cosmological issue. In pre-inflationary scenarios instead the Q 's would be diluted away by the exponential expansion and would be harmless. Therefore, condition (ii) restricts the viable R_Q only under the assumption that $U(1)_{PQ}$ is broken after inflation and that $m_Q < T_{RH}$. In this case the Q 's will attain, via their gauge interactions, a thermal distribution. This provides well defined initial conditions for their cosmological history, which then in principle depends only on their mass m_Q and representation R_Q .

For some R_Q , as for example the $SU(2)_L \times U(1)_Y$ singlets of the original KSVZ model [120, 121] as well as for the three representations in Eq. (254), Q decays into SM particles are forbidden. Moreover the heavy quarks can only hadronize into fractionally charged hadrons (see the Appendix in Ref. [509]). These Q -hadrons must then exist today as stable relics. Searches for fractionally charged particles in ordinary matter limit their abundance with respect to ordinary nucleons to $n_Q/n_b \lesssim 10^{-20}$ [513] which is orders of magnitude below any reasonable estimate of the Q 's cosmological relic abundance and of their expected concentration in bulk matter. The set of viable R_Q 's is then restricted to the much smaller subset that yields integrally charged or neutral color singlet Q -hadrons, in which case the limits on n_Q/n_b are less tight.

Whether this type of Q -hadrons can be excluded crucially depends on carrying out reliable estimates of their cosmological abundance Ω_Q , which is, however, a non-trivial task. In these estimates one generally assumes a symmetric scenario $n_Q = n_{\bar{Q}}$ since any asymmetry would eventually quench $Q\bar{Q}$ annihilation resulting in stronger bounds. At temperatures above the QCD phase transition the Q 's annihilate as free quarks, and the annihilation cross section can be computed perturbatively for any representation with reliable results. In this regime, for all masses above a few TeV one obtains $\Omega_Q \gg \Omega_{DM}$, which would firmly exclude stable Q 's if it were not for the fact that after confinement, Q -hadrons can restart annihilating. Obtaining reliable estimates of Ω_Q in this non-perturbative regime is challenging. A large cross section typical of inclusive hadronic scattering $\sigma_{ann} \sim (m_\pi^2 v)^{-1}$ was assumed in Ref. [514], however, it was remarked in Ref. [515] that the relevant process is exclusive containing no Q 's in the final state, resulting in a cross section a few orders of magnitude smaller. Ref. [516] suggested that annihilation could be catalysed by the formation of quarkonia-like bound states in the collision of a Q - and a \bar{Q} -hadron. Refs. [517, 518] reconsidered this mechanism arguing that Ω_Q could indeed be efficiently reduced to the level that energy

density considerations would not be able to exclude stable relics with $m_Q \lesssim 5 \cdot 10^3$ TeV. Ref. [519] studied this mechanism more quantitatively and remarked that the possible formation of $QQ\ldots$ bound states, besides $Q\bar{Q}$, would hinder annihilation rather than catalyse it. Even if consensus on how to estimate reliably Ω_Q has not been reached yet, and $\Omega_Q < \Omega_{\text{DM}}$ remains an open possibility, all estimates suggest that present concentrations would still be rather large, at least $10^{-8} \lesssim n_Q/n_b \lesssim 10^{-6}$. Although it can be questioned if similar concentrations have to be expected also in the Galactic disk [520, 521], searches for anomalously heavy isotopes in terrestrial, lunar, and meteoritic materials, yield limits on n_Q/n_b many orders of magnitude below these estimates [522]. Moreover, even tiny amounts of heavy Q 's in the interior of celestial bodies (stars, neutron stars, Earth) would produce all sorts of effects like instabilities [523], collapses [524], anomalously large heat flows [525]. Therefore, unless an extremely efficient mechanism exists that keeps Q -hadrons completely separated from ordinary matter, cosmologically stable heavy relics of this type are excluded. This implies that if exotic Q exist, they must decay.

As shown in Ref. [509], for each R_Q that allows for integrally charged or neutral color singlet Q -hadrons, it is always possible to construct gauge invariant operators of some dimension that can mediate their decay into SM particles. The issue is which range of lifetimes τ_Q are cosmologically safe, and this can then be translated into an upper bound on the dimension of the relevant decay operators. The larger is the dimension, the longer is the lifetime, the more dangerous is the relic. Cosmological observations severely constrain the allowed values of τ_Q . For $\tau_Q \sim (10^{-2} \div 10^{12})$ s the decays of superheavy quarks with $m_Q \gg 1$ TeV would affect BBN [526–529]. Early energy release from decays with lifetimes $\sim (10^6 \div 10^{12})$ s is strongly constrained also by limits on CMB spectral distortions [530–532]. Q 's decaying around the recombination era ($t_{\text{rec}} \sim 10^{13}$ s) are tightly constrained by measurements of CMB anisotropies. Decays after recombination would give rise to free-streaming photons visible in the diffuse gamma ray background [533], and Fermi LAT [534] excludes $\tau_Q \sim (10^{13} \div 10^{26})$ s. Note that these last constraints are also able to exclude lifetimes that are several order of magnitude larger than the age of the Universe, $t_U \sim 4 \cdot 10^{17}$ s. The conclusion is that for the post-inflationary case cosmologically stable heavy Q 's with $m_Q < T_{\text{RH}}$ are strongly disfavoured and likely ruled out, while for unstable Q 's the lifetime must satisfy $\tau_Q \lesssim 10^{-2}$ s.

All R_Q 's which allow for decays via renormalizable operators easily satisfy the above requirements, while for higher-dimensional operators suppressed by m_{Pl} and for $m_Q \gtrsim 800$ TeV operators of dimension not larger than $d = 5$ are needed [507]. For $d = 6$, even for the largest values compatible with post-inflationary scenarios $m_Q \sim f_a^{\text{max}} \sim 10^{12}$ GeV decays occur dangerously close to BBN. Operators of $d = 7$ and higher are always excluded. Table 5 (adpted from Ref. [507]) collects the representations that satisfy both the LP and the cosmological constraints. The largest value $E/N = 44/3$ is obtained for R_8 , while the weakest coupling is obtained for R_3 giving $E/N = 1.92 \sim -0.25$. These two values correspond to the two lines encompassing the green band in Fig. 19. Only the first two representations R_1 and R_2 have $N_{\text{DW}} = 1$, while only $R_3 = (3, 2, 1/6)$ is able to improve considerably unification with respect to the SM [507, 535].

With multiple representations sizeably larger values of E/N can be obtained. Saturating the LP condition using only cosmologically safe representations yields [507]

$$(3, 3, -4/3) \oplus (3, 3, -1/3) \ominus (\bar{6}, 1, -1/3) \quad \Rightarrow \quad E/N = 170/3, \quad (255)$$

which is only about 20% smaller than the value of $E/N = -135/2$ in Eq. (254) obtained by imposing only the LP condition. This maximum value for the $g_{a\gamma}$ coupling in KSVZ models is depicted with a dot-dashed line in Fig. 19. For $f_a > 5 \times 10^{11}$ GeV we forcedly have to assume a pre-inflationary scenario were the condition $m_Q > T_{\text{RH}}$ could be easily fulfilled. In this case the limit from cosmological considerations does not apply, however, the limit from the LP analysis still holds, so that the bound is only mildly relaxed. The corresponding region lies on the left-hand side of the purple vertical line in Fig. 19 labelled $f_a > 5 \times 10^{11}$ GeV.

Besides enhancing the axion-photon coupling, more R_Q 's can also weaken $g_{a\gamma}$, and even yield an approximate axion-photon decoupling. This requires an ad hoc choice of R_Q 's, but no numerical fine tuning. With two R_Q 's there are three such cases: $R_6 \oplus R_9$; $R_{10} \oplus R_{12}$ and $R_4 \oplus R_{13}$ which give respectively $E_c/N_c = (23/12, 64/33, 41/21) \approx (1.92, 1.94, 1.95)$ so that within theoretical errors even a complete decoupling is possible. In all these cases the axion could be eventually detected only via its (model-independent) coupling to the nucleons, given that the coupling to electrons is loop suppressed [111]. Finally, with multiple

	R_Q	\mathcal{O}_{Qq}	$\Lambda_{\text{LP}}^{R_Q} [\text{GeV}]$	E/N	N_{DW}
$d \leq 4$	$R_1: (3, 1, -\frac{1}{3})$	$\overline{Q}_L d_R$	$9.3 \cdot 10^{38}(g_1)$	$2/3$	1
	$R_2: (3, 1, +\frac{2}{3})$	$\overline{Q}_L u_R$	$5.4 \cdot 10^{34}(g_1)$	$8/3$	1
	$R_3: (3, 2, +\frac{1}{6})$	$\overline{Q}_R q_L$	$6.5 \cdot 10^{39}(g_1)$	$5/3$	2
	$R_4: (3, 2, -\frac{5}{6})$	$\overline{Q}_L d_R H^\dagger$	$4.3 \cdot 10^{27}(g_1)$	$17/3$	2
	$R_5: (3, 2, +\frac{7}{6})$	$\overline{Q}_L u_R H$	$5.6 \cdot 10^{22}(g_1)$	$29/3$	2
	$R_6: (3, 3, -\frac{1}{3})$	$\overline{Q}_R q_L H^\dagger$	$5.1 \cdot 10^{30}(g_2)$	$14/3$	3
	$R_7: (3, 3, +\frac{2}{3})$	$\overline{Q}_R q_L H$	$6.6 \cdot 10^{27}(g_2)$	$20/3$	3
$d = 5$	$R_8: (3, 3, -\frac{4}{3})$	$\overline{Q}_L d_R H^{\dagger 2}$	$3.5 \cdot 10^{18}(g_1)$	$44/3$	3
	$R_9: (\overline{6}, 1, -\frac{1}{3})$	$\overline{Q}_L \sigma d_R \cdot G$	$2.3 \cdot 10^{37}(g_1)$	$4/15$	5
	$R_{10}: (\overline{6}, 1, +\frac{2}{3})$	$\overline{Q}_L \sigma u_R \cdot G$	$5.1 \cdot 10^{30}(g_1)$	$16/15$	5
	$R_{11}: (\overline{6}, 2, +\frac{1}{6})$	$\overline{Q}_R \sigma q_L \cdot G$	$7.3 \cdot 10^{38}(g_1)$	$2/3$	10
	$R_{12}: (8, 1, -1)$	$\overline{Q}_L \sigma e_R \cdot G$	$7.6 \cdot 10^{22}(g_1)$	$8/3$	6
	$R_{13}: (8, 2, -\frac{1}{2})$	$\overline{Q}_R \sigma \ell_L \cdot G$	$6.7 \cdot 10^{27}(g_1)$	$4/3$	12
	$R_{14}: (15, 1, -\frac{1}{3})$	$\overline{Q}_L \sigma d_R \cdot G$	$8.3 \cdot 10^{21}(g_3)$	$1/6$	20
	$R_{15}: (15, 1, +\frac{2}{3})$	$\overline{Q}_L \sigma u_R \cdot G$	$7.6 \cdot 10^{21}(g_3)$	$2/3$	20

Table 5: R_Q allowing for $d \leq 4$ and $d = 5$ decay operators ($\sigma \cdot G \equiv \sigma_{\mu\nu} G^{\mu\nu}$) and yielding the first LP above 10^{18} GeV in the gauge coupling given in parenthesis in the fourth column. The anomaly contribution to $g_{a\gamma}$ is given in the fifth column, and the DW number in the sixth one. Table adapted from Ref. [507]

representations additional possibilities featuring $N_{\text{DW}} = 1$ open up as for example $R_{12} \oplus R_9$ or $R_{12} \oplus R_{10}$ for which $N = T(8) - T(6) = 3 - 5/2 = 1/2$ coincides with what is obtained with a single $SU(3)_c$ fundamental.

6.1.2. DFSZ-like scenarios

As we have seen in Section 2.7.2 in DFSZ-type of models [118, 119] besides the SM-singlet field Φ , two or more Higgs doublets H_i carrying PQ charges are introduced. The SM fermion content is not enlarged, but in general both quarks and leptons carry PQ charges since they are coupled to the Higgs fields. The electromagnetic and colour $U(1)_{PQ}$ anomalies then depend on the SM fermions gauge quantum numbers as well as on their model dependent PQ charge assignments. Hence, several variants of DFSZ axion models are possible, some of which have been discussed, for instance, in Refs. [506, 536]. For most of these variants the axion-photon coupling remains within the KSVZ regions highlighted in Fig. 19, and only in some specific cases the KSVZ upper limit $E/N = 170/3$ can be exceeded. We will now review under which conditions this can occur.

Let us assume $n_H \geq 2$ Higgs doublets H_i coupled to quarks and leptons via Yukawa interactions, and to the singlet field Φ through scalar potential terms. The kinetic term for the scalars carries a $U(1)^{n_H+1}$ rephasing symmetry that must be explicitly broken to $U(1)_{PQ} \times U(1)_Y$ so that the anomalous PQ current is unambiguously defined, and to avoid additional Goldstone bosons with couplings too mildly suppressed just by the electroweak scale. Renormalizable non-Hermitian monomials involving H_i and Φ are then required to provide an explicit breaking $U(1)^{n_H+1} \rightarrow U(1)_{PQ} \times U(1)_Y$. This implies that the PQ charges of all the Higgs doublets, and hence also of the SM fermions, are interrelated and cannot be arbitrarily chosen. To keep the discussion as general as possible let us use a notation in which each fermion bilinear is coupled to a specific scalar doublet, so that $\mathcal{X}(\bar{u}_{L_j} u_{R_j}) = -\mathcal{X}_{H_{u_j}}$, $\mathcal{X}(\bar{d}_{L_j} d_{R_j}) = -\mathcal{X}_{H_{d_j}}$, $\mathcal{X}(\bar{e}_{L_j} e_{R_j}) = -\mathcal{X}_{H_{e_j}}$ and we have taken the hypercharge of H_{d_j, e_j} opposite to that of H_{u_j} . The ratio of anomaly coefficients E/N can

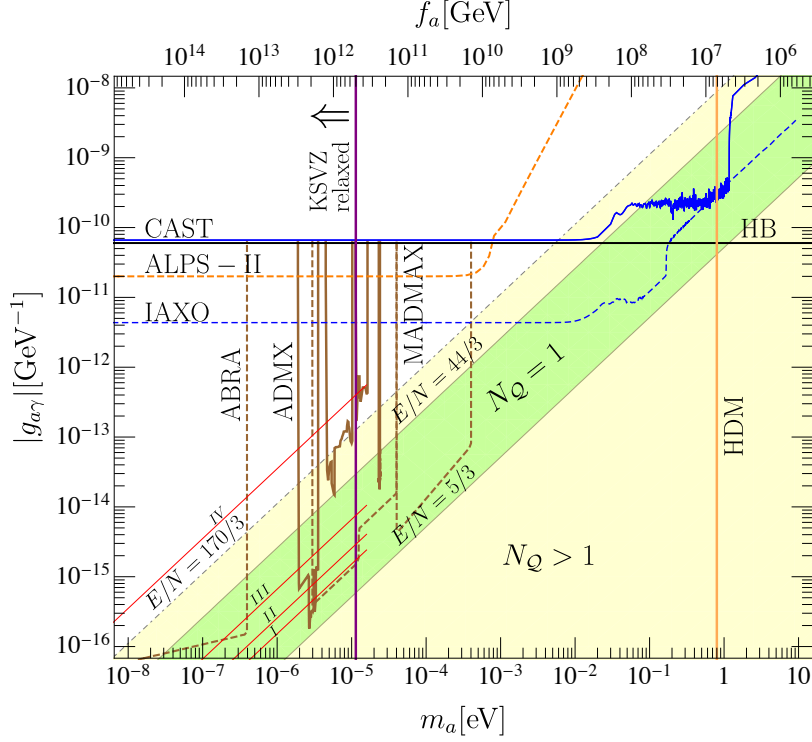


Figure 19: The $g_{a\gamma}$ - m_a window for preferred axion models. The two lines labeled $E/N = 44/3$ and $5/3$ encompass KSVZ models with a single R_Q , while the region below $E/N = 170/3$ allows for more R_Q 's satisfying both the conditions on the absence of LP and of stable relics. The red lines labeled from I to IV (only partially drawn not to clutter the figure) indicate where the DFSZ-type of models lie (see Section 6.1.2). Current exclusion regions and expected experimental sensitivities are delimited by solid and dashed lines respectively. To improve readability, only some experiment names are indicated. More details about the experimental panorama can be found in Fig. 16. On the left side of the vertical violet line, corresponding to a pre-inflationary PQ breaking scenario, the upper limit on E/N for KSVZ models can get relaxed (see text).

then be written as

$$\frac{E}{N} = \frac{\sum_j \left(\frac{4}{3} \mathcal{X}_{H_{u_j}} + \frac{1}{3} \mathcal{X}_{H_{d_j}} + \mathcal{X}_{H_{e_j}} \right)}{\sum_j \left(\frac{1}{2} \mathcal{X}_{H_{u_j}} + \frac{1}{2} \mathcal{X}_{H_{d_j}} \right)} = \frac{2}{3} + 2 \frac{\sum_j \left(\mathcal{X}_{H_{u_j}} + \mathcal{X}_{H_{e_j}} \right)}{\sum_j \left(\mathcal{X}_{H_{u_j}} + \mathcal{X}_{H_{d_j}} \right)}, \quad (256)$$

where the denominator, being proportional to the PQ-color anomaly, cannot vanish. The results for the two DFSZ models discussed in Section 2.7.2 are recovered from Eq. (256) by dropping the generation index and by setting for DFSZ-I $H_e = H_d$ which yields $E/N = 8/3$, and for DFSZ-II $H_e = \tilde{H}_u$ which yields $E/N = 2/3$. In both cases the axion-photon couplings, that correspond to the oblique red lines labeled I and II in Fig. 19, fall inside the $N_Q = 1$ KSVZ region.

Let us now consider the so called DFSZ-III variant [506] in which the leptons couple to a Higgs doublet H_e different from $H_{u,d}$. In order to enforce the breaking $U(1)^4 = U(1)_e \times U(1)_u \times U(1)_d \times U(1)_\Phi \rightarrow U(1)_{PQ}$, in the scalar potential the three doublets H_e , H_u and H_d must be appropriately coupled among them and/or to Φ^2 or Φ . To find which new values of E/N are allowed in DFSZ-III we follow Ref. [509]. Let us consider the mixed bilinear scalar monomials $(H_e H_u)$, $(H_e^\dagger H_d)$, $(H_u H_d)$. It is easy to see that these bilinear terms alone yield for E/N the same two possibilities obtained for DFSZ-I and II. Combining these bilinears among themselves or with their Hermitian conjugates to build quartic couplings two new possibilities arise:

$$\begin{aligned} (H_e H_u) \cdot (H_u H_d) &\implies \mathcal{X}_{H_e} = -(2\mathcal{X}_{H_u} + \mathcal{X}_{H_d}), & E/N = -4/3, \\ (H_e^\dagger H_d) \cdot (H_u H_d) &\implies \mathcal{X}_{H_e} = \mathcal{X}_{H_u} + 2\mathcal{X}_{H_d}, & E/N = 14/3. \end{aligned}$$

	$E/N(g_{a\gamma}^{\max})$	$E/N(g_{a\gamma}^{\min})$
KSVZ ($N_Q = 1$)	44/3	5/3
KSVZ ($N_Q > 1$)	170/3	23/12
DFSZ-I-II ($n_H = 2$)	2/3	8/3
DFSZ-III ($n_H = 3$)	-4/3	8/3
DFSZ-IV ($n_H = 9$)	524/3	23/12

Table 6: Values of E/N corresponding to the maximum and minimum values of $g_{a\gamma}$ for different classes of models. Only KSVZ models that satisfy the first two selection rules (i) and (ii) discussed in Section 6.1.1 are included.

The largest coupling is obtained for the first possibility giving $g_{a\gamma} \propto E/N - 1.92 \simeq -3.25$. We see that the largest axion-photon coupling allowed in DFSZ-III still falls within the $N_Q = 1$ band in Fig. 19.⁶⁵

More possibilities in choosing the PQ charges become possible if we allow for generation dependent PQ charge assignments, a scenario that was already mentioned in Section 2.9 and that will be studied more extensively in Section 6.3. The maximum freedom corresponds to the case in which there are three Higgs doublets for each fermion species ($H_{e_1}, H_{e_2}, H_{e_3}$, etc.) so that the scalar rephasing symmetry is $U(1)^{n_H+1}$ with $n_H = 9$, a scenario that was labeled DFSZ-IV in Ref. [509]. Differently from DFSZ-I, II and III, this scenario should not be understood as giving rise to realistic models, since it might be easily plagued by various phenomenological issues. However, it turns out to be useful to consider this construction since bounding from above the maximum possible E/N in DFSZ-IV automatically provides an upper bound on E/N for all cases with generation dependent PQ charges and $2 \leq n_H \leq 9$ Higgs doublets coupled to the SM fermions. For the derivation of this upper bound we refer to Ref. [509], the result is that the maximum possible axion-photon coupling in DFSZ-IV models corresponds to

$$(E/N)_{\max}^{\text{DFSZ-IV}} = 524/3. \quad (257)$$

Although the value in Eq. (257) exceeds by a factor of three the maximum KSVZ value $E/N = 170/3$ plotted in Fig. 19, the construction through which $(E/N)_{\max}$ was obtained in Ref. [509] is sufficiently cumbersome to suggest that the $N_Q > 1$ region in Fig. 19 can still be considered as representative also of most of DFSZ-IV type of models. In DFSZ-IV it is also possible to obtain axion-photon decoupling ensuring at the same time a correct breaking of the global symmetries $U(1)^{9+1} \rightarrow U(1)_{\text{PQ}} \times U(1)_Y$. One example is given by:

$$\mathcal{X}_{H_{u_j}} = (2, 4, 8) \mathcal{X}_\Phi, \quad \mathcal{X}_{H_{d_j}} = (0, -2, -4) \mathcal{X}_\Phi, \quad \mathcal{X}_{H_{e_j}} = (-1, -3, -5) \mathcal{X}_\Phi, \quad (258)$$

for which Eq. (256) yields $E/N = 23/12 \approx 1.92$ and hence $g_{a\gamma} \approx 0$ (within theoretical errors).

The values of E/N associated to the maximum and minimum of $g_{a\gamma}$ for the different classes of models discussed so far are summarised in Table 6. Note that differently from the KSVZ models analysed in Section 6.1.1, the limits on the axion-photon coupling in DFSZ models do not depend on the details of the cosmological evolution of the Universe, and therefore hold also within the region on the left of the violet vertical line labeled $f_a > 5 \times 10^{11}$ GeV in Fig. 19.

6.1.3. Enhancing $g_{a\gamma}$ above KSVZ- and DFSZ-like scenarios

The anomalous triangle diagrams responsible for the axion-photon coupling depend on the gauge and global charges of the fermions running in the loops. E/N can then be boosted either by increasing the contribution of the gauge charges (subject to LP constraints) or by increasing the value of the global charges (not subject to LP constraints). In the previous sections we have given some examples that exploit the former possibility. More elaborated scenarios that rely on the second possibility allow to enhance the axion coupling to photons by much larger (exponentially enhanced) factors, via mechanisms loosely inspired by

⁶⁵Note that the charges of the DFSZ-III variants in Ref. [506] do not allow to build PQ and gauge invariant mixed terms at the renormalizable level. Consequently, $U(1)^4$ cannot get broken to a single $U(1)_{\text{PQ}}$.

‘clockwork’ type of constructions [537–540]. One of such possibilities for the QCD axion was put forth in Ref. [541] (see also [542, 543]) and is based on a KSVZ type of model. Several singlet scalar fields Φ_k ($k = 0, 1, \dots, n$) are introduced, coupled among them through non-Hermitian monomials $\Phi_k^\dagger \Phi_{k+1}^3$ so that only a single global $U(1)$ remains unbroken, and a charge relation $\mathcal{X}_{\Phi_k} = 3^{-k} \mathcal{X}_{\Phi_0}$ is enforced. A vector-like representation of coloured quarks is coupled to Φ_n while another pair of electromagnetically charged but colour neutral leptons is coupled to a different scalar Φ_p with $p < n$. Hence the anomaly coefficient ratio E/N acquires from the ratio between the PQ charges of the coloured/uncoloured fermions an enhancement factor 3^{n-p} . Cosmological constraints on clockwork axions have been analysed in Ref. [544, 545].

A different possibility was proposed in Ref. [509]. This is based on a DFSZ type of construction and, for this reason, has the virtue of exponentially enhance also the axion-electron coupling (see Section 6.2). Let us consider a DFSZ-like scenarios with $2 + 1 + (n - 1)$ Higgs doublets. The up and down Higgs scalars are coupled to the PQ symmetry breaking singlet through the term $H_u H_d \Phi^2$ so that the PQ charge for H_u satisfies the relation $\mathcal{X}_{H_u} = -2\mathcal{X}_\Phi - \mathcal{X}_{H_d}$. Let us define $H_1 = H_u$ and add $n - 1$ additional scalar doublets H_k ($k = 2, 3, \dots, n$) with the same hypercharge of H_1 but whose couplings to the SM fermions are forbidden by the PQ symmetry. The additional doublets are coupled among each other via non-Hermitian quadrilinear terms $(H_k^\dagger H_{k-1})(H_{k-1} H_d)$, so that a single $U(1)$ global symmetry survives, while their PQ charges satisfy $\mathcal{X}_{H_k} = -2^k \mathcal{X}_\Phi - \mathcal{X}_{H_d}$. Finally, let us couple the lepton Higgs doublet H_e as $(H_e H_n)(H_n H_d)$ so that $\mathcal{X}_{H_e} = 2^{n+1} \mathcal{X}_\Phi + \mathcal{X}_{H_d}$. Inserting in Eq. (256) the expressions for \mathcal{X}_{H_u} and \mathcal{X}_{H_e} we readily obtain:

$$\frac{E}{N} = \frac{8}{3} - 2^{n+1}. \quad (259)$$

Since even in the most conservative case of doublets with electroweak scale masses, n can be as large as fifty before a LP is hit below the Planck scale, it is always possible to obtain exponentially large axion-photon couplings.

Other possibilities for large enhancement of $g_{a\gamma}$ exist. Some examples that are qualitatively different from the ones sketched above can be found in Ref. [546, 547].

6.2. Enhancing/suppressing g_{ae}

As discussed in Section 4.2, the axion-electron coupling g_{ae} can activate different processes that alter stellar evolution and that are particularly significant in the white dwarf and red giant evolutionary stages. The corresponding astrophysical bounds have been reviewed in Section 4.2. Although they are remarkably strong, translating them into constraints on fundamental parameters as the axion decay constant or the axion mass should be done with care, because the relation between g_{ae} and f_a (or m_a) depends crucially on the specific model (cf. Eq. (114) for its general expression). For example, in the KSVZ scenarios electrons do not carry a PQ charge, and hence they couple to the axion only through a photon-electron loop generated by the axion-photon coupling, so that the resulting g_{ae} is loop suppressed and tiny (see Eq. (69)). For this reason astrophysical limits on g_{ae} provide only weak constraints on KSVZ models (cf. also Fig. 11).

6.2.1. Enhancing g_{ae} in KSVZ-like scenarios

Large enhancements with respect to conventional KSVZ scenarios can be straightforwardly obtained by recalling that while in the original model $E/N = 0$, models that involve non-trivial heavy quarks representations like the ones discussed in Section 6.1.1, can yield particularly large E/N factors (see Table 5). In this case g_{ae} gets enhanced by the same factor that enhances $g_{a\gamma}$. In another class of KSVZ models the one-loop induced axion-electron coupling can get an extra contribution from loops involving new particles. This is what happens for example in type-I seesaw scenarios for neutrino masses in which the heavy RH neutrinos N_R obtain their mass M_R from a coupling $N_R N_R \Phi$ to the PQ symmetry breaking scalar singlet Φ . These models are soundly motivated by the fact that the seesaw and the PQ symmetry breaking scales naturally fall in the same intermediate range $M_R \sim f_a \sim 10^9 \div 10^{12}$ GeV so that an identification seems natural (see also Section 7.1). In this case, in order to acquire their mass, the RH neutrinos must carry a PQ charge, and their couplings to the axion give rise to new loops [548–550] that can enhance the axion-electron coupling by up to one or two orders of magnitude with respect to conventional hadronic axion models, see for example Refs. [147, 311, 548].

6.2.2. Enhancing g_{ae} in DFSZ-like scenarios

In DFSZ scenarios the axion-electron coupling arises at the tree level and hence the astrophysical limits on g_{ae} are more effective in providing tight constraints on the fundamental axion parameters. Clearly, in the DFSZ variants reviewed in Section 6.1.2 in which $g_{a\gamma}$ gets enhanced via an E/N value that is boosted by a large PQ electron charge, also g_{ae} is accordingly enhanced. However, defining correctly the coupling of electrons to the *physical* axion involves some subtleties. Let us consider for example the DFSZ construction with $2 + 1 + (n - 1)$ Higgs doublets outlined in Section 6.1.3 that produces an exponential enhancement in E/N , see Eq. (259). The physical axion is identified by imposing the orthogonality condition between the PQ and hypercharge currents $J_\mu^{\text{PQ}}|_a = \sum_i \mathcal{X}_i v_i \partial_\mu a_i$ and $J_\mu^Y|_a = \sum_i Y_i v_i \partial_\mu a_i$, where the sum runs over all the scalars $\{\Phi, H_u, H_d, H_e, H_{k \geq 2}\}$, a_i are the scalar (neutral) orbital modes, and v_i are the corresponding VEVs. Note that since $H_{u,d,e}$ need to pick-up a VEV to generate masses for the fermions, even in the case that all the $H_{k \geq 2}$ have positive mass squared terms, non-vanishing $v_{k \geq 2} \neq 0$ unavoidably arise because of the potential terms $(H_k^\dagger H_{k-1})(H_{k-1} H_d)$ in which they appear linearly. The size of these VEVs is controlled by the size of the quadrilinear coupling constant, hence it is natural to expect $v_k < v_u$ with a size that decreases with increasing k . To proceed, it is convenient to express the PQ charges \mathcal{X}_{H_d} , \mathcal{X}_{H_u} , and \mathcal{X}_{H_k} in terms of \mathcal{X}_{H_e} and \mathcal{X}_Φ by using the relations given above Eq. (259) as

$$\mathcal{X}_{H_d} = \mathcal{X}_{H_e} - 2^{n+1} \mathcal{X}_\Phi, \quad \mathcal{X}_{H_k} = -\mathcal{X}_{H_e} + (2^{n+1} - 2^k) \mathcal{X}_\Phi, \quad (260)$$

where again we have defined $H_u = H_1$. Recalling that $Y(H_e) = Y(H_d) = -Y(H_k) = \frac{1}{2}$ the orthogonality condition can be written as:

$$\sum_i 2Y_i \mathcal{X}_i v_i^2 = \mathcal{X}_{H_e} v^2 - \mathcal{X}_\Phi \left(2^{n+1} v_d^2 + \sum_{k=1}^n (2^{n+1} - 2^k) v_k^2 \right) = 0, \quad (261)$$

where $v^2 = v_e^2 + v_d^2 + \sum_{k=1}^n v_k^2$ is the electroweak VEV. The resulting PQ charge of the electron is:

$$\mathcal{X}_{H_e} = \frac{\mathcal{X}_\Phi}{v^2} \left(2^{n+1} v_d^2 + \sum_{k=1}^n (2^{n+1} - 2^k) v_k^2 \right), \quad (262)$$

and the axion-electron coupling can be written as

$$g_{ae} = \frac{\mathcal{X}_{H_e}}{2N} \frac{m_e}{f_a} = -2^{n+1} \frac{m_e}{6f_a} \left[\frac{v_d^2}{v^2} + \sum_{k=1}^n \left(1 - \frac{1}{2^{n+1-k}} \right) \frac{v_k^2}{v^2} \right], \quad (263)$$

where we have used $2N = 3(\mathcal{X}_{H_u} + \mathcal{X}_{H_d}) = -6\mathcal{X}_\Phi$. For large n the size of g_{ae} is bounded from below by

$$|g_{ae}| \gtrsim 2^{n+1} \left(\frac{v_u^2}{v^2} + \frac{v_d^2}{v^2} \right) \frac{m_e}{6f_a}, \quad (264)$$

where the inequality is saturated when all the $v_{k \geq 2}$ are negligible. Hence the axion coupling to the electrons is always exponentially enhanced.⁶⁶

6.2.3. Suppressing g_{ae} in DFSZ-like scenarios: the electrophobic axion

A more intriguing possibility within DFSZ-type of models is that of decoupling the axion from the electrons, especially if this could be done consistently with the conditions that enforce nucleophobia. In fact, in this case all the most stringent astrophysical limits would evaporate. Such an axion would be appropriately defined as *astrophobic* [551]. One might think that in order to decouple the electron from the axion it would be sufficient to introduce a third (leptonic) Higgs doublet neutral under the PQ symmetry,

⁶⁶Only for $v_e = v$ one could have $g_{ae} \rightarrow 0$. However, the sum of the VEV ratios in Eq. (264) is bounded by the perturbativity of the top Yukawa coupling to be $\gtrsim 0.1$.

so that the leptons would not carry PQ charges either. However, perhaps a bit unexpectedly, this can work only for a few specific values of the VEVs ratios of the two hadronic Higgs [124]. To see this let us consider a model with three-Higgs doublets, that is now convenient to define having the same hypercharge, wherein $H_{1,2}$ couple to quarks while H_3 couples to the leptons. We need to require that the four $U(1)$ rephasing symmetries of the kinetic term of the three scalar doublets $H_{1,2,3}$ and of the PQ symmetry breaking field Φ are broken by renormalizable potential terms so that $U(1)^4 \rightarrow U(1)_Y \times U(1)_{PQ}$. This can be done either by coupling the leptonic Higgs doublet H_3 to both hadronic Higgses ($H_{1,2}$), or by coupling one of the two hadronic Higgses to the other two doublets:

$$H_3^\dagger H_1 \Phi^m + H_3^\dagger H_2 \Phi^n \quad \text{or} \quad H_3^\dagger H_{1,2} \Phi^m + H_2^\dagger H_1 \Phi^n. \quad (265)$$

For renormalizable operators one has, without loss of generality, $m = 1, 2$ and $n = \pm 1, \pm 2$, with the convention that negative values of n mean Hermitian conjugation $\Phi^n \equiv (\Phi^\dagger)^{|n|}$. This implies certain conditions for the PQ charges of the scalar, for example for the first pair of operators we have

$$-\mathcal{X}_3 + \mathcal{X}_1 + m = 0, \quad -\mathcal{X}_3 + \mathcal{X}_2 + n = 0, \quad (266)$$

where for simplicity we have set $\mathcal{X}_\phi = 1$. Similar relations hold if the second pair of operators in Eq. (265) is chosen. Besides these two conditions, orthogonality between the physical axion and the Goldstone boson of hypercharge implies:

$$\mathcal{X}_1 v_1^2 + \mathcal{X}_2 v_2^2 + \mathcal{X}_3 v_3^2 = 0. \quad (267)$$

To see under which conditions the leptons can be decoupled from the axion, let us set $\mathcal{X}_3 \rightarrow 0$. We obtain

$$\tan^2 \beta \equiv \frac{v_2^2}{v_1^2} = -\frac{\mathcal{X}_1}{\mathcal{X}_2} = -\frac{m}{n}, \quad (268)$$

so that with the constraints in Eq. (266), $\mathcal{X}_3 \approx 0$ can be consistently enforced only for $\tan^2 \beta \approx \frac{1}{2}, 1, 2$. It can be verified that in the other two cases in Eq. (265) $\tan \beta = 1$ is the only possibility. As it was remarked in Ref. [124], it is intriguing that the condition for nucleophobia Eq. (276) which, as we have seen in Section 6.3.2, requires $\tan^2 \beta \approx \frac{m_d}{m_u} \approx 2$, is consistent with one of the $\tan \beta$ values that can enforce electrophobia or, said in another way, it is consistent with a suitable set of operators involving the three Higgs doublets, namely $H_3^\dagger H_1 \Phi^2 + H_3^\dagger H_2 \Phi^\dagger$.

6.3. Enhancing/suppressing g_{aN}

The defining property of axions is that they couple to gluons via the anomalous term, and hence they should couple as well to the nucleons $N = n, p$. In fact, from the model building point of view it is much more difficult to arrange for strong enhancements/suppressions of the axion-nucleon coupling g_{aN} than it is for $g_{a\gamma}$ and g_{ae} . Nevertheless, a handful of working mechanisms has been put forth, and will be reviewed in this section. Of special interest is the possibility of approximate axion-nucleon decoupling, that will be reviewed in Section 6.3.2, because in this case the tightest constraints on f_a and m_a , inferred from astrophysical bounds on g_{aN} by assuming a conventional axion model, see Section 4.3, would be accordingly relaxed, and regions in the $g_{a\gamma} - m_a$ plane that are generally considered excluded, would become allowed and thus worthwhile to be explored experimentally.

6.3.1. Enhancing g_{aN}

A possible way to enhance the axion coupling to nucleons is discussed in Ref. [552]. The idea is to uncorrelate the axion-nucleon coupling from the axion mass by assigning $U(1)_{PQ}$ charges to SM quarks such that the latter do not contribute to the QCD anomaly. Effective dimension five operators are introduced that couple the axion multiplet Φ to the light quarks and to the corresponding Higgs. Upon PQ symmetry breaking these terms give rise to the quark Yukawa couplings which, however, also involve the axion through a term $e^{-ia/f}$, where f is the $U(1)$ symmetry breaking order parameter. As usual, by reabsorbing the axion

via a quark field redefinition, derivative axion couplings are generated from the kinetic terms, and eventually an axion-nucleon interaction

$$\frac{\partial_\mu a}{f} \bar{N} \gamma^\mu \gamma_5 N \quad (269)$$

suppressed by the scale f results. The QCD anomaly of the PQ current is due instead to heavy vector-like fermions \mathcal{Q} that couple to a scalar Φ_k whose PQ charge is related to the charge of Φ as $\mathcal{X}_k = 3^{-k} \mathcal{X}_\Phi$, as the result of a clockwork-type of potential $\sum_j \Phi_j^\dagger \Phi_{j+1}^3 + \text{h.c.}$ (see Section 6.1.3). Hence the anomalous term reads

$$\frac{a}{3^k f} \frac{\alpha_s}{8\pi} G \tilde{G}, \quad (270)$$

where the factor 3^k in the denominator is due to the exponential suppression of the heavy quarks PQ charges $\mathcal{X}_\mathcal{Q} \sim 3^{-k}$. The axion decay constant is thus defined as $f_a = 3^k f$, so that the axion couplings to the nucleons in Eq. (269) is exponentially enhanced with respect to the usual $1/f_a$ scaling.

A different, and possibly simpler way to exponentially enhance g_{aN} was recently proposed in [553]. It relies on clockworking directly a set of Higgs doublets in a DFSZ-type of construction. Let us take $n+1$ doublets with hypercharge $Y = -\frac{1}{2}$ and let us consider the following scalar terms:

$$H_0^\dagger H_1 \Phi^2, \quad \sum_{k=2}^n \left(H_{k-1}^\dagger H_k \right) \left(H_{k-1}^\dagger H_0 \right). \quad (271)$$

It is easy to verify the charge relation $\mathcal{X}_k = \mathcal{X}_0 + 2^k \mathcal{X}_\Phi$ so that \mathcal{X}_n gets exponentially enhanced. Consider now the following generation dependent quark couplings:

$$\left(\bar{u}_{1L} u_{1R} H_n + \bar{d}_{1L} d_{1R} \tilde{H}_0 \right) + \left(\bar{u}_{2L} u_{2R} H_0 + \bar{d}_{2L} d_{2R} \tilde{H}_n \right) + \left(\bar{u}_{3L} u_{3R} H_1 + \bar{d}_{3L} d_{3R} \tilde{H}_0 \right), \quad (272)$$

where $\tilde{H} = i\sigma_2 H^*$. All CKM mixings can be generated by adding for example $(\bar{u}_{2L} u_{1R} H_1) + (\bar{u}_{3L} u_{1R} H_n)$ together with all the additional terms consistent with the charge assignments implied by these two terms plus the terms in Eq. (272). The anomalies of the first two generations that contain the Higgs multiplet H_n with the ‘large charge’ cancel each other, so that the QCD (and QED) anomaly coefficient is determined only by the third generation:

$$2N = (\mathcal{X}_{u_{3R}} - \mathcal{X}_{u_{3L}}) + (\mathcal{X}_{d_{3R}} - \mathcal{X}_{d_{3L}}) = -\mathcal{X}_{H_1} + \mathcal{X}_{H_0} = 2\mathcal{X}_\Phi. \quad (273)$$

As a result, the axion coupling to the light up-quark gets exponentially enhanced as

$$c_{u1}^0 = \frac{-\mathcal{X}_{u_{1L}} + \mathcal{X}_{u_{1R}}}{2N} \approx 2^{n-1}, \quad (274)$$

which in turn gives rise to an exponentially enhanced g_{aN} , see Eqs. (66)–(67), while the axion-photon coupling $g_{a\gamma}$ remains of standard size.

6.3.2. Suppressing g_{aN} : the nucleophobic axion

Arranging for a strong suppressions of the axion-nucleon coupling g_{aN} is difficult. In KSVZ models in which the SM fermions do not carry PQ charges this is not possible, because g_{aN} remains determined by a model-independent contribution that is induced by the axion coupling to the gluon fields. In DFSZ models the pathways to enforce $g_{aN} \approx 0$ must comply with tight theoretical constraints. For example, a necessary (but not sufficient) condition is that the PQ-colour anomaly is only determined by the light quarks, that is, either the two heavier generations are not charged under PQ, or they have cancelling anomalies [551]. This unavoidably requires generation dependent axion couplings to the quarks, which in turn implies that nucleophobic axions are mediators of flavour changing interactions, see Section 6.5. An early study in the direction of suppressing g_{aN} was presented in Ref. [554], where some phenomenological aspects connected

to nucleophobic axions were investigated, with the notably exception of SN1987A related limits, given that the Supernova explosion occurred only a few months before the completion of that paper. In another early reference [555] a class of models in which the axion couples to a single quark was studied, and it was found that when the coupling is only to the light up-quark it was possible to engineer for a strong suppression of g_{aN} . Clearly this is in agreement with the condition that to obtain $g_{aN} \approx 0$ only the light quark generation is allowed to contribute to the PQ anomaly. More recently, a dedicated study of the various possibilities for constructing nucleophobic axion models was presented in Ref. [551]. We will now review the main results following this reference.

To identify which conditions must be satisfied to suppress both axion couplings to protons and neutrons it is convenient to recast Eq. (66) and Eq. (67) into the following isospin conserving and isospin violating linear combinations:

$$C_{ap} + C_{an} = (c_u^0 + c_d^0 - 1) (\Delta u + \Delta d) - 2C_{a,\text{sea}}, \quad (275)$$

$$C_{ap} - C_{an} = (c_u^0 - c_d^0 - f_{ud}) (\Delta u - \Delta d), \quad (276)$$

where we have defined $f_{ud} = \frac{m_d - m_u}{m_d + m_u} \approx \frac{1}{3}$. The last term in Eq. (275) accounts for the contribution to the nucleon couplings of the sea quarks, that has been neglected in the treatment of Section 2.5.4 (but included in the full expressions for the couplings Eqs. (111)–(112)) and that cancels out in Eq. (276). The leading contribution comes from the strange quark $C_{a,\text{sea}} = 0.038 c_s^0 + \dots$, and the overall value of the correction is less than 10% of the contribution of the valence quarks.⁶⁷ The (approximate) vanishing of Eqs. (275)–(276) can then be taken as the defining condition for the nucleophobic axion. Note, also, that since the axion-pion coupling $C_{a\pi}$ is proportional to $C_{ap} - C_{an}$, see Eq. (58), nucleophobic axions are also pionphobic. In variant DFSZ models with two Higgs doublets $H_{1,2}$ and non-universal PQ charge assignment [551] both conditions $C_{ap} \pm C_{an} \approx 0$ can be realised [551]. To see this, let us focus on the first generation Yukawa terms

$$\bar{q}_{1L} u_{1R} H_1 + \bar{q}_{1L} d_{1R} \tilde{H}_2. \quad (277)$$

Neglecting the effects of flavour mixing, which are assumed to be small throughout this Section,⁶⁸ the axion couplings to the light quark fields are (cf. Eq. (75) for their UV origin in terms of PQ charges)

$$c_u^0 = \frac{1}{2N} (\mathcal{X}_{u_1} - \mathcal{X}_{q_1}) = -\frac{\mathcal{X}_1}{2N}, \quad (278)$$

$$c_d^0 = \frac{1}{2N} (\mathcal{X}_{d_1} - \mathcal{X}_{q_1}) = \frac{\mathcal{X}_2}{2N}. \quad (279)$$

Here $\mathcal{X}_{u_1} = \mathcal{X}(u_1)$, etc. denote the PQ charges of the fermion fields while $\mathcal{X}_{1,2} = \mathcal{X}(H_{1,2})$. The coefficient of the PQ colour anomaly is then

$$2N = \sum_{i=1}^3 (\mathcal{X}_{u_i} + \mathcal{X}_{d_i} - 2\mathcal{X}_{q_i}), \quad (280)$$

while the contribution to the colour anomaly from light quarks only can be written as:

$$2N_\ell = \mathcal{X}_{u_1} + \mathcal{X}_{d_1} - 2\mathcal{X}_{q_1} = \mathcal{X}_2 - \mathcal{X}_1. \quad (281)$$

Hence, the first condition for ensuring approximate nucleophobia reads (cf. Eq. (275))

$$c_u^0 + c_d^0 = \frac{N_\ell}{N} = 1. \quad (282)$$

This neatly shows that only models in which the color anomaly is determined solely by the light u, d quarks have a chance to be nucleophobic. This can be realised in two ways:

⁶⁷Unless otherwise noticed, it is understood that axion-nucleon decoupling will refer to a suppression of $\approx 10\%$ level compared to conventional KSVZ-like couplings.

⁶⁸In the presence of flavour mixing, $c_{u,d}^0 \rightarrow c_{u,d}^0 + \Delta c_{u,d}^0$, where $\Delta c_{u,d}^0$ involves quark mass diagonalization matrices. These effects will be discussed in Section 6.5, see also Ref. [551].

- (i) either the contributions of the two heavier generations vanish identically ($N_2 = N_3 = 0$);
- (ii) or they cancel each other ($N_2 = -N_3$ and $N_\ell = N_1$).

Assuming only two Higgs doublets, the first possibility can be easily realised by taking one Higgs doublet (say H_1) with a vanishing PQ

The first possibility was for example realised in a scenario in which the axion couples only to the up quark [555] (see also [556]) so that $2N = 2N_\ell$ is a straightforward result. Alternative possibilities in which the PQ charges for the two heavier generations are non-trivial were found in Ref. [557]. In the attempt of looking for connections between PQ symmetries and the quark flavour puzzle, with the aim of building predictive scenario for the quark masses and mixings, the authors of this last reference studied which PQ symmetries could force the vanishing of a certain number of entries in the Yukawa matrices, in such a way that a maximal parameter reduction consistent with observations is enforced.⁶⁹ Serendipitously, it was found that two specific PQ symmetries able to enforce maximal parameter reduction were also characterised by peculiar cancellations among the PQ charges of the heavier quarks resulting in $N_2 = N_3 = 0$.

The second possibility with non-vanishing anomaly coefficients for the heavier generations was thoroughly explored in Ref. [551].⁷⁰ With just two Higgs doublets, in order to have all three quark generations with different charges, some of the SM Yukawa operators are necessarily forbidden, so that zero textures are present in the quarks mass matrices [557]. In contrast, by imposing that the PQ symmetry does not forbid any of the SM Yukawa operators, then two quark generations must have the same charges, so that for example $N_1 = N_2 = -N_3$. The PQ charge assignments that satisfy this condition, and that can thus be compatible with nucleophobia, were classified in Ref. [551].

As regards the second condition, to enforce $C_{ap} - C_{an} \approx 0$ in Eq. (276) we need $c_u^0 - c_d^0 = f_{ud}$ where a value $f_{ud} = \frac{m_d - m_u}{m_d + m_u} \approx \frac{1}{3}$ corresponds to $\frac{m_d}{m_u} \approx 2$. Let us denote by $\tan \beta = v_2/v_1$ the ratio of the VEVs of $H_{1,2}$, and introduce the shorthand notation $s_\beta = \sin \beta$, $c_\beta = \cos \beta$. The ratio $\mathcal{X}_1/\mathcal{X}_2 = -\tan^2 \beta$ is fixed by the requirement that the PQ Goldstone boson is orthogonal to the Goldstone eaten up by the Z -boson, as in the standard DFSZ axion model (cf. Section 2.7.2). Labelling as H_1 the Higgs doublet that couples to the up and charm quarks and considering the case in which all the generations have a non-vanishing anomaly but there is a cancellation $N_2 + N_3 = 0$. The anomaly coefficient of the light quarks can be written as $2N_\ell = \mathcal{X}_2 - \mathcal{X}_1$, and from this we obtain $c_u^0 - c_d^0 = -\frac{1}{2N}(\mathcal{X}_1 + \mathcal{X}_2) = s_\beta^2 - c_\beta^2$. The second condition for nucleophobia that requires $c_u^0 - c_d^0 = f_{ud}$ is then realised for $s_\beta^2 \approx 2/3$ that is $\tan^2 \beta = \frac{m_d}{m_u} \approx 2$ (a value for which the top Yukawa coupling remains safely perturbative up to the Planck scale). In summary, while $C_{ap} + C_{an} \approx 0$ is enforced just by charge assignments and does not require any tuning of the parameters, $C_{ap} - C_{an} \approx 0$ requires a specific choice $\tan \beta \approx \sqrt{2}$.

It is also worthwhile mentioning that in nucleophobic models the requirement that a single generation of quarks contributes to the QCD anomaly also allows straightforwardly for $N_{\text{DW}} = 1$. There are in fact two ways in which $H_{1,2}$ can be coupled to the PQ symmetry breaking field: $H_2^\dagger H_1 \Phi$ in which case $|\mathcal{X}_\Phi| = 2N_\ell = 2N$, the axion field has the same periodicity than the θ term, and the number of domain walls is $N_{\text{DW}} = 1$. The other possibility is $H_2^\dagger H_1 \Phi^2$, in which case $|\mathcal{X}_\Phi| = N_\ell = N$ and $N_{\text{DW}} = 2$. In contrast, in conventional DFSZ models one gets respectively $N_{\text{DW}} = 3$ and 6.

6.4. Enhanced axion couplings and astrophysics

As seen in Section 4, limits from stellar evolution strongly constrain the allowed axion parameter space. The strongest astrophysical limit on the axion-photon coupling is derived from observations of the R-parameter in globular clusters. This is also known as the HB bound and constraints the axion-photon

⁶⁹In fact the requirement of no massless quarks, no vanishing mixings and one CP violating phase in the CKM matrix implies that no-less than seven non-vanishing Yukawa entries are required, so that the matching between fundamental parameters and observables is one-to-one, but within the SM there are no predictions. Conversely, in the lepton sector equipped with the type-I seesaw for neutrino masses, the same strategy yields precise numerical predictions for the leptonic Dirac phase and for the absolute scale of neutrino masses [558].

⁷⁰In this reference additional possibilities in which the contribution to the anomaly of two generations vanish identically were also identified.

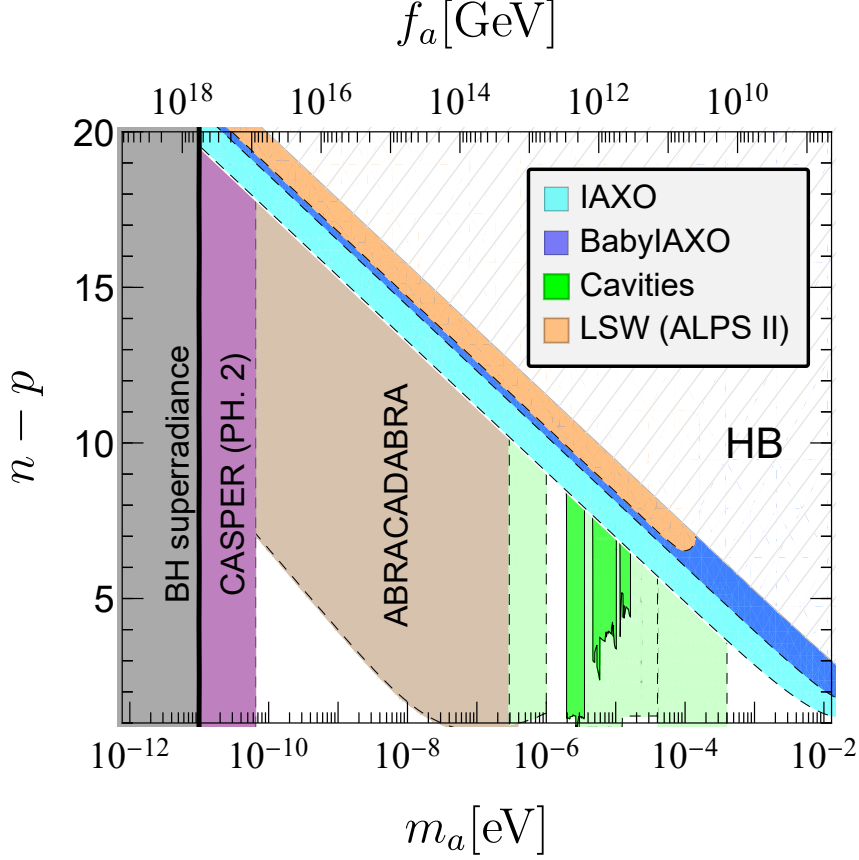


Figure 20: Parameter space (mass and $n - p$) for the clockwork construction (KSVZ type) discussed in Section 6.1.3. We remind that 3^n and 3^p are, respectively, the PQ charges of the scalar singlets that give masses to the exotic quarks and exotic leptons. Notice that $n - p$ is an integer ≥ 1 . Following the convention used in Section 5, we are shading with a lighter green the expected sensitivity of next generation axion cavity searches and in darker green the reported results of current haloscopes. Moreover, we are using a dashed contour line for sensitivity and a continuous line for experimental results. In light green, from left to right, we find KLASH, CULTASK (combined sensitivity of CAPP-12TB and CAPP-25T), and MADMAX.

coupling down to $g_{a\gamma} \lesssim 0.65 \times 10^{-10} \text{ GeV}^{-1}$ (cf. Section 4.1). The axion coupling to electrons is, instead, strongly constrained by RGB stars and by WDs. As discussed in Section 4.2, these bounds amount to roughly $g_{ae} \lesssim 2 - 3 \times 10^{-13}$, depending on the particular observable and analysis.

Interestingly, these astrophysical bounds do not depend on the pseudoscalar mass and are valid up to masses of the order of the stellar interior temperature (several keV). Therefore, such bounds can be readily applied to axion models beyond benchmark, like the ones discussed above in this section.

Let us first notice that the WD/RGB bound dominates over the HB constraint in all models in which C_{ae} and $C_{a\gamma}$, defined in Eq. (118), satisfy the condition $C_{ae}/C_{a\gamma} \gtrsim 10^{-2}$. This is easily satisfied in the KSVZ-like model discussed in Section 6.1.3 and 6.2.1, in which the coupling with electrons is suppressed by a loop factor $\sim 10^{-4}$ (cf. Eq. (114)). Hence, for such model the astrophysical bounds on the axion-electron coupling can be ignored, much the same as in the benchmark KSVZ axion. The parameter space is shown in Fig. 20. Notice that, thanks to the strong enhancement of the axion-photon coupling, the model is accessible to a large number of the axion experiments expected to take data in the near future, including ALPS II and BabyIAXO (cf. Section 5). The maximal value of n shown in figure can be easily accommodated and is well below the threshold required from the LP condition presented in Section 6.1.1.

A similar enhancement of the axion-photon coupling is expected in the DFSZ-type models discussed in

Section 6.1.2. However, in this case the axion electron coupling is also naturally very large and the condition $C_{ae}/C_{a\gamma} \gtrsim 10^{-2}$ is always expected, making the HB bound irrelevant. To see this, let us notice that from Eq. (259) and Eq. (262), it follows that (for large n)

$$\frac{C_{ae}}{C_{a\gamma}} \simeq \frac{1}{6} \left[\frac{v_d^2}{v^2} + \sum_{k=1}^n \left(1 - \frac{1}{2^{n+1-k}} \right) \frac{v_k^2}{v^2} \right], \quad (283)$$

where $v^2 = v_e^2 + v_d^2 + \sum_{k=1}^n v_k^2$ is the square of the electroweak VEV and $v_1 \equiv v_u$. Mathematically, the minimum of Eq. (283) corresponds to the (unphysical) condition $v_e = v$, which implies that all the other VEVs are zero and $C_{ae}/C_{a\gamma} = 0$. However, perturbative unitarity bounds on the top Yukawa coupling (cf. Section 2.7.2), de facto require the term in parenthesis in Eq. (283) to be always larger than ~ 0.1 , implying a finite lower bound on $C_{ae}/C_{a\gamma} \gtrsim 10^{-2}$. A lower value of $C_{ae}/C_{a\gamma}$ for such models is, if mathematically possible, very unnatural. The axion parameter space for the case of minimal $C_{ae}/C_{a\gamma}$ is shown in the left panel of Fig. 21. The potential of the axion helioscopes is minimally impacted. In fact, the increase of the RGB/WD bound is (partially) compensated by a more efficient production of solar axions, as discussed in Section 5.1. The predicted sensitivity of ALPS II is also sufficient to explore part of the region below the astrophysical bounds, though this section is clearly reduced with respect to the KSVZ-like model.

The axion parameter space for the higher coupling scenario, when the term in parenthesis in Eq. (283) is of order 1, is shown in the right panel of Fig. 21. In this cases, only a full scale IAXO (not BabyIAXO), among the planned future helioscopes, would have the capability to probe the axion parameter space allowed by the RGB/WD bounds. ALPS II would equally be unable to probe such model below the region excluded by astrophysics.

As evident from the figures, the large axion-photon couplings predicted in such models permit an almost complete exploration of their parameter space by the next generation of axion probes. In particular, several haloscope searches are expected to have enough sensitivity to probe the parameter region all the way to the minimal value of the axion-photon coupling (corresponding to $n = 2$).

Nucleophobic axion models are also phenomenologically interesting, in particular in relation to the SN 1987A and various NS axion bounds, discussed in Section 4.3. Although the SN and NS constraints on the axion couplings are still uncertain, they seem to restrict efficiently the axion parameter space at masses higher than a few 10 meV, if the standard mass-coupling relation is assumed (see, e.g., Fig. 12 for DFSZ axions). These constraints show some tension with the axion interpretation of the stellar cooling anomalies, which favor slightly higher masses [35]. In this respect, nucleophobia would improve the significance of the interpretation of the stellar cooling anomalies in terms of axions. Moreover, experimentally, nucleophobia opens up large sections of the parameter space to experiments, primarily helioscopes, which are sensitive to the higher axion mass region.

Models that enhance the axion nucleon coupling may also find interesting phenomenological applications. A recent analysis [559], which ascribes the observed excess of X-rays from a few nearby neutron stars to ALPs coupled to nucleons and photons, could be interpreted in terms of nucleophilic QCD axions of the kind described in Section 6.3.1. The interpretation given in Ref. [559] asks for a mass below a few μeV , with $g_{a\gamma}g_{aN} \sim \text{a few } 10^{-21} \text{ GeV}^{-1}$, a value several orders of magnitude larger than what expected, for example, in the DFSZ axion model. Such large couplings could, however, be possible in the case of the clockwork models described here, with enhanced coupling to photons and/or nucleons. Assuming, for example, a standard axion-photon coupling, the hinted region could be accessible to an axion of the kind presented in Section 6.3.1, with $m_a \sim 1 \mu\text{eV}$ and $n \sim 30$ (Cf. Eq. (274)), easily accessible to CASPER Electric (see Fig. 22).

Regardless of the phenomenological motivations, nucleophilic axions are viable axion models that could be probed in the near future, a fact that should encourage the exploration of the axion-nucleon parameter space, still quite poorly probed. An enhancement of the axion-neutron coupling by a factor larger than 10^3 with respect to the DFSZ axion, corresponding to $n \sim 10$ in the model in Eq. (274), would make the model sensitive to CASPER wind in phase II.

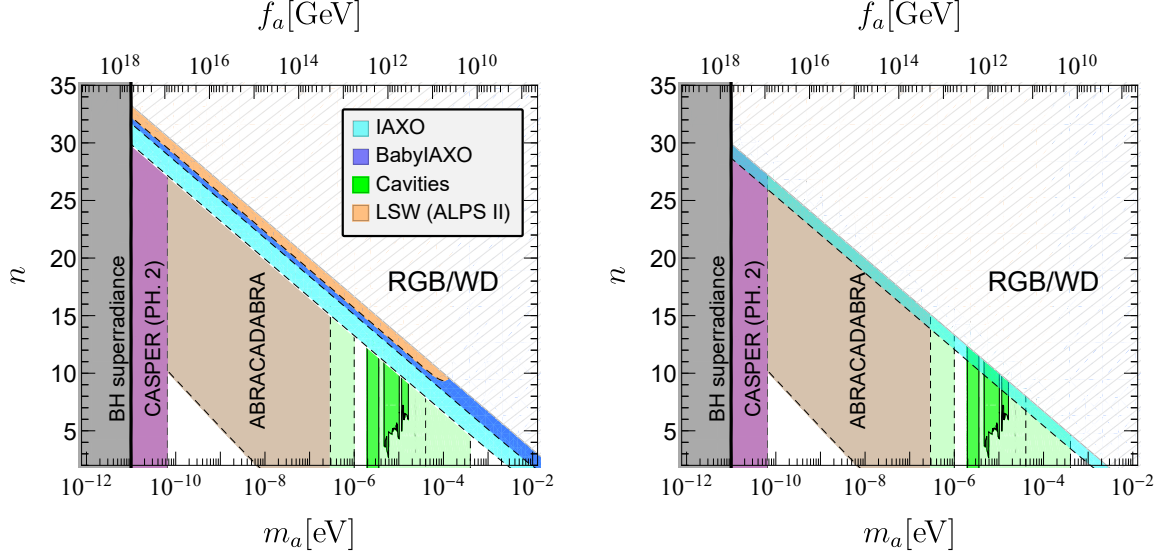


Figure 21: DFSZ model with enhanced axion-photon and axion-electron couplings, discussed in Section 6.1.2 and Section 6.2.2 for $C_{ae}/C_{a\gamma}$ minimal (left) and maximal (right). Following the convention used in Section 5, we are shading with a lighter green the expected sensitivity of next generation axion haloscope and in darker green the reported results of current haloscopes. Moreover, we are using a dashed contour line for sensitivity and a continuous line for experimental results. In light green, from left to right, we find KLASH, CULTASK (combined sensitivity of CAPP-12TB and CAPP-25T), and MADMAX.

6.5. Flavour violating axions

Assuming that axions exist and that the PQ symmetry acts on SM particles, the possibility that they couple differently to fermions of the same charge but of different generations is quite plausible. There is in fact no fundamental reason why the global and anomalous PQ symmetry should act universally in flavour space as the gauge interactions do. After all, this possibility is almost as old as the axion, as it was already contemplated in the Bardeen and Tye seminal paper [560] in 1978. This idea may then be daringly expanded to speculate whether the PQ symmetry can have something to do with flavour, that is with the pattern of fermions masses and mixing angles in the SM. The PQ symmetry could for example act as a flavour symmetry, or could emerge from a set of genuine flavour symmetries, a point of view that had been advocated by Wilczek already in the early 80's [561].

In the second half of the 80's the possibility of an axion coupled to the SM fermions in a generation dependent way was fired up by the observation in heavy ion collisions at GSI of a sharp peak at $E(e^+) \sim 300$ keV in the positron spectrum [562–564]. The positron data were later found to be correlated with the simultaneous detection of electrons also featuring in their energy spectrum a narrow peak at the same energy [565]. The data were consistent with the production of a particle of mass $1.6 - 1.8$ MeV, of probable pseudoscalar character [566], which then decayed into e^+e^- . Hence the characteristics of such a particle were well consistent with those of the original WW axion [16, 17]. However, this interpretation was challenged by the rather large value of the mass, which implied enhanced couplings, e.g. to either charm or bottom quarks, in conflict with limits from $J/\psi \rightarrow \gamma a$ or $\Upsilon \rightarrow \gamma a$. These limits, however, required the axion to escape from the detectors with no deposit of energy, and could have been circumvented by short lived axions $\tau_a \lesssim 6 \times 10^{-13}$ s [567], due to very large values of the axion-electron coupling g_{ae} . However, for generation independent PQ symmetries the ratio of the axion-electron and axion-muon couplings is determined by the ratio of the lepton masses as $g_{a\mu}/g_{ae} = m_\mu/m_e$, see Eq. (118). This predicted a large enhancement of $g_{a\mu}$, in plain conflict with existing measurements of $(g-2)_\mu$. Generation dependent axion couplings remained the only way out, and a series of interesting papers analysing this possibility appeared [117, 554, 568–570]. While eventually new experimental results quickly ruled out the 1.8 MeV GSI axion [282, 283, 571–575], the

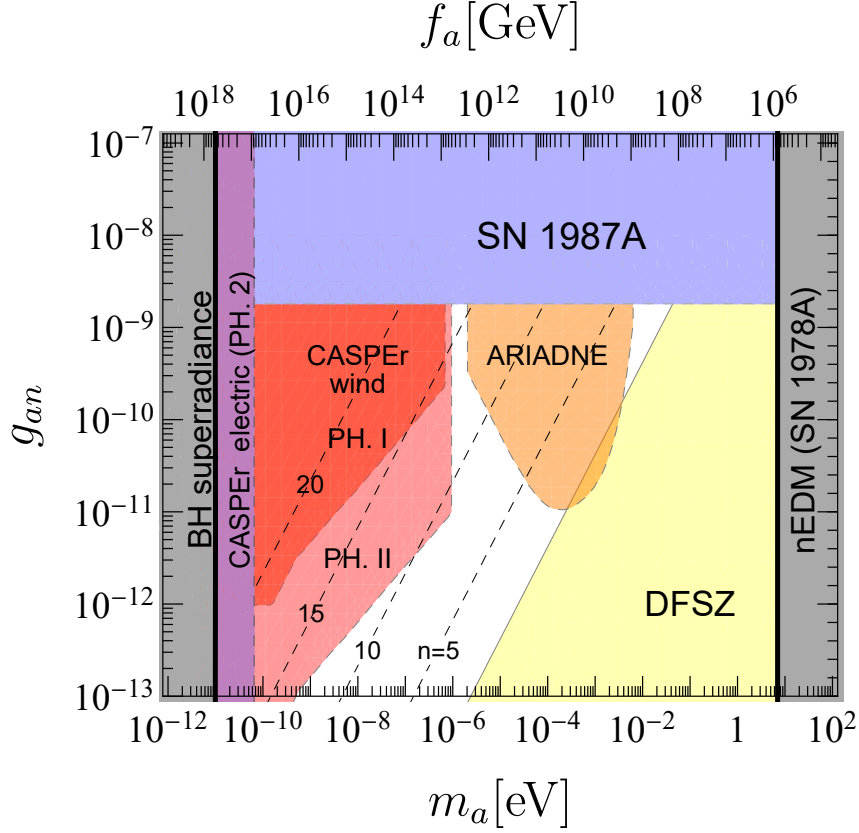


Figure 22: Current bounds and perspectives on the axion nucleon coupling. The black dashed lines correspond, from right to left, to $n = 5, 10, 15$, and 20 for the model discussed in Section 6.3.1 (see, in particular, Eq. (274)).

road to further develop generation dependent PQ scenarios, and to explore axion-flavour interconnections was paved.

Recently, several models attempting to relate fermion family symmetries to the PQ symmetry have been put forth. Well motivated realisations identify the $U(1)_{\text{PQ}}$ with the horizontal $U(1)$ symmetry responsible for the Yukawa hierarchies [576–578]. Models of Froggatt-Nielsen [579] type have recently regained some attention (see e.g. Refs. [580–583]), in relation to possible solutions to the strong CP problem. They typically predict axion flavour transitions controlled by the CKM matrix, although subject to built-in $O(1)$ uncertainties, which are intrinsic to most flavour models based on $U(1)$. Flavoured PQ symmetries can also arise in the context of Minimal Flavour Violation [584, 585] or in models based on non-abelian horizontal (gauge) symmetries like $SU(3)_F$, which can lead to an almost⁷¹ accidental global $U(1)$ ’s which can play the role of a PQ symmetry [586, 587]. In both these types of constructions the resulting axion corresponds to a pseudoscalar ‘familon’ that can mediate FCNC transitions much alike the axions of $U(1)$ flavour models. A different motivation for the non-universality of the PQ current, that was avocated in [124, 551], is that of constructing (nucleophobic) axion models in which the tightest astrophysical bounds can be circumvented, see the review in Section 6.3.2. A genuinely different approach is the attempt of maximize the predictive power of SM flavour data by searching for $U(1)$ symmetries that would enforce the maximal number of

⁷¹For three chiral families trilinear PQ symmetry breaking terms needs to be forbidden in the scalar potential, so although technically natural the PQ symmetry is still imposed by hand. On the other hand, in the presence of n_g chiral families the gauging of $SU(n_g)$ would have delivered a truly accidental axion for $n_g > 4$, since the first operator breaking the PQ symmetry is of dimension n_g .

textures zeros in the fermion mass matrices (compatibly with non-vanishing masses and mixings) [557, 558]. It was found in Ref. [557] that all $U(1)$ symmetries suitable to realise this requirement in the quark sector have a QCD anomaly, and thus correspond to generation dependent PQ symmetries. The particular realisations based on this approach are interesting because, differently from most (if not all) other models, allow to fix the structure of the axion couplings to SM fermions in terms of the values of quark masses and mixings, including the off-diagonal flavour changing ones, up to the values of f_a and $\tan\beta$, as in conventional DFSZ models.

Clearly all the constructions listed above do not have ‘natural flavour conservation’, and thus predict new sources of FCNC processes. However, the latter may be still consistent with experiments if the scale f_a suppressing all axion couplings were sufficiently large or if flavour transitions mainly affected the second and third generation SM fermions.

6.5.1. Generation dependent Peccei-Quinn symmetries

The important modifications in the structure of the axion couplings to the SM fermions, in the case when the PQ symmetry is generation dependent, was briefly addressed in Section 2.9. There it was shown that the consequences of dropping the assumption of generation independence of the PQ charges were twofold: firstly, flavour violating (FV) couplings arise, and secondly, besides coupling to axial-vector currents, ‘flavoured’ axions couple to vector currents as well. This latter point arises because the PQ charges of the fermions cannot maintain an exact chiral structure ($\mathcal{X}_L = -\mathcal{X}_R$), while in general $\mathcal{X}_L + \mathcal{X}_R \neq 0$ for the PQ symmetry to be anomalous.

Before discussing the existing bounds on axion FV interactions let us introduce some notations. In the simple scheme discussed in Section 2.9, with only two Higgs doublets and where only two generations were considered, the axion-fermion couplings could be easily expressed in terms of the PQ Higgs charges $\mathcal{X}_{1,2}$. Expressing the fermion couplings in terms of the charges of the (two or more) Higgs doublets is possible also in more complicated scenarios, however, the connection depends on the specific model. Hence, for the seek of generality, in this Section we will express the couplings simply in terms of the PQ charges of the SM fermions. Our starting point is the way the axion couples to the fermion current, as written in the first line of Eq. (73), except that $f_{L,R}$ have now to be understood as vectors of SM fermions of the same electric charge (e.g. $f = (u_1, u_2, u_3)^T$) while \mathbf{X}_f in the equation below is the diagonal matrix of the associated PQ charges. Going from the basis in which the PQ charges are well defined to the mass eigenstate basis $f_{L,R} \rightarrow U_{L,R}^f f_{L,R}$, with unitary matrices $U_{L,R}^f$, yields

$$\mathcal{L}_a = \frac{\partial_\mu a}{2f_a} \frac{1}{N} \left[\bar{f}_L \left(U_L^{f\dagger} \mathbf{X}_{f_L} U_L^f \right) f_L + \bar{f}_R \left(U_R^{f\dagger} \mathbf{X}_{f_R} U_R^f \right) f_R \right]. \quad (284)$$

The light quarks mass eigenstates u, d can then be redefined as in Eq. (39) in order to remove the anomalous $G\tilde{G}$ term from the Lagrangian, and again this results in adding to the couplings the model independent contribution in Eq. (42). The flavour-diagonal axion-fermion couplings receive corrections from the mixing: $c_{f_i}^0 \rightarrow c_{f_i}^0 + \delta c_{f_i}^0$ where

$$\delta c_{f_i}^0 = \frac{1}{2N} (W_{f_{iR}} - W_{f_{iL}}), \quad \text{with} \quad W_{f_{iR}} = \left[U_R^{f\dagger} (\mathbf{X}_{f_R} - \mathcal{X}_{f_{iR}} \mathbb{I}) U_R^f \right]_{ii}, \quad (285)$$

where \mathbb{I} is the identity matrix in generation space and a similar expression holds for $W_{f_{iL}}$ upon swapping $L \leftrightarrow R$. Such a correction can be invoked to improve nucleophobia by tuning a cancellation against $C_{a,\text{sea}}$ in Eq. (275), or to achieve electrophobia without recurring to a third Higgs by cancelling c_e^0 against the correction from mixings, as it was done in Ref. [551]; but except for these two cases the δc_f^0 contributions do not change much the overall picture. Of leading importance are instead the off-diagonal terms, that give

rise to FV axial-vector and vector axion couplings:

$$\mathcal{L}_{af_i f_j} = \frac{\partial_\mu a}{2f_a} \left[\bar{f}_i \gamma^\mu \left(C_{f_i f_j}^V - C_{f_i f_j}^A \gamma_5 \right) f_j \right], \quad (286)$$

$$C_{f_i f_j}^V = \frac{1}{2N} \left(U_L^{f\dagger} \mathbf{X}_{f_L} U_L^f + U_R^{f\dagger} \mathbf{X}_{f_R} U_R^f \right)_{ij}, \quad (287)$$

$$C_{f_i f_j}^A = \frac{1}{2N} \left(U_L^{f\dagger} \mathbf{X}_{f_L} U_L^f - U_R^{f\dagger} \mathbf{X}_{f_R} U_R^f \right)_{ij}. \quad (288)$$

The crucial point regarding these couplings is that, while the matrices of charges $\mathbf{X}_{f_{R,L}}$ are presumably fixed in any specific model, little is known about the mixing matrices $U_{R,L}^f$.⁷² In the quark sector, nothing is known about the RH matrices U_R^f , and their structure remains completely arbitrary. The LH mixings are instead constrained to satisfy $V_{\text{CKM}} = U_{u_L}^\dagger U_{d_L} \approx \mathbb{I}$. This, however, only implies $U_{u_L} \approx U_{d_L}$ but does not provide additional information on the size of the off-diagonal entries, and in particular it does not forbid large flavour mixings. Differently from the quark sector, the lepton sector is characterised by large mixings, but one does not know if they originate from the neutrino or from the charged lepton rotation matrices (or from both), so that for example also $U_L^\ell \approx \mathbb{I}$ remains a viable assumption.

6.5.2. Constraints on flavour violating axion couplings

Searches for FV decays involving invisible final states are the main experimental tool to probe the off-diagonal axion couplings $C_{f_i f_j}^{A,V}$. A general analysis of such flavour-changing processes involving a generic massless NGB, which holds also for FV axion, can be found in Ref. [588]. A recent thorough collection of limits on the FV couplings can be found in Ref. [589], and brief reviews about the status of the art are presented in Refs. [590, 591].⁷³ The currently best limits for each type of FV transition are listed in Table 7. They coincide with the limits given in Ref. [589] after the correspondence between their and our notations ($V_{ij}^f/v_{\text{PQ}} \equiv C_{f_i f_j}^V/(2f_a)$) is accounted for.

The strongest bounds on FV axion couplings to quarks come from meson decays into final states containing invisible particles. Note, however, that decays involving initial and final pseudo-scalar mesons like $P = K, B, D, \pi$ are only sensitive to the vector part of the FV quark current, since $\langle P' | J_\mu^5 | P \rangle = 0$ by the Wigner-Eckart theorem. Searches for $K^+ \rightarrow \pi^+ a$ decays provide the tightest limits. The current bound from E949/E787 [593] (see Table 7) implies $m_a < 17 \cdot |C_{sd}^V|^{-1} \mu\text{eV}$ which, if one assumes that C_{sd}^V is not particularly suppressed, is about three orders of magnitude stronger than typical astrophysical bounds. In the next future, NA62 is expected to improve the limit on $\text{Br}(K^+ \rightarrow \pi^+ a)$ by a factor of ~ 70 [594, 595], thus strengthening the axion mass bound by a factor ~ 8 . The most sensitive processes involving a quark of the third generation are $B^\pm \rightarrow \pi^\pm a$ and $B^\pm \rightarrow K^\pm a$. Present limit from CLEO [596] imply respectively $m_a < 11.4 \cdot 10^{-2} \cdot |C_{bd}^V|^{-1} \text{eV}$ and $m_a < 9.5 \cdot 10^{-2} \cdot |C_{bs}^V|^{-1} \text{eV}$ which, for maximal mixing, are close to the astrophysics bounds. Note that the latter bound could be presumably strengthened by a factor ~ 6 at BELLE II [597]. Processes involving FV transitions between up-type quarks are much less constrained. Decays of charmed mesons of the form $D \rightarrow \pi a$ are only subject to the trivial requirement $\text{Br}(D \rightarrow \pi a) < 1$, which can be translated into weak bounds, which are at least two orders of magnitude worse than the ones for down-type quarks and not competitive with limits from astrophysics.

As we have said meson decays can only constrain FV vector couplings. In order to set bounds on the axial-vector FV couplings one has to resort to other flavour changing processes, as for example neutral meson (K^0, D^0, B_d^0, B_s^0) mixing, since meson mass splittings receive from axion interactions an additional contribution $(\Delta m)_a$. However, in spite of the fact that, for example, the measurement of the mass difference in the neutral kaon system $\Delta m_K/m_K \simeq 0.7 \times 10^{-14}$ gives a number that is four orders of magnitude smaller

⁷² The models discussed in Ref. [557] are a remarkable exception since, thanks to the maximal reduction in the number of free parameters, both the quark mixing matrices remain fixed in terms of measured quantities.

⁷³ Close to the completion of this review, Ref. [592] appeared, where the importance of flavour violating transitions for axion searches was reiterated, and additional limits on FV axion couplings from three-body meson decays and baryonic decays, including the decay $\Lambda \rightarrow n a$ that would represent a new cooling mechanism for the SN1987A, were derived.

than the limit from kaon decays $\text{Br}(K^+ \rightarrow \pi^+ a) \lesssim 0.7 \times 10^{-10}$, the sensitivity to this type of new physics of the former observable is not competitive with the sensitivity of the latter. To understand the reasons for this, let us write the approximate expressions for the relevant quantities in the game:

$$\frac{(\Delta m_K)_a}{m_K} \simeq \frac{f_K^2}{f_a^2} |C_{sd}^A|^2, \quad (289)$$

$$\Gamma(K^+ \rightarrow \pi^+ a) \simeq \frac{m_K^3}{16\pi f_a^2} |C_{sd}^V|^2, \quad (290)$$

$$\Gamma(K^+ \rightarrow \mu^+ \nu) \simeq \frac{m_K}{8\pi} (G_F f_K m_\mu |V_{us}|)^2, \quad (291)$$

where f_K is the kaon decay constant, G_F the Fermi constant, and V_{us} the relevant element of the CKM matrix. The leptonic decay in Eq. (291) has the largest branching ratio $\simeq 63.4\%$, so we approximate $\Gamma_K^{\text{tot}} \approx \Gamma(K^+ \rightarrow \mu^+ \nu)$ and we obtain:

$$\text{Br}(K^+ \rightarrow \pi^+ a) \simeq (G_F f_K m_\mu |V_{us}|)^{-2} \times \frac{m_K^2}{f_a^2} |C_{sd}^V|^2. \quad (292)$$

The prefactor in the RHS of this equation accounts for chirality (and Cabibbo) suppression of the SM decays, and it is not present for $K^+ \rightarrow \pi^+ a$ decays. This factor is huge $\sim 5 \times 10^{14}$, and enhances the effects of C_{sd}^V largely overcompensating for the better precision of Δm_K . As a result the limits on $f_a/|C_{sd}^V|$ are more than five order of magnitude better than the corresponding limits on $f_a/|C_{sd}^A|$.

Differently from pseudoscalar mesons, for two-body charged lepton decays $\ell_i \rightarrow \ell_j a$ both vector and axial-vector couplings contribute because the decaying particle has non-zero spin. Experimentally it is more convenient to search for decays of anti-leptons. The angular differential decay rate for two-body decays is

$$\frac{d\Gamma(\ell_i^+ \rightarrow \ell_j^+ a)}{d \cos \theta} = \frac{m_{\ell_i}^3}{128\pi f_a^2} \left[|C_{\ell_i \ell_j}^V|^2 + |C_{\ell_i \ell_j}^A|^2 + 2\text{Re}(C_{\ell_i \ell_j}^A C_{\ell_i \ell_j}^{V*}) P_{\ell_i} \cos \theta \right], \quad (293)$$

where P_{ℓ_i} is the polarisation vector of the decaying particle. Strong bounds have been obtained from searches for $\mu^+ \rightarrow e^+ a$ decays, the best of which was obtained more than thirty years ago at TRIUMF, giving $\text{Br}(\mu^+ \rightarrow e^+ a) < 2.6 \cdot 10^{-6}$ [598]. This bound, however, was obtained by exploring a kinematical region forbidden for $\mu^+ \rightarrow e^+ \nu \bar{\nu}$ SM decays. Namely, the bound holds only if the decay is purely vector or purely axial-vector, implying in this case $m_a < 2.5 \cdot |C_{\mu e}^{V(A)}|^{-1} \text{ meV}$. However, the bound would evaporate for axion interactions with a SM-like $V - A$ structure. Slightly weaker bounds, which however do not depend on the chirality properties of the coupling, were obtained by the Crystal Box experiment by searching for the radiative decay $\mu^+ \rightarrow e^+ \gamma a$ [599, 600], see Table 7.

Assuming the decays are isotropic, or in case anisotropic decays are explicitly searched for, it is convenient to express the limits in terms of an effective coupling

$$C_{\ell_i \ell_j} = \left(|C_{\ell_i \ell_j}^V|^2 + |C_{\ell_i \ell_j}^A|^2 \right)^{1/2}. \quad (294)$$

Recent searches that explicitly evaluate limits for anisotropic two body muon decays have been carried out by the TWIST collaboration [601], and yield $f_a < (1.0 - 1.4) \cdot C_{\mu e}$ depending on the anisotropy of the decay. These bounds are slightly less stringent than the old limits from Crystal Box. In the next future, the MEG [602] and Mu3e [603] experiments at PSI are expected to improve the bounds on μ - e transitions by about one order of magnitude. Bounds on $\tau^+ \rightarrow \mu^+ a$ and $\tau^+ \rightarrow e^+ a$ FV decays have been obtained by the ARGUS collaboration [604], and are also reported in Table 7. However, they imply limits on the axion mass which remain well below the astrophysical limits.

6.6. Extending the mass region for dark matter axions

As we have discussed in Section 3.3, the contribution to DM from the axion misalignment mechanism is evaluated by solving a second order differential equation for the misalignment angle $\theta(t)$ with time dependent

Decay	Branching ratio	Experiment/Reference	f_a (GeV)
$K^+ \rightarrow \pi^+ a$	$< 0.73 \times 10^{-10}$	E949+E787 [593]	$> 3.4 \times 10^{11} C_{sd}^V $
$B^\pm \rightarrow \pi^\pm a$	$< 4.9 \times 10^{-5}$	CLEO [596]	$> 5.0 \times 10^7 C_{bd}^V $
$B^\pm \rightarrow K^\pm a$	$< 4.9 \times 10^{-5}$	CLEO [596]	$> 6.0 \times 10^7 C_{bs}^V $
$D^\pm \rightarrow \pi^\pm a$	< 1		$> 1.6 \times 10^5 C_{cu}^V $
$\mu^+ \rightarrow e^+ a$	$< 2.6 \times 10^{-6}$	TRIUMF [598]	$> 4.5 \times 10^9 C_{\mu e}^{V(A)} $
$\mu^+ \rightarrow e^+ \gamma a$	$< 1.1 \times 10^{-9}$	Crystal Box [600]	$> 1.6 \times 10^9 C_{\mu e}$
$\tau^+ \rightarrow e^+ a$	$< 1.5 \times 10^{-2}$	ARGUS [604]	$> 0.9 \times 10^6 C_{\tau e}$
$\tau^+ \rightarrow \mu^+ a$	$< 2.6 \times 10^{-2}$	ARGUS [604]	$> 0.8 \times 10^6 C_{\tau \mu}$

Table 7: Limits on FV axion couplings to the SM fermions. The TRIUMF limit on $\mu^+ \rightarrow e^+ a$ holds only for purely vector or purely axial-vector interactions. For the other leptonic transitions the total coupling $C_{\ell_i \ell_j}$ is defined in Eq. (294).

coefficients $H(t)$ and $m_a(t)$. In pre-inflationary scenarios the axion field is homogenised over distances much larger than the horizon, and the spatial derivative term in Eq. (153) can be dropped. In post-inflationary scenarios field modes with wavelength $\lambda(t) \ll t$ are quickly redshifted away, and restricting to the relevant super-horizon modes we can again drop spatial derivatives, so that Eq. (153) becomes

$$\ddot{\theta}(t) + 3H(t)\dot{\theta}(t) + m_a^2(T(t))\theta(t) = 0. \quad (295)$$

If the coefficients $H(t)$ and $m_a(t)$ have a power-law dependence on time, then Eq. (295) admits an exact solution. For example, let us assume that $R(t) \propto t^p$, where $p > 0$ is a new constant describing the cosmological model ($p = 1/2$ for radiation-domination). We also assume that $m_a(T) \propto T^{-\gamma}$, see Eq. (150), and γ is related to the exponent governing the temperature dependence of the topological susceptibility. Assuming that the entropy (see Eq. (145)) is conserved within a comoving volume, $d(sR^3)/dt = 0$, and neglecting the change in the number of degrees of freedom $g_S(T)$, we have $T \propto 1/R \propto t^{-p}$ and $m_a(t) \propto t^{\gamma p}$. Under these conditions, the general solution of Eq. (295) is

$$\theta(t) = \left(\frac{m_a t^\alpha}{2\alpha} \right)^\beta \left[C_1 \Gamma(1 + \beta) J_\beta \left(\frac{m_a t^\alpha}{\alpha} \right) + C_2 \Gamma(1 - \beta) J_{-\beta} \left(\frac{m_a t^\alpha}{\alpha} \right) \right], \quad (296)$$

where $\alpha = (2 + \gamma p)/2$, $\beta = (1 - 3p)/(2 + \gamma p)$, $\Gamma(x)$ is the Euler gamma function of argument x , $J_\kappa(x)$ is the Bessel function of the first kind of order κ , and $C_{1,2}$ are integration constants. The case studied in Section 3 corresponds to a cosmological evolution during radiation domination, that is $p = 1/2$, with the topological susceptibility obtained from lattice simulation, which roughly corresponds to $\gamma \approx 4$ for $T > T_C$ and $\gamma \approx 0$ for $T \ll T_C$, see the discussion below Eq. (150). We have also set the initial conditions $\dot{\theta} = 0$ and $\theta = \theta_i$ at the time at which the PQ symmetry breaking occurs, see Section 3.3. Several studies have been carried out under these assumptions, which suggest that the DM energy density is saturated for an axion mass lying within a window $m_a \sim (10 - 100) \mu\text{eV}$. This mass window can be significantly altered by various non-standard conditions:

1. Assuming $\theta_i \ll O(1)$ in pre-inflationary PQ breaking scenarios. This possibility has been already discussed in Section 3.3;
2. Assuming a non-standard cosmological evolution, that is by modifying the evolution of the Hubble parameter $H(t)$. This possibility will be explored in Section 6.6.1;
3. Altering the functional dependence of $m_a(t)$ by appealing to beyond-the-SM particle physics. Some examples that exploit this possibility will be reviewed in Section 6.6.2;
4. Assuming a sufficiently large initial value $\dot{\theta}_i \neq 0$, see Eq. (161).
5. Axion production via parametric resonance in the decay of the PQ field radial mode.

The last two possibilities will be reviewed in Section 6.6.3.

6.6.1. Non-standard cosmological evolution

The evolution of the Hubble parameter in the early Universe can be modified in different ways, and this can alter the mass region in which the relic density of axions saturates the DM density with respect to the conventional scenario reviewed in Section 3.6. We will now review some of these possibilities.

Entropy generation: The standard computation of the present axion energy density relies on the conservation of the entropy in a comoving volume, see Eq. (166). Suppose now that a new species X , like a massive scalar field with g_X degrees of freedom, is present in the early Universe and decays into thermalised products after the axion field starts to oscillate at T_{osc} , but prior to BBN. The present amount of entropy is increased by a factor $\Delta \equiv 1 + g_X/g_S$, where g_S is the number of entropy degrees of freedom in the SM at T_{osc} . In this scenario, the present axion energy density in Eq. (167) would be lowered by the entropy injection [605–608] by the same factor Δ . If we demand that the axion energy density matches that of CDM in spite of entropy dilution, then from Eq. (170) we obtain that the mass of the axion has to be lower with respect to the conventional value derived in Section 3.3 as

$$m_a \rightarrow m_a \Delta^{-\frac{2+\gamma}{3+\gamma}}. \quad (297)$$

In supersymmetric theories in which the axion forms a supermultiplet this scenario can be particularly motivated. Late decays of the scalar superpartner of the axion can release a large entropy at a late epoch of the Universe’s evolution [609, 610], diluting the axion energy density and raising the upper bound of the axion decay constant up to $f_a \sim 10^{15}$ GeV without conflicting with the observed amount of DM. Further studies of the supersymmetric realisation of the entropy dilution mechanism and specific models can be found in Refs. [611–614].

Unconventional cosmologies: If the evolution of the Universe at temperatures around or below ~ 1 GeV is characterised by a period of non-canonical expansion, the onset of axion oscillations would be altered and that would lead to a different axion relic density today. Thus, non-standard cosmologies can enlarge the mass range for axion DM.

Such a scenario might occur for example if the evolution of the Universe is described by a scalar-tensor gravity theory [615–617] rather than by general relativity. Scalar-tensor theories benefit from an attraction mechanism which at late times makes them flow towards standard general relativity, so that discrepancies with direct cosmological observations can be avoided. Some consequences of a modified expansion rate due to a scalar-tensor theory have already been discussed in the literature in relation to a possible large enhancements of the WIMP DM relic density [618–622], or to lower the scale of leptogenesis down to the TeV range [623].

Another possibility consists in enlarging the particle content of the SM, by including a new particle which at early times dominates the expansion rate of the Universe. This possibility also results into a modification of the cosmic evolution that departs from the Λ CDM predictions. Scenarios of this type have been extensively discussed in the literature, in relation to the expected abundance of WIMPs [624–629] and their free-stream velocity [630]. A similar possibility has been explored in relation to axion physics both for hot [631] and cold relics [632–636]. In brief, we assume that a new field ϕ coexists along with the SM particles and comes to dominate the energy density in the early Universe, down to a decay temperature T_{dec} that marks the transition to the standard cosmological scenario. If we assume that the new particle has an equation of state w_ϕ and energy density ρ_ϕ , and decays generating an extra radiation density $\rho_{\text{rad}}^{\text{ex}}$ at a rate Γ_ϕ , the transition can be modelled as [635]

$$\dot{\rho}_\phi + 3(1 + w_\phi)H\rho_\phi = -\Gamma_\phi\rho_\phi, \quad (298)$$

$$\dot{\rho}_{\text{rad}}^{\text{ex}} + 4H\rho_{\text{rad}}^{\text{ex}} = \Gamma_\phi\rho_\phi, \quad (299)$$

where a dot indicates a derivation with respect to cosmic time t . If it is assumed that the decay products are light SM particles, then the energy density of the surrounding plasma is increased.

A non-standard cosmology evolution alters the moment at which the coherent oscillations of the axion field commence and possibly dilutes their energy density thereafter, modifying the present axion energy

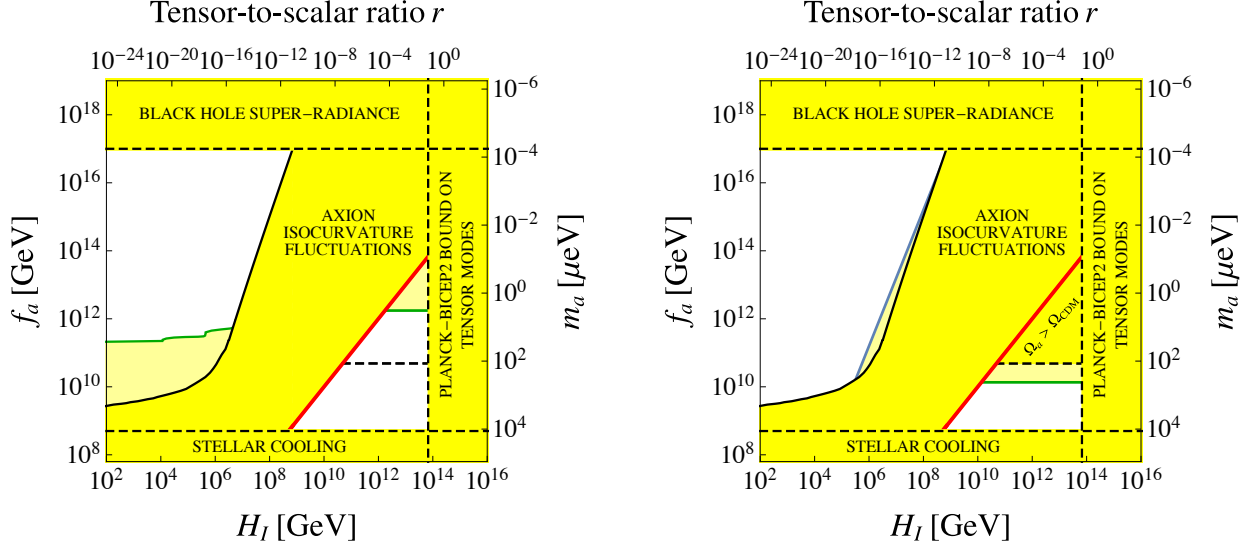


Figure 23: Region of axion parameter space where the axion constitutes the totality of the DM observed for an early matter-dominated period (left) and for an early kination period (right), see text for additional details. For each figure, axes and bounds have been described in Fig. 3.

density for a given axion mass and initial misalignment angle. Models that have been considered in the literature include an early matter-dominated period [172, 605, 637, 638], for which $w_\phi = 0$, and a period of dominance by a “fast-rolling” kination field [639, 640], with $w_\phi = 1$. We have summarised these modifications in Fig. 23, where we show the effects of an early matter-dominated period (left) or a kination domination (right) on the axion parameter space, assuming a decay temperature $T_{\text{dec}} = 100$ MeV. These results have to be compared with what has been obtained for the standard cosmological model in Fig. 3. In the pre-inflationary scenario described in Section 3.3, the bounds from the non-detection of axion isocurvature fluctuations give more stringent constraints on the allowed parameter space with respect to the result in the standard cosmology, bound in each of the figure by the contour in green and with additional yellow shading where excluded. For the matter-dominated scenario with $\theta_i \simeq 1$ and for a decay temperature $T_{\text{dec}} \ll 1$ GeV, the axion can be the DM for values of the axion decay constant that are generally larger than what obtained in the standard scenario, that is $f_a \gg 10^{11}$ GeV for a decay temperature $T_{\text{dec}} \ll 1$ GeV. Comparing to the standard scenario, the value of the DM axion mass is generally larger when an early kination period occurs, and smaller when in the presence of an early matter-dominated period. These changes are ultimately due to the effects of entropy dilution and to the production of a different number of axions from the altered T_{osc} in Eq. (154), as explained in detail in Ref. [632]. Unconventional cosmologies, such as early matter domination, can also modify the small scale structure of axion DM and lead to a linear growth of cosmological perturbations at early times, offering further opportunities for astrophysical tests [641].

6.6.2. Modifying the m_a - f_a relation or the axion mass function $m_a(T)$

The axion abundance would also change if the axion mass/decay constant or the mass dependence on the temperature were modified. We will now explore some scenarios that realise this possibility.

Axion dark matter with a non-conventional m_a - f_a relation: The estimate of the axion energy density due to the misalignment mechanism carried out in Section 3.3 led to Eq. (170), which shows that besides a dependence on the value of the initial misalignment angle, the axion contribution to the CDM crucially depends on the value of the axion mass. In the conventional axion model of Section 2, the product of the

zero temperature axion mass m_a and the PQ constant f_a is fixed by the value of the QCD topological susceptibility at zero temperature, $(m_a f_a)^2 = \chi(0)$ for which the standard value is $\chi(0) = (75.5 \text{ MeV})^4$. However, it is possible to conceive models in which the relation between the axion mass and its decay constant is modified, a condition that can be conveniently expressed as $(m_a f_a)^2 = \alpha_\chi \chi(0)$, with $\alpha_\chi \neq 1$. This would change the fraction of axion DM for a given mass and initial misalignment angle or, equivalently, the value of the mass required for the axion to account for all of the DM. Assuming that the misalignment mechanism dominates the cosmological axion production, to keep the energy density in axions constant it is easy to see from Eqs. (168)–(169) that the mass should be rescaled by the factor $\alpha_\chi^{(2+\gamma)/(3+\gamma)} \simeq \alpha_\chi^{6/7}$, where the numerical exponent in the last relation corresponds to the canonical value $\gamma = 4$. Hence, if $\alpha_\chi > 1$ a larger axion mass is needed to account for the totality of CDM in axions, while the opposite is true if $\alpha_\chi < 1$.

An example of a model in which m_a is decreased from its standard value was proposed in Ref. [642]. This model relies on a Z_N symmetry under which $a \rightarrow a + \frac{2\pi f_a}{N}$, and furthermore the axion interacts with N copies of QCD whose fermions transform under Z_N as $\psi_k \rightarrow \psi_{k+1}$. Surprisingly, adding up the contributions of all the sectors one finds that cancelations occur in the axion potential with a high degree of accuracy. As a result, the axion mass gets exponentially suppressed with respect to the standard case, and in the large N limit one obtains

$$m_a^{(N)} \approx \frac{m_a}{2^{(N-4)/2}}, \quad (300)$$

which corresponds to $\alpha_\chi \approx 2^{-N} < 1$ and, at constant relic density, to a rescaled axion mass $m_a \rightarrow 2^{-\frac{6N}{7}} m_a$. This construction can be particularly relevant for axion searches in the very low mass region. Another way to decouple m_a from f_a relies on an extra dimensional scenario with a large compactification radius [643]. The axion mass is bounded as $m_a \lesssim \min \left[\frac{1}{2R_c}, \frac{m_\pi f_\pi}{f_a} \right]$ where R_c is the compactification radius, and the second term inside square brackets represents the usual PQ axion mass. Present limits on deviations from gravitational Newtonian law at short distances constrain R_c to values well below $\sim 0.1 \text{ mm}$ [644, 645], so that this mechanism can yield axions lighter than expected only for relatively small values of the axion decay constant $f_a \lesssim 3 \cdot 10^9 \text{ GeV}$.

Axion dark matter with a modified mass function $m_a(T)$: Another interesting possibility are scenarios in which the zero temperature axion mass is unchanged but its temperature dependence is non-standard. In this case, the temperature at which the axion field oscillation commence differs from Eq. (168). Since the axion energy density scales as⁷⁴

$$\rho_a \propto m_a T_{\text{osc}}^{-1}, \quad (301)$$

shifting the temperature at which the oscillations start would change the energy density yield in axions even if the axion mass is unchanged. This effect is expected in the cosmological scenario predicted by the theory of the *mirror world* [646], extended to include the axion [647].

The mirror world idea is very old [648–651] and based on the assumption that the gauge group is the product of two identical groups, $G \times G'$. In the simplest possible model, G is the SM gauge group and G' an identical copy of it. Standard particles are singlets of G' and mirror particles are singlets of G . This implies the existence of mirror particles, identical to ours and interacting with our sector only through gravity (and possibly via other renormalizable portal couplings, which are assumed to be small). Since the gravitational interaction is very weak, mirror particles are not expected to come into thermal equilibrium with ordinary particles. Hence, there is no reason to expect that the standard and mirror Universe have the same temperature.⁷⁵ In fact, cosmological observations require a colder mirror Universe in order to

⁷⁴This can be seen as follows: $\rho_a = m_a n_a$ with $n_a \propto m_a(T_{\text{osc}}) T_{\text{osc}}^{-3} \propto H(T_{\text{osc}}) T_{\text{osc}}^{-3} \propto T_{\text{osc}}^{-1}$.

⁷⁵In the exact Z_2 symmetric case this requires an inflationary dynamics yielding different reheating temperatures in the standard and mirror sectors [646].

reduce the radiation energy density at the time of the BBN [646, 652]. Denoting with $x = T'/T$ the ratio of the mirror and standard temperatures, one finds that $x \lesssim 0.4$ is needed to accomodate the most recent combined analysis of the Cosmic Microwave Background from the Planck collaboration and observations of the Baryon Acoustic Oscillations [251].

The possibility to implement the PQ mechanism in the mirror world scenario was proposed in Refs. [653–655]. The general feature is that the total Lagrangian must be of the form $\mathcal{L} + \mathcal{L}' + \lambda \mathcal{L}_{\text{int}}$, where \mathcal{L} represents the ordinary Lagrangian, \mathcal{L}' is the Lagrangian describing the mirror world content, and \mathcal{L}_{int} is an interaction term with a coupling λ which is taken to be small enough to ensure that the two sectors do not come into thermal equilibrium. The simplest realisation of the mechanism restricts the interaction to the Higgs sector. Ordinary and mirror world have each two Higgses, which interact with each other. The axion emerges as a combination of their phases in a generalization of the Weinberg-Wilczek mechanism. For $\lambda = 0$, the total Lagrangian contains two identical $U(1)_{\text{axial}}$ symmetries, while the \mathcal{L}_{int} term breaks them into the usual $U(1)_{\text{PQ}}$, so that only one axion field results.

As long as the mirror-parity is an exact symmetry, the particle physics is exactly the same in the two worlds, and so the strong CP problem is simultaneously solved in both sectors. In particular, the axion couples to both sectors in the same way and their non-perturbative QCD dynamics produces the same contribution to the axion effective potential. Hence, the total zero temperature axion mass, which includes the mirror world contributions, is $m_{\text{tot}}(0) = \sqrt{2} m_a$, only slightly larger than the standard zero temperature axion mass m_a , given in Eq. (51). However, at temperature $T \sim 1$ GeV the axion mass could be considerably larger than its standard value. Assuming the same confinement temperature T_C in the two sectors, and neglecting a possible dependence of the exponent γ on the temperature so that $\gamma(T) \approx \gamma(xT) = \gamma \approx 4$, the expression in Eq. (150) for $T \gtrsim T_C$ gives

$$m_{\text{tot}}^2(T) = m_a^2 \left[\left(\frac{T_C}{T} \right)^{2\gamma} + \left(\frac{T_C}{xT} \right)^{2\gamma} \right] = m_a^2(T) \left(1 + \frac{1}{x^{2\gamma}} \right), \quad (302)$$

where $m_a(T)$ is the standard temperature dependent axion mass. Of course, this different temperature dependence implies a different value for T_{osc} . To estimate the contribution of the axion energy density, let us neglect the first term in the parenthesis in Eq. (302). This approximation is justified for $x \ll 1$. In this case, it is easy to see that the oscillation temperature in the mirror world scenario, T'_{osc} , is related to the standard oscillation temperature as

$$T'_{\text{osc}} \simeq x^{-\gamma/(\gamma+2)} T_{\text{osc}}. \quad (303)$$

The effect of this on the expected axion abundance can be inferred from Eq. (301):

$$\rho_a^{\text{mirror}} \simeq \sqrt{2} x^{\gamma/(\gamma+2)} \rho_a, \quad (304)$$

where the $\sqrt{2}$ accounts for the modification of the zero temperature axion mass. Although in this case the modification to the zero temperature axion mass is only a minor effect, corresponding to a factor $\alpha_\chi = 2$, the above result shows that in the mirror world scenario the present energy density in axions can be considerably smaller than expected, and this allows to saturate Ω_{DM} for large values of the PQ constant, a result that can be of interest for experiments searching for DM axions in mass regions well below the conventional window.

A different way to deplete the energy density of the QCD axion, thus allowing for larger f_a and smaller axion DM masses, was put forth in Ref. [656]. It is assumed that the axion couples to a massless $U(1)'$ dark photon via an $aF'\tilde{F}'$ term similar to the axion-photon coupling. The dark photon, however, is decoupled from the SM and does not interact with the thermal bath, a condition that has to be enforced to maintain it massless also at finite temperature. When the axion starts oscillating certain modes of the dark photon become tachyonic and start growing exponentially, and in this regime energy is efficiently transferred from the axion into the dark photons, leading to an exponential suppression of the axion density and drastically reducing its contribution to the DM, and opening a window for low mass values as small as $m_a \sim 10^{-10}$ eV.

However, the previous conclusion was based on a linear analysis and did not take into account the backreaction of the produced hidden photons on the axion dynamics, which becomes significant in the non-linear regime. Including the latter in a detailed lattice calculation Ref. [657] found that the axion abundance can be suppressed at most by a factor of $\mathcal{O}(10^2)$.

Another mechanism that brings in a hidden Abelian gauge field exploits the Witten effect [658] of hidden monopoles on the QCD axion dynamics. Long time ago Witten has shown that in the presence of a CP violating θ -term, monopoles acquire a non-zero electric charge and become dyons. When a dynamical axion field replaces θ , its potential receives additional contributions from interactions with the monopoles [659] and because of this the field oscillations begin much before the epoch of the QCD phase transition. This scenario does not work with QED monopoles, because of the extremely tight observational constraints on their abundance. For this reason Refs. [660, 661] attempted to implement the same mechanism exploiting monopoles of a hidden $U(1)'$ symmetry. The axion abundance turns out to be inversely proportional to the abundance of hidden monopoles, and when the density of monopoles is sufficiently large to make up a significant fraction of the DM, the abundance of axions with decay constant smaller than about 10^{12} GeV gets suppressed. While this mechanism does not seem to be able to extend by much the axion window towards low mass values, and moreover predicts that DM is accounted for by hidden monopoles, rather than by axions, it has some interesting features, as for example that of suppressing axion isocurvature perturbations, and of disposing of the domain wall problem.

Another way to allow for larger values of the axion decay constant for axion DM was discussed in Ref. [662]. It is based on the possibility of having a long period of supercooling in the early Universe proceeding down to temperatures $\lesssim T_{\text{osc}}$, so that after start oscillating the axion quickly relaxes to the minimum of its potential. At the end of supercooling, the Universe reheats to $T \sim \mathcal{O}(\text{TeV})$. A standard evolution begins, but now with an initial value of $\theta_i \ll 1$. Hence, this mechanism provides a dynamical way to arrange for small values of θ_i as initial condition also for post-inflationary scenarios.

6.6.3. Alternative mechanisms for axion dark matter production

In this section we review some mechanism for axion DM production that are alternative to the misalignment mechanism. Also in these cases the axion mass for which the DM density is saturated can be pushed to values sensibly larger than the conventional ones.

Axion dark matter from initial velocity. As we have seen in Section 3.3, oscillations of the axion field can start when the age of the Universe $t_U \sim H^{-1}$ is of the order of the oscillation period $\sim m_a^{-1}$. However, one additional condition must also be satisfied: at t_{osc} , as defined by Eq. (154), the axion kinetic energy $\dot{a}^2/2$ should not exceed the potential barrier $2m_a^2 f_a^2$, otherwise the axion field keeps rotating and oscillations are prevented. This implies that if $\dot{\theta}_i \gtrsim 2m_a(t_{\text{osc}})$, the conventional misalignment scenario is not realised. In this case the axion DM scenario would be genuinely different from the conventional misalignment scenario, hence it is worthwhile to investigate in some detail the consequences of this possibility, a task that was carried out in Refs. [663, 664]. The axion velocity $\dot{\theta}$ can be related to the density of the PQ charge associated with the symmetry $\Phi \rightarrow e^{i\alpha}\Phi$ of the field Φ introduced in Eq. (79):

$$n_\theta = i \left(\Phi \dot{\Phi}^\dagger - \Phi^\dagger \dot{\Phi} \right) = \dot{\theta} f_a^2, \quad (305)$$

where the last expression holds after replacing $\Phi \rightarrow f_a/\sqrt{2}$. The charge density in a comoving volume is conserved, hence the scaling $\dot{\theta} \sim R^{-3}$ in Eq. (156), and it is then convenient to introduce the (constant) comoving density $Y_\theta = n_\theta/T^3$. Saturating the condition $\dot{\theta} \sim m_a$ at T_{osc} the critical value for departing from the conventional misalignment scenario is obtained:

$$Y_\theta^c = \frac{n_\theta}{T^3} \simeq \frac{m_a(T_{\text{osc}}) f_a^2}{T_{\text{osc}}^3} \simeq \frac{f_a^2}{m_{\text{Pl}} T_{\text{osc}}}, \quad (306)$$

where $m_a(T_{\text{osc}}) \sim H(T_{\text{osc}}) \sim T_{\text{osc}}^2/m_{\text{Pl}}$ has been used. The energy density in axions can be written as $\rho_a = m_a Y_\theta^c T^3$ with m_a the zero temperature axion mass, and it saturates the DM density if at the temperature T_{eq} of matter-radiation equality $\rho_a \sim T_{\text{eq}}^4$, which yields $m_a f_a^2 \sim T_{\text{eq}} T_{\text{osc}} m_{\text{Pl}}$. For $Y_\theta > Y_\theta^c$ oscillations are delayed until some lower temperature $T_* < T_{\text{osc}}$ when the kinetic energy is insufficient to overcome the potential barrier. In this case relic axions are overproduced and one has to lower the scale f_a to match $\rho_a \approx \rho_{\text{DM}}$. The numerical studies in Refs. [663, 664] indeed confirm that at fixed values of f_a the axion kinetic mechanism can produce more DM than the conventional misalignment scenario, and this opens up an interesting mass window for axion DM in the range $m_a \in [10^2, 10^5] \mu\text{eV}$.

In post-inflationary scenarios, in terms of quantities defined at the PQ scale, the requirement that the kinetic energy overcomes the potential barrier ($\dot{\theta}_i \gtrsim 2m_a(t_{\text{osc}})$) translates into the condition $|\dot{\theta}_{\text{PQ}}|/H_{\text{PQ}} \gtrsim 10^{11} (f_a/10^{11} \text{ GeV})^{7/6}$ [664] (see also Eq. (161)), that is rather large values of $\dot{\theta}_{\text{PQ}}$ are needed. In the models of Ref. [663] the PQ symmetry is broken during inflation, the scaling $\dot{\theta} \sim R^{-3}$ is delayed until the radial mode settles to the minimum due to new dynamics of the rotation, which can occur at temperatures well below f_a , and the condition on $|\dot{\theta}|/H$ is accordingly relaxed. The basic mechanism to generate $\dot{\theta}_{\text{PQ}} \neq 0$ is to introduce at the high scale an explicit breaking of the PQ symmetry via higher dimensional operators similar to the ones discussed in Section 2.11. In this way the potential gets tilted, and the axion starts moving towards the potential minimum acquiring a velocity. Of course an explicit breaking can shift the axion from the CP conserving minimum, so that while it must be effective in the early Universe, it must become negligible at lower temperatures. This can be arranged by assuming very flat potentials, so that the expectation value of the radial mode is initially large $\langle \varrho_a \rangle \gg f_a$ enhancing the effects of the operators that at later times, when eventually ϱ_a relaxes to f_a , become sufficiently suppressed [663].

Axion dark matter from parametric resonance. This mechanism represents another alternative way for producing axion DM, and allows saturating the DM relic density for $f_a \ll 10^{12} \text{ GeV}$, that is for relatively large axion mass values $m_a \in [10^{-3}-10^{-1}] \text{ eV}$ [665]. As in the previous mechanism, it is assumed that the axion radial mode $\langle \varrho_a \rangle$ has a large initial value $\langle \varrho_a \rangle \gg f_a$. Axion production becomes efficient when the field ϱ_a starts oscillating near the minimum of its effective potential, and rapidly decays into axions due to a broad parametric resonance, in a way similar to particle production by the oscillating inflaton field in the preheating stage after inflation [666–668]. Axions are initially produced with momenta of order of the mass of the radial mode and thus, in contrast to the misalignment mechanism, the axions produced in this way are initially relativistic. They can redshift sufficiently to be CDM, although for large values of the initial momentum they can remain sufficiently warm to leave a signature in structure formation. Even warmer axions are produced in the model of Ref. [669] where the PQ phase transition and the parametric production of axions is delayed to temperature much below the PQ scale f_a . Axion production via parametric resonance in a supersymmetric model, due to oscillation of the axion superpartner, was studied in Ref. [670]. Although some cosmological consequences like the production of an axion dark radiation component or the possibility of detecting gravitational waves from explosive axion production were considered, possible consequences for axion CDM were not addressed.

6.7. Super-heavy axions

In Sections 6.1–6.3, we showed how axions can be made more or less strongly coupled to SM fields through the dynamics of additional fields. In such models, the modification of the interaction strength was realized by altering the C_{af} parameters, defined in Eq. (109), while preserving the relation between the axion mass and decay constant f_a given in Eq. (108). In this Section we consider instead the possibility that the m_a – f_a relation is modified (still keeping the solution of the strong CP problem), thus allowing for $m_a \gtrsim 100 \text{ keV}$ axions (the 100 keV threshold is actually needed in order to evade (most) of the astrophysical constraints). We denote the latter *super-heavy* axions, in contrast to the canonical heavy axion regime up to $m_a \lesssim 0.1 \text{ eV}$. It should be first noted that such super-heavy axions are cosmologically unstable. For instance, the decay channel $a \rightarrow \gamma + \gamma$ yields

$$\Gamma(a \rightarrow \gamma + \gamma) = \frac{g_{a\gamma}^2 m_a^3}{64\pi} = \frac{E/N - 1.92}{0.318 \text{ s}} \left(\frac{m_a}{100 \text{ keV}} \right)^5, \quad (307)$$

where in the last step we used the numerical values of the axion-photon coupling and the standard QCD m_a – f_a relation⁷⁶ (cf. Eq. (118), (108) and (116)). Hence, barring an unrealistic cancellation in the axion-photon coupling, an axion with $m_a \gtrsim 100$ keV cannot be DM.

Relaxing the relation between m_a and f_a requires some modifications of the gauge structure of the SM, particularly of the strong interaction sector. Yet, models which envisioned a large axion mass for some fixed couplings appeared early on (see, e.g., Refs. [134, 671–676]). The reason can be perhaps traced, at least in part, in the desire of avoiding the requirements of extremely small (experimentally prohibitive) axion couplings, which seemed an inevitable consequence of the experimental and astrophysical constraints. Early experimental tests of the original WW axion model (cf. footnote (19) in Section 2.7) ruled out the range $f_a \lesssim 10^4$ GeV. According to the standard QCD relation in Eq. (108), this constraint implies an axion mass below 0.1 keV. However, light axions with masses below a few keV, can be easily produced in stars and impact their evolution possibly beyond what is observationally allowed (cf. Section 4). As it turns out, astrophysical constraints are considerably more restrictive than the original bounds, pushing the range of excluded couplings all the way up to $f_a \sim 10^8$ GeV, implying extremely weakly interacting axions. Hence, somewhat surprisingly, the relatively weak bounds that ruled out the WW model brought to a rather dramatic result. The only two viable options left were either to make the axion extremely weakly coupled (invisible axion) or to make it heavier.⁷⁷ Either way, the axion could avoid the astrophysical bounds. Both roads were pursued. Models with a larger mass for fixed coupling have the additional appeal to be more easily tested in the laboratory while invisible axions were, at the time, truly thought to be beyond the foreseeable experimental potential (this, of course, before the seminal paper of Sikivie [444]).

Additional motivations for super-heavy axions can be found in connection with the PQ quality problem [133–138] (cf. Section 2.11), since explicit PQ-breaking terms would produce a shift, in some cases very large, to the axion mass (for an application in the context of Gamma Ray Bursts see [678]). This, however, would generically also shift the minimum of the axion potential away from its CP conserving point, thus spoiling the solution of the strong CP problem.⁷⁸ Indeed, some of the original models did not satisfy this condition.

An even earlier strategy to raise the axion mass was put forth by Holdom and Peskin [674] (see also [675]), which pointed out that the contribution of the small color instantons to the axion potential could be made sizable by some nontrivial dynamics above the electroweak scale which reversed the sign of the color β function at some mass above 1 TeV or so. This idea was later reconsidered in Refs. [134, 676] in the context of GUTs, where it was argued that in the presence of new sources of chiral symmetry breaking at high energies there is no generic reason for the small instanton contribution to the axion potential to be aligned to the long-distance QCD contribution. Hence, also in this case raising the axion mass could have spoiled the solution of the strong CP problem. Interestingly, the idea that small instantons could contribute to the axion mass was resuscitated very recently in Ref. [680], in a model where QCD is embedded in a theory with one compact extra dimension. In this scenario, it was shown that the contribution of the small instantons to the axion mass can be larger than the usual large instantons contribution, though it is required that the theory is close to the non-perturbative limit. At any rate, the θ angle is not shifted in this construction and hence the axion solution to the strong CP problem naturally preserved.

Another, perhaps less economic, strategy is to assume that additional mass contribution emerges from the $U(1)_{\text{PQ}}$ current anomaly, related to some hidden gauge sector with a confinement scale larger than Λ_{QCD} . One of the earliest attempts in this direction is the mirror world axion scenario, already introduced in Section 6.6.2. In this case, a whole new SM sector is introduced, with mirror and ordinary particles interacting

⁷⁶For fixed f_a , this provides a lower bound on the decay rate, compared to the case where m_a is enhanced.

⁷⁷Another non-trivial option would have been to relax the hypothesis of the universality of the PQ current (see for instance the discussion at the beginning of Section 6.5). More recently, it was shown in Ref. [677] that an $\mathcal{O}(10$ MeV) axion with the standard m_a – f_a QCD relation could still be viable under the following conditions: *i*) the axion couples only to first generation fermions, with dominant decaying channel into electrons *ii*) the axion-pion coupling is suppressed (pion-phobia) and *iii*) large hadronic uncertainties in rare K decays are invoked. The UV completion of such an axion is however non-trivial, and it requires several extra fields beyond those of benchmark axion models.

⁷⁸Turning up the argument, one can observe that generic PQ-breaking effective operators would spoil the axion solution for f_a above a few GeV or, if we forbid $d = 5$ operators, for f_a a few TeV. Hence, such scales are interesting for a theoretical point of view. However, unless we make the axions super-heavy, $f_a \sim 1$ TeV implies $m_a \sim 1$ keV which is excluded by stellar argument. This is a strong motivation to consider super-heavy axions [679].

with each other only gravitationally and, possibly, through some other very weak couplings, insufficient to bring the two sectors in thermal equilibrium during the cosmological evolution (cf. Section 6.6.2). The first example of such models [653] was based on a mirror extended GUT theory, with gauge group $SU(5) \times SU(5)'$, each one with its own PQ symmetry. A Z_2 symmetry (*mirror parity*) for exchange of ordinary and mirror particles guarantees the equality of the θ parameters in the two sectors. The $U(1) \times U(1)'$ symmetry is reduced to just one PQ symmetry through the introduction of an $SU(5) \times SU(5)'$ singlet complex scalar field, of PQ charge different from zero, that interacts with both ordinary and mirror Higgs. As explained in Section 6.6.2, in such a symmetric model the contribution to the axion mass from the hidden mirror sector would be a factor of $\sqrt{2}$ larger than in the standard case. To have a larger mass gain, one has to assume a breaking of the mirror symmetry which does not, however, spoil the solution of the strong CP in both sectors. The way to do that is to have the mirror parity broken softly in the Higgs sector, without affecting the structure of the Yukawa couplings which has to remain the same in the two sectors (so that $\arg \det Y_u Y_d = \arg \det Y'_u Y'_d$). In Ref. [653], it was assumed that the mirror parity is broken by soft terms and that the breaking of $SU(5)'$ to the mirror SM happens at a much lower scale than in the ordinary sector. Since the coupling constant of $SU(5)$ runs faster than that of $SU(3)$, it results that $\Lambda'_{\text{QCD}} \gg \Lambda_{\text{QCD}}$. Hence, the axion mass takes most of its contribution from the mirror sector.

Somewhat simpler models, which did not require a GUT but just a $\text{SM} \times \text{SM}'$ gauge group, were considered in Ref. [654] and in its supersymmetric extension [655]. The mirror parity is spontaneously broken and induces a larger electroweak scale in the mirror sector, without affecting the Yukawa sectors. The higher mirror Higgs VEV generates heavier mirror fermions and, consequently, a faster renormalization group evolution and a larger confinement scale $\Lambda'_{\text{QCD}} \gg \Lambda_{\text{QCD}}$. These constructions were also motivated by the need to avoid Planck induced corrections which afflicted the model in Ref. [653] and could hence spoil the solution of the strong CP.

More recently, Ref. [681] considered a mirror KSVZ model. The construction assumes a $\text{SM} \times \text{SM}'$ gauge group, with a softly broken Z_2 symmetry to ensure the alignment of the effective θ angles in the two sectors. Just like in the models in Ref. [654, 655], described above, soft breaking terms induce a larger electroweak symmetry breaking scale (and hence heavier quarks) in the mirror sector. In order to get a considerable enhancement of the axion mass, however, the model in Ref. [681] requires the addition of scalar quarks in both sectors. The choice of scalar, rather than fermionic, quarks is motivated by the fact that they do not contribute to the effective θ angles. The ratio of the mirror and standard confinement scales turns out to be roughly equal to the ratio of the mirror and standard scalar masses. The somewhat more complicated construction permits a larger mass for a fixed PQ scale than in the case of the models in Ref. [654, 655], with masses of 100 MeV or so achievable for $f_a \sim 10^{3-5}$ GeV.

In recent times, several more models (see e.g. [682–684]) reconsidered the Z_2 symmetry to ensure CP conservation in super-heavy axion models with a scale f_a all the way down to $\sim \text{TeV}$, hence accessible to detector searches such as ATLAS and CMS [683]. For instance, in the latter construction there is only one massless exotic quark transforming under $SU(\mathcal{N})$ and an axion whose mass is induced by $SU(\mathcal{N})$ instantons, so that in the limit of vanishing QCD coupling it remains massive. The problem with the two vacuum angles θ_{QCD} and $\theta_{\mathcal{N}}$ is again solved by imposing a Z_2 symmetry that implies vacuum angles alignment.

A critical analysis of the Z_2 symmetry mechanism to guarantee the solution of the strong CP problem in models with a hidden QCD sector is presented in Ref. [685]. Indeed, the requirement of an additional parity symmetry can be circumvented and mechanisms that avoid its use have been proposed in recent years. In Ref. [686], it is assumed that the $SU(3)_c$ group is a subgroup of an enlarged QCD color group, $SU(3 + \mathcal{N})$, which breaks into $SU(\mathcal{N}) \times SU(3)_c$. After the breaking, the unique θ angle of the $SU(3 + \mathcal{N})$ group becomes a common factor of the $G\tilde{G}$ terms of $SU(\mathcal{N})$ and of $SU(3)_c$. Thus, the axion dynamics can take care of the CP violation in both sectors, while the axion mass gets most of its contribution from the $SU(\mathcal{N})$ sector, which can have a substantially larger confinement scale than the QCD.

Another proposal that avoids the introduction of the discrete Z_2 symmetry was put forth in [687] (see also [688–690]). At high energies the gauge group is a product of factors $SU(3)^{\mathcal{N}}$ and $SU(3)_c$ is the diagonal subgroup that survives at low energies. Non-perturbative effects in each individual $SU(3)$ factor generate a potential for the corresponding axion. The vacuum is naturally aligned to ensure $\theta = 0$, while the masses of these axions can be much larger than for the standard QCD axion, reaching values well above the GeV.

Gaillard et al. [691] also consider a solution with massless new fermions. The solution is based on an enlarged but *unified* color sector, where unification solves the issue of the different θ parameters that arise in the presence of two or more individual confining groups. The unified color group breaks spontaneously to QCD and to another confining group. Instantons of the unified group with a large characteristic scale contribute to breaking of a PQ symmetry and provide a source of large masses for the axions, so that no light pseudoscalar particles remain at low scales. This construction can yield both, dynamical and fundamental axions, with masses that can lie in the several TeV range.

7. Axions and...

This Section is devoted to the collection of various topics in which axion physics can be related to other open issues of the SM, such as massive neutrinos (Section 7.1), the baryon asymmetry (Section 7.2) and inflation (Section 7.3). In Section 7.4 we touch on possible observational signals of the PQ phase transition from the detection of gravitational waves (GW). We then discuss possible solutions of the DW issue (Section 7.5) and of the PQ quality problem (Section 7.6), as well as the embedding of axions in UV motivated frameworks, such as composite dynamics (Section 7.7), grand unified theories (GUTs) (Section 7.8) and String Theory (Section 7.9). Every topic is briefly sketched, with the scope of mainly redirecting to the relevant literature.

7.1. Axions and neutrino masses

Axions and neutrinos share various properties: they are both extremely lighter than charged leptons and possess a feeble coupling to SM fermions. In fact, the idea of connecting massive neutrinos with a spontaneously broken $U(1)_{\text{PQ}}$ comes a long way. Early studies (such as [586, 692–694]) were actually motivated by the natural emergence of intermediate mass scales in grand-unified theories. In particular, the axion-neutrino connection has been largely explored in the context of the type-I seesaw [147, 311–313, 548, 694–699], in which the heavy RH neutrinos N_R obtain their mass M_R from a coupling $N_R N_R \Phi$ to the PQ symmetry breaking scalar singlet Φ . This connection is soundly motivated by the fact that the RH neutrino and the PQ symmetry breaking scales naturally fall in the same intermediate range $M_R \sim f_a \sim 10^9 \div 10^{12}$ GeV, and further supported by the possibility of naturally producing a cosmological baryon asymmetry of the correct size via leptogenesis [695]. Considering instead only scalar extensions of the SM a simple setup based on the Zee model for radiative neutrino masses was discussed in Refs. [700, 701], while extensions based on the type-II (III) seesaw and other radiative neutrino mass models were explored later on [702–704]. Scenarios implementing Dirac neutrinos have also been discussed [705–708]. The latter, however, miss the main motivation behind the axion-neutrino connection, that is the identification of the PQ scale with the scale suppressing neutrino masses.

The constructions above often aim at providing a minimal SM extension addressing most of the shortcomings of the SM. It is fair to say, however, that they often lack in predictivity being the collection of somewhat orthogonal ingredients. The most genuine signature of the axion-neutrino connection would in fact be an axion coupling to neutrinos, of the type $\mathcal{L} \supset (m_\nu/f_a) a \bar{\nu} i \gamma_5 \nu$, which is clearly beyond any experimental accessibility due to the huge m_ν/f_a suppression. Hence, any chance for predictivity beyond the single ingredients in isolation (e.g. Type-I seesaw and PQ mechanism) can only arise indirectly as a self-consistency of the whole setup.

A non-trivial step in this direction was achieved recently, in the context of the SMASH model of Refs. [311–313], in which the modulus of the PQ scalar is also the key ingredient for successful inflation. A robust prediction of this setup is that the PQ symmetry is broken after inflation and never restored after it, thus making the range for axion DM in principle calculable.

A different predictive approach, involving also flavour, was instead pursued recently in Ref. [558], which classified all the generation dependent $U(1)$ symmetries which, in the presence of two leptonic Higgs doublets, can reduce the number of independent high-energy parameters of type-I seesaw to the minimum number compatible with non-vanishing neutrino mixings and CP violation in the leptonic sector. This setup leads to definite predictions for the charged leptons and neutrino mass matrices and, if extended to the quark

sector, necessarily leads to a QCD anomalous $U(1)_{\text{PQ}}$ [557], thus predicting the existence of a QCD axion, with couplings to SM fermions fixed in terms of SM fermion masses and mixings.

7.2. Axions and the cosmological baryon asymmetry

The strong CP-violating parameter must be extremely small today, as required by the non-observation of the nEDM. However, if the smallness of the theta angle were due to the cosmological evolution of an axion field, it is plausible that θ was $\mathcal{O}(1)$ in the early Universe and, conceivably, such source of CP violation could have played a role for baryogenesis. This idea was first put forth by Kuzmin, Tkachev and Shaposhnikov in Ref. [709], which considered the possible effects on electroweak baryogenesis of strong CP-violation related to an axion field with a large background value. The conclusions of this work were, however, negative: SM baryon number violating processes are only effective at temperatures above $T_{\text{EW}} \sim 100$ GeV, however, at these temperatures strong CP violating effects are suppressed by an exceedingly small exponential factor $\exp(-8\pi^2/g_s^2)$ where g_s is the strong gauge coupling. They concluded that the only possibility was to diminish the temperature of the electroweak phase transition down to Λ_{QCD} , and to require that no entropy was injected in the plasma after the phase transition to avoid diluting the baryon asymmetry. This, however, also implied that the Universe got over-dominated by axion DM, contrary to observations.

More recently, this problem was reconsidered in Ref. [710] in the context of cold electroweak baryogenesis (see e.g. Refs. [711, 712]), a scenario that can lead to a very efficient production of baryon number if the electroweak symmetry breaking is triggered through a fast tachyonic instability (‘Higgs quenching’) and if it occurs in a range of temperatures $10 \text{ MeV} \lesssim T_{\text{EW}} \lesssim 1 \text{ GeV}$. In this scenario baryon production occurs strongly out of equilibrium so that there are no washout effects and the efficiency can be very large. The corresponding rates can be described in terms of an effective equilibrium temperature T_{eff} much larger than T_{EW} and one or two orders of magnitude larger than the reheating temperature of the plasma after the phase transition T_{RH} . The baryon-to-photons ratio scales as $(T_{\text{eff}}/T_{\text{RH}})^3$ so that it can easily reach the observed value. Axion oscillations start well after reheating, and are not delayed with respect to the conventional scenario, so that the cold DM energy density from axion misalignment remains as in the standard case.

A different approach to overcome the no-go of Ref. [709] was put forth more recently in Refs. [713, 714]. Instead of delaying the electroweak phase transition down to 1 GeV or below, the idea is to increase the QCD confinement scale $\Lambda_{\text{QCD}} \gtrsim T_{\text{EW}}$. This is achieved by promoting the strong coupling to a dynamical quantity, which evolves through the vacuum expectation value of a singlet scalar field that mixes with the Higgs field. QCD confinement and electroweak symmetry breaking occur simultaneously close to the TeV scale, providing large CP violation from an axion field value $\theta(T)$ of $\mathcal{O}(1)$ together with baryon number violation and the out-of-equilibrium condition from the phase transitions, which are expected to be first order.

Finally, Ref. [715] proposed a mechanism wherein the cosmological matter-antimatter asymmetry stems from initial conditions in which the axion field is fastly rotating, much alike in the alternative scenario for axion DM production reviewed in Section 6.6.3. A $\dot{\theta} \neq 0$ corresponds to an asymmetry-density of the PQ charge, which is converted into the baryon asymmetry via QCD and electroweak sphalerons. This rotation can be induced at the PQ scale by effective operators that break explicitly the symmetry, tilting the bottom of the mexican-hat potential. However, these operators must fade away rapidly enough at lower temperatures not to spoil the solution of the strong CP problem, that is the zero temperature minimum of the axion potential must remain determined by the QCD non-perturbative effects. The mechanism encounters difficulties because to preserve the baryon asymmetry from being washed out, $\dot{\theta}$ must remain large down to the temperature when sphaleron transitions get out of equilibrium. This, however, implies that at the QCD phase transition the axion kinetic energy would dominate the potential energy, thus delaying the onset of oscillations which results in an unacceptable overproduction of DM. The proposed way out is to engineer a way to increase the temperature of the electroweak phase transition in order to suppress sphalerons transitions at much earlier times.

7.3. Axions and inflation

A period of accelerated expansion in the very early Universe called *inflation* [716, 717] is usually invoked to address various problems of the standard cosmology, namely the absence of monopoles [219, 717, 718] and domain walls [719], the fact that the Universe appears to be homogeneous and isotropic (the *horizon problem*) [720], and the fact that the Universe appears to possess fine-tuned initial conditions that lead to its exceptionally flatness already at recombination (the *flatness problem*). One class of inflationary models relies on the dynamics of a field that is responsible for the inflationary period, the *inflaton*, which evolves under the influence of a nearly flat potential. In the simplest model of *single field* inflation the equation of motion for the inflaton field (denoted by ϕ) evolving under the potential $V(\phi)$ is similar to Eq. (152),

$$\ddot{\phi} + 3H\dot{\phi} - \frac{1}{R^2}\nabla^2\phi + \frac{dV(\phi)}{d\phi} = 0. \quad (308)$$

For super-horizon modes, the spatial derivative can be neglected. A nearly flat potential grants an inflationary period in which the inflaton evolves under a *slow-roll* dynamics if *i)* $\ddot{\phi} \ll H\dot{\phi}$, and *ii)* $\dot{\phi}^2 \ll V(\phi)$. Condition *i)* leads to $3H\dot{\phi} \simeq -dV(\phi)/d\phi$, while condition *ii)* gives the equation of state

$$w_\phi = \frac{\frac{1}{2}\dot{\phi}^2 - V(\phi)}{\frac{1}{2}\dot{\phi}^2 + V(\phi)} \simeq -1. \quad (309)$$

If both conditions *i)* and *ii)* are satisfied, the energy density of the ϕ field is constant during inflation, which yields a quasi-exponential growth of the scale factor according to Eq. (140).

Different models have been considered so far in order to embed inflation into an axion framework. One possibility consists in considering the dynamics of the PQ complex field during inflation [266] and identify the inflaton field with the radial mode ϱ_a of the PQ complex field (see Eq. (79)). At sufficiently high temperatures, the potential of ϱ_a in Eq. (78) can be approximated by a quartic potential. However, such a form of inflaton potential has been excluded to a high level of confidence by the measurements of the CMB spectra by the *Planck* mission [721–723]. For this reason, Ref. [315] considered a non-minimal coupling to gravity so that the potential at large values of ϱ_a is flattened out (see e.g. Ref. [724]) and the model reconciles with observations. This model also circumvents the problem that, for relatively high values of the Hubble rate during inflation H_I , axion isocurvature fluctuations during inflation are too large with respect to what is allowed by measurements [252], see Section 3.5. The reason being that the radial field has not yet relaxed to its minimum value during inflation and it evolves in the regime $\varrho_a \gg f_a$, thus suppressing isocurvature fluctuations.⁷⁹

A less minimal kind of embedding has been carried out in the SMASH model [311–313], in which the inflaton field is a linear combination of the radial modes of the PQ field Φ and the Higgs doublet H , both coupled non-minimally to gravity. The model shares some similarities with the Higgs inflation model of [725], but thanks to the mixed embedding of the inflaton field it provides a solution of the unitarity problem of standard Higgs inflation [726, 727], thus making inflationary predictions more reliable.

Within the single field slow-roll inflation model, it is possible to obtain predictions for the scalar and tensor power spectra on super-horizon scales. As discussed in Section 3.5, tensor modes for single-field inflation are defined in terms of the tensor-to-scalar ratio r which, if measured in the future at the level of $r \sim 10^{-3}$, would shut off the pre-inflationary scenario completely [188, 315, 728–731], see also Fig. 3. It has recently been shown [317] that a model of inflation with the SM Higgs field, in which the Higgs field is coupled non-minimally to *Palatini* gravity [732] leads to an inflation energy scale $H_I \sim 10^8$ GeV and a low tensor-to-scalar ratio $r \sim 10^{-13}$. In this model, axion isocurvature fluctuations that would evade the current bounds can be accommodated, and it is then possible to realise axion DM in the pre-inflationary scenario with a value of the axion energy scale of the order of $\sim 10^{14}$ GeV.

The QCD axion itself could have driven inflation, evolving via a series of tunnelling events in the so-called chain inflation model [733, 734]. Assuming an axion model in which the continuous shift symmetry is broken

⁷⁹Another way to circumvent isocurvature bounds in low-scale models of hybrid inflation has been proposed in Ref. [272].

down to a discrete $\mathbb{Z}_{N_{\text{DW}}}$ symmetry, with a large number $\mathcal{O}(100)$ of local minima N_{DW} , and a tilting term parametrized via a soft breaking contribution with height η , the potential reads

$$V(a) = V_0 \left[1 - \cos \left(\frac{N_{\text{DW}} a}{v_a} \right) \right] + \eta \cos \left(\frac{a}{v_a} \right). \quad (310)$$

The axion evolves in one of the false vacua described by the potential in Eq. (310), providing about one e -fold of inflation before tunnelling to the next false vacuum and approaching the true vacuum of the theory. Chain inflation is a viable model for solving the horizon, entropy and flatness problem of standard cosmology and for generating the right amount of adiabatic cosmological perturbations [735, 736], although a considerable effort in model building is necessary since a large number of tunnelling events, $\gtrsim 10^8$ per Hubble volume per e -fold, are required [737]. Finally, two classes of inflation models which come from superstring axion scenarios (see Section 7.9) are axion inflation [738–741] where the inflationary potential is given by the standard cosine potential, and axion monodromy [742–744], in which the potential includes extra terms like a linear term.

7.4. Gravitational waves from the Peccei-Quinn phase transition

The detection of GW by LIGO [745] has rendered clear that a new powerful tool is now available for the exploration of the Universe. In particular, first-order phase transitions in the early Universe can produce stochastic GW signals which could be potentially observed. The LIGO/VIRGO frequency band corresponds to first-order phase transitions which could have happened at temperatures around 10^7 - 10^8 GeV. This is intriguingly close to the lowest possible energy scale where the PQ symmetry can be broken [746]. Although the astrophysical bounds reviewed in Section 4 require f_a to lie above the scales at which LIGO/VIRGO are most sensitive, in the presence of a certain amount of supercooling the nucleation temperature of the PQ phase transition can be actually smaller than f_a by an order of magnitude or more [747, 748], thus motivating studies of the potential of GW experiments to detect the imprint of the phase transition that gave birth to the axion. A GW signature could be detected only if the PQ phase transition occurred after the end of inflation and if it is of strong first order. In weakly coupled models the transition, however, is typically second order, except in the region of parameters where the PQ symmetry is broken through the Coleman-Weinberg mechanism, while in strongly coupled realisations of axion models the transition is often first order. This restricts the type of models that can produce the sought signals. Recent studies of the energy density stored in stochastic GW from a first order PQ transition and of the corresponding peak frequency have been presented in [747, 748]. Ref. [749] studies the GW signal in a dynamical super-heavy axion models where the phase transition is associated with a new color-like gauge group confining around the TeV scale. In this case, however, the signal frequency remains well below the LIGO/VIRGO sensitivity range. A study of the axion (and ALP) parameter space which may be probed by future GW detectors can be found in Ref. [750].

7.5. Solutions to the domain walls problem

The DW problem arises from the fact that the axion field a , being an angular variable, takes values in the interval $[0, 2\pi v_a)$. The axion potential is periodic in a with period $\Delta a = 2\pi v_a/N_{\text{DW}}$, and thus it enjoys an exact $\mathbb{Z}_{N_{\text{DW}}}$ discrete symmetry. Once at $T \sim \Lambda_{\text{QCD}}$ the non-perturbative QCD effects lift the axion potential, N_{DW} degenerate vacua appear. In general the initial value of a at the bottom of the originally flat potential is randomly selected and it differs in different patches of the Universe, so that in each patch the axion will eventually flow towards a different minimum, breaking spontaneously $\mathbb{Z}_{N_{\text{DW}}}$. DWs will then form at the boundaries between regions of different vacua. The cosmological DW problem [510] consists in the fact that the energy density of the DWs would largely overshoot the critical density of the Universe. There are, however, two scenarios in which this there is no DW problem: (i) The first corresponds to the pre-inflationary scenario in which an initial patch characterised by some value of θ_i gets exponentially inflated to super-horizon scales, so that after inflation the whole observable Universe is characterised by a unique minimum of the axion potential, and is thus free from topological defects. (ii) The second scenario encloses

the models in which $N_{\text{DW}} = 1$, so that there is a single value of θ where the potential has a minimum. Although the vacuum is unique, a particular type of DWs still form, but they are harmless. The reason can be pictured as follows: when $U(1)_{\text{PQ}}$ gets broken, strings form, and in circulating around a string θ changes by 2π . When the temperature approaches the QCD scale and the axion potential gets tilted, the unique minimum $\theta = 0$ is selected. Still, in a two dimensional region attached to the string the phase must jump from 0 to 2π and back to 0, and this region corresponds to a wall with one edge attached to the string. However, a configuration of walls bounded by strings tends to rapidly collapse [226], and eventually the whole system of walls and strings disappears without ever coming to dominate the energy density of the Universe. Hence, axion models with $N_{\text{DW}} = 1$ are safe with respect to the DW problem also in post-inflationary scenarios.

A first example of a construction with $N_{\text{DW}} = 1$ is the original KSVZ model [120, 121] that we have reviewed in Section 2.7.1, where a single pair of electroweak singlet exotic quarks in the fundamental of $SU(3)_c$ yields a colour anomaly $2N = N_{\text{DW}} = 1$. Georgi and Wise [751] considered instead the possibility of canceling part of the QCD anomaly of DFSZ-type of models by introducing suitable representations of exotic quarks of KSVZ-type with PQ charge of the opposite sign, so that a total anomaly $2N = 1$ eventually results.

A different kind of construction features an apparent value $N_{\text{DW}} > 1$, while the physical number of DW is in fact $N_{\text{DW}} = 1$. These constructions rely on the introduction of extra symmetries, in such a way that the degenerate vacua of the axion potential are connected by symmetry transformations. The first realisation of this mechanism is due to Lazarides and Shafi (LS) [752] which observed that the DW problem does not exist if the discrete subgroup $\mathbb{Z}_{N_{\text{DW}}}$ in $U(1)_{\text{PQ}}$ can be embedded in the center of a continuous gauge group, and they provided a neat example based on the GUT symmetry $SO(10) \times U(1)_{\text{PQ}}$. A different possibility was proposed in Ref. [152]. The axion arises from an accidental $U(1)$ enforced on the potential of a scalar multiplet Y_{LR} by a gauge symmetry $SU(\mathcal{N})_L \times SU(\mathcal{N})_R$. Y_{LR} transforms under the group as $(\mathcal{N}, \bar{\mathcal{N}})$ and is responsible for the spontaneous breaking of the gauge group down to $SU(\mathcal{N})_{L+R}$. Although the construction gives a QCD anomaly with coefficient $N = \mathcal{N}/2$, all the minima can be connected by gauge transformations corresponding to the center $\mathbb{Z}_{\mathcal{N}}$ of the unbroken group, and hence they are gauge equivalent. While in the original LS model $\mathbb{Z}_{N_{\text{DW}}}$ was embedded into a local group, embedding in global groups can also yield the same result. For example, models with global family groups were considered in Ref. [753].

A different type of constructions in which $N_{\text{DW}} = 1$ can be engineered, rely on the presence of more than one global $U(1)$ symmetry [754]. The anomalous PQ will in general correspond to a combination of the various Abelian groups, and it can be arranged so that QCD effects break this specific combination to the trivial subgroup \mathbb{Z}_1 .

A horizontal realisation of the PQ symmetry that, together with $B-L$ global invariance, can solve the DW problem for any arbitrary number of fermion generations was discussed in Ref. [755]. Other models enforce $N_{\text{DW}} = 1$ making use in different ways of generation dependent PQ symmetries. For example a partial cancellation of the anomaly contributions between different generations can be arranged [124, 551], or the PQ charges are chosen in such a way that two generations give vanishing contributions to the anomaly [557], or more in general it can be assumed that some SM quark flavours have a special status with respect to the PQ symmetry [570], for example it can happen that only one or two out of all the SM quarks contribute to the anomaly [555]. Of course, as was discussed in Section 6.5, all these models feature flavour violating axion couplings, and can be thoroughly tested by searching for flavour changing processes.

Models for which none of the above two conditions (i) and (ii) are satisfied, that is the PQ symmetry is broken after inflation, and $N_{\text{DW}} > 1$ gives rise to the same number of physically inequivalent degenerate vacua, can also remain viable, but additional assumptions are needed. The DW problem can be disposed of in a simple way by introducing an explicit breaking of the PQ symmetry so that the degeneracy between the different vacua is removed and there is a unique minimum of the potential. This can be done either by introducing an explicit breaking of the PQ symmetry via Planck-suppressed effective operators [510] or by non-perturbative potential terms induced by a new confining gauge group [756–758]. Breaking explicitly the PQ symmetry is, however, a delicate issue: sufficiently large breaking effects are needed to guarantee that regions trapped in false vacua will cross over to the true vacuum before DWs start dominating the Universe

energy density.⁸⁰ However, at the same time they should not be too large, otherwise they would spoil the PQ solution. The present limit $\theta \lesssim 10^{-10}$ still leaves a viable region in parameter space where these two conditions can be simultaneously matched [27, 29, 758].

7.6. Solutions to the Peccei-Quinn quality problem

As we have discussed in Section 2.11 in order to ensure the effectiveness of the PQ mechanism in solving the strong CP problem a strong requirement needs to be satisfied: the PQ symmetry must remain a good symmetry well beyond the level of renormalizable operators, and arguably up to effective operators of dimensions $d > 10$. However, the PQ symmetry is a global symmetry, and in QFT global symmetries are not deemed to be fundamental or exact. Moreover, the PQ symmetry is anomalous, and as such at the quantum level it is not even a real symmetry. Analogies with baryon and lepton $U(1)$ symmetries in the SM, which are also global and anomalous, but whose origin as accidental symmetries is well understood, naturally lead to speculate whether the PQ symmetry might also arise accidentally, in the sense that other fundamental symmetries (gauge and Lorentz) might forbid, up to the required dimension, operators that do not conserve the PQ charge. Several constructions have been put forth to realise this idea. Probably the simplest possibility is that of a discrete gauge symmetry. For instance a \mathbb{Z}_n acting on Φ as $\Phi \rightarrow e^{i2\pi/n}\Phi$ would forbid all effective operators $(\Phi^\dagger\Phi)^m\Phi^k$ with $k < n$. A possible way to generate discrete gauge symmetries in 4-dimensional QFT was suggested in Ref. [760]. Consider a $U(1)$ gauge symmetry under which the axion multiplet Φ carries charge 1, while a second field ξ carries charge n : $\Phi \rightarrow e^{i\alpha}\Phi$, $\xi \rightarrow e^{in\alpha}\xi$. Suppose that ξ undergoes condensation at some high-energy scale $\langle\xi\rangle \gg f_a$. The invariance of the VEV $\langle\xi\rangle \rightarrow e^{in\alpha}\langle\xi\rangle$ with $\alpha = 2\pi/n$ corresponds to a \mathbb{Z}_n discrete gauge symmetry, unbroken above f_a , under which Φ transforms as $\Phi \rightarrow e^{i\alpha}\Phi = e^{i2\pi/n}\Phi$. This ensures that the first allowed operator breaking PQ explicitly is Φ^n . Mechanisms with large local discrete symmetries have been for example invoked in Ref. [144–148].

Other models rely on the introduction of a new local Abelian symmetry $U(1)'$ that, as in Ref. [135], can be directly added to enlarge the SM gauge group. In this reference two singlet scalars Φ and S are also introduced, with $U(1)'$ charges respectively p and q , and these charges are chosen in such a way that the lowest order effective operator that breaks the PQ symmetry, namely $(S^\dagger)^p\Phi^q$, is of the required high dimension $d = p + q$. Ref. [137] considers instead a supersymmetric GUT extension $E_6 \times U(1)'$, where the usual trilinear superpotential Yukawa coupling $\mathbf{27}^3$ is forbidden by the new Abelian symmetry, and is replaced by a coupling involving a new unconventional representation $\mathbf{27}_1\mathbf{27}_{-1}\mathbf{351}_0$, where subscripts refers to the $U(1)'$ gauge charges. A global PQ symmetry under which with $\mathcal{X}(\mathbf{27}) = 1$ and $\mathcal{X}(\mathbf{351}) = -2$ arises accidentally, and the lowest order gauge invariant PQ violating operators $\mathbf{27}^6$ or $\mathbf{351}^6$ are of the required large dimension. Soft supersymmetry breaking effects might, however, endanger this solution [155]. Ref. [149] considers instead the possibility of embedding the PQ symmetry into a gauged $U(1)'$, which is rendered non anomalous by adding exotic fermions coupled to the SM only via gauge interactions, so that the subset of gauge rotations acting only on the SM quarks can be interpreted as an accidental (global and anomalous) $U(1) \subset U(1)'$. Ref. [150] promotes baryon number to a local gauge symmetry by canceling the anomaly via the introduction of exotic fermions which play the role of KSVZ exotic quarks. The authors show that the PQ symmetry remains sufficiently protected by this gauged baryon number. Finally, Ref. [151] addresses the axion quality problem in a 4-dimensional clockwork model, with the PQ global symmetry arising accidentally due to a gauged $U(1)^N$ symmetry.

Other approaches exploit instead new non-Abelian gauge groups. Georgi, Hall and Wise [133] provided the first example⁸¹ of an accidental PQ symmetry arising from a grand-unified gauge group based on $SU(9)$, which incorporates the usual $SU(5)$ GUT as a subgroup. The construction is non-trivial, since it involves several $SU(9)$ representations (left-handed fermions in a $\mathbf{36} \oplus 5 \times \bar{\mathbf{9}}$ and scalar fields in a $\mathbf{80} \oplus 5 \times \mathbf{9} \oplus \mathbf{126}$). Writing the most general renormalizable Lagrangian allowed by the $SU(9)$ gauge symmetry enforces a QCD

⁸⁰A stronger bound actually originates from requiring that the axions produced from the collapse of DWs do not have an abundance larger than the DM one [207, 208, 295]. An early matter domination era around the MeV scale can help in relaxing this bound [759].

⁸¹Incidentally, this is also the first paper where the issue of the PQ quality problem was clearly laid down.

anomalous $U(1)$ symmetry that is spontaneously broken at the unification scale. Although in this work the authors did not explicitly address the question of at which operator level the PQ breaking is explicitly broken, one can see that this happens due to the “baryon-like” invariant $\epsilon_{ijk\dots} \mathbf{9}^i \mathbf{9}^j \mathbf{9}^k \dots$ and hence at $d = 9$. The complexity of this construction shows that it is highly nontrivial to get an accidental PQ symmetry in GUTs (without resorting to extra gauged $U(1)$ ’s) and we are not aware of other successful attempts, apart from the original one in Ref. [133]. Instead the construction discussed in Ref. [152] takes inspiration from a type of flavour models in which the SM Yukawa couplings are promoted to dynamical scalar fields $Y(x)$ transforming in the bi-fundamental of a gauge group $SU(3)_L \times SU(3)_R$. As it was remarked in Ref. [761], gauge invariant operators in the scalar potential for $Y(x)$ are Hermitian and thus respect an accidental $U(1)$ rephasing invariance, with the sole exception of $\det Y(x)$ which is non-Hermitian and of dimension $d = 3$. Then, generalising the construction to an $SU(\mathcal{N})_L \times SU(\mathcal{N})_R$ invariant potential with $\mathcal{N} > 4$, the dimension of the symmetry breaking operator is promoted to $d = \mathcal{N}$, so that the quality of the accidental $U(1)$ remains determined by the dimension of the gauge group which can be arbitrarily chosen. An even simpler possibility based on the same approach is to replace the SM flavour symmetry $SU(3)_L \times SU(3)_R$ with a different one $SU(M)_L \times SU(N)_R$ ($M \neq N$) and require that the Yukawa field transforms as (M, \bar{N}) (for M and/or $N > 3$ this can be done by introducing new exotic vectorlike quarks) [762]. In this case the dimension of the first flavour-singlet non-Hermitian scalar operator is at least as large as the least common multiple of M and N , so that large operator dimensions for the PQ breaking operators can be obtained with group factors of relatively small degree. Finally, scalar-gauge theories in which $Y(x)$ transforms as the symmetric (anti-symmetric) of $SU(\mathcal{N})$ broken into $SO(\mathcal{N})$ ($Sp(\mathcal{N})$) also lead to an accidental Goldstone for $\mathcal{N} > 4$ [763], and they might be used to construct models for the PQ protection along the lines of [152].

Ref. [153] introduces an exotic sector equipped with an $SU(\mathcal{N})$ gauge symmetry where a hidden baryon number $U(1)_{B_N}$ appears accidentally, similarly to what happens in the SM with ordinary $U(1)_B$. However, differently from the SM where B violating effective operators are allowed already at $d = 6$, the B_N violating operators of lowest dimension are the gauge (and, assuming \mathcal{N} even, also Lorentz) invariant $SU(\mathcal{N})$ singlets $\epsilon_{\alpha_1 \alpha_2 \dots \alpha_{\mathcal{N}}} Q^{\alpha_1} Q^{\alpha_2} \dots Q^{\alpha_{\mathcal{N}}}$ with dimension $d = 3\mathcal{N}/2 \gg 3$. In the presence of fermion species chiral under $SU(\mathcal{N}) \times SU(2)_C$ a $U(1)_{B_N}$ - $SU(3)_C^2$ anomaly can arise, so that the new baryon symmetry can act in the SM as a PQ symmetry. In Ref. [161] instead the SM quark flavour symmetry has been used directly, and the required level of suppression for the PQ breaking operators is obtained by assuming that quark masses are generated radiatively, so that the Yukawa couplings do not correspond to fundamental symmetry breaking scalars, but result from a more complicated set of spurions that allow to keep the PQ symmetry exact up to $d = 12$.

Composite axion models (reviewed in Section 7.7) are also well suited to arrange for approximate PQ symmetries preserved up to operators of high dimension. One of the first constructions exploiting compositeness with this aim was the Randall model [154]. The relevant gauge symmetry is $SU(\mathcal{N}) \times SU(m) \times SU(3)_C$. Exotic fermions transform under the group factors with suitable chiral assignments in such a way that an accidental global $U(1)$ arises, which is non-anomalous with respect to the first two factors but has an $SU(3)_C$ anomaly. $SU(\mathcal{N})$ becomes strong at a large scale breaking spontaneously $SU(m)$ (much alike $SU(3)_C$ condensates in the SM break spontaneously $SU(2)_L$) and breaking also the global $U(1)$, but not $SU(3)_C$. In this model the lowest dimensional operator consistent with the gauge and Lorentz symmetries, but not respecting the $U(1)$, can be built with $2m$ uncoloured fermions. Hence the quality of the PQ symmetry is controlled by the dimension of the $SU(m)$ group. Other composite models for PQ symmetry protection exploiting similar ideas can be found in Refs. [155–158].

Extra-dimensional setups are also well suited to protect the PQ symmetry. For instance, in the proposal of Ref. [159] the axion is identified with the 5-th component of a gauge field in a 5D orbifold field theory compactified on S^1/Z_2 , for which all PQ breaking terms other than the QCD anomaly are naturally suppressed by the higher-dimensional gauge symmetry and the 5D locality. A recent geometrical solution of PQ quality problem was considered in Ref. [160], by modelling the axion with a bulk complex scalar field in a slice of AdS_5 , where the $U(1)_{PQ}$ symmetry is spontaneously broken in the bulk but explicitly broken on the UV brane. By localising the axion field towards the IR brane, gravitational violations of the PQ symmetry on the UV brane are sufficiently suppressed by the warp factor.

7.7. Axions and composite dynamics

Composite axion models were originally motivated by the possibility of dynamically explaining the hierarchy $f_a \ll m_{\text{Pl}}$, as a consequence of a confining non-abelian gauge theory, largely inspired by pions and chiral symmetry breaking in QCD as well as technicolor models for the electroweak scale.

For instance, the original model of Kim [505] (see also [508]) was based on a new gauge group $SU(\mathcal{N})$ that confines at a scale $\Lambda_{SU(\mathcal{N})} \sim f_a$, and comprises the following vector-like fermion content with transformation properties under $SU(\mathcal{N}) \times SU(3)_c$: $\psi_{L,R} \sim (\mathcal{N}, 3)$ and $\xi_{L,R} \sim (\mathcal{N}, 1)$. In the limit of zero fermion masses and for $g_s \rightarrow 0$ the model has an $SU(4)_L \times SU(4)_R \times U(1)_V$ global symmetry, which is spontaneously broken down to $SU(4)_{L+R} \times U(1)_V$ by the fermion condensates $\langle \bar{\psi}_L \psi_R \rangle = \langle \bar{\xi}_L \xi_R \rangle \sim \Lambda_{SU(\mathcal{N})}^3$. The resulting 15 NGB transform as $1 + 3 + \bar{3} + 8$ under $SU(3)_c$. The color singlet, with a $(\bar{\psi}_L \psi_R - 3 \bar{\xi}_L \xi_R)$ content, is identified with the composite axion and $U(1)_{\text{PQ}}$ corresponds to the $[(T^{15})_L \times \mathbb{I}_R + \mathbb{I}_L \times (T^{15})_R]/\sqrt{2}$ broken generator of $SU(4)_L \times SU(4)_R$, with $T^{15} = \frac{1}{2\sqrt{6}} \text{diag}(1, 1, 1, -3)$ belonging to the $SU(4)$ Cartan sub-algebra, so that the $U(1)_{\text{PQ}}$ is anomalous under QCD but not under $SU(\mathcal{N})$. When g_s is turned on, the $SU(4)_{L+R}$ global symmetry is explicitly broken down to the gauged $SU(3)_c$. The axion gets a tiny mass from QCD instantons, since the associated current is QCD anomalous

$$J_{\text{PQ}}^\mu = \frac{1}{2\sqrt{6}} [\bar{\psi} \gamma^\mu \gamma_5 \psi - 3 \bar{\xi} \gamma^\mu \gamma_5 \xi] \quad \implies \quad \partial_\mu J_{\text{PQ}}^\mu = \frac{g_s}{16\pi^2} \frac{\mathcal{N}}{2\sqrt{6}} G\tilde{G}, \quad (311)$$

while the other pseudo NGB in non-trivial color representations get masses of order $g_s \Lambda_{SU(\mathcal{N})}/(4\pi)$ via perturbative gluon loops (similarly to the QED contribution to the mass of the charged pion of order $e \Lambda_{\text{QCD}}/(4\pi)$). The axion couplings to SM fields in Kim's composite axion model follow from the expression of the PQ current in Eq. (311) and from the definition of the 'axi-pion' constant [112] $\langle 0 | J_{\text{PQ}}^\mu | a \rangle = i F_a p^\mu$ (with F_a of order $\Lambda_{SU(\mathcal{N})}$, analogously to $f_\pi \sim \Lambda_{\text{QCD}}$). Matching with the axion effective Lagrangian in Eq. (36) one gets $f_a = \sqrt{6} F_a / \mathcal{N} \sim \sqrt{6} \Lambda_{SU(\mathcal{N})} / \mathcal{N}$. Note that similarly to KSVZ-like models where SM fields (f) are uncharged under the PQ, the model-dependent axion coupling to SM fermions vanish, $c_f^0 = 0$, and also $g_{a\gamma}^0 = 0$. The latter actually depends on the specific choice of the exotic fermion representations in Kim's model. By assigning to them non-trivial electroweak quantum numbers one can also get direct EM anomaly contributions to $g_{a\gamma}^0 \neq 0$ [112], as discussed in Section 6.1.1.

It should be noted that in Kim's original composite axion model, similarly to standard KSVZ constructions, vector-like exotic fermion masses need to be forbidden in order not to spoil the whole framework. In fact, bare mass terms, $m_{\psi, \xi}$, even if $\ll \Lambda_{SU(\mathcal{N})}$, would still misalign the minimum of the QCD axion potential unless extremely suppressed, since they contribute to the composite NGB axion mass as $m_a \sim \sqrt{\Lambda_{SU(\mathcal{N})} m_{\psi, \xi}}$. The model is also prone to the PQ quality problem (see Section 2.11), since Planck-suppressed $U(1)_{\text{PQ}}$ breaking operators, which are in principle allowed by gauge symmetries, could spoil the solution of the strong CP problem. This motivated the construction of composite axion models in which an extra, chiral gauge symmetry avoids the presence of exotic fermion mass terms and protects as well from higher-order PQ symmetry breaking operators. Models of this type were briefly reviewed towards the end of Section 7.6.

7.8. Axions and GUTs

Unified gauged theories provide a rationale for the large value of the axion decay constant f_a , which for phenomenological reasons must lie between 10^8 GeV and the Planck scale. In fact, if the axion field is embedded into a scalar representation responsible for the breaking of the GUT symmetry (e.g. in the global phase of a complexified adjoint representation) one has $f_a = v_a / N_{\text{DW}} \approx M_G / N_{\text{DW}}$, where $M_G \gtrsim 10^{15}$ GeV denotes the scale of GUT breaking, which is bounded from below by the non-observation of proton decay. Models of this type, in which the global $U(1)_{\text{PQ}}$ commutes with the GUT group, were first proposed in the context of $SU(5)$ [764] and $SO(10)$ [765] (for modern variants see also [766–770]). A remarkable feature of these models is the connection between proton decay and standard axion searches, which will start to probe the GUT-scale axion in the coming decade (cf. the reach of Casper-Electric and ABRACADABRA in Section 5.3). For instance, the minimal $SU(5) \times U(1)_{\text{PQ}}$ model of Ref. [767], based on the original Georgi-Glashow [771] field content plus a 24_F representation that fixes both neutrino masses and gauge coupling

unification [772–774], provides a rather sharp prediction (arising from gauge coupling unification and proton decay constraints) for the value of the axion mass $m_a \sim 5 \text{ neV}$, setting a well-defined target for axion DM experiments. Regarding the connection with axion DM let us recall that, in order not to over-produce axion DM, GUT-scale values of f_a require the PQ symmetry to be broken before inflation (pre-inflationary PQ breaking scenario) together with a certain tuning of the initial misalignment angle to small values (for $f_a \sim 10^{15} \text{ GeV}$, $\theta_i \sim 1\%$).⁸² Note that values of $f_a \ll M_G$ can still be obtained for $v_a \sim M_G$, but these require values of N_{DW} is unrealistically large. Another class of models which allows for $f_a \ll M_G$ and that at the same time can be compatible with post-inflationary PQ breaking scenarios is based on $SO(10)$ GUTs in which the axion is embedded into a representation responsible for an intermediate symmetry breaking stage, possibly related to the scale of right-handed neutrinos [693, 766, 775–778]. In such a case, however, the scale f_a turns out to be “sliding”, since it is only weakly constrained by gauge coupling unification [766].

Regarding the structure of axion couplings in GUTs, these are fixed up to some minor model-dependent factors, thus providing a well-defined and motivated benchmark for axion searches. Most notably, the value of the group theory factor that determines the axion coupling to photons is fixed to be $E/N = 8/3$. This can be seen from the explicit expression

$$\frac{E}{N} = \frac{\text{Tr } Q^2}{\text{Tr } T_C^2} = \frac{\text{Tr } (T_L^3)^2 + \frac{5}{3} \text{Tr } T_Y^2}{\text{Tr } T_C^2} = \frac{8}{3}, \quad (312)$$

where $Q = T_L^3 + \sqrt{5/3} T_Y$, in terms of the GUT-normalized hypercharge generator T_Y . This result follows from the fact that all the generators of the GUT group, and in particular T_C, T_L^3 and T_Y , have the same normalization.⁸³

The Yukawa sector of an axion GUT model is similar (as far as concerns global PQ charges) to that of the DFSZ-I model with Yukawa Lagrangian in Eq. (91). E.g. in minimal $SU(5)$ one has (neglecting for simplicity neutrino masses and corrections to the charged fermion mass relations)

$$\mathcal{L}_{\text{SU}(5)}^Y \supset -Y_{10} 10_F 10_F \bar{5}_{H_u} - Y_5 \bar{5}_F 10_F \bar{5}_{H_d}, \quad (313)$$

which after projecting onto the SM components matches Eq. (91), with the following GUT-scale boundary values for the Yukawa matrices: $Y_{10} = Y_U$ and $Y_5 = Y_E = Y_D^T$. Hence, we can take over the derivation of the axion couplings to SM fermions in the DFSZ-I model (cf. Eqs. (103)–(105)), which yields

$$c_{u_i}^0 = -\frac{1}{N} \cos^2 \beta, \quad c_{d_i}^0 = -\frac{1}{N} \sin^2 \beta, \quad c_{e_i}^0 = -\frac{1}{N} \sin^2 \beta, \quad (314)$$

where we used $v_a = f_a(2N)$ and with the important difference (compared to DFSZ-I) that the color anomaly N is a model-dependent factor that can be computed only after specifying the full GUT model.

While we have exemplified this derivation in the context of $SU(5)$, similar results apply to the $SO(10)$ case, where however care must be taken in order to properly orthogonalize the physical axion field with respect to the Goldstone fields of all the broken gauge generators (see Ref. [766] for a detailed account). Another peculiarity of GUTs like is $SO(10)$ is also the fact that some vacua of the axion potential can be connected by gauge transformations, and hence the naive identification $N_{\text{DW}} = 2N$ does not hold [752, 766].

7.9. Axions from superstrings

In this Review we have focussed on QFT axion solutions to the strong CP problem for which a spontaneously broken PQ symmetry, of which the axion is the resulting pNGB, is a necessary ingredient. As

⁸²This condition can, however, be circumvented by appealing for example to the mechanism of axion dilution by late entropy production reviewed in Section 6.6.1, as is done e.g. in the supersymmetric GUT model of Ref. [614].

⁸³Differ values of E/N are instead possible in the ‘unificaxion’ framework of Ref. [535], which assumes that the anomaly factors are due to intermediate-scale KSVZ-like fermions which form incomplete GUT multiplets and assist gauge coupling unification. It should be noted, however, that such scenarios are not easily motivated from a UV point of view. Indeed, as long as the $U(1)_{PQ}$ symmetry commutes with the GUT group, the full GUT representation contributes to the anomaly coefficients, yielding the result in Eq. (312). Moreover, all the fragments of the original GUT multiplet obtain mass of order f_a , and thus do not improve gauge coupling unification.

already noted, the PQ symmetry is global and anomalous, hence with good reason it can be considered unsatisfactory to impose PQ as a fundamental symmetry of a Lagrangian. Indeed, a more sound possibility is that it arises automatically as a consequence of other fundamental principles.

Another avenue that has been ventured is exploring whether axions can arise naturally from a more fundamental theory as for example superstring theory, supergravity or M-theory. At first glance, candidates featuring the qualitative properties of the QCD axion are superabundant in string theory. They arise from ten-dimensional antisymmetric gauge field tensors that, upon compactifying six internal coordinates $M_{10} \rightarrow M_4 \times V_6$, with V_6 some compact manifold, behave like pseudoscalars in the 4D effective theory. Each string theory realisation has antisymmetric p -forms that can host the axion, and that go under different names: the Ramond-Ramond (RR) C -fields for Type II strings, the C_3 -form for supergravity, the NS-NS B_2 -field for the heterotic string (NS stands for Neveu-Schwartz), the RR C_2 -field for the Type I string. Their relations with possible QCD axions in four dimensions has been studied and reviewed in several papers, see for example Refs. [738, 739, 779, 780]. Let us consider for definiteness the gravity supermultiplet, that is present in all string theories. Besides the 10D graviton g_{MN} , it contains an antisymmetric tensor B_{MN} and the dilaton. After compactification, the fields in B_{MN} can be categorized into a set of tangential fields $B_{\mu\nu}$ with indices in Minkowski space M_4 , and a set of fields B_{ij} with indices in the internal space V_6 . Let us consider $B_{\mu\nu}$ first: it has only one transverse degree of freedom so that, denoting by $H_{\mu\nu\sigma}$ its field strength tensor, one can define a scalar dualization $H_{\mu\nu\sigma} \propto f_a \epsilon_{\mu\nu\sigma\rho} \partial^\rho a$.⁸⁴ In the effective theory coming from the heterotic string the pseudoscalar a has the qualitative features of an axion: since it originates from a gauge field it has no potential at the renormalizable level, and hence enjoys a shift symmetry. However, since the shift symmetry is anomalous, the field a also couples to the QCD $G\tilde{G}$ term and it acquires non-perturbatively a small mass from QCD instantons (and in general also a much larger mass from other string-related non-perturbative effects, in which case, however, it would not serve as a QCD axion, see below). Since $B_{\mu\nu}$ can be discussed independently of the particular string compactification, it is called the Model Independent (MI) axion. A MI axion exists also in type-I strings, it arises from a RR two form C_2 in a way similar to the MI heterotic string axion, to which is in fact related by S -duality. Discrete symmetries arising from string compactification might also help in obtaining an accidental, intermediate-scale axion (see e.g. Refs. [781, 782]).

If the MI pseudoscalar fails to incarnate a useful QCD axion, one can resort to the B_{ij} components. These can be decomposed as $B_{ij} = \sum_n a_n(x_\mu) b_{ij}^n(y_k)$ with $x_\mu \in M_4$, $y_k \in V_6$, b_{ij}^n are harmonic two-form on V_6 , and a_n correspond to scalars living in 4D. Massless pseudoscalars arise from the b_{ij}^n zero modes, which correspond to $\int_C d\Sigma^{ij} b_{ij}$ where the integral over two-manifolds C in V_6 does not vanish if C has non-trivial topology. The properties of these states will clearly depend on the compactification scheme, and for this reason the corresponding axions are called Model Dependent (MD). The number of zero modes corresponds to the number of non-trivial two-cycles in V_6 , which is the Hodge number of the compact manifold [779]. When considering manifolds sufficiently complicated to have some chance of resulting in an effective theory containing the SM, the Hodge number could be as large as $\mathcal{O}(100)$ [783].

Plenty of others axion candidates are found in Type II A and B superstrings as well as in 11D supergravity.⁸⁵ Nevertheless, obtaining a phenomenologically acceptable QCD axion from these theories is not an easy task. Superstring axion constructions encounter a certain number of obstacles, among which the most serious are the following:

1. *String-related contributions to the axion potential.* Although at the renormalizable level string axions are massless because they originate from 10D gauge fields, the shift symmetry of the effective Lagrangian can

⁸⁴One defines $A^\mu = \frac{1}{6} \epsilon^{\mu\nu\alpha\beta} H_{\nu\alpha\beta}$, then from the equation of motion $\partial^\mu H_{\mu\alpha\beta} = 0$ for the 2-form field strength tensor $H^{\mu\alpha\beta} = \frac{1}{2} \partial_{[\mu} B_{\alpha\beta]}$, one has $\partial_\mu A_\nu - \partial_\nu A_\mu = 0$, that is $A_\mu = f_a \partial_\mu a$ for some scalar a and for some scale f_a that normalizes canonically the scalar field a in 4D.

⁸⁵This abundance of pseudoscalars, a large number of which could remain ultralight, has led to concoct the so called *string axiverse* [784–786], wherein hundreds of light axion-like particles populate a logarithmically distributed mass spectrum possibly down to the Hubble scale $\sim 10^{-33}$ eV. Constraints on this scenario from cosmological considerations are discussed e.g. in Refs. [787, 788].

be violated by all sort of string-related effects: worldsheet instantons [789, 790], brane instantons [791] gravitational instantons, gauge instantons from other factors of the gauge group. These effects can easily overwhelm the breaking induced by low energy QCD instantons, and this would exclude the possibility that these pseudoscalars could serve as QCD axions. This is basically the same issue that we have discussed in Section 2.11: suppose that the axion couples to a string instanton of action S with a natural mass scale $M \sim m_{\text{Pl}}$. Such instantons with their anti-instantons will then generate a contribution to the axion potential

$$V_S(\theta) = -2M^4 e^{-S} \cos(\theta + \xi), \quad (315)$$

where the phase ξ is unrelated with QCD or with complex quark mass phases. Upon minimizing V_S together with the QCD potential $V(\theta) \sim -m_\pi^2 f_\pi^2 \cos \theta$ it is found that in order not to spoil the axion solution to the strong CP problem one needs to require

$$M^4 e^{-S} \lesssim 10^{-10} f_\pi^2 m_\pi^2. \quad (316)$$

This implies $S \gtrsim 200$ which is a serious constraint on string axion models [270]. A few solutions to this problem have been proposed. If supersymmetry survives down to a scale μ lower than M then the contribution in the LH side of Eq. (315) could be reduced as $M^4 \rightarrow M^2 \mu^2$ [738, 739, 779]. For MD axions of type IIB superstring, Ref. [786] (see also Ref. [792]) put forth the possibility that in a large volume scenario, characterised by an exponentially large volume of the extra dimensions, a strong suppression $M \sim m_{\text{Pl}}/\sqrt{V_6}$, with $V_6 \gg 1$ in units of the string length, can be engineered.

2. Cosmological constraints on the axion scale f_a . As we have seen in Section 3.7, there is a phenomenologically preferred window for the axion decay constant $10^9 \lesssim f_a/\text{GeV} \lesssim 10^{12}$. The upper bound on f_a leads to some tension with string theory which naturally predicts much larger values. For example, for the MI axion of the heterotic string the value $f_a \simeq 1.1 \times 10^{16}$ GeV was first obtained in Ref. [793], and later confirmed by a more refined computation in Ref. [728]. Analogous predictions for the MD heterotic string axion as well as for other types of string models were derived in Ref. [739], which concluded that it is generally difficult to push f_a drastically below $\sim 10^{16}$ GeV, while more natural values are close to the reduced Planck mass $(8\pi G_N)^{-1/2} \sim 2.4 \times 10^{18}$ GeV. This would imply a very large overproduction of axion DM. Some possible ways out have been proposed, as for example the early attempt of Barr within the $E_8 \times E_8$ heterotic string [794] and more recently Conlon's construction in Ref. [780], which are both able to arrange for values of f_a within the canonical window.

Despite the promising initial conditions for a string origin of the axion, it appears surprisingly hard to construct explicit string theoretic examples with a successful QCD axion candidate. It seems then fair to say that, given the present status of the art, there are no sufficient reasons to theoretically disfavour the QFT axion with respect to their superstring homologues.

8. Concluding remarks and *desiderata*

Axion physics is witnessing an exponential growth of interest from the particle physics community. According to the inSPIRE database, during the first lustrum of this millennium less than 250 papers were published containing the word *axion* in the title. In the following years, the number of publications has steadily grown, reaching the stunning number of more than 1,250 papers published in the last quinquennium, and there is no hint that this growth is going to diminish in the forthcoming years. It is an experimental fact that particle physicists interests and wishes do not render a theory correct (as LHC results have recently reconfirmed). However, scientific attention gets naturally focussed by theories that, besides being highly consistent and remarkably elegant, are able to explain some longstanding theoretical conundrums and are also particularly promising as far as regards the possibility of experimental verification. Undoubtedly axion physics belongs to this class of theories. For this reason we are convinced that any effort to develop further

crucial theoretical issues in axion physics is soundly justified while, at the same time, experimental axion searches should be pursued along all viable pathways.

A major aim of this Review was that of motivating experimental colleagues to explore all the accessible regions in the axion parameter space. We have shown how axions can hide in regions that lie well beyond the boundaries of canonical windows. Axions can, for example, embody the whole DM also for mass values much larger or much smaller than what it is generally assumed. Axion searches which exploit their couplings to nucleons and electrons are complementary to traditional experimental searches which exploit their coupling to photons. As we have stressed, each type of axion couplings to SM particles could be suppressed well below their benchmark values, while leaving the other couplings substantially unaffected. In particular, it is possible to decouple the axion from the photon, in which case experimental searches that rely on the couplings to nucleons and electrons would play a crucial role. It is also conceivable that a strong suppression would instead occur for the axion-nucleon and axion-electron interactions. This would relax the tightest astrophysical bounds rendering viable regions in the m_a - $g_{a\gamma}$ parameter space that are generally regarded as excluded. Conversely, large enhancements of a single type of coupling are also possible. For this reason, new leading-edge experiments based on novel search techniques, which in many cases are characterised by limited sensitivities, can still contribute to circumscribe the landscape of phenomenologically viable axion models.

While the current blossoming of the field of axion physics is certainly driven by experiments, there exist important calls also for the theory community. We have collected in a (personal) list of *desiderata* those theoretical advancements that we consider crucial for further developments of axion physics, and that is conceivable that could be accomplished in the forthcoming years.

Origin of the Peccei-Quinn symmetry. Undoubtedly the PQ symmetry can be considered the ‘standard model’ for generating in a QFT the effective axion-gluon interaction needed to solve the strong CP problem. However, a ‘standard model’ for explaining the origin of the PQ symmetry is still missing. The remarkably large number of model realisations that have been reviewed in this work provides the best evidence of this statement. Candidate models should in first place provide a cogent explanation for how a global PQ symmetry arises, and should also naturally embed some mechanism to preserve it at an exceptionally good level. However, they would acquire real credibility if, with no additional or ad hoc theoretical inputs, they could automatically shed light on some other unsettled issue of the SM, like for example the flavour problem, the origin of neutrino masses, etc. We believe that any progress in this direction would represent an important milestone to strengthen the plausibility of the axion hypothesis.

Topological defects. Assessing the axion contribution to the DM arising from axion-related topological defects (in post-inflationary PQ breaking scenarios, and within $N_{\text{DW}} = 1$ models) is, at the time of writing, a major unsettled question. Tackling this problem requires extensive numerical simulations of the string network evolution and an extrapolation through several orders of magnitude between the PQ scale down to the Hubble scale at the time the axion acquires its mass. Although this appears as a remarkably difficult task, the importance of converging towards a reliable estimate cannot be overstated, since it would drive the scanning strategy of axion DM experiments.

Temperature dependence of the axion mass. Lattice studies of the temperature dependence of the axion mass have made remarkable progresses in the last few years. However, it seems that universal consensus on the behaviour of the mass function $m_a(T)$ has not yet been reached. A final convergence on this issue is highly desirable in order to refine estimates of the misalignment contribution to axion DM. We believe that it is realistic to expect that this goal will be achieved in the not so far future.

Axion emissivity from supernova cores. Our understanding of nuclear matter in the extreme conditions of proton-neutron stars in the cooling phase, shortly after a SN explosion, is still limited. Also this issue has recently witnessed important advancements. However, a detailed and reliable treatment of axion emissivity is, at least in part, still lacking. Any improvement in this direction would be of utmost importance. In fact, although the bound has been reassessed more than one time since first established, constraints from the

observed neutrino signal from SN1987A still provide one of the strongest limits for axion models, and this in spite of the fact that the collected data were very sparse. A new galactic SN explosion would produce an immensely richer data set, which could be optimally interpreted only if a better understanding of this issue will be available.

We do not know if the axion exists. What we do know, is that this hypothetical particle has been able to focus an enormous amount of theoretical and experimental efforts in the attempt of understanding its properties and arrive at its discovery. It might be deemed surprising that so much commitment is devoted to prove what remains, admittedly, essentially a theoretical speculation. We believe that the explanation lies in the beauty and in the elegance of the theoretical construction. Whether these two paradigms can really provide insight into the way nature works, only future experiments will tell. For the moment axion physics, in all its aspects, is healthy and frisky. May it remain so until the axion is discovered.

Acknowledgments

We thank Claudio Bonati, Andrea Caputo, Luc Darmé, Giovanni Grilli di Cortona, Axel Lindner, David J. E. Marsh, Pablo Quílez and Sunny Vagnozzi, for reviewing parts of the manuscript. We acknowledge Stefano Bertolini, Dmitry Budker, Marco Gorghetto, Igor G. Irastorza, Derek Jackson Kimball, Giacomo Landini, Federico Mescia, Alessandro Mirizzi, Fabrizio Nesti, Alessio Notari, Michele Redi, Javier Redondo, Andreas Ringwald, Giuseppe Ruoso, Oscar Straniero, Daniele Teresi, Andrea Tesi and Giovanni Villadoro for discussions and inputs, and Michael Wiescher for permission to reproduce the picture in the left panel of Fig. 4. We thank Hai-Yang Cheng, Raymond Co, Jordy de Vries, Patrick Draper, Keisuke Harigaya, Gioacchino Piazza, Mario Reig and Armen Sedrakian for comments and feedbacks on the first arXiv version of this review. L.D.L., M.G. and L.V. acknowledge the INFN Laboratori Nazionali di Frascati, where this project was first laid down, and where relevant portions of their work was performed, for hospitality and partial financial support. A large part of the work of L.D.L., M.G. and E.N. was performed at the Aspen Center for Physics, which is supported by National Science Foundation grant PHY-1607611. The participation of L.D.L. and E.N. at the Aspen Center for Physics was supported in part by a grant from the Simons Foundation. L.D.L. acknowledges hospitality from the Theoretical Physics Group at the University of Padova during the final stages of this work. E.N. acknowledges hospitality and support from the Munich Institute for Astro- and Particle Physics (MIAPP), which is funded by the Deutsche Forschungsgemeinschaft (DFG, German Research Foundation) under Germany's Excellence Strategy – EXC-2094 – 390783311, where this project was brought to completion. L.V. thanks the kind hospitality of the Leinweber Center for Theoretical Physics, the University of Michigan, and Barry University, where part of this work was carried out. L.D.L. is supported by the Marie Skłodowska-Curie Individual Fellowship grant AXION-RUSH (GA 840791). E.N. is supported by the Italian Istituto Nazionale di Fisica Nucleare (INFN) through the ‘Theoretical Astroparticle Physics’ project TAsP. L.V. acknowledges support by the Vetenskapsrådet (Swedish Research Council) through contract No. 638-2013-8993 and the Oskar Klein Centre for Cosmoparticle Physics. The work of L.V. is part of the research program ‘The Hidden Universe of Weakly Interacting Particles’ with project number 680.92.18.03 (NWO Vrije Programma), which is (partly) financed by the Dutch Research Council (NWO). L.V. acknowledges support by the Department of Physics and Astronomy, Uppsala University, by Nordita, KTH Royal Institute of Technology and Stockholm University, by GRAPPA University of Amsterdam.

Appendix: Tables of notations and of acronyms

Symbol	Meaning	Equation
θ	CP violating QCD angle	1
$\epsilon^{\mu\nu\rho\sigma}$	Levi-Civita symbol ($\epsilon^{0123} = -1$)	4
N	$U(1)_{\text{PQ}}\text{-}SU(3)_{\text{QCD}}$ anomaly coefficient	70
E	$U(1)_{\text{PQ}}\text{-}U(1)_{\text{QED}}$ anomaly coefficient	70
Φ	axion multiplet $\Phi(x) = \frac{1}{\sqrt{2}}(v_a + \varrho_a(x)) e^{i\frac{a(x)}{v_a}}$	79
ϱ_a	axion multiplet radial mode	79
a	axion field: axion multiplet orbital mode	79
v_a	Peccei-Quinn symmetry breaking VEV $v_a = \sqrt{2}\langle\Phi\rangle$	79
f_a	axion decay constant $f_a = v_a/(2N)$	72
N_{DW}	domain wall number $N_{\text{DW}} = 2N$	88
m_a	axion mass	108
$C_{a\gamma}$	axion-photon coupling	110
C_{ap}	axion-proton coupling	111
C_{an}	axion-neutron coupling	112
C_{ae}	axion-electron coupling	114
$C_{a\pi}$	axion-pion coupling	115
$C_{an\gamma}$	axion coupling to the neutron EDM	116
$g_{a\gamma}$	dimensional axion-photon coupling (GeV^{-1})	118
g_{af}	rescaled axion-fermion coupling	118
g_d	rescaled axion coupling to the neutron EDM	118
g_{aN}^S	CP-violating scalar axion-nucleon coupling	127
χ	topological susceptibility	131
R	cosmological scale factor	139
H	Hubble parameter $H = \dot{R}/R$	140
m_{Pl}	Planck mass	140
ρ, s	energy and entropy density ($(\rho, s) \simeq (\rho, s)_{\text{rad}}$ in rad. domination)	145
g_*, g_S	effective energy and entropy degrees of freedom	146
$m_a(T)$	axion mass at temperature T	149
t_{osc}	time for the onset of axion oscillations	154
$\theta_{\text{PQ}}, \dot{\theta}_{\text{PQ}}$	misalignment angle, axion velocity at the PQ scale	155
$\theta_i, \dot{\theta}_i$	misalignment angle, axion velocity at t_{osc}	158
Ω_a^{mis}	fractional axion energy density from misalignment	170
ε	energy-loss rate per unit mass	208
\mathcal{R}	ratio of number of stars in Horizontal and Red Giant branches	210
$g_{e12}, g_{\gamma10}$	respectively $g_{ae}/10^{-12}$ and $g_{a\gamma}/10^{-10} \text{ GeV}^{-1}$	240

Table 8: Notations introduced in the text, their meaning, and equations where they are defined.

Acronym	Meaning
ABC	Atomic recombination and de-excitation, Bremsstrahlung, Compton
ALP	Axion-like Particle
BBN	Big-Bang Nucleosynthesis
(C)DM	(Cold) Dark Matter
CL	Confidence Level
CMB	Cosmic Microwave Background
CMD	Color Magnitude Diagram
CP	Charge Parity
χ PT	Chiral Perturbation Theory
DFSZ	Dine-Fischler-Srednicki-Zhitnitsky
DIGA	Dilute Instanton Gas Approximation
DW	Domain Wall
EFT	Effective Field Theory
FCNC	Flavour Changing Neutral Currents
FLRW	Friedmann-Lemaître-Robertson-Walker
FV	Flavour Violating
GUT	Grand Unified Theory
GW	Gravitational Waves
HB	Horizontal Branch
HDM	Hot Dark Matter
HR	Hertzsprung-Russell
IR	Infrared
KSVZ	Kim-Shifman-Vainshtein-Zakharov
LP	Landau Pole
LSW	Light Shining Through a Wall
MI(D)	Model Independent (Dependent)
(n)EDM	(neutron) Electric Dipole Moment
(p)NGB	(pseudo) Nambu-Goldstone Boson
NMR	Nuclear Magnetic Resonance
(N)LO	(Next-to) Leading Order
NS	Neutron Star
OPE	One Pion Exchange
PQ	Peccei Quinn
QCD	Quantum Chromo Dynamics
QED	Quantum Electro Dynamics
QFT	Quantum Field Theory
RGB	Red Giant Branch
SM	Standard Model
SMASH	Standard Model–Axion–Seesaw–Higgs inflation portal
SN	Supernova
UV	Ultraviolet
VEV	Vacuum Expectation Value
WD(LF)	White Dwarf (Luminosity Function)
WIMP	Weakly Interacting Massive Particle
WW	Weinberg-Wilczek

Table 9: Acronyms used in the text and their meaning.

Experiment	Meaning
ABRACADABRA [319]	A Broadband/Resonant Approach to Cosmic Axion Detection
ADMX [795]	Axion Dark Matter Experiment
ALPS (II) [796]	Any Light Particle Search (II)
ARGUS [604]	A Russian-German-United States-Swedish Collaboration
ARIADNE [482]	Axion Resonant InterAction Detection Experiment
ATLAS [797]	A Toroidal LHC ApparatuS
AXIOMA [501]	AXION dark MATter detection
BEAST [497]	Broadband Electric Axion Sensing Technique
BELLE II [597]	
CAPP-8TB [463]	Center for Axion and Precision Physics
CASPEr [318]	Cosmic Axion Spin Precession Experiment
CAST [451]	CERN Axion Solar Telescope
CLEO [596]	
CMS [798]	Compact Muon Solenoid
Crystal Box [600]	
CULTASK [799]	CAPP's Ultra Low Temperature Axion Search in Korea
DARWIN [800]	Dark Matter WIMP Search With Liquid Xenon
E949+E787 [593]	
Fermi LAT [487]	Fermi Large Area Telescope
GAIA [419]	Global Astrometric Interferometer for Astrophysics
GNOME [503]	Global Network of Optical Magnetometers for Exotic Physics
HAYSTACK [464]	Haloscope at Yale Sensitive to Axion CDM
HST [801]	Hubble Space Telescope
IAXO [802]	International Axion Observatory
KLASH [322]	KLoe magnet for Axion Search
LHC [803]	Large Hadron Collider
LIGO [804]	Laser Interferometer Gravitational-Wave Observatory
LSST [402]	Large Synoptic Survey Telescope
LUX [455]	Large Underground Xenon
LZ [455]	LUX-ZEPLIN
MADMAX [331]	Magnetized Disc and Mirror Axion eXperiment
ORGAN [465]	Oscillating Resonant Group AxioN
ORPHEUS [493]	
OSQAR [479]	Optical Search for QED vacuum birefringence, Axions, and photon Regeneration
PandaX [456]	Particle aND Astrophysical Xenon experiment
PVLAS [480]	Polarisation of Vacuum with LASer
QUAX [469]	QUaerere AXion
RADES [494]	Relic Axion Detector Exploratory Setup
SCSS [805]	SuperCOSMOS Sky Survey
SDSS [806]	Sloan Digital Sky Survey
SKA [474]	Square Kilometer Array
STAX [498]	Sub-THz-AXion
TASTE [492]	Troitsk Axion Solar Telescope Experiment
TOORAD [468]	Topological Resonant Axion Detection
TRIUMF [598]	TRI University Meson Facility
VIRGO [807]	
VMB@CERN [481]	Vacuum Magnetic Birefringence experiment at CERN
WMAP [808]	Wilkinson Microwave Anisotropy Probe
XENON100 [454]	100 kg liquid Xenon target

Table 10: Experiment acronyms and their meaning. Blank entries correspond to experiment names that are not acronyms.

References

References

- [1] S. Weinberg, Anthropic Bound on the Cosmological Constant, *Phys. Rev. Lett.* 59 (1987) 2607. [doi:10.1103/PhysRevLett.59.2607](#).
- [2] V. Agrawal, S. M. Barr, J. F. Donoghue, D. Seckel, Viable range of the mass scale of the standard model, *Phys. Rev. D* 57 (1998) 5480–5492. [arXiv:hep-ph/9707380](#), [doi:10.1103/PhysRevD.57.5480](#).
- [3] V. Agrawal, S. M. Barr, J. F. Donoghue, D. Seckel, Anthropic considerations in multiple domain theories and the scale of electroweak symmetry breaking, *Phys. Rev. Lett.* 80 (1998) 1822–1825. [arXiv:hep-ph/9801253](#), [doi:10.1103/PhysRevLett.80.1822](#).
- [4] L. Ubaldi, Effects of theta on the deuteron binding energy and the triple-alpha process, *Phys. Rev. D* 81 (2010) 025011. [arXiv:0811.1599](#), [doi:10.1103/PhysRevD.81.025011](#).
- [5] M. Dine, L. Stephenson Haskins, L. Ubaldi, D. Xu, Some Remarks on Anthropic Approaches to the Strong CP Problem, *JHEP* 05 (2018) 171. [arXiv:1801.03466](#), [doi:10.1007/JHEP05\(2018\)171](#).
- [6] P. Minkowski, $\mu \rightarrow e\gamma$ at a Rate of One Out of 10^9 Muon Decays?, *Phys. Lett.* 67B (1977) 421–428. [doi:10.1016/0370-2693\(77\)90435-X](#).
- [7] T. Yanagida, Horizontal gauge symmetry and masses of neutrinos, *Conf. Proc. C7902131* (1979) 95–99.
- [8] M. Gell-Mann, P. Ramond, R. Slansky, Complex Spinors and Unified Theories, *Conf. Proc. C790927* (1979) 315–321. [arXiv:1306.4669](#).
- [9] R. N. Mohapatra, G. Senjanovic, Neutrino Masses and Mixings in Gauge Models with Spontaneous Parity Violation, *Phys. Rev. D* 23 (1981) 165. [doi:10.1103/PhysRevD.23.165](#).
- [10] M. Fukugita, T. Yanagida, Baryogenesis Without Grand Unification, *Phys. Lett. B* 174 (1986) 45–47. [doi:10.1016/0370-2693\(86\)91126-3](#).
- [11] S. Davidson, A. Ibarra, A Lower bound on the right-handed neutrino mass from leptogenesis, *Phys. Lett. B* 535 (2002) 25–32. [arXiv:hep-ph/0202239](#), [doi:10.1016/S0370-2693\(02\)01735-5](#).
- [12] W. Buchmuller, P. Di Bari, M. Plumacher, Leptogenesis for pedestrians, *Annals Phys.* 315 (2005) 305–351. [arXiv:hep-ph/0401240](#), [doi:10.1016/j.aop.2004.02.003](#).
- [13] S. Davidson, E. Nardi, Y. Nir, Leptogenesis, *Phys. Rept.* 466 (2008) 105–177. [arXiv:0802.2962](#), [doi:10.1016/j.physrep.2008.06.002](#).
- [14] C. S. Fong, E. Nardi, A. Riotto, Leptogenesis in the Universe, *Adv. High Energy Phys.* 2012 (2012) 158303. [arXiv:1301.3062](#), [doi:10.1155/2012/158303](#).
- [15] E. J. Chun, et al., Probing Leptogenesis, *Int. J. Mod. Phys. A* 33 (05n06) (2018) 1842005. [arXiv:1711.02865](#), [doi:10.1142/S0217751X18420058](#).
- [16] S. Weinberg, A New Light Boson?, *Phys. Rev. Lett.* 40 (1978) 223–226. [doi:10.1103/PhysRevLett.40.223](#).
- [17] F. Wilczek, Problem of Strong p and t Invariance in the Presence of Instantons, *Phys. Rev. Lett.* 40 (1978) 279–282. [doi:10.1103/PhysRevLett.40.279](#).
- [18] C. Vafa, E. Witten, Parity Conservation in QCD, *Phys. Rev. Lett.* 53 (1984) 535. [doi:10.1103/PhysRevLett.53.535](#).
- [19] R. D. Peccei, H. R. Quinn, CP Conservation in the Presence of Instantons, *Phys. Rev. Lett.* 38 (1977) 1440–1443. [doi:10.1103/PhysRevLett.38.1440](#).
- [20] R. D. Peccei, H. R. Quinn, Constraints Imposed by CP Conservation in the Presence of Instantons, *Phys. Rev. D* 16 (1977) 1791–1797. [doi:10.1103/PhysRevD.16.1791](#).
- [21] S. Coleman, *Aspects of Symmetry*, Cambridge University Press, Cambridge, U.K., 1985. [doi:10.1017/CB09780511565045](#).
- [22] J. E. Kim, Light Pseudoscalars, *Particle Physics and Cosmology, Phys. Rept.* 150 (1987) 1–177. [doi:10.1016/0370-1573\(87\)90017-2](#).
- [23] H.-Y. Cheng, The Strong CP Problem Revisited, *Phys. Rept.* 158 (1988) 1. [doi:10.1016/0370-1573\(88\)90135-4](#).
- [24] R. D. Peccei, The Strong CP Problem, *Adv. Ser. Direct. High Energy Phys.* 3 (1989) 503–551. [doi:10.1142/9789814503280_0013](#).
- [25] R. D. Peccei, The Strong CP problem and axions, *Lect. Notes Phys.* 741 (2008) 3–17, [3(2006)]. [arXiv:hep-ph/0607268](#), [doi:10.1007/978-3-540-73518-2_1](#).
- [26] J. E. Kim, G. Carosi, Axions and the Strong CP Problem, *Rev. Mod. Phys.* 82 (2010) 557–602, [erratum: *Rev. Mod. Phys.* 91, no. 4, 049902 (2019)]. [arXiv:0807.3125](#), [doi:10.1103/RevModPhys.82.557](#), [doi:10.1103/RevModPhys.91.049902](#).
- [27] P. Sikivie, Axion Cosmology, *Lect. Notes Phys.* 741 (2008) 19–50, [19(2006)]. [arXiv:astro-ph/0610440](#), [doi:10.1007/978-3-540-73518-2_2](#).
- [28] M. Kawasaki, K. Nakayama, Axions: Theory and Cosmological Role, *Ann. Rev. Nucl. Part. Sci.* 63 (2013) 69–95. [arXiv:1301.1123](#), [doi:10.1146/annurev-nucl-102212-170536](#).
- [29] D. J. E. Marsh, Axion Cosmology, *Phys. Rept.* 643 (2016) 1–79. [arXiv:1510.07633](#), [doi:10.1016/j.physrep.2016.06.005](#).
- [30] H.-Y. Cheng, Tabulation of Astrophysical Constraints on Axions and Nambu-goldstone Bosons, *Phys. Rev. D* 36 (1987) 1649. [doi:10.1103/PhysRevD.36.1649](#).
- [31] M. S. Turner, Windows on the Axion, *Phys. Rept.* 197 (1990) 67–97. [doi:10.1016/0370-1573\(90\)90172-X](#).
- [32] G. G. Raffelt, Astrophysical methods to constrain axions and other novel particle phenomena, *Phys. Rept.* 198 (1990) 1–113. [doi:10.1016/0370-1573\(90\)90054-6](#).
- [33] G. G. Raffelt, Astrophysical axion bounds, *Lect. Notes Phys.* 741 (2008) 51–71, [51(2006)]. [arXiv:hep-ph/0611350](#), [doi:10.1007/978-3-540-73518-2_3](#).

- [34] S. J. Asztalos, L. J. Rosenberg, K. van Bibber, P. Sikivie, K. Zioutas, Searches for astrophysical and cosmological axions, *Ann. Rev. Nucl. Part. Sci.* 56 (2006) 293–326. [doi:10.1146/annurev.nucl.56.080805.140513](#).
- [35] M. Giannotti, I. G. Irastorza, J. Redondo, A. Ringwald, K. Saikawa, Stellar Recipes for Axion Hunters, *JCAP* 1710 (10) (2017) 010. [arXiv:1708.02111](#), [doi:10.1088/1475-7516/2017/10/010](#).
- [36] L. J. Rosenberg, K. A. van Bibber, Searches for invisible axions, *Phys. Rept.* 325 (2000) 1–39. [doi:10.1016/S0370-1573\(99\)00045-9](#).
- [37] R. Battesti, B. Beltran, H. Davoudiasl, M. Kuster, P. Pagnat, R. Rabadan, A. Ringwald, N. Spooner, K. Zioutas, Axion searches in the past, at present, and in the near future, *Lect. Notes Phys.* 741 (2008) 199–237, [199(2007)]. [arXiv:0705.0615](#), [doi:10.1007/978-3-540-73518-2_10](#).
- [38] P. W. Graham, I. G. Irastorza, S. K. Lamoreaux, A. Lindner, K. A. van Bibber, Experimental Searches for the Axion and Axion-Like Particles, *Ann. Rev. Nucl. Part. Sci.* 65 (2015) 485–514. [arXiv:1602.00039](#), [doi:10.1146/annurev-nucl-102014-022120](#).
- [39] I. G. Irastorza, J. Redondo, New experimental approaches in the search for axion-like particles, *Prog. Part. Nucl. Phys.* 102 (2018) 89–159. [arXiv:1801.08127](#), [doi:10.1016/j.pnpnp.2018.05.003](#).
- [40] P. Sikivie, Invisible Axion Search Methods (2020). [arXiv:2003.02206](#).
- [41] S. Weinberg, The U(1) Problem, *Phys. Rev. D* 11 (1975) 3583–3593. [doi:10.1103/PhysRevD.11.3583](#).
- [42] D. V. Nanopoulos, Towards a renormalizable unified gauge theory of strong, electromagnetic and weak interactions, *Lett. Nuovo Cim.* 8S2 (1973) 873–877, [*Lett. Nuovo Cim.* 8, 873 (1973)]. [doi:10.1007/BF02727401](#).
- [43] S. Weinberg, Nonabelian Gauge Theories of the Strong Interactions, *Phys. Rev. Lett.* 31 (1973) 494–497. [doi:10.1103/PhysRevLett.31.494](#).
- [44] A. A. Belavin, A. M. Polyakov, A. S. Schwartz, Yu. S. Tyupkin, Pseudoparticle Solutions of the Yang-Mills Equations, *Phys. Lett. B* 59 (1975) 85–87, [350(1975)]. [doi:10.1016/0370-2693\(75\)90163-X](#).
- [45] C. G. Callan, Jr., R. F. Dashen, D. J. Gross, The Structure of the Gauge Theory Vacuum, *Phys. Lett. B* 63 (1976) 334–340, [357(1976)]. [doi:10.1016/0370-2693\(76\)90277-X](#).
- [46] R. Jackiw, C. Rebbi, Vacuum Periodicity in a Yang-Mills Quantum Theory, *Phys. Rev. Lett.* 37 (1976) 172–175, [353(1976)]. [doi:10.1103/PhysRevLett.37.172](#).
- [47] G. Grilli di Cortona, E. Hardy, J. Pardo Vega, G. Villadoro, The QCD axion, precisely, *JHEP* 01 (2016) 034. [arXiv:1511.02867](#), [doi:10.1007/JHEP01\(2016\)034](#).
- [48] R. Bott, On the iteration of closed geodesics and the sturm intersection theory, *Communications on Pure and Applied Mathematics* 9 (2) (1956) 171–206. [doi:10.1002/cpa.3160090204](#).
- [49] G. 't Hooft, Symmetry Breaking Through Bell-Jackiw Anomalies, *Phys. Rev. Lett.* 37 (1976) 8–11, [226(1976)]. [doi:10.1103/PhysRevLett.37.8](#).
- [50] G. 't Hooft, Computation of the Quantum Effects Due to a Four-Dimensional Pseudoparticle, *Phys. Rev. D* 14 (1976) 3432–3450, [70(1976)]. [doi:10.1103/PhysRevD.14.3432](#), [doi:10.1103/PhysRevD.18.2199.3](#), [doi:10.1103/PhysRevD.14.3432](#).
- [51] E. Witten, Some Exact Multi - Instanton Solutions of Classical Yang-Mills Theory, *Phys. Rev. Lett.* 38 (1977) 121–124, [124(1976)]. [doi:10.1103/PhysRevLett.38.121](#).
- [52] R. Jackiw, C. Nohl, C. Rebbi, Conformal Properties of Pseudoparticle Configurations, *Phys. Rev. D* 15 (1977) 1642, [128(1976)]. [doi:10.1103/PhysRevD.15.1642](#).
- [53] R. Jackiw, Introduction to the Yang-Mills Quantum Theory, *Rev. Mod. Phys.* 52 (1980) 661–673. [doi:10.1103/RevModPhys.52.661](#).
- [54] S. Weinberg, The quantum theory of fields. Vol. 2: Modern applications, Cambridge University Press, 2013.
- [55] G. 't Hooft, How Instantons Solve the U(1) Problem, *Phys. Rept.* 142 (1986) 357–387. [doi:10.1016/0370-1573\(86\)90117-1](#).
- [56] D. J. Gross, R. D. Pisarski, L. G. Yaffe, QCD and Instantons at Finite Temperature, *Rev. Mod. Phys.* 53 (1981) 43. [doi:10.1103/RevModPhys.53.43](#).
- [57] K. Fujikawa, Path Integral Measure for Gauge Invariant Fermion Theories, *Phys. Rev. Lett.* 42 (1979) 1195–1198. [doi:10.1103/PhysRevLett.42.1195](#).
- [58] C. Vafa, E. Witten, Restrictions on Symmetry Breaking in Vector-Like Gauge Theories, *Nucl. Phys. B* 234 (1984) 173–188. [doi:10.1016/0550-3213\(84\)90230-X](#).
- [59] J. M. Pendlebury, et al., Revised experimental upper limit on the electric dipole moment of the neutron, *Phys. Rev. D* 92 (9) (2015) 092003. [arXiv:1509.04411](#), [doi:10.1103/PhysRevD.92.092003](#).
- [60] C. Abel, et al., Measurement of the permanent electric dipole moment of the neutron, *Phys. Rev. Lett.* 124 (2020) 081803. [arXiv:2001.11966](#), [doi:10.1103/PhysRevLett.124.081803](#).
- [61] B. W. Filippone, Worldwide Search for the Neutron EDM, in: 13th Conference on the Intersections of Particle and Nuclear Physics (CIPANP 2018) Palm Springs, California, USA, May 29-June 3, 2018, 2018. [arXiv:1810.03718](#).
- [62] V. Baluni, CP Violating Effects in QCD, *Phys. Rev. D* 19 (1979) 2227–2230. [doi:10.1103/PhysRevD.19.2227](#).
- [63] R. J. Crewther, P. Di Vecchia, G. Veneziano, E. Witten, Chiral Estimate of the Electric Dipole Moment of the Neutron in Quantum Chromodynamics, *Phys. Lett.* 88B (1979) 123, [Erratum: *Phys. Lett.* 91B, 487 (1980)]. [doi:10.1016/0370-2693\(80\)91025-4](#), [doi:10.1016/0370-2693\(79\)90128-X](#).
- [64] A. Pich, E. de Rafael, Strong CP violation in an effective chiral Lagrangian approach, *Nucl. Phys. B* 367 (1991) 313–333. [doi:10.1016/0550-3213\(91\)90019-T](#).
- [65] M. Pospelov, A. Ritz, Theta vacua, QCD sum rules, and the neutron electric dipole moment, *Nucl. Phys. B* 573 (2000) 177–200. [arXiv:hep-ph/9908508](#), [doi:10.1016/S0550-3213\(99\)00817-2](#).
- [66] L. Bartolini, F. Bigazzi, S. Bolognesi, A. L. Cotrone, A. Manenti, Neutron electric dipole moment from gauge/string duality, *Phys. Rev. Lett.* 118 (9) (2017) 091601. [arXiv:1609.09513](#), [doi:10.1103/PhysRevLett.118.091601](#).

- [67] M. Abramczyk, S. Aoki, T. Blum, T. Izubuchi, H. Ohki, S. Syritsyn, Lattice calculation of electric dipole moments and form factors of the nucleon, *Phys. Rev. D* 96 (1) (2017) 014501. [arXiv:1701.07792](#), [doi:10.1103/PhysRevD.96.014501](#).
- [68] J. Dragos, T. Luu, A. Shindler, J. de Vries, A. Yousif, Confirming the Existence of the strong CP Problem in Lattice QCD with the Gradient Flow (2019). [arXiv:1902.03254](#).
- [69] M. Pospelov, A. Ritz, Electric dipole moments as probes of new physics, *Annals Phys.* 318 (2005) 119–169. [arXiv:hep-ph/0504231](#), [doi:10.1016/j.aop.2005.04.002](#).
- [70] M. Pospelov, A. Ritz, Probing CP violation with electric dipole moments, *Adv. Ser. Direct. High Energy Phys.* 20 (2009) 439–518. [doi:10.1142/9789814271844_0013](#).
- [71] V. V. Flambaum, M. Pospelov, A. Ritz, Y. V. Stadnik, Sensitivity of EDM experiments in paramagnetic atoms and molecules to hadronic CP violation. (2019). [arXiv:1912.13129](#).
- [72] J. R. Ellis, M. K. Gaillard, Strong and Weak CP Violation, *Nucl. Phys. B* 150 (1979) 141–162. [doi:10.1016/0550-3213\(79\)90297-9](#).
- [73] I. B. Khriplovich, A. I. Vainshtein, Infinite renormalization of Theta term and Jarlskog invariant for CP violation, *Nucl. Phys. B* 414 (1994) 27–32. [arXiv:hep-ph/9308334](#), [doi:10.1016/0550-3213\(94\)90419-7](#).
- [74] C. Jarlskog, Commutator of the Quark Mass Matrices in the Standard Electroweak Model and a Measure of Maximal CP Violation, *Phys. Rev. Lett.* 55 (1985) 1039. [doi:10.1103/PhysRevLett.55.1039](#).
- [75] J. E. Kim, D. Y. Mo, S. Nam, Final state interaction phases obtained by data from CP asymmetries, *J. Korean Phys. Soc.* 66 (6) (2015) 894–899. [arXiv:1402.2978](#), [doi:10.3938/jkps.66.894](#).
- [76] I. B. Khriplovich, Quark Electric Dipole Moment and Induced θ Term in the Kobayashi-Maskawa Model, *Phys. Lett. B* 173 (1986) 193–196, [*Sov. J. Nucl. Phys.* 44,659(1986); *Yad. Fiz.* 44,1019(1986)]. [doi:10.1016/0370-2693\(86\)90245-5](#).
- [77] J. de Vries, P. Draper, K. Fuyuto, J. Kozaczuk, D. Sutherland, Indirect Signs of the Peccei-Quinn Mechanism, *Phys. Rev. D* 99 (1) (2019) 015042. [arXiv:1809.10143](#), [doi:10.1103/PhysRevD.99.015042](#).
- [78] N. Weiss, The cosmological constant and the strong CP problem, *Phys. Rev. D* 37 (1988) 3760. [doi:10.1103/PhysRevD.37.3760](#).
- [79] F. Takahashi, A possible solution to the strong CP problem, *Prog. Theor. Phys.* 121 (2009) 711–725. [arXiv:0804.2478](#), [doi:10.1143/PTP.121.711](#).
- [80] N. Kaloper, J. Terning, Landscaping the Strong CP Problem, *JHEP* 03 (2019) 032. [arXiv:1710.01740](#), [doi:10.1007/JHEP03\(2019\)032](#).
- [81] G. Dvali, A Vacuum accumulation solution to the strong CP problem, *Phys. Rev. D* 74 (2006) 025019. [arXiv:hep-th/0510053](#), [doi:10.1103/PhysRevD.74.025019](#).
- [82] D. B. Kaplan, A. V. Manohar, Current Mass Ratios of the Light Quarks, *Phys. Rev. Lett.* 56 (1986) 2004. [doi:10.1103/PhysRevLett.56.2004](#).
- [83] H. Georgi, I. N. McArthur, Instantons And The Mu Quark Mass (1981).
- [84] K. Choi, C. W. Kim, W. K. Sze, Mass Renormalization by Instantons and the Strong CP Problem, *Phys. Rev. Lett.* 61 (1988) 794. [doi:10.1103/PhysRevLett.61.794](#).
- [85] T. Banks, Y. Nir, N. Seiberg, Missing (up) mass, accidental anomalous symmetries, and the strong CP problem, in: Yukawa couplings and the origins of mass. Proceedings, 2nd IFT Workshop, Gainesville, USA, February 11-13, 1994, 1994, pp. 26–41. [arXiv:hep-ph/9403203](#).
- [86] M. Tanabashi, et al., Review of Particle Physics, *Phys. Rev. D* 98 (3) (2018) 030001. [doi:10.1103/PhysRevD.98.030001](#).
- [87] A. G. Cohen, D. B. Kaplan, A. E. Nelson, Testing $m(u)=0$ on the lattice, *JHEP* 11 (1999) 027. [arXiv:hep-lat/9909091](#), [doi:10.1088/1126-6708/1999/11/027](#).
- [88] M. Dine, P. Draper, G. Festuccia, Instanton Effects in Three Flavor QCD, *Phys. Rev. D* 92 (5) (2015) 054004. [arXiv:1410.8505](#), [doi:10.1103/PhysRevD.92.054004](#).
- [89] C. Alexandrou, J. Finkenrath, L. Funcke, K. Jansen, B. Kostrzewa, F. Pittler, C. Urbach, Ruling out the massless up-quark solution to the strong CP problem by computing the topological mass contribution with lattice QCD (2020). [arXiv:2002.07802](#).
- [90] M. A. B. Beg, H. S. Tsao, Strong P , T Noninvariances in a Superweak Theory, *Phys. Rev. Lett.* 41 (1978) 278. [doi:10.1103/PhysRevLett.41.278](#).
- [91] H. Georgi, A Model of Soft CP Violation, *Hadronic J.* 1 (1978) 155.
- [92] R. N. Mohapatra, G. Senjanovic, Natural Suppression of Strong p and t Noninvariance, *Phys. Lett.* 79B (1978) 283–286. [doi:10.1016/0370-2693\(78\)90243-5](#).
- [93] A. E. Nelson, Naturally Weak CP Violation, *Phys. Lett. B* 136 (1984) 387–391. [doi:10.1016/0370-2693\(84\)92025-2](#).
- [94] S. M. Barr, Solving the Strong CP Problem Without the Peccei-Quinn Symmetry, *Phys. Rev. Lett.* 53 (1984) 329. [doi:10.1103/PhysRevLett.53.329](#).
- [95] M. Dine, P. Draper, Challenges for the Nelson-Barr Mechanism, *JHEP* 08 (2015) 132. [arXiv:1506.05433](#), [doi:10.1007/JHEP08\(2015\)132](#).
- [96] L. Vecchi, Spontaneous CP violation and the strong CP problem, *JHEP* 04 (2017) 149. [arXiv:1412.3805](#), [doi:10.1007/JHEP04\(2017\)149](#).
- [97] S. Yu. Khlebnikov, M. E. Shaposhnikov, Extra Space-time Dimensions: Towards a Solution to the Strong CP Problem, *Phys. Lett. B* 203 (1988) 121–124. [doi:10.1016/0370-2693\(88\)91582-1](#).
- [98] M. Chaichian, A. Kobakhidze, Extra dimensions and the strong CP problem, *Phys. Rev. Lett.* 87 (2001) 171601. [arXiv:hep-ph/0104158](#), [doi:10.1103/PhysRevLett.87.171601](#).
- [99] S. Khlebnikov, M. Shaposhnikov, Brane-worlds and theta-vacua, *Phys. Rev. D* 71 (2005) 104024. [arXiv:hep-th/0412306](#), [doi:10.1103/PhysRevD.71.104024](#).
- [100] F. L. Bezrukov, Y. Burnier, Towards a solution of the strong CP problem by compact extra dimensions, *Phys. Rev. D* 80

- (2009) 125004. [arXiv:0811.1163](#), [doi:10.1103/PhysRevD.80.125004](#).
- [101] S. Samuel, Does the Yang-Mills theory solve the strong CP problem by itself?, *Mod. Phys. Lett. A7* (1992) 2007–2016. [doi:10.1142/S0217732392001737](#).
 - [102] N. J. Dowrick, N. A. McDougall, On the Samuel solution to the strong CP problem within QCD, *Nucl. Phys. B399* (1993) 426–440. [doi:10.1016/0550-3213\(93\)90503-H](#).
 - [103] G. Gabadadze, M. Shifman, QCD vacuum and axions: What’s happening?, *Int. J. Mod. Phys. A17* (2002) 3689–3728, [521(2002)]. [arXiv:hep-ph/0206123](#), [doi:10.1142/S0217751X02011357](#).
 - [104] H. Georgi, D. B. Kaplan, L. Randall, Manifesting the Invisible Axion at Low-energies, *Phys. Lett. 169B* (1986) 73–78. [doi:10.1016/0370-2693\(86\)90688-X](#).
 - [105] J. Kodaira, QCD Higher Order Effects in Polarized Electroproduction: Flavor Singlet Coefficient Functions, *Nucl. Phys. B165* (1980) 129–140. [doi:10.1016/0550-3213\(80\)90310-7](#).
 - [106] S. A. Larin, The Renormalization of the axial anomaly in dimensional regularization, *Phys. Lett. B303* (1993) 113–118. [arXiv:hep-ph/9302240](#), [doi:10.1016/0370-2693\(93\)90053-K](#).
 - [107] E. Witten, Large N Chiral Dynamics, *Annals Phys. 128* (1980) 363. [doi:10.1016/0003-4916\(80\)90325-5](#).
 - [108] P. Di Vecchia, G. Veneziano, Chiral Dynamics in the Large n Limit, *Nucl. Phys. B171* (1980) 253–272. [doi:10.1016/0550-3213\(80\)90370-3](#).
 - [109] L. Di Luzio, M. Redi, A. Strumia, D. Teresi, Coset Cosmology, *JHEP 06* (2019) 110. [arXiv:1902.05933](#), [doi:10.1007/JHEP06\(2019\)110](#).
 - [110] S. Chang, K. Choi, Hadronic axion window and the big bang nucleosynthesis, *Phys. Lett. B316* (1993) 51–56. [arXiv:hep-ph/9306216](#), [doi:10.1016/0370-2693\(93\)90656-3](#).
 - [111] M. Srednicki, Axion Couplings to Matter. 1. CP Conserving Parts, *Nucl. Phys. B260* (1985) 689–700. [doi:10.1016/0550-3213\(85\)90054-9](#).
 - [112] D. B. Kaplan, Opening the Axion Window, *Nucl. Phys. B260* (1985) 215–226. [doi:10.1016/0550-3213\(85\)90319-0](#).
 - [113] T. W. Donnelly, S. J. Freedman, R. S. Lytel, R. D. Peccei, M. Schwartz, Do Axions Exist?, *Phys. Rev. D18* (1978) 1607. [doi:10.1103/PhysRevD.18.1607](#).
 - [114] L. J. Hall, M. B. Wise, Flavor changing Higgs - boson couplings, *Nucl. Phys. B187* (1981) 397–408. [doi:10.1016/0550-3213\(81\)90469-7](#).
 - [115] F. Wilczek, Decays of Heavy Vector Mesons Into Higgs Particles, *Phys. Rev. Lett. 39* (1977) 1304. [doi:10.1103/PhysRevLett.39.1304](#).
 - [116] M. Davier, Searches for New Particles, in: *Proceedings, 23RD International Conference on High Energy Physics, JULY 16-23, 1986, Berkeley, CA, 1986*.
 - [117] W. A. Bardeen, R. D. Peccei, T. Yanagida, Constraints on variant axion models, *Nucl. Phys. B279* (1987) 401–428. [doi:10.1016/0550-3213\(87\)90003-4](#).
 - [118] A. R. Zhitnitsky, On Possible Suppression of the Axion Hadron Interactions. (In Russian), *Sov. J. Nucl. Phys. 31* (1980) 260, [*Yad. Fiz.*31,497(1980)].
 - [119] M. Dine, W. Fischler, M. Srednicki, A Simple Solution to the Strong CP Problem with a Harmless Axion, *Phys. Lett. B104* (1981) 199–202. [doi:10.1016/0370-2693\(81\)90590-6](#).
 - [120] J. E. Kim, Weak Interaction Singlet and Strong CP Invariance, *Phys. Rev. Lett. 43* (1979) 103. [doi:10.1103/PhysRevLett.43.103](#).
 - [121] M. A. Shifman, A. I. Vainshtein, V. I. Zakharov, Can Confinement Ensure Natural CP Invariance of Strong Interactions?, *Nucl. Phys. B166* (1980) 493. [doi:10.1016/0550-3213\(80\)90209-6](#).
 - [122] L. Di Luzio, J. F. Kamenik, M. Nardecchia, Implications of perturbative unitarity for scalar di-boson resonance searches at LHC, *Eur. Phys. J. C77* (1) (2017) 30. [arXiv:1604.05746](#), [doi:10.1140/epjc/s10052-017-4594-2](#).
 - [123] L. Di Luzio, M. Nardecchia, What is the scale of new physics behind the B -flavour anomalies?, *Eur. Phys. J. C77* (8) (2017) 536. [arXiv:1706.01868](#), [doi:10.1140/epjc/s10052-017-5118-9](#).
 - [124] F. Björkeröth, L. Di Luzio, F. Mescia, E. Nardi, P. Panci, R. Ziegler, Axion-electron decoupling in nucleophobic axion models, *Phys. Rev. D 101* (3) (2020) 035027. [arXiv:1907.06575](#), [doi:10.1103/PhysRevD.101.035027](#).
 - [125] M. Gorghetto, G. Villadoro, Topological Susceptibility and QCD Axion Mass: QED and NNLO corrections, *JHEP 03* (2019) 033. [arXiv:1812.01008](#), [doi:10.1007/JHEP03\(2019\)033](#).
 - [126] S. Borsanyi, et al., Calculation of the axion mass based on high-temperature lattice quantum chromodynamics, *Nature 539* (7627) (2016) 69–71. [arXiv:1606.07494](#), [doi:10.1038/nature20115](#).
 - [127] T. Vonk, F.-K. Guo, U.-G. Meißner, Precision calculation of the axion-nucleon coupling in chiral perturbation theory, *JHEP 03* (2020) 138. [arXiv:2001.05327](#), [doi:10.1007/JHEP03\(2020\)138](#).
 - [128] J. E. Moody, F. Wilczek, New macroscopic forces?, *Phys. Rev. D30* (1984) 130. [doi:10.1103/PhysRevD.30.130](#).
 - [129] S. Durr, et al., Lattice computation of the nucleon scalar quark contents at the physical point, *Phys. Rev. Lett. 116* (17) (2016) 172001. [arXiv:1510.08013](#), [doi:10.1103/PhysRevLett.116.172001](#).
 - [130] F. Bigazzi, A. L. Cotrone, M. Järvinen, E. Kiritsis, Non-derivative Axionic Couplings to Nucleons at large and small N, *JHEP 01* (2020) 100. [arXiv:1906.12132](#), [doi:10.1007/JHEP01\(2020\)100](#).
 - [131] H. Georgi, L. Randall, Flavor Conserving CP Violation in Invisible Axion Models, *Nucl. Phys. B276* (1986) 241–252. [doi:10.1016/0550-3213\(86\)90022-2](#).
 - [132] M. Pospelov, CP odd interaction of axion with matter, *Phys. Rev. D58* (1998) 097703. [arXiv:hep-ph/9707431](#), [doi:10.1103/PhysRevD.58.097703](#).
 - [133] H. M. Georgi, L. J. Hall, M. B. Wise, Grand Unified Models With an Automatic Peccei-Quinn Symmetry, *Nucl. Phys. B192* (1981) 409–416. [doi:10.1016/0550-3213\(81\)90433-8](#).
 - [134] M. Dine, N. Seiberg, String Theory and the Strong CP Problem, *Nucl. Phys. B273* (1986) 109–124. [doi:10.1016/](#)

- 0550-3213(86)90043-X.
- [135] S. M. Barr, D. Seckel, Planck scale corrections to axion models, *Phys. Rev. D* 46 (1992) 539–549. [doi:10.1103/PhysRevD.46.539](#).
 - [136] M. Kamionkowski, J. March-Russell, Planck scale physics and the Peccei-Quinn mechanism, *Phys. Lett. B* 282 (1992) 137–141. [arXiv:hep-th/9202003](#), [doi:10.1016/0370-2693\(92\)90492-M](#).
 - [137] R. Holman, S. D. H. Hsu, T. W. Kephart, E. W. Kolb, R. Watkins, L. M. Widrow, Solutions to the strong CP problem in a world with gravity, *Phys. Lett. B* 282 (1992) 132–136. [arXiv:hep-ph/9203206](#), [doi:10.1016/0370-2693\(92\)90491-L](#).
 - [138] S. Ghigna, M. Lusignoli, M. Roncadelli, Instability of the invisible axion, *Phys. Lett. B* 283 (1992) 278–281. [doi:10.1016/0370-2693\(92\)90019-Z](#).
 - [139] S. W. Hawking, Particle Creation by Black Holes, *Commun. Math. Phys.* 43 (1975) 199–220, [167(1975)]. [doi:10.1007/BF02345020](#), [doi:10.1007/BF01608497](#).
 - [140] L. F. Abbott, M. B. Wise, Wormholes and Global Symmetries, *Nucl. Phys. B* 325 (1989) 687–704. [doi:10.1016/0550-3213\(89\)90503-8](#).
 - [141] S. R. Coleman, K.-M. Lee, Wormholes made without massless matter fields, *Nucl. Phys. B* 329 (1990) 387–409. [doi:10.1016/0550-3213\(90\)90149-8](#).
 - [142] R. Kallosh, A. D. Linde, D. A. Linde, L. Susskind, Gravity and global symmetries, *Phys. Rev. D* 52 (1995) 912–935. [arXiv:hep-th/9502069](#), [doi:10.1103/PhysRevD.52.912](#).
 - [143] R. Alonso, A. Urbano, Wormholes and masses for Goldstone bosons, *JHEP* 02 (2019) 136. [arXiv:1706.07415](#), [doi:10.1007/JHEP02\(2019\)136](#).
 - [144] A. G. Dias, V. Pleitez, M. D. Tonasse, Naturally light invisible axion in models with large local discrete symmetries, *Phys. Rev. D* 67 (2003) 095008. [arXiv:hep-ph/0211107](#), [doi:10.1103/PhysRevD.67.095008](#).
 - [145] L. M. Carpenter, M. Dine, G. Festuccia, Dynamics of the Peccei Quinn Scale, *Phys. Rev. D* 80 (2009) 125017. [arXiv:0906.1273](#), [doi:10.1103/PhysRevD.80.125017](#).
 - [146] K. Harigaya, M. Ibe, K. Schmitz, T. T. Yanagida, Peccei-Quinn symmetry from a gauged discrete R symmetry, *Phys. Rev. D* 88 (7) (2013) 075022. [arXiv:1308.1227](#), [doi:10.1103/PhysRevD.88.075022](#).
 - [147] A. G. Dias, A. C. B. Machado, C. C. Nishi, A. Ringwald, P. Vaudrevange, The Quest for an Intermediate-Scale Accidental Axion and Further ALPs, *JHEP* 06 (2014) 037. [arXiv:1403.5760](#), [doi:10.1007/JHEP06\(2014\)037](#).
 - [148] K. Harigaya, M. Ibe, K. Schmitz, T. T. Yanagida, Peccei-Quinn Symmetry from Dynamical Supersymmetry Breaking, *Phys. Rev. D* 92 (7) (2015) 075003. [arXiv:1505.07388](#), [doi:10.1103/PhysRevD.92.075003](#).
 - [149] H. Fukuda, M. Ibe, M. Suzuki, T. T. Yanagida, A “gauged” $U(1)$ Peccei-Quinn symmetry, *Phys. Lett. B* 771 (2017) 327–331. [arXiv:1703.01112](#), [doi:10.1016/j.physletb.2017.05.071](#).
 - [150] M. Duerr, K. Schmidt-Hoberg, J. Unwin, Protecting the Axion with Local Baryon Number, *Phys. Lett. B* 780 (2018) 553–556. [arXiv:1712.01841](#), [doi:10.1016/j.physletb.2018.03.054](#).
 - [151] Q. Bonnefoy, E. Dudas, S. Pokorski, Axions in a highly protected gauge symmetry model, *Eur. Phys. J. C* 79 (1) (2019) 31. [arXiv:1804.01112](#), [doi:10.1140/epjc/s10052-018-6528-z](#).
 - [152] L. Di Luzio, E. Nardi, L. Ubaldi, Accidental Peccei-Quinn symmetry protected to arbitrary order, *Phys. Rev. Lett.* 119 (1) (2017) 011801. [arXiv:1704.01122](#), [doi:10.1103/PhysRevLett.119.011801](#).
 - [153] H.-S. Lee, W. Yin, Peccei-Quinn symmetry from a hidden gauge group structure, *Phys. Rev. D* 99 (1) (2019) 015041. [arXiv:1811.04039](#), [doi:10.1103/PhysRevD.99.015041](#).
 - [154] L. Randall, Composite axion models and Planck scale physics, *Phys. Lett. B* 284 (1992) 77–80. [doi:10.1016/0370-2693\(92\)91928-3](#).
 - [155] B. A. Dobrescu, The Strong CP problem versus Planck scale physics, *Phys. Rev. D* 55 (1997) 5826–5833. [arXiv:hep-ph/9609221](#), [doi:10.1103/PhysRevD.55.5826](#).
 - [156] M. Redi, R. Sato, Composite Accidental Axions, *JHEP* 05 (2016) 104. [arXiv:1602.05427](#), [doi:10.1007/JHEP05\(2016\)104](#).
 - [157] B. Lillard, T. M. P. Tait, A High Quality Composite Axion, *JHEP* 11 (2018) 199. [arXiv:1811.03089](#), [doi:10.1007/JHEP11\(2018\)199](#).
 - [158] M. B. Gavela, M. Ibe, P. Quilez, T. T. Yanagida, Automatic Peccei-Quinn symmetry, *Eur. Phys. J. C* 79 (6) (2019) 542. [arXiv:1812.08174](#), [doi:10.1140/epjc/s10052-019-7046-3](#).
 - [159] K.-w. Choi, A QCD axion from higher dimensional gauge field, *Phys. Rev. Lett.* 92 (2004) 101602. [arXiv:hep-ph/0308024](#), [doi:10.1103/PhysRevLett.92.101602](#).
 - [160] P. Cox, T. Gherghetta, M. D. Nguyen, A Holographic Perspective on the Axion Quality Problem, *JHEP* 01 (2020) 188. [arXiv:1911.09385](#), [doi:10.1007/JHEP01\(2020\)188](#).
 - [161] C. Cheung, Axion Protection from Flavor, *JHEP* 06 (2010) 074. [arXiv:1003.0941](#), [doi:10.1007/JHEP06\(2010\)074](#).
 - [162] C. G. Callan, Jr., R. F. Dashen, D. J. Gross, Toward a Theory of the Strong Interactions, *Phys. Rev. D* 17 (1978) 2717, [36(1977)]. [doi:10.1103/PhysRevD.17.2717](#).
 - [163] M. Dine, P. Draper, L. Stephenson-Haskins, D. Xu, Axions, Instantons, and the Lattice, *Phys. Rev. D* 96 (9) (2017) 095001. [arXiv:1705.00676](#), [doi:10.1103/PhysRevD.96.095001](#).
 - [164] C. Bonati, M. D’Elia, M. Mariti, G. Martinelli, M. Mesiti, F. Negro, F. Sanfilippo, G. Villadoro, Axion phenomenology and θ -dependence from $N_f = 2+1$ lattice QCD, *JHEP* 03 (2016) 155. [arXiv:1512.06746](#), [doi:10.1007/JHEP03\(2016\)155](#).
 - [165] O. Wantz, E. P. S. Shellard, The Topological susceptibility from grand canonical simulations in the interacting instanton liquid model: Chiral phase transition and axion mass, *Nucl. Phys. B* 829 (2010) 110–160. [arXiv:0908.0324](#), [doi:10.1016/j.nuclphysb.2009.12.005](#).
 - [166] O. Wantz, E. P. S. Shellard, Axion Cosmology Revisited, *Phys. Rev. D* 82 (2010) 123508. [arXiv:0910.1066](#), [doi:10.1103/PhysRevD.82.123508](#).
 - [167] P. Petreczky, H.-P. Schadler, S. Sharma, The topological susceptibility in finite temperature QCD and axion cosmology,

- Phys. Lett. B762 (2016) 498–505. [arXiv:1606.03145](#), [doi:10.1016/j.physletb.2016.09.063](#).
- [168] C. Bonati, M. D’Elia, G. Martinelli, F. Negro, F. Sanfilippo, A. Todaro, Topology in full QCD at high temperature: a multicanonical approach, JHEP 11 (2018) 170. [arXiv:1807.07954](#), [doi:10.1007/JHEP11\(2018\)170](#).
 - [169] F. Burger, E.-M. Ilgenfritz, M. P. Lombardo, A. Trunin, Chiral observables and topology in hot QCD with two families of quarks, Phys. Rev. D98 (9) (2018) 094501. [arXiv:1805.06001](#), [doi:10.1103/PhysRevD.98.094501](#).
 - [170] A. Bazavov, et al., The chiral and deconfinement aspects of the QCD transition, Phys. Rev. D85 (2012) 054503. [arXiv:1111.1710](#), [doi:10.1103/PhysRevD.85.054503](#).
 - [171] L. F. Abbott, P. Sikivie, A Cosmological Bound on the Invisible Axion, Phys. Lett. B120 (1983) 133–136. [doi:10.1016/0370-2693\(83\)90638-X](#).
 - [172] M. Dine, W. Fischler, The Not So Harmless Axion, Phys. Lett. B120 (1983) 137–141. [doi:10.1016/0370-2693\(83\)90639-1](#).
 - [173] J. Preskill, M. B. Wise, F. Wilczek, Cosmology of the Invisible Axion, Phys. Lett. B120 (1983) 127–132. [doi:10.1016/0370-2693\(83\)90637-8](#).
 - [174] A. D. Linde, Generation of Isothermal Density Perturbations in the Inflationary Universe, Phys. Lett. 158B (1985) 375–380. [doi:10.1016/0370-2693\(85\)90436-8](#).
 - [175] D. Seckel, M. S. Turner, "Isothermal" Density Perturbations in an Axion Dominated Inflationary Universe, Phys. Rev. D 32 (1985) 3178. [doi:10.1103/PhysRevD.32.3178](#).
 - [176] D. H. Lyth, A limit on the inflationary energy density from axion isocurvature fluctuations, Physics Letters B 236 (4) (1990) 408 – 410. [doi:http://dx.doi.org/10.1016/0370-2693\(90\)90374-F](#).
 - [177] A. D. Linde, D. H. Lyth, Axionic domain wall production during inflation, Phys. Lett. B246 (1990) 353–358. [doi:10.1016/0370-2693\(90\)90613-B](#).
 - [178] M. S. Turner, F. Wilczek, Inflationary axion cosmology, Phys. Rev. Lett. 66 (1991) 5–8. [doi:10.1103/PhysRevLett.66.5.3394](#).
 - [179] D. H. Lyth, Axions and inflation: Vacuum fluctuations, Phys. Rev. D 45 (1992) 3394–3404. [doi:10.1103/PhysRevD.45.3394](#).
 - [180] D. H. Lyth, E. D. Stewart, Constraining the inflationary energy scale from axion cosmology, Physics Letters B 283 (3) (1992) 189 – 193. [doi:http://dx.doi.org/10.1016/0370-2693\(92\)90006-P](#).
 - [181] P. Crotty, J. Garcia-Bellido, J. Lesgourgues, A. Riazuelo, Bounds on isocurvature perturbations from CMB and LSS data, Phys. Rev. Lett. 91 (2003) 171301. [arXiv:astro-ph/0306286](#), [doi:10.1103/PhysRevLett.91.171301](#).
 - [182] M. Beltran, J. Garcia-Bellido, J. Lesgourgues, A. R. Liddle, A. Slosar, Bayesian model selection and isocurvature perturbations, Phys. Rev. D71 (2005) 063532. [arXiv:astro-ph/0501477](#), [doi:10.1103/PhysRevD.71.063532](#).
 - [183] M. Beltran, J. Garcia-Bellido, J. Lesgourgues, Isocurvature bounds on axions revisited, Phys. Rev. D75 (2007) 103507. [arXiv:hep-ph/0606107](#), [doi:10.1103/PhysRevD.75.103507](#).
 - [184] M. S. Turner, Cosmic and Local Mass Density of Invisible Axions, Phys. Rev. D33 (1986) 889–896. [doi:10.1103/PhysRevD.33.889](#).
 - [185] D. H. Lyth, Axions and inflation: Sitting in the vacuum, Phys. Rev. D45 (1992) 3394–3404. [doi:10.1103/PhysRevD.45.3394](#).
 - [186] K. Strobl, T. J. Weiler, Anharmonic evolution of the cosmic axion density spectrum, Phys. Rev. D50 (1994) 7690–7702. [arXiv:astro-ph/9405028](#), [doi:10.1103/PhysRevD.50.7690](#).
 - [187] K. J. Bae, J.-H. Huh, J. E. Kim, Update of axion CDM energy, JCAP 0809 (2008) 005. [arXiv:0806.0497](#), [doi:10.1088/1475-7516/2008/09/005](#).
 - [188] L. Visinelli, P. Gondolo, Dark Matter Axions Revisited, Phys. Rev. D80 (2009) 035024. [arXiv:0903.4377](#), [doi:10.1103/PhysRevD.80.035024](#).
 - [189] T. A. DeGrand, T. W. Kephart, T. J. Weiler, Invisible Axions and the QCD Phase Transition in the Early Universe, Phys. Rev. D 33 (1986) 910. [doi:10.1103/PhysRevD.33.910](#).
 - [190] J. E. Kim, S.-J. Kim, "Invisible" QCD axion rolling through the QCD phase transition, Phys. Lett. B 783 (2018) 357–363. [arXiv:1804.05173](#), [doi:10.1016/j.physletb.2018.07.020](#).
 - [191] A. Vilenkin, E. P. S. Shellard, Cosmic Strings and Other Topological Defects, Cambridge University Press, 2000.
 - [192] T. W. B. Kibble, Topology of cosmic domains and strings, Journal of Physics A Mathematical General 9 (1976) 1387–1398. [doi:10.1088/0305-4470/9/8/029](#).
 - [193] T. W. B. Kibble, G. Lazarides, Q. Shafi, Walls Bounded by Strings, Phys. Rev. D26 (1982) 435. [doi:10.1103/PhysRevD.26.435](#).
 - [194] T. Kibble, Some Implications of a Cosmological Phase Transition, Phys. Rept. 67 (1980) 183. [doi:10.1016/0370-1573\(80\)90091-5](#).
 - [195] A. Vilenkin, Cosmic Strings, Phys. Rev. D24 (1981) 2082–2089. [doi:10.1103/PhysRevD.24.2082](#).
 - [196] R. L. Davis, Cosmic Axions from Cosmic Strings, Phys. Lett. B180 (1986) 225–230. [doi:10.1016/0370-2693\(86\)90300-X](#).
 - [197] A. Vilenkin, A. E. Everett, Cosmic Strings and Domain Walls in Models with Goldstone and PseudoGoldstone Bosons, Phys. Rev. Lett. 48 (1982) 1867–1870. [doi:10.1103/PhysRevLett.48.1867](#).
 - [198] A. Vilenkin, T. Vachaspati, Radiation of Goldstone Bosons From Cosmic Strings, Phys. Rev. D35 (1987) 1138. [doi:10.1103/PhysRevD.35.1138](#).
 - [199] D. Harari, P. Sikivie, On the Evolution of Global Strings in the Early Universe, Phys. Lett. B195 (1987) 361–365. [doi:10.1016/0370-2693\(87\)90032-3](#).
 - [200] R. L. Davis, E. P. S. Shellard, Do Axions Need Inflation?, Nucl. Phys. B324 (1989) 167–186. [doi:10.1016/0550-3213\(89\)90187-9](#).
 - [201] D. H. Lyth, Estimates of the cosmological axion density, Physics Letters B 275 (3) (1992) 279 – 283. [doi:https://doi.org/10.1016/0370-2693\(92\)91590-6](#).

- [202] R. A. Battye, E. P. S. Shellard, Global string radiation, Nucl. Phys. B423 (1994) 260–304. [arXiv:astro-ph/9311017](#), [doi:10.1016/0550-3213\(94\)90573-8](#).
- [203] R. A. Battye, E. P. S. Shellard, Axion string constraints, Phys. Rev. Lett. 73 (1994) 2954–2957, [Erratum: Phys. Rev. Lett.76,2203(1996)]. [arXiv:astro-ph/9403018](#), [doi:10.1103/PhysRevLett.73.2954](#), [doi:10.1103/PhysRevLett.76.2203](#).
- [204] M. Yamaguchi, M. Kawasaki, J. Yokoyama, Evolution of axionic strings and spectrum of axions radiated from them, Phys. Rev. Lett. 82 (1999) 4578–4581. [arXiv:hep-ph/9811311](#), [doi:10.1103/PhysRevLett.82.4578](#).
- [205] M. Yamaguchi, J. Yokoyama, M. Kawasaki, Evolution of a global string network in a matter dominated universe, Phys. Rev. D61 (2000) 061301. [arXiv:hep-ph/9910352](#), [doi:10.1103/PhysRevD.61.061301](#).
- [206] T. Hiramatsu, M. Kawasaki, T. Sekiguchi, M. Yamaguchi, J. Yokoyama, Improved estimation of radiated axions from cosmological axionic strings, Phys. Rev. D83 (2011) 123531. [arXiv:1012.5502](#), [doi:10.1103/PhysRevD.83.123531](#).
- [207] T. Hiramatsu, M. Kawasaki, K. Saikawa, Evolution of String-Wall Networks and Axionic Domain Wall Problem, JCAP 1108 (2011) 030. [arXiv:1012.4558](#), [doi:10.1088/1475-7516/2011/08/030](#).
- [208] T. Hiramatsu, M. Kawasaki, K. Saikawa, T. Sekiguchi, Axion cosmology with long-lived domain walls, JCAP 1301 (2013) 001. [arXiv:1207.3166](#), [doi:10.1088/1475-7516/2013/01/001](#).
- [209] T. Hiramatsu, M. Kawasaki, K. Saikawa, T. Sekiguchi, Production of dark matter axions from collapse of string-wall systems, Phys. Rev. D85 (2012) 105020, [Erratum: Phys. Rev.D86,089902(2012)]. [arXiv:1202.5851](#), [doi:10.1103/PhysRevD.86.089902](#), [doi:10.1103/PhysRevD.85.105020](#).
- [210] L. Fleury, G. D. Moore, Axion dark matter: strings and their cores, JCAP 1601 (2016) 004. [arXiv:1509.00026](#), [doi:10.1088/1475-7516/2016/01/004](#).
- [211] V. B. Klaer, G. D. Moore, How to simulate global cosmic strings with large string tension, JCAP 1710 (2017) 043. [arXiv:1707.05566](#), [doi:10.1088/1475-7516/2017/10/043](#).
- [212] V. B. Klaer, G. D. Moore, The dark-matter axion mass, JCAP 1711 (11) (2017) 049. [arXiv:1708.07521](#), [doi:10.1088/1475-7516/2017/11/049](#).
- [213] M. Gorghetto, E. Hardy, G. Villadoro, Axions from Strings: the Attractive Solution, JHEP 07 (2018) 151. [arXiv:1806.04677](#), [doi:10.1007/JHEP07\(2018\)151](#).
- [214] A. Vaquero, J. Redondo, J. Stadler, Early seeds of axion miniclusters, JCAP 1904 (04) (2019) 012. [arXiv:1809.09241](#), [doi:10.1088/1475-7516/2019/04/012](#).
- [215] M. Buschmann, J. W. Foster, B. R. Safdi, Early-Universe Simulations of the Cosmological Axion, Phys. Rev. Lett. 124 (16) (2020) 161103. [arXiv:1906.00967](#), [doi:10.1103/PhysRevLett.124.161103](#).
- [216] M. Gorghetto, Axions from Strings, Ph.D. thesis, SISSA, Trieste (2019).
- [217] Ya. B. Zeldovich, M. Yu. Khlopov, On the Concentration of Relic Magnetic Monopoles in the Universe, Phys. Lett. 79B (1978) 239–241. [doi:10.1016/0370-2693\(78\)90232-0](#).
- [218] J. Preskill, Cosmological Production of Superheavy Magnetic Monopoles, Phys. Rev. Lett. 43 (1979) 1365. [doi:10.1103/PhysRevLett.43.1365](#).
- [219] A. H. Guth, S. H. H. Tye, Phase Transitions and Magnetic Monopole Production in the Very Early Universe, Phys. Rev. Lett. 44 (1980) 631, [Erratum: Phys. Rev. Lett.44,963(1980)]. [doi:10.1103/PhysRevLett.44.631](#), [doi:10.1103/PhysRevLett.44.963.2](#).
- [220] M. Yamaguchi, Scaling property of the global string in the radiation dominated universe, Phys. Rev. D 60 (1999) 103511. [arXiv:hep-ph/9907506](#), [doi:10.1103/PhysRevD.60.103511](#).
- [221] A. Albrecht, N. Turok, Evolution of Cosmic String Networks, Phys. Rev. D40 (1989) 973–1001. [doi:10.1103/PhysRevD.40.973](#).
- [222] D. P. Bennett, F. R. Bouchet, Evidence for a Scaling Solution in Cosmic String Evolution, Phys. Rev. Lett. 60 (1988) 257. [doi:10.1103/PhysRevLett.60.257](#).
- [223] C. J. A. P. Martins, E. P. S. Shellard, Quantitative string evolution, Phys. Rev. D54 (1996) 2535–2556. [arXiv:hep-ph/9602271](#), [doi:10.1103/PhysRevD.54.2535](#).
- [224] C. J. A. P. Martins, E. P. S. Shellard, Extending the velocity dependent one scale string evolution model, Phys. Rev. D65 (2002) 043514. [arXiv:hep-ph/0003298](#), [doi:10.1103/PhysRevD.65.043514](#).
- [225] C. J. A. P. Martins, J. N. Moore, E. P. S. Shellard, A Unified model for vortex string network evolution, Phys. Rev. Lett. 92 (2004) 251601. [arXiv:hep-ph/0310255](#), [doi:10.1103/PhysRevLett.92.251601](#).
- [226] A. Vilenkin, Cosmic Strings and Domain Walls, Phys. Rept. 121 (1985) 263–315. [doi:10.1016/0370-1573\(85\)90033-X](#).
- [227] C. J. A. P. Martins, E. P. S. Shellard, String evolution with friction, Phys. Rev. D53 (1996) 575–579. [arXiv:hep-ph/9507335](#), [doi:10.1103/PhysRevD.53.R575](#).
- [228] T. Vachaspati, A. Vilenkin, Evolution of cosmic networks, Phys. Rev. D35 (1987) 1131. [doi:10.1103/PhysRevD.35.1131](#).
- [229] C. J. A. P. Martins, Scaling properties of cosmological axion strings, Phys. Lett. B788 (2019) 147–151. [arXiv:1811.12678](#), [doi:10.1016/j.physletb.2018.11.031](#).
- [230] R. A. Battye, E. P. S. Shellard, String radiative back reaction, Phys. Rev. Lett. 75 (1995) 4354–4357. [arXiv:astro-ph/9408078](#), [doi:10.1103/PhysRevLett.75.4354](#).
- [231] M. Sakellariadou, Gravitational waves emitted from infinite strings, Phys. Rev. D42 (1990) 354–360, [Erratum: Phys. Rev.D43,4150(1991)]. [doi:10.1103/PhysRevD.42.354](#), [doi:10.1103/PhysRevD.43.4150.2](#).
- [232] M. Sakellariadou, Radiation of Nambu-Goldstone bosons from infinitely long cosmic strings, Phys. Rev. D44 (1991) 3767–3773. [doi:10.1103/PhysRevD.44.3767](#).
- [233] V. Vanchurin, K. D. Olum, A. Vilenkin, Scaling of cosmic string loops, Phys. Rev. D74 (2006) 063527. [arXiv:gr-qc/0511159](#), [doi:10.1103/PhysRevD.74.063527](#).
- [234] C. J. A. P. Martins, E. P. S. Shellard, Fractal properties and small-scale structure of cosmic string networks, Phys. Rev. D73 (2006) 043515. [arXiv:astro-ph/0511792](#), [doi:10.1103/PhysRevD.73.043515](#).

- [235] C. Ringeval, M. Sakellariadou, F. Bouchet, Cosmological evolution of cosmic string loops, JCAP 0702 (2007) 023. [arXiv:astro-ph/0511646](#), [doi:10.1088/1475-7516/2007/02/023](#).
- [236] K. D. Olum, V. Vanchurin, Cosmic string loops in the expanding Universe, Phys. Rev. D75 (2007) 063521. [arXiv:astro-ph/0610419](#), [doi:10.1103/PhysRevD.75.063521](#).
- [237] J. J. Blanco-Pillado, K. D. Olum, B. Shlaer, Large parallel cosmic string simulations: New results on loop production, Phys. Rev. D83 (2011) 083514. [arXiv:1101.5173](#), [doi:10.1103/PhysRevD.83.083514](#).
- [238] J. J. Blanco-Pillado, K. D. Olum, Stochastic gravitational wave background from smoothed cosmic string loops, Phys. Rev. D96 (10) (2017) 104046. [arXiv:1709.02693](#), [doi:10.1103/PhysRevD.96.104046](#).
- [239] T. W. B. Kibble, Evolution of a system of cosmic strings, Nucl. Phys. B252 (1985) 227, [Erratum: Nucl. Phys. B261,750(1985)]. [doi:10.1016/0550-3213\(85\)90439-0](#), [doi:10.1016/0550-3213\(85\)90596-6](#).
- [240] Y. Cui, D. E. Morrissey, Non-Thermal Dark Matter from Cosmic Strings, Phys. Rev. D79 (2009) 083532. [arXiv:0805.1060](#), [doi:10.1103/PhysRevD.79.083532](#).
- [241] C. Hagmann, P. Sikivie, Computer simulations of the motion and decay of global strings, Nucl. Phys. B363 (1991) 247–280. [doi:10.1016/0550-3213\(91\)90243-Q](#).
- [242] S. Chang, C. Hagmann, P. Sikivie, Studies of the motion and decay of axion walls bounded by strings, Phys. Rev. D59 (1999) 023505. [arXiv:hep-ph/9807374](#), [doi:10.1103/PhysRevD.59.023505](#).
- [243] S. M. Barr, K. Choi, J. E. Kim, Axion Cosmology in Superstring Models, Nucl. Phys. B283 (1987) 591–604. [doi:10.1016/0550-3213\(87\)90288-4](#).
- [244] V. F. Mukhanov, G. V. Chibisov, Quantum Fluctuations and a Nonsingular Universe, JETP Lett. 33 (1981) 532–535, [Pisma Zh. Eksp. Teor. Fiz.33,549(1981)].
- [245] A. H. Guth, S. Y. Pi, Fluctuations in the New Inflationary Universe, Phys. Rev. Lett. 49 (1982) 1110–1113. [doi:10.1103/PhysRevLett.49.1110](#).
- [246] S. W. Hawking, The Development of Irregularities in a Single Bubble Inflationary Universe, Phys. Lett. 115B (1982) 295. [doi:10.1016/0370-2693\(82\)90373-2](#).
- [247] A. A. Starobinsky, Dynamics of Phase Transition in the New Inflationary Universe Scenario and Generation of Perturbations, Phys. Lett. 117B (1982) 175–178. [doi:10.1016/0370-2693\(82\)90541-X](#).
- [248] J. M. Bardeen, P. J. Steinhardt, M. S. Turner, Spontaneous Creation of Almost Scale - Free Density Perturbations in an Inflationary Universe, Phys. Rev. D28 (1983) 679. [doi:10.1103/PhysRevD.28.679](#).
- [249] P. J. Steinhardt, M. S. Turner, A Prescription for Successful New Inflation, Phys. Rev. D29 (1984) 2162–2171. [doi:10.1103/PhysRevD.29.2162](#).
- [250] Y. Akrami, et al., Planck 2018 results. I. Overview and the cosmological legacy of Planck. (2018). [arXiv:1807.06205](#).
- [251] N. Aghanim, et al., Planck 2018 results. VI. Cosmological parameters. (2018). [arXiv:1807.06209](#).
- [252] Y. Akrami, et al., Planck 2018 results. X. Constraints on inflation. (2018). [arXiv:1807.06211](#).
- [253] A. Kosowsky, M. S. Turner, CBR anisotropy and the running of the scalar spectral index, Phys. Rev. D52 (1995) R1739–R1743. [arXiv:astro-ph/9504071](#), [doi:10.1103/PhysRevD.52.R1739](#).
- [254] S. M. Leach, A. R. Liddle, Microwave background constraints on inflationary parameters, Mon. Not. Roy. Astron. Soc. 341 (2003) 1151. [arXiv:astro-ph/0207213](#), [doi:10.1046/j.1365-8711.2003.06445.x](#).
- [255] A. R. Liddle, S. M. Leach, How long before the end of inflation were observable perturbations produced?, Phys. Rev. D68 (2003) 103503. [arXiv:astro-ph/0305263](#), [doi:10.1103/PhysRevD.68.103503](#).
- [256] A. Riotto, Inflation and the theory of cosmological perturbations, ICTP Lect. Notes Ser. 14 (2003) 317–413. [arXiv:hep-ph/0210162](#).
- [257] V. Bozza, M. Gasperini, M. Giovannini, G. Veneziano, Assisting pre - big bang phenomenology through short lived axions, Phys. Lett. B543 (2002) 14–22. [arXiv:hep-ph/0206131](#), [doi:10.1016/S0370-2693\(02\)02387-0](#).
- [258] V. Bozza, M. Gasperini, M. Giovannini, G. Veneziano, Constraints on pre big bang parameter space from CMBR anisotropies, Phys. Rev. D67 (2003) 063514. [arXiv:hep-ph/0212112](#), [doi:10.1103/PhysRevD.67.063514](#).
- [259] T. Kobayashi, R. Kurematsu, F. Takahashi, Isocurvature Constraints and Anharmonic Effects on QCD Axion Dark Matter, JCAP 1309 (2013) 032. [arXiv:1304.0922](#), [doi:10.1088/1475-7516/2013/09/032](#).
- [260] P. A. R. Ade, et al., Planck 2013 results. XVI. Cosmological parameters, Astron. Astrophys. 571 (2014) A16. [arXiv:1303.5076](#), [doi:10.1051/0004-6361/201321591](#).
- [261] P. A. R. Ade, et al., Planck 2013 results. XXII. Constraints on inflation, Astron. Astrophys. 571 (2014) A22. [arXiv:1303.5082](#), [doi:10.1051/0004-6361/201321569](#).
- [262] D. Barkats, et al., Degree-Scale CMB Polarization Measurements from Three Years of BICEP1 Data, Astrophys. J. 783 (2014) 67. [arXiv:1310.1422](#), [doi:10.1088/0004-637X/783/2/67](#).
- [263] P. A. R. Ade, et al., Joint Analysis of BICEP2/KeckArray and Planck Data, Phys. Rev. Lett. 114 (2015) 101301. [arXiv:1502.00612](#), [doi:10.1103/PhysRevLett.114.101301](#).
- [264] P. A. R. Ade, et al., Planck 2015 results. XX. Constraints on inflation, Astron. Astrophys. 594 (2016) A20. [arXiv:1502.02114](#), [doi:10.1051/0004-6361/201525898](#).
- [265] P. A. R. Ade, et al., BICEP2 / Keck Array x: Constraints on Primordial Gravitational Waves using Planck, WMAP, and New BICEP2/Keck Observations through the 2015 Season, Phys. Rev. Lett. 121 (2018) 221301. [arXiv:1810.05216](#), [doi:10.1103/PhysRevLett.121.221301](#).
- [266] A. D. Linde, Axions in inflationary cosmology, Phys. Lett. B259 (1991) 38–47. [doi:10.1016/0370-2693\(91\)90130-I](#).
- [267] S. Folkerts, C. Germani, J. Redondo, Axion Dark Matter and Planck favor non-minimal couplings to gravity, Phys. Lett. B728 (2014) 532–536. [arXiv:1304.7270](#), [doi:10.1016/j.physletb.2013.12.026](#).
- [268] K. S. Jeong, F. Takahashi, Suppressing Isocurvature Perturbations of QCD Axion Dark Matter, Phys. Lett. B 727 (2013) 448–451. [arXiv:1304.8131](#), [doi:10.1016/j.physletb.2013.10.061](#).

- [269] G. R. Dvali, Removing the cosmological bound on the axion scale (1995). [arXiv:hep-ph/9505253](#).
- [270] T. Banks, M. Dine, The Cosmology of string theoretic axions, Nucl. Phys. B505 (1997) 445–460. [arXiv:hep-th/9608197](#), [doi:10.1016/S0550-3213\(97\)00413-6](#).
- [271] K. Choi, E. J. Chun, S. H. Im, K. S. Jeong, Diluting the inflationary axion fluctuation by a stronger QCD in the early Universe, Phys. Lett. B750 (2015) 26–30. [arXiv:1505.00306](#), [doi:10.1016/j.physletb.2015.08.041](#).
- [272] K. Schmitz, T. T. Yanagida, Axion Isocurvature Perturbations in Low-Scale Models of Hybrid Inflation, Phys. Rev. D98 (7) (2018) 075003. [arXiv:1806.06056](#), [doi:10.1103/PhysRevD.98.075003](#).
- [273] J. E. Kim, H. P. Nilles, M. Peloso, Completing natural inflation, JCAP 0501 (2005) 005. [arXiv:hep-ph/0409138](#), [doi:10.1088/1475-7516/2005/01/005](#).
- [274] S. Hannestad, A. Mirizzi, G. G. Raffelt, Y. Y. Y. Wong, Neutrino and axion hot dark matter bounds after WMAP-7, JCAP 1008 (2010) 001. [arXiv:1004.0695](#), [doi:10.1088/1475-7516/2010/08/001](#).
- [275] M. Archidiacono, S. Hannestad, A. Mirizzi, G. Raffelt, Y. Y. Y. Wong, Axion hot dark matter bounds after Planck, JCAP 1310 (2013) 020. [arXiv:1307.0615](#), [doi:10.1088/1475-7516/2013/10/020](#).
- [276] E. Di Valentino, E. Giusarma, M. Lattanzi, O. Mena, A. Melchiorri, J. Silk, Cosmological Axion and neutrino mass constraints from Planck 2015 temperature and polarization data, Phys. Lett. B752 (2016) 182–185. [arXiv:1507.08665](#), [doi:10.1016/j.physletb.2015.11.025](#).
- [277] M. Archidiacono, T. Basse, J. Hamann, S. Hannestad, G. Raffelt, Y. Y. Y. Wong, Future cosmological sensitivity for hot dark matter axions, JCAP 1505 (05) (2015) 050. [arXiv:1502.03325](#), [doi:10.1088/1475-7516/2015/05/050](#).
- [278] E. Masso, R. Toldra, New constraints on a light spinless particle coupled to photons, Phys. Rev. D55 (1997) 7967–7969. [arXiv:hep-ph/9702275](#), [doi:10.1103/PhysRevD.55.7967](#).
- [279] D. Cadamuro, S. Hannestad, G. Raffelt, J. Redondo, Cosmological bounds on sub-MeV mass axions, JCAP 1102 (2011) 003. [arXiv:1011.3694](#), [doi:10.1088/1475-7516/2011/02/003](#).
- [280] M. Millea, L. Knox, B. Fields, New Bounds for Axions and Axion-Like Particles with keV-GeV Masses, Phys. Rev. D92 (2) (2015) 023010. [arXiv:1501.04097](#), [doi:10.1103/PhysRevD.92.023010](#).
- [281] P. F. Depta, M. Hufnagel, K. Schmidt-Hoberg, Robust cosmological constraints on axion-like particles (2020). [arXiv:2002.08370](#).
- [282] E. M. Riordan, et al., A Search for Short Lived Axions in an Electron Beam Dump Experiment, Phys. Rev. Lett. 59 (1987) 755. [doi:10.1103/PhysRevLett.59.755](#).
- [283] J. Bjorken, S. Ecklund, W. Nelson, A. Abashian, C. Church, B. Lu, L. Mo, T. Nunamaker, P. Rassmann, Search for Neutral Metastable Penetrating Particles Produced in the SLAC Beam Dump, Phys. Rev. D 38 (1988) 3375. [doi:10.1103/PhysRevD.38.3375](#).
- [284] J. Blumlein, et al., Limits on neutral light scalar and pseudoscalar particles in a proton beam dump experiment, Z. Phys. C51 (1991) 341–350. [doi:10.1007/BF01548556](#).
- [285] J. Blumlein, et al., Limits on the mass of light (pseudo)scalar particles from Bethe-Heitler e^+e^- and $\mu^+\mu^-$ pair production in a proton - iron beam dump experiment, Int. J. Mod. Phys. A7 (1992) 3835–3850. [doi:10.1142/S0217751X9200171X](#).
- [286] ALPs at Colliders, JHEP 06 (2015) 173. [arXiv:1409.4792](#), [doi:10.1007/JHEP06\(2015\)173](#).
- [287] J. Jaeckel, M. Spannowsky, Probing MeV to 90 GeV axion-like particles with LEP and LHC, Phys. Lett. B753 (2016) 482–487. [arXiv:1509.00476](#), [doi:10.1016/j.physletb.2015.12.037](#).
- [288] B. Döbrich, J. Jaeckel, F. Kahlhoefer, A. Ringwald, K. Schmidt-Hoberg, ALPtraum: ALP production in proton beam dump experiments, JHEP 02 (2016) 018, [JHEP02,018(2016)]. [arXiv:1512.03069](#), [doi:10.1007/JHEP02\(2016\)018](#).
- [289] I. Brivio, M. B. Gavela, L. Merlo, K. Mimasu, J. M. No, R. del Rey, V. Sanz, ALPs Effective Field Theory and Collider Signatures, Eur. Phys. J. C77 (8) (2017) 572. [arXiv:1701.05379](#), [doi:10.1140/epjc/s10052-017-5111-3](#).
- [290] M. Bauer, M. Neubert, A. Thamm, Collider Probes of Axion-Like Particles, JHEP 12 (2017) 044. [arXiv:1708.00443](#), [doi:10.1007/JHEP12\(2017\)044](#).
- [291] M. J. Dolan, T. Ferber, C. Hearty, F. Kahlhoefer, K. Schmidt-Hoberg, Revised constraints and Belle II sensitivity for visible and invisible axion-like particles, JHEP 12 (2017) 094. [arXiv:1709.00009](#), [doi:10.1007/JHEP12\(2017\)094](#).
- [292] B. Döbrich, J. Jaeckel, T. Spadaro, Light in the beam dump. Axion-Like Particle production from decay photons in proton beam-dumps, JHEP 05 (2019) 213. [arXiv:1904.02091](#), [doi:10.1007/JHEP05\(2019\)213](#).
- [293] M. Gavela, J. No, V. Sanz, J. de Trocóniz, Nonresonant Searches for Axionlike Particles at the LHC, Phys. Rev. Lett. 124 (5) (2020) 051802. [arXiv:1905.12953](#), [doi:10.1103/PhysRevLett.124.051802](#).
- [294] L. M. Fleury, G. D. Moore, Axion String Dynamics I: $2+1D$, JCAP 1605 (05) (2016) 005. [arXiv:1602.04818](#), [doi:10.1088/1475-7516/2016/05/005](#).
- [295] M. Kawasaki, K. Saikawa, T. Sekiguchi, Axion dark matter from topological defects, Phys. Rev. D91 (6) (2015) 065014. [arXiv:1412.0789](#), [doi:10.1103/PhysRevD.91.065014](#).
- [296] J. N. Moore, E. P. S. Shellard, C. J. A. P. Martins, On the evolution of Abelian-Higgs string networks, Phys. Rev. D65 (2002) 023503. [arXiv:hep-ph/0107171](#), [doi:10.1103/PhysRevD.65.023503](#).
- [297] S. Hoof, F. Kahlhoefer, P. Scott, C. Weniger, M. White, Axion global fits with Peccei-Quinn symmetry breaking before inflation using GAMBIT, JHEP 03 (2019) 191. [arXiv:1810.07192](#), [doi:10.1007/JHEP03\(2019\)191](#).
- [298] T. Bringmann, et al., DarkBit: A GAMBIT module for computing dark matter observables and likelihoods, Eur. Phys. J. C77 (12) (2017) 831. [arXiv:1705.07920](#), [doi:10.1140/epjc/s10052-017-5155-4](#).
- [299] P. Athron, et al., GAMBIT: The Global and Modular Beyond-the-Standard-Model Inference Tool, Eur. Phys. J. C77 (11) (2017) 784, [Addendum: Eur. Phys. J. C78, no.2, 98(2018)]. [arXiv:1705.07908](#), [doi:10.1140/epjc/s10052-017-5513-2](#), [doi:10.1140/epjc/s10052-017-5321-8](#).
- [300] P. W. Graham, A. Scherlis, Stochastic axion scenario, Phys. Rev. D98 (3) (2018) 035017. [arXiv:1805.07362](#), [doi:10.1103/PhysRevD.98.035017](#).

- [301] F. Takahashi, W. Yin, A. H. Guth, QCD axion window and low-scale inflation, *Phys. Rev. D* **98** (1) (2018) 015042. [arXiv:1805.08763](#), [doi:10.1103/PhysRevD.98.015042](#).
- [302] K. Choi, H. B. Kim, J. E. Kim, Axion cosmology with a stronger QCD in the early universe, *Nucl. Phys. B* **490** (1997) 349–364. [arXiv:hep-ph/9606372](#), [doi:10.1016/S0550-3213\(97\)00066-7](#).
- [303] R. T. Co, E. Gonzalez, K. Harigaya, Axion Misalignment Driven to the Bottom, *JHEP* **05** (2019) 162. [arXiv:1812.11186](#), [doi:10.1007/JHEP05\(2019\)162](#).
- [304] R. T. Co, E. Gonzalez, K. Harigaya, Axion Misalignment Driven to the Hilltop, *JHEP* **05** (2019) 163. [arXiv:1812.11192](#), [doi:10.1007/JHEP05\(2019\)163](#).
- [305] F. Takahashi, W. Yin, QCD axion on hilltop by a phase shift of π , *JHEP* **10** (2019) 120. [arXiv:1908.06071](#), [doi:10.1007/JHEP10\(2019\)120](#).
- [306] G. G. Raffelt, Axion constraints from white dwarf cooling times, *Physics Letters B* **166** (4) (1986) 402 – 406. [doi:https://doi.org/10.1016/0370-2693\(86\)91588-1](#).
- [307] N. Viaux, M. Catelan, P. B. Stetson, G. Raffelt, J. Redondo, A. A. R. Valcarce, A. Weiss, Neutrino and axion bounds from the globular cluster M5 (NGC 5904), *Phys. Rev. Lett.* **111** (2013) 231301. [arXiv:1311.1669](#), [doi:10.1103/PhysRevLett.111.231301](#).
- [308] A. Arvanitaki, S. Dubovsky, Exploring the String Axiverse with Precision Black Hole Physics, *Phys. Rev. D* **83** (2011) 044026. [arXiv:1004.3558](#), [doi:10.1103/PhysRevD.83.044026](#).
- [309] A. Arvanitaki, M. Baryakhtar, X. Huang, Discovering the QCD Axion with Black Holes and Gravitational Waves, *Phys. Rev. D* **91** (8) (2015) 084011. [arXiv:1411.2263](#), [doi:10.1103/PhysRevD.91.084011](#).
- [310] P. A. R. Ade, et al., Planck 2015 results. XIII. Cosmological parameters, *Astron. Astrophys.* **594** (2016) A13. [arXiv:1502.01589](#), [doi:10.1051/0004-6361/201525830](#).
- [311] G. Ballesteros, J. Redondo, A. Ringwald, C. Tamarit, Unifying inflation with the axion, dark matter, baryogenesis and the seesaw mechanism, *Phys. Rev. Lett.* **118** (7) (2017) 071802. [arXiv:1608.05414](#), [doi:10.1103/PhysRevLett.118.071802](#).
- [312] G. Ballesteros, J. Redondo, A. Ringwald, C. Tamarit, Standard Model—axion—seesaw—Higgs portal inflation. Five problems of particle physics and cosmology solved in one stroke, *JCAP* **1708** (08) (2017) 001. [arXiv:1610.01639](#), [doi:10.1088/1475-7516/2017/08/001](#).
- [313] G. Ballesteros, J. Redondo, A. Ringwald, C. Tamarit, Several Problems in Particle Physics and Cosmology Solved in One SMASH, *Front. Astron. Space Sci.* **6** (2019) 55. [arXiv:1904.05594](#), [doi:10.3389/fspas.2019.00055](#).
- [314] N. Kitajima, F. Takahashi, Resonant conversions of QCD axions into hidden axions and suppressed isocurvature perturbations, *JCAP* **1501** (01) (2015) 032. [arXiv:1411.2011](#), [doi:10.1088/1475-7516/2015/01/032](#).
- [315] M. Fairbairn, R. Hogan, D. J. E. Marsh, Unifying inflation and dark matter with the Peccei-Quinn field: observable axions and observable tensors, *Phys. Rev. D* **91** (2) (2015) 023509. [arXiv:1410.1752](#), [doi:10.1103/PhysRevD.91.023509](#).
- [316] K. N. Abazajian, et al., CMB-S4 Science Book, First Edition. (2016). [arXiv:1610.02743](#).
- [317] T. Tenkanen, L. Visinelli, Axion dark matter from Higgs inflation with an intermediate H_* , *JCAP* **1908** (08) (2019) 033. [arXiv:1906.11837](#), [doi:10.1088/1475-7516/2019/08/033](#).
- [318] D. Budker, P. W. Graham, M. Ledbetter, S. Rajendran, A. Sushkov, Proposal for a Cosmic Axion Spin Precession Experiment (CASPER), *Phys. Rev. X* **4** (2) (2014) 021030. [arXiv:1306.6089](#), [doi:10.1103/PhysRevX.4.021030](#).
- [319] Y. Kahn, B. R. Safdi, J. Thaler, Broadband and Resonant Approaches to Axion Dark Matter Detection, *Phys. Rev. Lett.* **117** (14) (2016) 141801. [arXiv:1602.01086](#), [doi:10.1103/PhysRevLett.117.141801](#).
- [320] J. L. Ouellet, et al., First Results from ABRACADABRA-10 cm: A Search for Sub- μ eV Axion Dark Matter, *Phys. Rev. Lett.* **122** (12) (2019) 121802. [arXiv:1810.12257](#), [doi:10.1103/PhysRevLett.122.121802](#).
- [321] D. Alesini, D. Babusci, D. Di Gioacchino, C. Gatti, G. Lamanna, C. Ligi, The KLASH Proposal. (2017). [arXiv:1707.06010](#).
- [322] D. Alesini, et al., KLASH Conceptual Design Report (2019). [arXiv:1911.02427](#).
- [323] L. D. Duffy, P. Sikivie, D. B. Tanner, S. J. Asztalos, C. Hagmann, D. Kinion, L. J. Rosenberg, K. van Bibber, D. B. Yu, R. F. Bradley, A high resolution search for dark-matter axions, *Phys. Rev. D* **74** (2006) 012006. [arXiv:astro-ph/0603108](#), [doi:10.1103/PhysRevD.74.012006](#).
- [324] S. J. Asztalos, et al., A SQUID-based microwave cavity search for dark-matter axions, *Phys. Rev. Lett.* **104** (2010) 041301. [arXiv:0910.5914](#), [doi:10.1103/PhysRevLett.104.041301](#).
- [325] S. J. Asztalos, et al., Design and performance of the ADMX SQUID-based microwave receiver, *Nucl. Instrum. Meth. A* **656** (2011) 39–44. [arXiv:1105.4203](#), [doi:10.1016/j.nima.2011.07.019](#).
- [326] I. Stern, ADMX Status, *PoS ICHEP2016* (2016) 198. [arXiv:1612.08296](#).
- [327] T. Braine, et al., Extended Search for the Invisible Axion with the Axion Dark Matter Experiment, *Phys. Rev. Lett.* **124** (10) (2020) 101303. [arXiv:1910.08638](#), [doi:10.1103/PhysRevLett.124.101303](#).
- [328] Y. K. Semertzidis, et al., Axion Dark Matter Research with IBS/CAPP. (2019). [arXiv:1910.11591](#).
- [329] S. Lee, S. Ahn, J. Choi, B. Ko, Y. Semertzidis, Axion Dark Matter Search around 6.7 μ eV, *Phys. Rev. Lett.* **124** (10) (2020) 101802. [arXiv:2001.05102](#), [doi:10.1103/PhysRevLett.124.101802](#).
- [330] D. Kim, J. Jeong, S. Youn, Y. Kim, Y. K. Semertzidis, Revisiting the detection rate for axion haloscopes, *JCAP* **03** (2020) 066. [arXiv:2001.05605](#), [doi:10.1088/1475-7516/2020/03/066](#).
- [331] A. Caldwell, G. Dvali, B. Majorovits, A. Millar, G. Raffelt, J. Redondo, O. Reimann, F. Simon, F. Steffen, Dielectric Haloscopes: A New Way to Detect Axion Dark Matter, *Phys. Rev. Lett.* **118** (9) (2017) 091801. [arXiv:1611.05865](#), [doi:10.1103/PhysRevLett.118.091801](#).
- [332] J. K. Vogel, et al., IAXO - The International Axion Observatory, in: 8th Patras Workshop on Axions, WIMPs and WISPs (AXION-WIMP 2012) Chicago, Illinois, July 18–22, 2012, 2013. [arXiv:1302.3273](#).
- [333] J. K. Vogel, et al., The Next Generation of Axion Helioscopes: The International Axion Observatory (IAXO), *Phys.*

- Procedia 61 (2015) 193–200. [doi:10.1016/j.phpro.2014.12.031](#).
- [334] E. Armengaud, et al., Physics potential of the International Axion Observatory (IAXO), JCAP 1906 (06) (2019) 047. [arXiv:1904.09155](#), [doi:10.1088/1475-7516/2019/06/047](#).
 - [335] P. F. de Salas, S. Pastor, Relic neutrino decoupling with flavour oscillations revisited, JCAP 1607 (07) (2016) 051. [arXiv:1606.06986](#), [doi:10.1088/1475-7516/2016/07/051](#).
 - [336] G. Mangano, G. Miele, S. Pastor, T. Pinto, O. Pisanti, P. D. Serpico, Relic neutrino decoupling including flavor oscillations, Nucl. Phys. B729 (2005) 221–234. [arXiv:hep-ph/0506164](#), [doi:10.1016/j.nuclphysb.2005.09.041](#).
 - [337] S. Dodelson, M. S. Turner, Nonequilibrium neutrino statistical mechanics in the expanding universe, Phys. Rev. D46 (1992) 3372–3387. [doi:10.1103/PhysRevD.46.3372](#).
 - [338] S. Hannestad, J. Madsen, Neutrino decoupling in the early universe, Phys. Rev. D52 (1995) 1764–1769. [arXiv:astro-ph/9506015](#), [doi:10.1103/PhysRevD.52.1764](#).
 - [339] A. D. Dolgov, S. H. Hansen, D. V. Semikoz, Nonequilibrium corrections to the spectra of massless neutrinos in the early universe, Nucl. Phys. B503 (1997) 426–444. [arXiv:hep-ph/9703315](#), [doi:10.1016/S0550-3213\(97\)00479-3](#).
 - [340] M. Archidiacono, E. Giusarma, S. Hannestad, O. Mena, Cosmic dark radiation and neutrinos, Adv. High Energy Phys. 2013 (2013) 191047. [arXiv:1307.0637](#), [doi:10.1155/2013/191047](#).
 - [341] J. Lesgourgues, S. Pastor, Neutrino cosmology and Planck, New J. Phys. 16 (2014) 065002. [arXiv:1404.1740](#), [doi:10.1088/1367-2630/16/6/065002](#).
 - [342] S. Hannestad, A. Mirizzi, G. Raffelt, New cosmological mass limit on thermal relic axions, JCAP 0507 (2005) 002. [arXiv:hep-ph/0504059](#), [doi:10.1088/1475-7516/2005/07/002](#).
 - [343] A. Melchiorri, O. Mena, A. Slosar, An improved cosmological bound on the thermal axion mass, Phys. Rev. D76 (2007) 041303. [arXiv:0705.2695](#), [doi:10.1103/PhysRevD.76.041303](#).
 - [344] E. Di Valentino, S. Gariazzo, E. Giusarma, O. Mena, Robustness of cosmological axion mass limits, Phys. Rev. D91 (12) (2015) 123505. [arXiv:1503.00911](#), [doi:10.1103/PhysRevD.91.123505](#).
 - [345] R. Z. Ferreira, A. Notari, Observable Windows for the QCD Axion Through the Number of Relativistic Species, Phys. Rev. Lett. 120 (19) (2018) 191301. [arXiv:1801.06090](#), [doi:10.1103/PhysRevLett.120.191301](#).
 - [346] M. S. Turner, Thermal Production of Not So Invisible Axions in the Early Universe, Phys. Rev. Lett. 59 (1987) 2489, [Erratum: Phys. Rev. Lett. 60, 1101 (1988)]. [doi:10.1103/PhysRevLett.59.2489](#), [doi:10.1103/PhysRevLett.60.1101.3](#).
 - [347] E. Masso, F. Rota, G. Zsembinszki, On axion thermalization in the early universe, Phys. Rev. D66 (2002) 023004. [arXiv:hep-ph/0203221](#), [doi:10.1103/PhysRevD.66.023004](#).
 - [348] P. Graf, F. D. Steffen, Thermal axion production in the primordial quark-gluon plasma, Phys. Rev. D83 (2011) 075011. [arXiv:1008.4528](#), [doi:10.1103/PhysRevD.83.075011](#).
 - [349] A. Salvio, A. Strumia, W. Xue, Thermal axion production, JCAP 1401 (2014) 011. [arXiv:1310.6982](#), [doi:10.1088/1475-7516/2014/01/011](#).
 - [350] F. D’Eramo, R. Z. Ferreira, A. Notari, J. L. Bernal, Hot Axions and the H_0 tension, JCAP 1811 (11) (2018) 014. [arXiv:1808.07430](#), [doi:10.1088/1475-7516/2018/11/014](#).
 - [351] D. Baumann, D. Green, B. Wallisch, New Target for Cosmic Axion Searches, Phys. Rev. Lett. 117 (17) (2016) 171301. [arXiv:1604.08614](#), [doi:10.1103/PhysRevLett.117.171301](#).
 - [352] L. Verde, T. Treu, A. Riess, Tensions between the Early and the Late Universe, 2019. [arXiv:1907.10625](#), [doi:10.1038/s41550-019-0902-0](#).
 - [353] C. J. Hogan, M. J. Rees, Axion Miniclusters, Phys. Lett. B205 (1988) 228–230. [doi:10.1016/0370-2693\(88\)91655-3](#).
 - [354] E. W. Kolb, I. I. Tkachev, Axion miniclusters and Bose stars, Phys. Rev. Lett. 71 (1993) 3051–3054. [arXiv:hep-ph/9303313](#), [doi:10.1103/PhysRevLett.71.3051](#).
 - [355] E. W. Kolb, I. I. Tkachev, Nonlinear axion dynamics and formation of cosmological pseudosolitons, Phys. Rev. D49 (1994) 5040–5051. [arXiv:astro-ph/9311037](#), [doi:10.1103/PhysRevD.49.5040](#).
 - [356] E. W. Kolb, I. I. Tkachev, Large amplitude isothermal fluctuations and high density dark matter clumps, Phys. Rev. D50 (1994) 769–773. [arXiv:astro-ph/9403011](#), [doi:10.1103/PhysRevD.50.769](#).
 - [357] J. Enander, A. Pargner, T. Schwetz, Axion minicluster power spectrum and mass function, JCAP 1712 (12) (2017) 038. [arXiv:1708.04466](#), [doi:10.1088/1475-7516/2017/12/038](#).
 - [358] A. E. Nelson, H. Xiao, Axion Cosmology with Early Matter Domination, Phys. Rev. D98 (6) (2018) 063516. [arXiv:1807.07176](#), [doi:10.1103/PhysRevD.98.063516](#).
 - [359] L. Visinelli, J. Redondo, Axion Miniclusters in Modified Cosmological Histories, Phys. Rev. D101 (2) (2020) 023008. [arXiv:1808.01879](#), [doi:10.1103/PhysRevD.101.023008](#).
 - [360] M. Fairbairn, D. J. E. Marsh, J. Quevillon, S. Rozier, Structure formation and microlensing with axion miniclusters, Phys. Rev. D97 (8) (2018) 083502. [arXiv:1707.03310](#), [doi:10.1103/PhysRevD.97.083502](#).
 - [361] M. Fairbairn, D. J. E. Marsh, J. Quevillon, Searching for the QCD Axion with Gravitational Microlensing, Phys. Rev. Lett. 119 (2) (2017) 021101. [arXiv:1701.04787](#), [doi:10.1103/PhysRevLett.119.021101](#).
 - [362] B. Eggemeier, J. Redondo, K. Dolag, J. C. Niemeyer, A. Vaquero, First simulations of axion minicluster halos (11 2019). [arXiv:1911.09417](#).
 - [363] A. K. Drukier, K. Freese, D. N. Spergel, Detecting Cold Dark Matter Candidates, Phys. Rev. D33 (1986) 3495–3508. [doi:10.1103/PhysRevD.33.3495](#).
 - [364] S. Knirck, A. J. Millar, C. A. J. O’Hare, J. Redondo, F. D. Steffen, Directional axion detection, JCAP 1811 (11) (2018) 051. [arXiv:1806.05927](#), [doi:10.1088/1475-7516/2018/11/051](#).
 - [365] E. W. Kolb, I. I. Tkachev, Femtolensing and picolensing by axion miniclusters, Astrophys. J. 460 (1996) L25–L28. [arXiv:astro-ph/9510043](#), [doi:10.1086/309962](#).
 - [366] P. Tinyakov, I. Tkachev, K. Zioutas, Tidal streams from axion miniclusters and direct axion searches, JCAP 1601 (01)

- (2016) 035. [arXiv:1512.02884](#), [doi:10.1088/1475-7516/2016/01/035](#).
- [367] I. I. Tkachev, On the possibility of Bose star formation, *Phys. Lett. B* 261 (1991) 289–293. [doi:10.1016/0370-2693\(91\)90330-S](#).
- [368] H.-Y. Schive, T. Chiueh, T. Broadhurst, Cosmic Structure as the Quantum Interference of a Coherent Dark Wave, *Nature Phys.* 10 (2014) 496–499. [arXiv:1406.6586](#), [doi:10.1038/nphys2996](#).
- [369] B. Eggemeier, J. C. Niemeyer, Formation and mass growth of axion stars in axion miniclusters, *Phys. Rev. D* 100 (6) (2019) 063528. [arXiv:1906.01348](#), [doi:10.1103/PhysRevD.100.063528](#).
- [370] D. J. Kaup, Klein-Gordon Geon, *Phys. Rev.* 172 (1968) 1331–1342. [doi:10.1103/PhysRev.172.1331](#).
- [371] R. Ruffini, S. Bonazzola, Systems of selfgravitating particles in general relativity and the concept of an equation of state, *Phys. Rev.* 187 (1969) 1767–1783. [doi:10.1103/PhysRev.187.1767](#).
- [372] J. D. Breit, S. Gupta, A. Zaks, Cold Bose Stars, *Phys. Lett.* 140B (1984) 329–332. [doi:10.1016/0370-2693\(84\)90764-0](#).
- [373] L. A. Urena-Lopez, T. Matos, R. Becerril, Inside oscillatons, *Class. Quant. Grav.* 19 (2002) 6259–6277. [doi:10.1088/0264-9381/19/23/320](#).
- [374] T. Helfer, D. J. E. Marsh, K. Clough, M. Fairbairn, E. A. Lim, R. Becerril, Black hole formation from axion stars, *JCAP* 1703 (03) (2017) 055. [arXiv:1609.04724](#), [doi:10.1088/1475-7516/2017/03/055](#).
- [375] E. Seidel, W.-M. Suen, Formation of solitonic stars through gravitational cooling, *Phys. Rev. Lett.* 72 (1994) 2516–2519. [arXiv:gr-qc/9309015](#), [doi:10.1103/PhysRevLett.72.2516](#).
- [376] F. S. Guzman, L. A. Urena-Lopez, Gravitational cooling of self-gravitating Bose-Condensates, *Astrophys. J.* 645 (2006) 814–819. [arXiv:astro-ph/0603613](#), [doi:10.1086/504508](#).
- [377] D. G. Levkov, A. G. Panin, I. I. Tkachev, Gravitational Bose-Einstein condensation in the kinetic regime, *Phys. Rev. Lett.* 121 (15) (2018) 151301. [arXiv:1804.05857](#), [doi:10.1103/PhysRevLett.121.151301](#).
- [378] P.-H. Chavanis, Mass-radius relation of Newtonian self-gravitating Bose-Einstein condensates with short-range interactions: I. Analytical results, *Phys. Rev. D* 84 (2011) 043531. [arXiv:1103.2050](#), [doi:10.1103/PhysRevD.84.043531](#).
- [379] P. H. Chavanis, L. Delfini, Mass-radius relation of Newtonian self-gravitating Bose-Einstein condensates with short-range interactions: II. Numerical results, *Phys. Rev. D* 84 (2011) 043532. [arXiv:1103.2054](#), [doi:10.1103/PhysRevD.84.043532](#).
- [380] M. Membrado, J. Abad, A. Pacheco, J. Sanudo, NEWTONIAN BOSON SPHERES, *Phys. Rev. D* 40 (1989) 2736–2738. [doi:10.1103/PhysRevD.40.2736](#).
- [381] D. G. Levkov, A. G. Panin, I. I. Tkachev, Relativistic axions from collapsing Bose stars, *Phys. Rev. Lett.* 118 (1) (2017) 011301. [arXiv:1609.03611](#), [doi:10.1103/PhysRevLett.118.011301](#).
- [382] L. Visinelli, S. Baum, J. Redondo, K. Freese, F. Wilczek, Dilute and dense axion stars, *Phys. Lett. B* 777 (2018) 64–72. [arXiv:1710.08910](#), [doi:10.1016/j.physletb.2017.12.010](#).
- [383] G. Raffelt, Stars as laboratories for fundamental physics: The astrophysics of neutrinos, axions, and other weakly interacting particles, 1996.
- [384] P. Di Vecchia, M. Giannotti, M. Lattanzi, A. Lindner, Round Table on Axions and Axion-like Particles, in: 13th Conference on Quark Confinement and the Hadron Spectrum (Confinement XIII) Maynooth, Ireland, July 31-August 6, 2018, 2019. [arXiv:1902.06567](#).
- [385] A. Friedland, M. Giannotti, M. Wise, Constraining the Axion-Photon Coupling with Massive Stars., *Phys.Rev.Lett.* 110 (2013) 061101. [arXiv:1210.1271](#), [doi:10.1103/PhysRevLett.110.061101](#).
- [386] A. Ayala, I. Dominguez, M. Giannotti, A. Mirizzi, O. Straniero, Revisiting the bound on axion-photon coupling from Globular Clusters, *Phys. Rev. Lett.* 113 (19) (2014) 191302. [arXiv:1406.6053](#), [doi:10.1103/PhysRevLett.113.191302](#).
- [387] O. Straniero, A. Ayala, M. Giannotti, A. Mirizzi, I. Dominguez, Axion-Photon Coupling: Astrophysical Constraints, in: Proceedings, 11th Patras Workshop on Axions, WIMPs and WISPs (Axion-WIMP 2015): Zaragoza, Spain, June 22-26, 2015, 2015, pp. 77–81. [doi:10.3204/DESY-PROC-2015-02/straniero_oscar](#).
- [388] N. Vinyoles, A. M. Serenelli, F. L. Villante, S. Basu, J. Bergström, M. C. Gonzalez-Garcia, M. Maltoni, C. Peña-Garay, N. Song, A new Generation of Standard Solar Models, *Astrophys. J.* 835 (2) (2017) 202. [arXiv:1611.09867](#), [doi:10.3847/1538-4357/835/2/202](#).
- [389] O. Straniero, I. Dominguez, L. Piersanti, M. Giannotti, A. Mirizzi, The Initial Mass–Final Luminosity Relation of Type II Supernova Progenitors: Hints of New Physics?, *Astrophys. J.* 881 (2) (2019) 158. [arXiv:1907.06367](#), [doi:10.3847/1538-4357/ab3222](#).
- [390] G. G. Raffelt, D. S. P. Dearborn, Bounds on Hadronic Axions From Stellar Evolution, *Phys. Rev. D* 36 (1987) 2211. [doi:10.1103/PhysRevD.36.2211](#).
- [391] H. Schlattl, A. Weiss, G. Raffelt, Helioseismological constraint on solar axion emission, *Astropart. Phys.* 10 (1999) 353–359. [arXiv:hep-ph/9807476](#), [doi:10.1016/S0927-6505\(98\)00063-2](#).
- [392] N. Vinyoles, A. Serenelli, F. L. Villante, S. Basu, J. Redondo, J. Isern, New axion and hidden photon constraints from a solar data global fit, *JCAP* 1510 (10) (2015) 015. [arXiv:1501.01639](#), [doi:10.1088/1475-7516/2015/10/015](#).
- [393] P. Gondolo, G. G. Raffelt, Solar neutrino limit on axions and keV-mass bosons, *Phys. Rev. D* 79 (2009) 107301. [arXiv:0807.2926](#), [doi:10.1103/PhysRevD.79.107301](#).
- [394] M. Giannotti, I. Irastorza, J. Redondo, A. Ringwald, Cool WISPs for stellar cooling excesses, *JCAP* 1605 (05) (2016) 057. [arXiv:1512.08108](#), [doi:10.1088/1475-7516/2016/05/057](#).
- [395] Y. I. Izotov, G. Stasinska, N. G. Guseva, Primordial 4He abundance: a determination based on the largest sample of HII regions with a methodology tested on model HII regions, *Astron. Astrophys.* 558 (2013) A57. [arXiv:1308.2100](#), [doi:10.1051/0004-6361/201220782](#).
- [396] Y. I. Izotov, T. X. Thuan, N. G. Guseva, A new determination of the primordial He abundance using the He I $\lambda 10830$ radA emission line: cosmological implications, *Mon. Not. Roy. Astron. Soc.* 445 (1) (2014) 778–793. [arXiv:1408.6953](#), [doi:10.1093/mnras/stu1771](#).

- [397] E. Aver, K. A. Olive, E. D. Skillman, The effects of He I λ 10830 on helium abundance determinations, JCAP 1507 (07) (2015) 011. [arXiv:1503.08146](#), [doi:10.1088/1475-7516/2015/07/011](#).
- [398] G. Carosi, A. Friedland, M. Giannotti, M. Pivovarov, J. Ruz, et al., Probing the axion-photon coupling: phenomenological and experimental perspectives. A snowmass white paper. (2013). [arXiv:1309.7035](#).
- [399] R. Kippenhahn, A. Weigert, Stellar Structure and Evolution., Springer-Verlag, 1994.
- [400] K. B. McQuinn, E. D. Skillman, J. J. Dalcanton, A. E. Dolphin, J. Holtzman, et al., Observational Constraints on Red and Blue Helium Burning Sequences., Astrophys.J. 740 (2011) 48. [arXiv:1108.1405](#), [doi:10.1088/0004-637X/740/1/48](#).
- [401] M. Giannotti, ALP hints from cooling anomalies, in: Proceedings, 11th Patras Workshop on Axions, WIMPs and WISPs (Axion-WIMP 2015): Zaragoza, Spain, June 22-26, 2015, 2015, pp. 26–30. [arXiv:1508.07576](#), [doi:10.3204/DESY-PROC-2015-02/giannotti_maurizio](#).
- [402] LSST Science Collaboration, P. A. Abell, J. Allison, S. F. Anderson, J. R. Andrew, J. R. P. Angel, L. Armus, D. Arnett, S. J. Asztalos, T. S. Axelrod, LSST Science Book, Version 2.0. (Dec 2009). [arXiv:0912.0201](#).
- [403] A. Drlica-Wagner, et al., Probing the Fundamental Nature of Dark Matter with the Large Synoptic Survey Telescope. (2019). [arXiv:1902.01055](#).
- [404] A. Pantziris, K. Kang, Axion Emission Rates in Stars and Constraints on Its Mass, Phys. Rev. D33 (1986) 3509. [doi:10.1103/PhysRevD.33.3509](#).
- [405] J. Redondo, Solar axion flux from the axion-electron coupling, JCAP 1312 (2013) 008. [arXiv:1310.0823](#), [doi:10.1088/1475-7516/2013/12/008](#).
- [406] G. Raffelt, A. Weiss, Red giant bound on the axion - electron coupling revisited, Phys. Rev. D51 (1995) 1495–1498. [arXiv:hep-ph/9410205](#), [doi:10.1103/PhysRevD.51.1495](#).
- [407] M. Giannotti, Hints of new physics from stars., PoS ICHEP2016 (2016) 076. [arXiv:1611.04651](#), [doi:10.22323/1.282.0076](#).
- [408] A. H. Córscico, L. G. Althaus, M. M. Miller Bertolami, S. O. Kepler, Pulsating white dwarfs: new insights, Astron. Astrophys. Rev. 27 (1) (2019) 7. [arXiv:1907.00115](#), [doi:10.1007/s00159-019-0118-4](#).
- [409] M. M. Miller Bertolami, B. E. Melendez, L. G. Althaus, J. Isern, Revisiting the axion bounds from the Galactic white dwarf luminosity function, JCAP 1410 (10) (2014) 069. [arXiv:1406.7712](#), [doi:10.1088/1475-7516/2014/10/069](#).
- [410] C.-F. Chang, Hidden Photon Compton and Bremsstrahlung in White Dwarf Anomalous Cooling and Luminosity Functions. (2016). [arXiv:1607.03347](#).
- [411] M. M. Miller Bertolami, Limits on the neutrino magnetic dipole moment from the luminosity function of hot white dwarfs, Astron. Astrophys. 562 (2014) A123. [arXiv:1407.1404](#), [doi:10.1051/0004-6361/201322641](#).
- [412] J. Isern, E. Garcia-Berro, S. Torres, R. Cojocaru, S. Catalan, Axions and the luminosity function of white dwarfs: the thin and thick discs, and the halo, Mon. Not. Roy. Astron. Soc. 478 (2) (2018) 2569–2575. [arXiv:1805.00135](#), [doi:10.1093/mnras/sty1162](#).
- [413] M. Kilic, N. C. Hambly, P. Bergeron, C. Genest-Beaulieu, N. Rowell, Gaia reveals evidence for merged white dwarfs, MNRAS 479 (1) (2018) L113–L117. [arXiv:1805.01227](#), [doi:10.1093/mnrasl/sly110](#).
- [414] N. P. Gentile Fusillo, P.-E. Tremblay, B. T. Gänsicke, C. J. Manser, T. Cunningham, E. Cukanovaite, M. Hollands, T. Marsh, R. Raddi, S. Jordan, A Gaia Data Release 2 catalogue of white dwarfs and a comparison with SDSS, MNRAS 482 (4) (2019) 4570–4591. [arXiv:1807.03315](#), [doi:10.1093/mnras/sty3016](#).
- [415] S. A. Diaz, K.-P. Schröder, K. Zuber, D. Jack, E. E. B. Barrios, Constraint on the axion-electron coupling constant and the neutrino magnetic dipole moment by using the tip-RGB luminosity of fifty globular clusters. (2019). [arXiv:1910.10568](#).
- [416] O. Straniero, I. Dominguez, M. Giannotti, A. Mirizzi, Axion-electron coupling from the RGB tip of Globular Clusters, in: Proceedings, 13th Patras Workshop on Axions, WIMPs and WISPs, (PATRAS 2017): Thessaloniki, Greece, 15 May 2017 - 19, 2017, 2018, pp. 172–176. [arXiv:1802.10357](#), [doi:10.3204/DESY-PROC-2017-02/straniero_oscar](#).
- [417] A. Serenelli, A. Weiss, S. Cassisi, M. Salaris, A. Pietrinferni, The brightness of the red giant branch tip, Astronomy & Astrophysics 606 (2017) A33. [doi:10.1051/0004-6361/201731004](#).
- [418] N. Viaux, M. Catelan, P. B. Stetson, G. Raffelt, J. Redondo, A. A. R. Valcarce, A. Weiss, Particle-physics constraints from the globular cluster M5: Neutrino Dipole Moments, Astron. Astrophys. 558 (2013) A12. [arXiv:1308.4627](#), [doi:10.1051/0004-6361/201322004](#).
- [419] E. Pancino, M. Bellazzini, G. Giuffrida, S. Marinoni, Globular clusters with Gaia, Monthly Notices of the Royal Astronomical Society 467 (2017) 412–427. [arXiv:1701.03003](#).
- [420] C. Hanhart, D. R. Phillips, S. Reddy, Neutrino and axion emissivities of neutron stars from nucleon-nucleon scattering data, Phys. Lett. B499 (2001) 9–15. [arXiv:astro-ph/0003445](#), [doi:10.1016/S0370-2693\(00\)01382-4](#).
- [421] P. Carenza, T. Fischer, M. Giannotti, G. Guo, G. Martinez-Pinedo, A. Mirizzi, Improved axion emissivity from a supernova via nucleon-nucleon bremsstrahlung, JCAP 1910 (10) (2019) 016. [arXiv:1906.11844](#), [doi:10.1088/1475-7516/2019/10/016](#).
- [422] W. Keil, H.-T. Janka, D. N. Schramm, G. Sigl, M. S. Turner, J. R. Ellis, A Fresh look at axions and SN-1987A, Phys. Rev. D56 (1997) 2419–2432. [arXiv:astro-ph/9612222](#), [doi:10.1103/PhysRevD.56.2419](#).
- [423] R. Balkin, J. Serra, K. Springmann, A. Weiler, The QCD Axion at Finite Density, arXiv e-prints (Mar. 2020). [arXiv:2003.04903](#).
- [424] M. S. Turner, Axions from SN 1987a, Phys. Rev. Lett. 60 (1988) 1797. [doi:10.1103/PhysRevLett.60.1797](#).
- [425] A. Burrows, M. S. Turner, R. P. Brinkmann, Axions and SN 1987a, Phys. Rev. D39 (1989) 1020. [doi:10.1103/PhysRevD.39.1020](#).
- [426] G. Raffelt, D. Seckel, Bounds on Exotic Particle Interactions from SN 1987a, Phys. Rev. Lett. 60 (1988) 1793. [doi:10.1103/PhysRevLett.60.1793](#).
- [427] J. Keller, A. Sedrakian, Axions from cooling compact stars, Nucl. Phys. A897 (2013) 62–69. [arXiv:1205.6940](#), [doi:](#)

- 10.1016/j.nuclphysa.2012.11.004.
- [428] A. Sedrakian, Axion cooling of neutron stars, *Phys. Rev. D* 93 (6) (2016) 065044. [arXiv:1512.07828](#), [doi:10.1103/PhysRevD.93.065044](#).
 - [429] K. Hamaguchi, N. Nagata, K. Yanagi, J. Zheng, Limit on the Axion Decay Constant from the Cooling Neutron Star in Cassiopeia A, *Phys. Rev. D* 98 (10) (2018) 103015. [arXiv:1806.07151](#), [doi:10.1103/PhysRevD.98.103015](#).
 - [430] M. V. Beznogov, E. Rrapaj, D. Page, S. Reddy, Constraints on Axion-like Particles and Nucleon Pairing in Dense Matter from the Hot Neutron Star in HESS J1731-347, *Phys. Rev. C* 98 (3) (2018) 035802. [arXiv:1806.07991](#), [doi:10.1103/PhysRevC.98.035802](#).
 - [431] A. Sedrakian, Axion cooling of neutron stars. II. Beyond hadronic axions, *Phys. Rev. D* 99 (4) (2019) 043011. [arXiv:1810.00190](#), [doi:10.1103/PhysRevD.99.043011](#).
 - [432] L. B. Leinson, Axion mass limit from observations of the neutron star in Cassiopeia A, *JCAP* 1408 (2014) 031. [arXiv:1405.6873](#), [doi:10.1088/1475-7516/2014/08/031](#).
 - [433] L. B. Leinson, Superfluid phases of triplet pairing and rapid cooling of the neutron star in Cassiopeia A, *Phys. Lett. B* 741 (2015) 87–91. [arXiv:1411.6833](#), [doi:10.1016/j.physletb.2014.12.017](#).
 - [434] P. W. Graham, S. Rajendran, New Observables for Direct Detection of Axion Dark Matter, *Phys. Rev. D* 88 (2013) 035023. [arXiv:1306.6088](#), [doi:10.1103/PhysRevD.88.035023](#).
 - [435] G. Raffelt, Limits on a CP-violating scalar axion-nucleon interaction, *Phys. Rev. D* 86 (2012) 015001. [arXiv:1205.1776](#), [doi:10.1103/PhysRevD.86.015001](#).
 - [436] E. Hardy, R. Lasenby, Stellar cooling bounds on new light particles: plasma mixing effects, *JHEP* 02 (2017) 033. [arXiv:1611.05852](#), [doi:10.1007/JHEP02\(2017\)033](#).
 - [437] R. Penrose, Gravitational collapse: The role of general relativity, *Riv. Nuovo Cim.* 1 (1969) 252–276, [Gen. Rel. Grav. 34,1141(2002)].
 - [438] V. Cardoso, Ó. J. C. Dias, G. S. Hartnett, M. Middleton, P. Pani, J. E. Santos, Constraining the mass of dark photons and axion-like particles through black-hole superradiance, *JCAP* 1803 (03) (2018) 043. [arXiv:1801.01420](#), [doi:10.1088/1475-7516/2018/03/043](#).
 - [439] A. Arvanitaki, M. Baryakhtar, S. Dimopoulos, S. Dubovsky, R. Lasenby, Black Hole Mergers and the QCD Axion at Advanced LIGO, *Phys. Rev. D* 95 (4) (2017) 043001. [arXiv:1604.03958](#), [doi:10.1103/PhysRevD.95.043001](#).
 - [440] T. Fischer, S. Chakraborty, M. Giannotti, A. Mirizzi, A. Payez, A. Ringwald, Probing axions with the neutrino signal from the next galactic supernova, *Phys. Rev. D* 94 (8) (2016) 085012. [arXiv:1605.08780](#), [doi:10.1103/PhysRevD.94.085012](#).
 - [441] S. Andriamonje, et al., An Improved limit on the axion-photon coupling from the CAST experiment, *JCAP* 0704 (2007) 010. [arXiv:hep-ex/0702006](#), [doi:10.1088/1475-7516/2007/04/010](#).
 - [442] K. Barth, et al., CAST constraints on the axion-electron coupling, *JCAP* 1305 (2013) 010. [arXiv:1302.6283](#), [doi:10.1088/1475-7516/2013/05/010](#).
 - [443] J. Jaeckel, L. J. Thormaehlen, Distinguishing Axion Models with IAXO, *JCAP* 1903 (03) (2019) 039. [arXiv:1811.09278](#), [doi:10.1088/1475-7516/2019/03/039](#).
 - [444] P. Sikivie, Experimental Tests of the Invisible Axion, *Phys. Rev. Lett.* 51 (1983) 1415–1417, [321(1983)]. [doi:10.1103/PhysRevLett.51.1415](#), [doi:10.1103/PhysRevLett.52.695.2](#).
 - [445] E. A. Paschos, K. Zioutas, A Proposal for solar axion detection via Bragg scattering, *Phys. Lett. B* 323 (1994) 367–372. [doi:10.1016/0370-2693\(94\)91233-5](#).
 - [446] A. V. Derbin, A. S. Kayunov, V. N. Muratova, D. A. Semenov, E. V. Unzhakov, Constraints on the axion-electron coupling for solar axions produced by Compton process and bremsstrahlung, *Phys. Rev. D* 83 (2011) 023505. [arXiv:1101.2290](#), [doi:10.1103/PhysRevD.83.023505](#).
 - [447] K. Arisaka, P. Beltrame, C. Ghag, J. Kaidi, K. Lung, A. Lyashenko, R. D. Peccei, P. Smith, K. Ye, Expected Sensitivity to Galactic/Solar Axions and Bosonic Super-WIMPs based on the Axio-electric Effect in Liquid Xenon Dark Matter Detectors, *Astropart. Phys.* 44 (2013) 59–67. [arXiv:1209.3810](#), [doi:10.1016/j.astropartphys.2012.12.009](#).
 - [448] T. Dafni, C. A. J. O’Hare, B. Lakić, J. Galán, F. J. Iguaiz, I. G. Irastorza, K. Jakovčić, G. Luzón, J. Redondo, E. Ruiz Chóliz, Weighing the solar axion, *Phys. Rev. D* 99 (3) (2019) 035037. [arXiv:1811.09290](#), [doi:10.1103/PhysRevD.99.035037](#).
 - [449] K. van Bibber, P. M. McIntyre, D. E. Morris, G. G. Raffelt, A Practical Laboratory Detector for Solar Axions, *Phys. Rev. D* 39 (1989) 2089. [doi:10.1103/PhysRevD.39.2089](#).
 - [450] K. Zioutas, et al., A Decommissioned LHC model magnet as an axion telescope, *Nucl. Instrum. Meth. A* 425 (1999) 480–489. [arXiv:astro-ph/9801176](#), [doi:10.1016/S0168-9002\(98\)01442-9](#).
 - [451] V. Anastassopoulos, et al., New CAST Limit on the Axion-Photon Interaction, *Nature Phys.* 13 (2017) 584–590. [arXiv:1705.02290](#), [doi:10.1038/nphys4109](#).
 - [452] I. G. Irastorza, et al., Towards a new generation axion helioscope, *JCAP* 1106 (2011) 013. [arXiv:1103.5334](#), [doi:10.1088/1475-7516/2011/06/013](#).
 - [453] F. T. Avignone, III, et al., Experimental search for solar axions via coherent Primakoff conversion in a germanium spectrometer, *Phys. Rev. Lett.* 81 (1998) 5068–5071. [arXiv:astro-ph/9708008](#), [doi:10.1103/PhysRevLett.81.5068](#).
 - [454] E. Aprile, et al., First Axion Results from the XENON100 Experiment, *Phys. Rev. D* 90 (6) (2014) 062009, [Erratum: *Phys. Rev. D* 95, no. 2, 029904 (2017)]. [arXiv:1404.1455](#), [doi:10.1103/PhysRevD.90.062009](#), [doi:10.1103/PhysRevD.95.029904](#).
 - [455] D. S. Akerib, et al., First Searches for Axions and Axionlike Particles with the LUX Experiment, *Phys. Rev. Lett.* 118 (26) (2017) 261301. [arXiv:1704.02297](#), [doi:10.1103/PhysRevLett.118.261301](#).
 - [456] C. Fu, et al., Limits on Axion Couplings from the First 80 Days of Data of the PandaX-II Experiment, *Phys. Rev. Lett.* 119 (18) (2017) 181806. [arXiv:1707.07921](#), [doi:10.1103/PhysRevLett.119.181806](#).
 - [457] S. Dimopoulos, G. D. Starkman, B. W. Lynn, Atomic Enhancements in the Detection of Axions, *Mod. Phys. Lett. A* 1

- (1986) 491–500. [doi:10.1142/S0217732386000622](#).
- [458] M. Pospelov, A. Ritz, M. B. Voloshin, Bosonic super-WIMPs as keV-scale dark matter, *Phys. Rev. D* 78 (2008) 115012. [arXiv:0807.3279](#), [doi:10.1103/PhysRevD.78.115012](#).
- [459] A. Derevianko, V. A. Dzuba, V. V. Flambaum, M. Pospelov, Axio-electric effect, *Phys. Rev. D* 82 (2010) 065006. [arXiv:1007.1833](#), [doi:10.1103/PhysRevD.82.065006](#).
- [460] N. Du, et al., A Search for Invisible Axion Dark Matter with the Axion Dark Matter Experiment, *Phys. Rev. Lett.* 120 (15) (2018) 151301. [arXiv:1804.05750](#), [doi:10.1103/PhysRevLett.120.151301](#).
- [461] R. Dicke, The Measurement of Thermal Radiation at Microwave Frequencies, *Rev. of Sci. Instr.* 17 (1946) 268–275. [doi:10.1063/1.1770483](#).
- [462] J. Kim, S. Youn, J. Jeong, W. Chung, O. Kwon, Y. K. Semertzidis, Exploiting higher-order resonant modes for axion haloscopes, *J. Phys. G* 47 (3) (2020) 035203. [arXiv:1910.00793](#), [doi:10.1088/1361-6471/ab5ace](#).
- [463] S. Lee, S. Ahn, J. Choi, B. R. Ko, Y. K. Semertzidis, CAPP-8TB: Search for Axion Dark Matter in a Mass Range of 6.62 to 7.04 μeV , 2019. [arXiv:1910.00047](#).
- [464] B. M. Brubaker, et al., First results from a microwave cavity axion search at 24 μeV , *Phys. Rev. Lett.* 118 (6) (2017) 061302. [arXiv:1610.02580](#), [doi:10.1103/PhysRevLett.118.061302](#).
- [465] B. T. McAllister, G. Flower, E. N. Ivanov, M. Goryachev, J. Bourhill, M. E. Tobar, The ORGAN Experiment: An axion haloscope above 15 GHz, *Phys. Dark Univ.* 18 (2017) 67–72. [arXiv:1706.00209](#), [doi:10.1016/j.dark.2017.09.010](#).
- [466] P. Brun, et al., A new experimental approach to probe QCD axion dark matter in the mass range above 40 μeV , *Eur. Phys. J. C* 79 (3) (2019) 186. [arXiv:1901.07401](#), [doi:10.1140/epjc/s10052-019-6683-x](#).
- [467] M. Lawson, A. J. Millar, M. Pancaldi, E. Vitagliano, F. Wilczek, Tunable axion plasma haloscopes, *Phys. Rev. Lett.* 123 (2019) 141802. [arXiv:1904.11872](#), [doi:10.1103/PhysRevLett.123.141802](#).
- [468] D. J. E. Marsh, K.-C. Fong, E. W. Lentz, L. Smejkal, M. N. Ali, Proposal to Detect Dark Matter using Axionic Topological Antiferromagnets, *Phys. Rev. Lett.* 123 (12) (2019) 121601. [arXiv:1807.08810](#), [doi:10.1103/PhysRevLett.123.121601](#).
- [469] R. Barbieri, C. Braggio, G. Carugno, C. S. Gallo, A. Lombardi, A. Ortolan, R. Pengo, G. Ruoso, C. C. Speake, Searching for galactic axions through magnetized media: the QUAX proposal, *Phys. Dark Univ.* 15 (2017) 135–141. [arXiv:1606.02201](#), [doi:10.1016/j.dark.2017.01.003](#).
- [470] N. Crescini, et al., Operation of a ferromagnetic axion haloscope at $m_a = 58 \mu\text{eV}$, *Eur. Phys. J. C* 78 (9) (2018) 703, [Erratum: *Eur. Phys. J. C* 78, no. 9, 813 (2018)]. [arXiv:1806.00310](#), [doi:10.1140/epjc/s10052-018-6262-6](#), [doi:10.1140/epjc/s10052-018-6163-8](#).
- [471] A. Hook, Y. Kahn, B. R. Safdi, Z. Sun, Radio Signals from Axion Dark Matter Conversion in Neutron Star Magnetospheres, *Phys. Rev. Lett.* 121 (24) (2018) 241102. [arXiv:1804.03145](#), [doi:10.1103/PhysRevLett.121.241102](#).
- [472] T. D. Edwards, M. Chianese, B. J. Kavanagh, S. M. Nissanke, C. Weniger, A Unique Multi-Messenger Signal of QCD Axion Dark Matter, *Phys. Rev. Lett.* 124 (16) (2020) 161101. [arXiv:1905.04686](#), [doi:10.1103/PhysRevLett.124.161101](#).
- [473] M. Leroy, M. Chianese, T. D. P. Edwards, C. Weniger, Radio Signal of Axion Photon Conversion in Neutron Stars: A Ray Tracing Analysis (2019). [arXiv:1912.08815](#).
- [474] D. J. Bacon, et al., Cosmology with Phase 1 of the Square Kilometre Array: Red Book 2018: Technical specifications and performance forecasts, Submitted to: *Publ. Astron. Soc. Austral.* (2018). [arXiv:1811.02743](#).
- [475] A. Caputo, C. P. Garay, S. J. Witte, Looking for Axion Dark Matter in Dwarf Spheroidals, *Phys. Rev. D* 98 (8) (2018) 083024, [Erratum: *Phys. Rev. D* 99, no. 8, 089901 (2019)]. [arXiv:1805.08780](#), [doi:10.1103/PhysRevD.98.083024](#).
- [476] A. Caputo, M. Regis, M. Taoso, S. J. Witte, Detecting the Stimulated Decay of Axions at RadioFrequencies, *JCAP* 1903 (03) (2019) 027. [arXiv:1811.08436](#), [doi:10.1088/1475-7516/2019/03/027](#).
- [477] D. F. Jackson Kimball, et al., Overview of the Cosmic Axion Spin Precession Experiment (CASPER). (2017). [arXiv:1711.08999](#).
- [478] K. Van Bibber, N. R. Dagdeviren, S. E. Koonin, A. Kerman, H. N. Nelson, Proposed experiment to produce and detect light pseudoscalars, *Phys. Rev. Lett.* 59 (1987) 759–762. [doi:10.1103/PhysRevLett.59.759](#).
- [479] R. Ballou, et al., New exclusion limits on scalar and pseudoscalar axionlike particles from light shining through a wall, *Phys. Rev. D* 92 (9) (2015) 092002. [arXiv:1506.08082](#), [doi:10.1103/PhysRevD.92.092002](#).
- [480] F. Della Valle, A. Ejlli, U. Gastaldi, G. Messineo, E. Milotti, R. Pengo, G. Ruoso, G. Zavattini, The PVLAS experiment: measuring vacuum magnetic birefringence and dichroism with a birefringent Fabry–Perot cavity, *Eur. Phys. J. C* 76 (1) (2016) 24. [arXiv:1510.08052](#), [doi:10.1140/epjc/s10052-015-3869-8](#).
- [481] R. Ballou, F. Della Valle, A. Ejlli, U. Gastaldi, H. Grote, S. Kunc, K. Meissner, E. Milotti, W.-T. Ni, S.-s. Pan, R. Pengo, P. Pugnat, G. Ruoso, A. Siemko, M. Sulc, G. Zavattini, Letter of Intent to measure Vacuum Magnetic Birefringence: the VMB@CERN experiment, *Tech. Rep. CERN-SPSC-2018-036. SPSC-I-249*, CERN, Geneva (Dec 2018).
- [482] A. Arvanitaki, A. A. Geraci, Resonantly Detecting Axion-Mediated Forces with Nuclear Magnetic Resonance, *Phys. Rev. Lett.* 113 (16) (2014) 161801. [arXiv:1403.1290](#), [doi:10.1103/PhysRevLett.113.161801](#).
- [483] A. A. Geraci, et al., Progress on the ARIADNE axion experiment, *Springer Proc. Phys.* 211 (2018) 151–161. [arXiv:1710.05413](#), [doi:10.1007/978-3-319-92726-8_18](#).
- [484] N. Crescini, C. Braggio, G. Carugno, P. Falferi, A. Ortolan, G. Ruoso, Improved constraints on monopole-dipole interaction mediated by pseudo-scalar bosons, *Phys. Lett. B* 773 (2017) 677–680. [arXiv:1705.06044](#), [doi:10.1016/j.physletb.2017.09.019](#).
- [485] M. Ajello, et al., Search for Spectral Irregularities due to Photon–Axionlike-Particle Oscillations with the Fermi Large Area Telescope, *Phys. Rev. Lett.* 116 (16) (2016) 161101. [arXiv:1603.06978](#), [doi:10.1103/PhysRevLett.116.161101](#).
- [486] A. Payez, C. Evoli, T. Fischer, M. Giannotti, A. Mirizzi, A. Ringwald, Revisiting the SN1987A gamma-ray limit on ultralight axion-like particles, *JCAP* 1502 (02) (2015) 006. [arXiv:1410.3747](#), [doi:10.1088/1475-7516/2015/02/006](#).
- [487] M. Meyer, M. Giannotti, A. Mirizzi, J. Conrad, M. A. Sánchez-Conde, Fermi Large Area Telescope as a Galactic

- Supernovae Axionscope, Phys. Rev. Lett. 118 (1) (2017) 011103. [arXiv:1609.02350](#), [doi:10.1103/PhysRevLett.118.011103](#).
- [488] T. Schmidt, Über die magnetischen Momente der Atomkerne. , Zeitschrift für Physik 106 (5-6) (1937) 358–361. [doi:10.1007/BF01338744](#).
- [489] D. F. Jackson Kimball, Nuclear spin content and constraints on exotic spin-dependent couplings. , New J. Phys. 17 (7) (2015) 073008. [arXiv:1407.2671](#), [doi:10.1088/1367-2630/17/7/073008](#).
- [490] T. Wu, et al., Search for Axionlike Dark Matter with a Liquid-State Nuclear Spin Comagnetometer. , Phys. Rev. Lett. 122 (19) (2019) 191302. [arXiv:1901.10843](#), [doi:10.1103/PhysRevLett.123.169002](#), [doi:10.1103/PhysRevLett.122.191302](#).
- [491] N. Crisosto, G. Rybka, P. Sikivie, N. S. Sullivan, D. B. Tanner, J. Yang, ADMX SLIC: Results from a Superconducting LC Circuit Investigating Cold Axions (2019). [arXiv:1911.05772](#).
- [492] V. Anastassopoulos, et al., Towards a medium-scale axion helioscope and haloscope, JINST 12 (11) (2017) P11019. [arXiv:1706.09378](#), [doi:10.1088/1748-0221/12/11/P11019](#).
- [493] G. Rybka, A. Wagner, A. Brill, K. Ramos, R. Percival, K. Patel, Search for dark matter axions with the Orpheus experiment, Phys. Rev. D91 (1) (2015) 011701. [arXiv:1403.3121](#), [doi:10.1103/PhysRevD.91.011701](#).
- [494] A. Á. Melcón, et al., Axion Searches with Microwave Filters: the RADES project, JCAP 1805 (05) (2018) 040. [arXiv:1803.01243](#), [doi:10.1088/1475-7516/2018/05/040](#).
- [495] A. Á. Melcón, et al., Scalable haloscopes for axion dark matter detection in the $30\mu\text{eV}$ range with RADES (2020). [arXiv:2002.07639](#).
- [496] M. Baryakhtar, J. Huang, R. Lasenby, Axion and hidden photon dark matter detection with multilayer optical haloscopes, Phys. Rev. D98 (3) (2018) 035006. [arXiv:1803.11455](#), [doi:10.1103/PhysRevD.98.035006](#).
- [497] B. T. McAllister, M. Goryachev, J. Bourhill, E. N. Ivanov, M. E. Tobar, Broadband Axion Dark Matter Haloscopes via Electric Sensing (2018). [arXiv:1803.07755](#).
- [498] L. Capparelli, G. Cavoto, J. Ferretti, F. Giazotto, A. D. Polosa, P. Spagnolo, Axion-like particle searches with sub-THz photons, Phys. Dark Univ. 12 (2016) 37–44. [arXiv:1510.06892](#), [doi:10.1016/j.dark.2016.01.003](#).
- [499] P. Spagnolo, STAX: a new technique for detecting Axions, PoS ICHEP2016 (2016) 207. [doi:10.22323/1.282.0207](#).
- [500] J. Ferretti, STAX. An Axion-like Particle Search with Microwave Photons, in: Proceedings, 12th Patras Workshop on Axions, WIMPs and WISPs (PATRAS 2016): Jeju Island, South Korea, June 20–24, 2016, 2017, pp. 35–38. [arXiv:1609.05105](#), [doi:10.3204/DESY-PROC-2009-03/Ferretti_Jacopo](#).
- [501] L. Santamaria, C. Braggio, G. Carugno, V. D. Sarno, P. Maddaloni, G. Ruoso, Axion dark matter detection by laser spectroscopy of ultracold molecular oxygen: a proposal, New Journal of Physics 17 (11) (2015) 113025. [doi:10.1088/1367-2630/17/11/113025](#).
- [502] C. Braggio, et al., New detectors for axions, PoS IFD2015 (2017) 032. [doi:10.22323/1.266.0032](#).
- [503] S. Pustelny, et al., The Global Network of Optical Magnetometers for Exotic physics (GNOME): A novel scheme to search for physics beyond the Standard Model, Annalen Phys. 525 (8–9) (2013) 659–670. [arXiv:1303.5524](#), [doi:10.1002/andp.201300061](#).
- [504] E. Farhi, L. Susskind, Technicolor, Phys. Rept. 74 (1981) 277. [doi:10.1016/0370-1573\(81\)90173-3](#).
- [505] J. E. Kim, A composite invisible axion, Phys. Rev. D31 (1985) 1733. [doi:10.1103/PhysRevD.31.1733](#).
- [506] S. L. Cheng, C. Q. Geng, W. T. Ni, Axion - photon couplings in invisible axion models, Phys. Rev. D52 (1995) 3132–3135. [arXiv:hep-ph/9506295](#), [doi:10.1103/PhysRevD.52.3132](#).
- [507] L. Di Luzio, F. Mescia, E. Nardi, Redefining the Axion Window, Phys. Rev. Lett. 118 (2017) 031801. [arXiv:1610.07593](#), [doi:10.1103/PhysRevLett.118.031801](#).
- [508] K. Choi, J. E. Kim, DYNAMICAL AXION, Phys. Rev. D32 (1985) 1828. [doi:10.1103/PhysRevD.32.1828](#).
- [509] L. Di Luzio, F. Mescia, E. Nardi, Window for preferred axion models, Phys. Rev. D96 (7) (2017) 075003. [arXiv:1705.05370](#), [doi:10.1103/PhysRevD.96.075003](#).
- [510] P. Sikivie, Of Axions, Domain Walls and the Early Universe, Phys. Rev. Lett. 48 (1982) 1156–1159. [doi:10.1103/PhysRevLett.48.1156](#).
- [511] S. P. Robinson, F. Wilczek, Gravitational correction to running of gauge couplings, Phys. Rev. Lett. 96 (2006) 231601. [arXiv:hep-th/0509050](#), [doi:10.1103/PhysRevLett.96.231601](#).
- [512] L. Di Luzio, R. Grober, J. F. Kamenik, M. Nardecchia, Accidental matter at the LHC, JHEP 07 (2015) 074. [arXiv:1504.00359](#), [doi:10.1007/JHEP07\(2015\)074](#).
- [513] M. L. Perl, E. R. Lee, D. Loomba, Searches for fractionally charged particles, Ann. Rev. Nucl. Part. Sci. 59 (2009) 47–65. [doi:10.1146/annurev-nucl-121908-122035](#).
- [514] C. B. Dover, T. K. Gaisser, G. Steigman, Cosmological constraints on new stable hadrons, Phys. Rev. Lett. 42 (1979) 1117. [doi:10.1103/PhysRevLett.42.1117](#).
- [515] E. Nardi, E. Roulet, Are exotic stable quarks cosmologically allowed?, Phys. Lett. B245 (1990) 105–110. [doi:10.1016/0370-2693\(90\)90172-3](#).
- [516] A. Arvanitaki, C. Davis, P. W. Graham, A. Pierce, J. G. Wacker, Limits on split supersymmetry from gluino cosmology, Phys. Rev. D72 (2005) 075011. [arXiv:hep-ph/0504210](#), [doi:10.1103/PhysRevD.72.075011](#).
- [517] J. Kang, M. A. Luty, S. Nasri, The Relic abundance of long-lived heavy colored particles, JHEP 09 (2008) 086. [arXiv:hep-ph/0611322](#), [doi:10.1088/1126-6708/2008/09/086](#).
- [518] C. Jacoby, S. Nussinov, The Relic Abundance of Massive Colored Particles after a Late Hadronic Annihilation Stage. (2007). [arXiv:0712.2681](#).
- [519] M. Kusakabe, T. Takesako, Resonant annihilation of long-lived massive colored particles through hadronic collisions, Phys. Rev. D85 (2012) 015005. [arXiv:1112.0860](#), [doi:10.1103/PhysRevD.85.015005](#).
- [520] S. Dimopoulos, D. Eichler, R. Esmailzadeh, G. D. Starkman, Getting a Charge Out of Dark Matter, Phys. Rev. D41

- (1990) 2388. [doi:10.1103/PhysRevD.41.2388](#).
- [521] L. Chuzhoy, E. W. Kolb, Reopening the window on charged dark matter, JCAP 0907 (2009) 014. [arXiv:0809.0436](#), [doi:10.1088/1475-7516/2009/07/014](#).
 - [522] S. Burdin, M. Fairbairn, P. Mermod, D. Milstead, J. Pinfold, T. Sloan, W. Taylor, Non-collider searches for stable massive particles, Phys. Rept. 582 (2015) 1–52. [arXiv:1410.1374](#), [doi:10.1016/j.physrep.2015.03.004](#).
 - [523] M. P. Hertzberg, A. Masoumi, Astrophysical Constraints on Singlet Scalars at LHC, JCAP 1704 (04) (2017) 028. [arXiv:1607.06445](#), [doi:10.1088/1475-7516/2017/04/028](#).
 - [524] A. Gould, B. T. Draine, R. W. Romani, S. Nussinov, Neutron Stars: Graveyard of Charged Dark Matter, Phys. Lett. B238 (1990) 337. [doi:10.1016/0370-2693\(90\)91745-W](#).
 - [525] G. D. Mack, J. F. Beacom, G. Bertone, Towards Closing the Window on Strongly Interacting Dark Matter: Far-Reaching Constraints from Earth's Heat Flow, Phys. Rev. D76 (2007) 043523. [arXiv:0705.4298](#), [doi:10.1103/PhysRevD.76.043523](#).
 - [526] M. Kawasaki, K. Kohri, T. Moroi, Big-Bang nucleosynthesis and hadronic decay of long-lived massive particles, Phys. Rev. D71 (2005) 083502. [arXiv:astro-ph/0408426](#), [doi:10.1103/PhysRevD.71.083502](#).
 - [527] K. Jedamzik, Big bang nucleosynthesis constraints on hadronically and electromagnetically decaying relic neutral particles, Phys. Rev. D74 (2006) 103509. [arXiv:hep-ph/0604251](#), [doi:10.1103/PhysRevD.74.103509](#).
 - [528] K. Jedamzik, Bounds on long-lived charged massive particles from Big Bang nucleosynthesis, JCAP 0803 (2008) 008. [arXiv:0710.5153](#), [doi:10.1088/1475-7516/2008/03/008](#).
 - [529] M. Kawasaki, K. Kohri, T. Moroi, Y. Takaesu, Revisiting Big-Bang Nucleosynthesis Constraints on Long-Lived Decaying Particles, Phys. Rev. D97 (2) (2018) 023502. [arXiv:1709.01211](#), [doi:10.1103/PhysRevD.97.023502](#).
 - [530] W. Hu, J. Silk, Thermalization constraints and spectral distortions for massive unstable relic particles, Phys. Rev. Lett. 70 (1993) 2661–2664. [doi:10.1103/PhysRevLett.70.2661](#).
 - [531] J. Chluba, R. A. Sunyaev, The evolution of CMB spectral distortions in the early Universe, Mon. Not. Roy. Astron. Soc. 419 (2012) 1294–1314. [arXiv:1109.6552](#), [doi:10.1111/j.1365-2966.2011.19786.x](#).
 - [532] J. Chluba, Distinguishing different scenarios of early energy release with spectral distortions of the cosmic microwave background, Mon. Not. Roy. Astron. Soc. 436 (2013) 2232–2243. [arXiv:1304.6121](#), [doi:10.1093/mnras/stt1733](#).
 - [533] G. D. Kribs, I. Z. Rothstein, Bounds on longlived relics from diffuse gamma-ray observations, Phys. Rev. D55 (1997) 4435–4449, [Erratum: Phys. Rev.D56,1822(1997)]. [arXiv:hep-ph/9610468](#), [doi:10.1103/PhysRevD.56.1822](#), [doi:10.1103/PhysRevD.55.4435](#).
 - [534] M. Ackermann, et al., Fermi LAT Search for Dark Matter in Gamma-ray Lines and the Inclusive Photon Spectrum, Phys. Rev. D86 (2012) 022002. [arXiv:1205.2739](#), [doi:10.1103/PhysRevD.86.022002](#).
 - [535] G. F. Giudice, R. Rattazzi, A. Strumia, Unification, Phys. Lett. B715 (2012) 142–148. [arXiv:1204.5465](#), [doi:10.1016/j.physletb.2012.07.028](#).
 - [536] J. E. Kim, Constraints on very light axions from cavity experiments, Phys. Rev. D58 (1998) 055006. [arXiv:hep-ph/9802220](#), [doi:10.1103/PhysRevD.58.055006](#).
 - [537] K. Choi, H. Kim, S. Yun, Natural inflation with multiple sub-Planckian axions, Phys. Rev. D90 (2014) 023545. [arXiv:1404.6209](#), [doi:10.1103/PhysRevD.90.023545](#).
 - [538] K. Choi, S. H. Im, Realizing the relaxation from multiple axions and its UV completion with high scale supersymmetry, JHEP 01 (2016) 149. [arXiv:1511.00132](#), [doi:10.1007/JHEP01\(2016\)149](#).
 - [539] D. E. Kaplan, R. Rattazzi, Large field excursions and approximate discrete symmetries from a clockwork axion, Phys. Rev. D93 (8) (2016) 085007. [arXiv:1511.01827](#), [doi:10.1103/PhysRevD.93.085007](#).
 - [540] G. F. Giudice, M. McCullough, A Clockwork Theory, JHEP 02 (2017) 036. [arXiv:1610.07962](#), [doi:10.1007/JHEP02\(2017\)036](#).
 - [541] M. Farina, D. Pappadopulo, F. Rompineve, A. Tesi, The photo-philic QCD axion, JHEP 01 (2017) 095. [arXiv:1611.09855](#), [doi:10.1007/JHEP01\(2017\)095](#).
 - [542] T. Higaki, K. S. Jeong, N. Kitajima, F. Takahashi, The QCD Axion from Aligned Axions and Diphoton Excess, Phys. Lett. B755 (2016) 13–16. [arXiv:1512.05295](#), [doi:10.1016/j.physletb.2016.01.055](#).
 - [543] T. Higaki, K. S. Jeong, N. Kitajima, F. Takahashi, Quality of the Peccei-Quinn symmetry in the Aligned QCD Axion and Cosmological Implications, JHEP 06 (2016) 150. [arXiv:1603.02090](#), [doi:10.1007/JHEP06\(2016\)150](#).
 - [544] T. Higaki, K. S. Jeong, N. Kitajima, T. Sekiguchi, F. Takahashi, Topological Defects and nano-Hz Gravitational Waves in Aligned Axion Models, JHEP 08 (2016) 044. [arXiv:1606.05552](#), [doi:10.1007/JHEP08\(2016\)044](#).
 - [545] A. J. Long, Cosmological Aspects of the Clockwork Axion, JHEP 07 (2018) 066. [arXiv:1803.07086](#), [doi:10.1007/JHEP07\(2018\)066](#).
 - [546] P. Agrawal, J. Fan, M. Reece, L.-T. Wang, Experimental Targets for Photon Couplings of the QCD Axion, JHEP 02 (2018) 006. [arXiv:1709.06085](#), [doi:10.1007/JHEP02\(2018\)006](#).
 - [547] R. Daido, F. Takahashi, N. Yokozaki, Enhanced axion-photon coupling in GUT with hidden photon, Phys. Lett. B780 (2018) 538–542. [arXiv:1801.10344](#), [doi:10.1016/j.physletb.2018.03.039](#).
 - [548] M. Shin, Light Neutrino Masses and Strong CP Problem, Phys. Rev. Lett. 59 (1987) 2515, [Erratum: Phys. Rev. Lett. 60,383(1988)]. [doi:10.1103/PhysRevLett.60.383](#), [doi:10.1103/PhysRevLett.59.2515](#).
 - [549] A. Pilaftsis, Astrophysical and terrestrial constraints on singlet Majoron models, Phys. Rev. D49 (1994) 2398–2404. [arXiv:hep-ph/9308258](#), [doi:10.1103/PhysRevD.49.2398](#).
 - [550] C. Garcia-Cely, J. Heck, Neutrino Lines from Majoron Dark Matter, JHEP 05 (2017) 102. [arXiv:1701.07209](#), [doi:10.1007/JHEP05\(2017\)102](#).
 - [551] L. Di Luzio, F. Mescia, E. Nardi, P. Panci, R. Ziegler, Astrophobic Axions, Phys. Rev. Lett. 120 (26) (2018) 261803. [arXiv:1712.04940](#), [doi:10.1103/PhysRevLett.120.261803](#).

- [552] G. Marques-Tavares, M. Teo, Light axions with large hadronic couplings, JHEP 05 (2018) 180. [arXiv:1803.07575](#), [doi:10.1007/JHEP05\(2018\)180](#).
- [553] L. Darmé, L. Di Luzio, E. Nardi, Exponential enhancement of the axion coupling to nucleons. In preparation (2020).
- [554] L. M. Krauss, D. J. Nash, A viable weak interaction axion?, Phys. Lett. B202 (1988) 560–567. [doi:10.1016/0370-2693\(88\)91864-3](#).
- [555] M. Hindmarsh, P. Moulatsiotis, Constraints on variant axion models, Phys. Rev. D56 (1997) 8074–8081. [arXiv:hep-ph/9708281](#), [doi:10.1103/PhysRevD.56.8074](#).
- [556] K. Saikawa, T. T. Yanagida, Stellar cooling anomalies and variant axion models, JCAP 03 (2020) 007. [arXiv:1907.07662](#), [doi:10.1088/1475-7516/2020/03/007](#).
- [557] F. Björkeröth, L. Di Luzio, F. Mescia, E. Nardi, $U(1)$ flavour symmetries as Peccei-Quinn symmetries, JHEP 02 (2019) 133. [arXiv:1811.09637](#), [doi:10.1007/JHEP02\(2019\)133](#).
- [558] F. Björkeröth, L. Di Luzio, F. Mescia, E. Nardi, Covert symmetries in the neutrino mass matrix, JHEP 02 (2020) 066. [arXiv:1910.00576](#), [doi:10.1007/JHEP02\(2020\)066](#).
- [559] M. Buschmann, R. T. Co, C. Dessert, B. R. Safdi, X-ray Search for Axions from Nearby Isolated Neutron Stars (2019). [arXiv:1910.04164](#).
- [560] W. A. Bardeen, S. H. H. Tye, Current Algebra Applied to Properties of the Light Higgs Boson, Phys. Lett. 74B (1978) 229–232. [doi:10.1016/0370-2693\(78\)90560-9](#).
- [561] F. Wilczek, Axions and Family Symmetry Breaking, Phys. Rev. Lett. 49 (1982) 1549–1552. [doi:10.1103/PhysRevLett.49.1549](#).
- [562] J. Schweppe, et al., Observation of a peak structure in positron spectra from $U + Cm$ collisions, Phys. Rev. Lett. 51 (1983) 2261–2264. [doi:10.1103/PhysRevLett.51.2261](#).
- [563] M. Clemente, E. Berdermann, P. Kienle, H. Tsertos, W. Wagner, C. Kozhuharov, F. Bosch, W. König, Narrow positron lines from $U - U$ and $U - Th$ collisions, Phys. Lett. 137B (1984) 41–46. [doi:10.1016/0370-2693\(84\)91102-X](#).
- [564] T. Cowan, et al., Anomalous positron peaks from supercritical collisions systems, Phys. Rev. Lett. 54 (1985) 1761–1764. [doi:10.1103/PhysRevLett.54.1761](#).
- [565] T. Cowan, et al., Observation of Correlated Narrow Peak Structures in Positron and electron Spectra from Superheavy Collision Systems, Phys. Rev. Lett. 56 (1986) 444–447. [doi:10.1103/PhysRevLett.56.444](#).
- [566] A. Schafer, J. Reinhardt, B. Müller, W. Greiner, G. Soff, Is there Evidence for the Production of a New Particle in Heavy Ion Collisions?, J. Phys. G11 (1985) L69–L74. [doi:10.1088/0305-4616/11/5/001](#).
- [567] A. B. Balantekin, C. Bottcher, M. R. Strayer, S. J. Lee, Phenomenology of New Particle Production in Heavy Ion Collisions, Phys. Rev. Lett. 55 (1985) 461. [doi:10.1103/PhysRevLett.55.461](#).
- [568] R. D. Peccei, T. T. Wu, T. Yanagida, A viable axion model, Phys. Lett. B172 (1986) 435–440. [doi:10.1016/0370-2693\(86\)90284-4](#).
- [569] L. M. Krauss, F. Wilczek, A short lived axion variant, Phys. Lett. B173 (1986) 189–192. [doi:10.1016/0370-2693\(86\)90244-3](#).
- [570] C. Q. Geng, J. N. Ng, Flavor Connections and Neutrino Mass Hierarchy Invariant Invisible Axion Models Without Domain Wall Problem, Phys. Rev. D39 (1989) 1449. [doi:10.1103/PhysRevD.39.1449](#).
- [571] G. Mageras, P. Franzini, P. M. Tuts, S. Youssef, T. Zhao, J. Lee-Franzini, R. D. Schamberger, Search for Shortlived Axions in Radiative Υ Decays, Phys. Rev. Lett. 56 (1986) 2672–2675. [doi:10.1103/PhysRevLett.56.2672](#).
- [572] T. J. V. Bowcock, et al., Upper Limits for the Production of Light Shortlived Neutral Particles in Radiative Υ Decay, Phys. Rev. Lett. 56 (1986) 2676. [doi:10.1103/PhysRevLett.56.2676](#).
- [573] C. N. Brown, et al., A New Limit on Axion Production in 800-GeV Hadronic Showers, Phys. Rev. Lett. 57 (1986) 2101. [doi:10.1103/PhysRevLett.57.2101](#).
- [574] A. L. Hallin, F. P. Calaprice, R. W. Dunford, A. B. McDonald, Restrictions on a 1.7-MeV Axion From Nuclear Pair Transitions, Phys. Rev. Lett. 57 (1986) 2105–2108. [doi:10.1103/PhysRevLett.57.2105](#).
- [575] M. Davier, J. Jeanjean, H. Nguyen Ngoc, Search for Axions in Electron Bremsstrahlung, Phys. Lett. B180 (1986) 295–298. [doi:10.1016/0370-2693\(86\)90313-8](#).
- [576] A. Davidson, K. C. Wali, Minimal flavor unification via multigenerational peccei-quinn symmetry, Phys. Rev. Lett. 48 (1982) 11. [doi:10.1103/PhysRevLett.48.11](#).
- [577] A. Davidson, V. P. Nair, K. C. Wali, Peccei-Quinn Symmetry as Flavor Symmetry and Grand Unification, Phys. Rev. D29 (1984) 1504. [doi:10.1103/PhysRevD.29.1504](#).
- [578] A. Davidson, M. A. H. Vozmediano, The Horizontal Axion Alternative: The Interplay of Vacuum Structure and Flavor Interactions, Nucl. Phys. B248 (1984) 647–670. [doi:10.1016/0550-3213\(84\)90616-3](#).
- [579] C. D. Froggatt, H. B. Nielsen, Hierarchy of Quark Masses, Cabibbo Angles and CP Violation, Nucl. Phys. B147 (1979) 277–298. [doi:10.1016/0550-3213\(79\)90316-X](#).
- [580] Y. Ema, K. Hamaguchi, T. Moroi, K. Nakayama, Flaxion: a minimal extension to solve puzzles in the standard model, JHEP 01 (2017) 096. [arXiv:1612.05492](#), [doi:10.1007/JHEP01\(2017\)096](#).
- [581] L. Calibbi, F. Goertz, D. Redigolo, R. Ziegler, J. Zupan, Minimal axion model from flavor, Phys. Rev. D95 (9) (2017) 095009. [arXiv:1612.08040](#), [doi:10.1103/PhysRevD.95.095009](#).
- [582] Q. Bonnefoy, E. Dudas, S. Pokorski, Chiral Froggatt-Nielsen models, gauge anomalies and flavourful axions, JHEP 01 (2020) 191. [arXiv:1909.05336](#), [doi:10.1007/JHEP01\(2020\)191](#).
- [583] T. Alanne, S. Blasi, F. Goertz, Common source for scalars: Flavored axion-Higgs unification, Phys. Rev. D99 (1) (2019) 015028. [arXiv:1807.10156](#), [doi:10.1103/PhysRevD.99.015028](#).
- [584] M. E. Albrecht, T. Feldmann, T. Mannel, Goldstone Bosons in Effective Theories with Spontaneously Broken Flavour Symmetry, JHEP 10 (2010) 089. [arXiv:1002.4798](#), [doi:10.1007/JHEP10\(2010\)089](#).

- [585] F. Arias-Aragon, L. Merlo, The Minimal Flavour Violating Axion, JHEP 10 (2017) 168, [Erratum: JHEP11,152(2019)]. [arXiv:1709.07039](#), [doi:10.1007/JHEP10\(2017\)168](#), [10.1007/JHEP11\(2019\)152](#).
- [586] Z. G. Berezhiani, Horizontal Symmetry and Quark - Lepton Mass Spectrum: The SU(5) \times SU(3)-h Model, Phys. Lett. 150B (1985) 177–181. [doi:10.1016/0370-2693\(85\)90164-9](#).
- [587] Z. G. Berezhiani, M. Yu. Khlopov, Cosmology of Spontaneously Broken Gauge Family Symmetry, Z. Phys. C49 (1991) 73–78. [doi:10.1007/BF01570798](#).
- [588] J. L. Feng, T. Moroi, H. Murayama, E. Schnapka, Third generation familons, b factories, and neutrino cosmology, Phys. Rev. D57 (1998) 5875–5892. [arXiv:hep-ph/9709411](#), [doi:10.1103/PhysRevD.57.5875](#).
- [589] F. Bjorkerth, E. J. Chun, S. F. King, Flavourful Axion Phenomenology, JHEP 08 (2018) 117. [arXiv:1806.00660](#), [doi:10.1007/JHEP08\(2018\)117](#).
- [590] R. Ziegler, Flavored Axions, PoS CORFU2018 (2019) 035. [arXiv:1905.01084](#), [doi:10.22323/1.347.0035](#).
- [591] L. Di Luzio, Flavour Violating Axions, in: Workshop on Flavour changing and conserving processes (FCCP2019) Anacapri, Capri Island, Italy, August 29-31, 2019, 2019. [arXiv:1911.02591](#).
- [592] J. Martin Camalich, M. Pospelov, P. N. H. Vuong, R. Ziegler, J. Zupan, Quark Flavor Phenomenology of the QCD Axion. (2020). [arXiv:2002.04623](#).
- [593] S. Adler, et al., Measurement of the $K^+ \rightarrow \pi^+ \nu \bar{\nu}$ branching ratio, Phys. Rev. D77 (2008) 052003. [arXiv:0709.1000](#), [doi:10.1103/PhysRevD.77.052003](#).
- [594] G. Anelli, et al., Proposal to measure the rare decay $K^+ \rightarrow \pi^+ \nu \bar{\nu}$ at the CERN SPS (2005).
- [595] R. Fantechi, The NA62 experiment at CERN: status and perspectives, in: 12th Conference on Flavor Physics and CP Violation (FPCP 2014) Marseille, France, May 26-30, 2014, 2014. [arXiv:1407.8213](#).
- [596] R. Ammar, et al., Search for the familon via $B^+ \rightarrow \pi^+ X_0$, $B^+ \rightarrow K^+ X_0$, and $B_0 \rightarrow K_0(S) X_0$ decays, Phys. Rev. Lett. 87 (2001) 271801. [arXiv:hep-ex/0106038](#), [doi:10.1103/PhysRevLett.87.271801](#).
- [597] T. Abe, et al., Belle II Technical Design Report. (2010). [arXiv:1011.0352](#).
- [598] A. Jodidio, et al., Search for Right-Handed Currents in Muon Decay, Phys. Rev. D34 (1986) 1967, [Erratum: Phys. Rev.D37,237(1988)]. [doi:10.1103/PhysRevD.34.1967](#), [10.1103/PhysRevD.37.237](#).
- [599] J. T. Goldman, et al., Light Boson Emission in the Decay of the μ^+ , Phys. Rev. D36 (1987) 1543–1546. [doi:10.1103/PhysRevD.36.1543](#).
- [600] R. D. Bolton, et al., Search for Rare Muon Decays with the Crystal Box Detector, Phys. Rev. D38 (1988) 2077. [doi:10.1103/PhysRevD.38.2077](#).
- [601] R. Bayes, et al., Search for two body muon decay signals, Phys. Rev. D91 (5) (2015) 052020. [arXiv:1409.0638](#), [doi:10.1103/PhysRevD.91.052020](#).
- [602] F. Renga, The quest for $\mu \rightarrow e \gamma$: present and future, Hyperfine Interact. 239 (1) (2018) 58. [arXiv:1811.05921](#), [doi:10.1007/s10751-018-1534-y](#).
- [603] A. Blondel, et al., Research Proposal for an Experiment to Search for the Decay $\mu \rightarrow e e e$. (2013). [arXiv:1301.6113](#).
- [604] H. Albrecht, et al., A Search for lepton flavor violating decays $\tau \rightarrow e \alpha$, $\tau \rightarrow \mu \alpha$, Z. Phys. C68 (1995) 25–28. [doi:10.1007/BF01579801](#).
- [605] P. J. Steinhardt, M. S. Turner, Saving the invisible axion, Phys. Lett. B129 (1983) 51. [doi:10.1016/0370-2693\(83\)90727-X](#).
- [606] G. Lazarides, C. Panagiotakopoulos, Q. Shafi, Relaxing the cosmological bound on axions, Phys. Lett. B192 (1987) 323. [doi:10.1016/0370-2693\(87\)90115-8](#).
- [607] G. Lazarides, R. K. Schaefer, D. Seckel, Q. Shafi, Dilution of Cosmological Axions by Entropy Production, Nucl. Phys. B346 (1990) 193–212. [doi:10.1016/0550-3213\(90\)90244-8](#).
- [608] M. Kawasaki, T. Moroi, T. Yanagida, Can decaying particles raise the upper bound on the Peccei-Quinn scale?, Phys. Lett. B383 (1996) 313–316. [arXiv:hep-ph/9510461](#), [doi:10.1016/0370-2693\(96\)00743-5](#).
- [609] K. Choi, E. J. Chun, J. E. Kim, Cosmological implications of radiatively generated axion scale, Phys. Lett. B403 (1997) 209–217. [arXiv:hep-ph/9608222](#), [doi:10.1016/S0370-2693\(97\)00465-6](#).
- [610] M. Hashimoto, K. I. Izawa, M. Yamaguchi, T. Yanagida, Axion cosmology with its scalar superpartner, Phys. Lett. B437 (1998) 44–50. [arXiv:hep-ph/9803263](#), [doi:10.1016/S0370-2693\(98\)00887-9](#).
- [611] M. Kawasaki, N. Kitajima, K. Nakayama, Cosmological Aspects of Inflation in a Supersymmetric Axion Model, Phys. Rev. D83 (2011) 123521. [arXiv:1104.1262](#), [doi:10.1103/PhysRevD.83.123521](#).
- [612] H. Baer, A. Lessa, Some necessary conditions for allowing the PQ scale as high as M_{GUT} in SUSY models with an axino or neutralino LSP, JHEP 06 (2011) 027. [arXiv:1104.4807](#), [doi:10.1007/JHEP06\(2011\)027](#).
- [613] K. J. Bae, H. Baer, A. Lessa, H. Serce, Coupled Boltzmann computation of mixed axion neutralino dark matter in the SUSY DFSZ axion model, JCAP 1410 (10) (2014) 082. [arXiv:1406.4138](#), [doi:10.1088/1475-7516/2014/10/082](#).
- [614] R. T. Co, F. D’Eramo, L. J. Hall, Supersymmetric axion grand unified theories and their predictions, Phys. Rev. D94 (7) (2016) 075001. [arXiv:1603.04439](#), [doi:10.1103/PhysRevD.94.075001](#).
- [615] P. Jordan, Schwerkraft und Weltall: Grundlagen der theoretische Kosmologie, Vol. 107, Vieweg. (Braunschweig: und Sohns), 1955.
- [616] M. Fierz, On the physical interpretation of P.Jordan’s extended theory of gravitation, Helv. Phys. Acta 29 (1956) 128–134.
- [617] C. Brans, R. H. Dicke, Mach’s principle and a relativistic theory of gravitation, Phys. Rev. 124 (1961) 925–935. [doi:10.1103/PhysRev.124.925](#).
- [618] R. Catena, N. Fornengo, A. Masiero, M. Pietroni, F. Rosati, Dark matter relic abundance and scalar - tensor dark energy, Phys. Rev. D70 (2004) 063519. [arXiv:astro-ph/0403614](#), [doi:10.1103/PhysRevD.70.063519](#).
- [619] R. Catena, N. Fornengo, M. Pato, L. Pieri, A. Masiero, Thermal Relics in Modified Cosmologies: Bounds on Evolution Histories of the Early Universe and Cosmological Boosts for PAMELA, Phys. Rev. D81 (2010) 123522. [arXiv:0912.4421](#),

- doi:10.1103/PhysRevD.81.123522.
- [620] M. T. Meehan, I. B. Whittingham, Dark matter relic density in scalar-tensor gravity revisited, JCAP 1512 (12) (2015) 011. [arXiv:1508.05174](#), doi:10.1088/1475-7516/2015/12/011.
 - [621] B. Dutta, E. Jimenez, I. Zavala, Dark Matter Relics and the Expansion Rate in Scalar-Tensor Theories, JCAP 1706 (06) (2017) 032. [arXiv:1612.05553](#), doi:10.1088/1475-7516/2017/06/032.
 - [622] B. Dutta, E. Jimenez, I. Zavala, D-brane Disformal Coupling and Thermal Dark Matter, Phys. Rev. D96 (10) (2017) 103506. [arXiv:1708.07153](#), doi:10.1103/PhysRevD.96.103506.
 - [623] B. Dutta, C. S. Fong, E. Jimenez, E. Nardi, A cosmological pathway to testable leptogenesis, JCAP 1810 (10) (2018) 025. [arXiv:1804.07676](#), doi:10.1088/1475-7516/2018/10/025.
 - [624] G. Gelmini, P. Gondolo, A. Soldatenko, C. E. Yaguna, The Effect of a late decaying scalar on the neutralino relic density, Phys. Rev. D74 (2006) 083514. [arXiv:hep-ph/0605016](#), doi:10.1103/PhysRevD.74.083514.
 - [625] G. B. Gelmini, P. Gondolo, A. Soldatenko, C. E. Yaguna, Direct detection of neutralino dark matter in non-standard cosmologies, Phys. Rev. D76 (2007) 015010. [arXiv:hep-ph/0610379](#), doi:10.1103/PhysRevD.76.015010.
 - [626] G. B. Gelmini, P. Gondolo, Ultra-cold WIMPs: relics of non-standard pre-BBN cosmologies, JCAP 0810 (2008) 002. [arXiv:0803.2349](#), doi:10.1088/1475-7516/2008/10/002.
 - [627] A. L. Erickcek, K. Sigurdson, Reheating Effects in the Matter Power Spectrum and Implications for Substructure, Phys. Rev. D84 (2011) 083503. [arXiv:1106.0536](#), doi:10.1103/PhysRevD.84.083503.
 - [628] K. Redmond, A. L. Erickcek, New Constraints on Dark Matter Production during Kination, Phys. Rev. D96 (4) (2017) 043511. [arXiv:1704.01056](#), doi:10.1103/PhysRevD.96.043511.
 - [629] L. Visinelli, (Non-)thermal production of WIMPs during kination, Symmetry 10 (11) (2018) 546. [arXiv:1710.11006](#), doi:10.3390/sym10110546.
 - [630] L. Visinelli, P. Gondolo, Kinetic decoupling of WIMPs: analytic expressions, Phys. Rev. D91 (8) (2015) 083526. [arXiv:1501.02233](#), doi:10.1103/PhysRevD.91.083526.
 - [631] D. Grin, T. L. Smith, M. Kamionkowski, Axion constraints in non-standard thermal histories, Phys. Rev. D77 (2008) 085020. [arXiv:0711.1352](#), doi:10.1103/PhysRevD.77.085020.
 - [632] L. Visinelli, P. Gondolo, Axion cold dark matter in non-standard cosmologies, Phys. Rev. D81 (2010) 063508. [arXiv:0912.0015](#), doi:10.1103/PhysRevD.81.063508.
 - [633] L. Visinelli, Light axion-like dark matter must be present during inflation, Phys. Rev. D96 (2) (2017) 023013. [arXiv:1703.08798](#), doi:10.1103/PhysRevD.96.023013.
 - [634] P. Draper, J. Kozaczuk, J.-H. Yu, Theta in new QCD-like sectors, Phys. Rev. D98 (1) (2018) 015028. [arXiv:1803.00015](#), doi:10.1103/PhysRevD.98.015028.
 - [635] N. Ramberg, L. Visinelli, Probing the Early Universe with Axion Physics and Gravitational Waves, Phys. Rev. D99 (12) (2019) 123513. [arXiv:1904.05707](#), doi:10.1103/PhysRevD.99.123513.
 - [636] N. Blinov, M. J. Dolan, P. Draper, J. Kozaczuk, Dark matter targets for axionlike particle searches, Phys. Rev. D100 (1) (2019) 015049. [arXiv:1905.06952](#), doi:10.1103/PhysRevD.100.015049.
 - [637] M. S. Turner, Coherent Scalar Field Oscillations in an Expanding Universe, Phys. Rev. D28 (1983) 1243. doi:10.1103/PhysRevD.28.1243.
 - [638] R. J. Scherrer, M. S. Turner, Decaying Particles Do Not Heat Up the Universe, Phys. Rev. D31 (1985) 681. doi:10.1103/PhysRevD.31.681.
 - [639] J. D. Barrow, Massive Particles As A Probe Of The Early Universe, Nucl. Phys. B208 (1982) 501–508. doi:10.1016/0550-3213(82)90233-4.
 - [640] L. H. Ford, Gravitational Particle Creation and Inflation, Phys. Rev. D35 (1987) 2955. doi:10.1103/PhysRevD.35.2955.
 - [641] N. Blinov, M. J. Dolan, P. Draper, Imprints of the Early Universe on Axion Dark Matter Substructure, Phys. Rev. D101 (3) (2020) 035002. [arXiv:1911.07853](#), doi:10.1103/PhysRevD.101.035002.
 - [642] A. Hook, Solving the Hierarchy Problem Discretely, Phys. Rev. Lett. 120 (26) (2018) 261802. [arXiv:1802.10093](#), doi:10.1103/PhysRevLett.120.261802.
 - [643] K. R. Dienes, E. Dudas, T. Gherghetta, Invisible axions and large radius compactifications, Phys. Rev. D62 (2000) 105023. [arXiv:hep-ph/9912455](#), doi:10.1103/PhysRevD.62.105023.
 - [644] A. A. Geraci, S. J. Smullin, D. M. Weld, J. Chiaiverini, A. Kapitulnik, Improved constraints on non-Newtonian forces at 10 microns, Phys. Rev. D78 (2008) 022002. [arXiv:0802.2350](#), doi:10.1103/PhysRevD.78.022002.
 - [645] A. O. Sushkov, W. J. Kim, D. A. R. Dalvit, S. K. Lamoreaux, New Experimental Limits on Non-Newtonian Forces in the Micrometer Range, Phys. Rev. Lett. 107 (2011) 171101. [arXiv:1108.2547](#), doi:10.1103/PhysRevLett.107.171101.
 - [646] Z. Berezhiani, D. Comelli, F. L. Villante, The Early mirror universe: Inflation, baryogenesis, nucleosynthesis and dark matter, Phys. Lett. B503 (2001) 362–375. [arXiv:hep-ph/0008105](#), doi:10.1016/S0370-2693(01)00217-9.
 - [647] M. Giannotti, Mirror world and axion: Relaxing cosmological bounds, Int. J. Mod. Phys. A20 (2005) 2454–2458. [arXiv:astro-ph/0504636](#), doi:10.1142/S0217751X05024766.
 - [648] T. D. Lee, C.-N. Yang, Question of Parity Conservation in Weak Interactions, Phys. Rev. 104 (1956) 254–258. doi:10.1103/PhysRev.104.254.
 - [649] B. Holdom, Two U(1)’s and Epsilon Charge Shifts, Phys. Lett. 166B (1986) 196–198. doi:10.1016/0370-2693(86)91377-8.
 - [650] S. L. Glashow, Positronium Versus the Mirror Universe, Phys. Lett. 167B (1986) 35–36. doi:10.1016/0370-2693(86)90540-X.
 - [651] M. Yu. Khlopov, G. M. Beskin, N. E. Bochkarev, L. A. Pustynnik, S. A. Pustynnik, Observational Physics of Mirror World, Sov. Astron. 35 (1991) 21, [Astron. Zh.68,42(1991)].
 - [652] J.-S. Roux, J. M. Cline, Constraining galactic structures of mirror dark matter. (2020). [arXiv:2001.11504](#).

- [653] V. A. Rubakov, Grand unification and heavy axion, JETP Lett. 65 (1997) 621–624. [arXiv:hep-ph/9703409](#), [doi:10.1134/1.567390](#).
- [654] Z. Berezhiani, L. Gianfagna, M. Giannotti, Strong CP problem and mirror world: The Weinberg-Wilczek axion revisited, Phys. Lett. B500 (2001) 286–296. [arXiv:hep-ph/0009290](#), [doi:10.1016/S0370-2693\(00\)01392-7](#).
- [655] L. Gianfagna, M. Giannotti, F. Nesti, Mirror world, supersymmetric axion and gamma ray bursts, JHEP 10 (2004) 044. [arXiv:hep-ph/0409185](#), [doi:10.1088/1126-6708/2004/10/044](#).
- [656] P. Agrawal, G. Marques-Tavares, W. Xue, Opening up the QCD axion window, JHEP 03 (2018) 049. [arXiv:1708.05008](#), [doi:10.1007/JHEP03\(2018\)049](#).
- [657] N. Kitajima, T. Sekiguchi, F. Takahashi, Cosmological abundance of the QCD axion coupled to hidden photons, Phys. Lett. B781 (2018) 684–687. [arXiv:1711.06590](#), [doi:10.1016/j.physletb.2018.04.024](#).
- [658] E. Witten, Dyons of Charge $e\theta/2\pi$, Phys. Lett. B86 (1979) 283–287, [283(1979)]. [doi:10.1016/0370-2693\(79\)90838-4](#).
- [659] W. Fischler, J. Preskill, Dyon-axion dynamics, Phys. Lett. 125B (1983) 165–170. [doi:10.1016/0370-2693\(83\)91260-1](#).
- [660] M. Kawasaki, F. Takahashi, M. Yamada, Suppressing the QCD Axion Abundance by Hidden Monopoles, Phys. Lett. B753 (2016) 677–681. [arXiv:1511.05030](#), [doi:10.1016/j.physletb.2015.12.075](#).
- [661] M. Kawasaki, F. Takahashi, M. Yamada, Adiabatic suppression of the axion abundance and isocurvature due to coupling to hidden monopoles, JHEP 01 (2018) 053. [arXiv:1708.06047](#), [doi:10.1007/JHEP01\(2018\)053](#).
- [662] P. Baratella, A. Pomarol, F. Rompineve, The Supercooled Universe, JHEP 03 (2019) 100. [arXiv:1812.06996](#), [doi:10.1007/JHEP03\(2019\)100](#).
- [663] R. T. Co, L. J. Hall, K. Harigaya, Kinetic Misalignment Mechanism. (2019). [arXiv:1910.14152](#).
- [664] C.-F. Chang, Y. Cui, New Perspectives on Axion Misalignment Mechanism. (2019). [arXiv:1911.11885](#).
- [665] R. T. Co, L. J. Hall, K. Harigaya, QCD Axion Dark Matter with a Small Decay Constant, Phys. Rev. Lett. 120 (21) (2018) 211602. [arXiv:1711.10486](#), [doi:10.1103/PhysRevLett.120.211602](#).
- [666] L. Kofman, A. D. Linde, A. A. Starobinsky, Reheating after inflation, Phys. Rev. Lett. 73 (1994) 3195–3198. [arXiv:hep-th/9405187](#), [doi:10.1103/PhysRevLett.73.3195](#).
- [667] Y. Shtanov, J. H. Traschen, R. H. Brandenberger, Universe reheating after inflation, Phys. Rev. D51 (1995) 5438–5455. [arXiv:hep-ph/9407247](#), [doi:10.1103/PhysRevD.51.5438](#).
- [668] L. Kofman, A. D. Linde, A. A. Starobinsky, Towards the theory of reheating after inflation, Phys. Rev. D56 (1997) 3258–3295. [arXiv:hep-ph/9704452](#), [doi:10.1103/PhysRevD.56.3258](#).
- [669] K. Harigaya, J. M. Leedom, QCD Axion Dark Matter from a Late Time Phase Transition (2019). [arXiv:1910.04163](#).
- [670] Y. Ema, K. Nakayama, Explosive Axion Production from Saxion, Phys. Lett. B776 (2018) 174–181. [arXiv:1710.02461](#), [doi:10.1016/j.physletb.2017.11.035](#).
- [671] T. C. Yang, Gauge Chiral U(1) Symmetry and CP Invariance in the Presence of Instantons, Phys. Rev. Lett. 41 (1978) 523–526. [doi:10.1103/PhysRevLett.41.523](#).
- [672] S. Dimopoulos, A Solution of the Strong CP Problem in Models With Scalars, Phys. Lett. 84B (1979) 435–439. [doi:10.1016/0370-2693\(79\)91233-4](#).
- [673] S. H. H. Tye, A Superstrong Force With a Heavy Axion, Phys. Rev. Lett. 47 (1981) 1035. [doi:10.1103/PhysRevLett.47.1035](#).
- [674] B. Holdom, M. E. Peskin, Raising the Axion Mass, Nucl. Phys. B208 (1982) 397–412. [doi:10.1016/0550-3213\(82\)90228-0](#).
- [675] B. Holdom, Strong QCD at High-energies and a Heavy Axion, Phys. Lett. 154B (1985) 316, [Erratum: Phys. Lett. 156B, 452(1985)]. [doi:10.1016/0370-2693\(85\)90371-5](#).
- [676] J. M. Flynn, L. Randall, A Computation of the Small Instanton Contribution to the Axion Potential, Nucl. Phys. B293 (1987) 731–739. [doi:10.1016/0550-3213\(87\)90089-7](#).
- [677] D. S. M. Alves, N. Weiner, A viable QCD axion in the MeV mass range, JHEP 07 (2018) 092. [arXiv:1710.03764](#), [doi:10.1007/JHEP07\(2018\)092](#).
- [678] Z. Berezhiani, A. Drago, Gamma-ray bursts via emission of axion - like particles, Phys. Lett. B473 (2000) 281–290. [arXiv:hep-ph/9911333](#), [doi:10.1016/S0370-2693\(99\)01449-5](#).
- [679] X. Cid Vidal, A. Mariotti, D. Redigolo, F. Sala, K. Tobioka, New Axion Searches at Flavor Factories, JHEP 01 (2019) 113. [arXiv:1810.09452](#), [doi:10.1007/JHEP01\(2019\)113](#).
- [680] T. Gherghetta, V. V. Khoze, A. Pomarol, Y. Shirman, The Axion Mass from 5D Small Instantons, JHEP 03 (2020) 063. [arXiv:2001.05610](#), [doi:10.1007/JHEP03\(2020\)063](#).
- [681] H. Fukuda, K. Harigaya, M. Ibe, T. T. Yanagida, Model of visible QCD axion, Phys. Rev. D92 (1) (2015) 015021. [arXiv:1504.06084](#), [doi:10.1103/PhysRevD.92.015021](#).
- [682] A. Hook, Anomalous solutions to the strong CP problem, Phys. Rev. Lett. 114 (14) (2015) 141801. [arXiv:1411.3325](#), [doi:10.1103/PhysRevLett.114.141801](#).
- [683] S. Dimopoulos, A. Hook, J. Huang, G. Marques-Tavares, A collider observable QCD axion, JHEP 11 (2016) 052. [arXiv:1606.03097](#), [doi:10.1007/JHEP11\(2016\)052](#).
- [684] A. Hook, S. Kumar, Z. Liu, R. Sundrum, The High Quality QCD Axion and the LHC (11 2019). [arXiv:1911.12364](#).
- [685] A. Albaid, M. Dine, P. Draper, Strong CP and SUZ₂, JHEP 12 (2015) 046. [arXiv:1510.03392](#), [doi:10.1007/JHEP12\(2015\)046](#).
- [686] T. Gherghetta, N. Nagata, M. Shifman, A Visible QCD Axion from an Enlarged Color Group, Phys. Rev. D93 (11) (2016) 115010. [arXiv:1604.01127](#), [doi:10.1103/PhysRevD.93.115010](#).
- [687] P. Agrawal, K. Howe, Factoring the Strong CP Problem, JHEP 12 (2018) 029. [arXiv:1710.04213](#), [doi:10.1007/JHEP12\(2018\)029](#).

- [688] P. Agrawal, K. Howe, A Flavorful Factoring of the Strong CP Problem, JHEP 12 (2018) 035. [arXiv:1712.05803](#), [doi:10.1007/JHEP12\(2018\)035](#).
- [689] J. Fuentes-Martin, M. Reig, A. Vicente, Strong CP problem with low-energy emergent QCD: The 4321 case, Phys. Rev. D100 (11) (2019) 115028. [arXiv:1907.02550](#), [doi:10.1103/PhysRevD.100.115028](#).
- [690] C. Csaki, M. Ruhdorfer, Y. Shirman, UV Sensitivity of the Axion Mass from Instantons in Partially Broken Gauge Groups. (2019). [arXiv:1912.02197](#).
- [691] M. K. Gaillard, M. B. Gavela, R. Houtz, P. Quilez, R. Del Rey, Color unified dynamical axion, Eur. Phys. J. C78 (11) (2018) 972. [arXiv:1805.06465](#), [doi:10.1140/epjc/s10052-018-6396-6](#).
- [692] J. E. Kim, Reason for $SU(6)$ Grand Unification, Phys. Lett. 107B (1981) 69–72. [doi:10.1016/0370-2693\(81\)91149-7](#).
- [693] R. N. Mohapatra, G. Senjanovic, The Superlight Axion and Neutrino Masses, Z. Phys. C17 (1983) 53–56. [doi:10.1007/BF01577819](#).
- [694] Q. Shafi, F. W. Stecker, Implications of a Class of Grand Unified Theories for Large Scale Structure in the Universe, Phys. Rev. Lett. 53 (1984) 1292. [doi:10.1103/PhysRevLett.53.1292](#).
- [695] P. Langacker, R. D. Peccei, T. Yanagida, Invisible Axions and Light Neutrinos: Are They Connected?, Mod. Phys. Lett. A1 (1986) 541. [doi:10.1142/S0217732386000683](#).
- [696] X. G. He, R. R. Volkas, Models Featuring Spontaneous CP Violation: An Invisible Axion and Light Neutrino Masses, Phys. Lett. B208 (1988) 261, [Erratum: Phys. Lett. B218,508(1989)]. [doi:10.1016/0370-2693\(88\)90427-3](#), [doi:10.1016/0370-2693\(89\)91457-3](#).
- [697] A. G. Dias, V. Pleitez, The Invisible axion and neutrino masses, Phys. Rev. D73 (2006) 017701. [arXiv:hep-ph/0511104](#), [doi:10.1103/PhysRevD.73.017701](#).
- [698] A. Salvio, A Simple Motivated Completion of the Standard Model below the Planck Scale: Axions and Right-Handed Neutrinos, Phys. Lett. B743 (2015) 428–434. [arXiv:1501.03781](#), [doi:10.1016/j.physletb.2015.03.015](#).
- [699] J. D. Clarke, R. R. Volkas, Technically natural nonsupersymmetric model of neutrino masses, baryogenesis, the strong CP problem, and dark matter, Phys. Rev. D93 (3) (2016) 035001, [Phys. Rev. D93,035001(2016)]. [arXiv:1509.07243](#), [doi:10.1103/PhysRevD.93.035001](#).
- [700] S. Bertolini, A. Santamaria, The Strong CP problem and the solar neutrino puzzle: Are they related?, Nucl. Phys. B357 (1991) 222–240. [doi:10.1016/0550-3213\(91\)90467-C](#).
- [701] H. Arason, P. Ramond, B. D. Wright, A Standard model extension with neutrino masses and an invisible axion, Phys. Rev. D43 (1991) 2337–2350. [doi:10.1103/PhysRevD.43.2337](#).
- [702] S. Bertolini, L. Di Luzio, H. Kolesová, M. Malinský, Massive neutrinos and invisible axion minimally connected, Phys. Rev. D91 (5) (2015) 055014. [arXiv:1412.7105](#), [doi:10.1103/PhysRevD.91.055014](#).
- [703] Y. H. Ahn, E. J. Chun, Minimal Models for Axion and Neutrino, Phys. Lett. B752 (2016) 333–337. [arXiv:1510.01015](#), [doi:10.1016/j.physletb.2015.11.067](#).
- [704] S. Bertolini, L. Di Luzio, H. Kolesova, M. Malinsky, J. C. Vazquez, Neutrino-axion-dilaton interconnection, Phys. Rev. D93 (1) (2016) 015009. [arXiv:1510.03668](#), [doi:10.1103/PhysRevD.93.015009](#).
- [705] C.-S. Chen, L.-H. Tsai, Peccei-Quinn symmetry as the origin of Dirac Neutrino Masses, Phys. Rev. D88 (5) (2013) 055015. [arXiv:1210.6264](#), [doi:10.1103/PhysRevD.88.055015](#).
- [706] P.-H. Gu, Peccei-Quinn symmetry for Dirac seesaw and leptogenesis, JCAP 1607 (07) (2016) 004. [arXiv:1603.05070](#), [doi:10.1088/1475-7516/2016/07/004](#).
- [707] C. D. R. Carvajal, Ó. Zapata, One-loop Dirac neutrino mass and mixed axion-WIMP dark matter, Phys. Rev. D99 (7) (2019) 075009. [arXiv:1812.06364](#), [doi:10.1103/PhysRevD.99.075009](#).
- [708] E. Peinado, M. Reig, R. Srivastava, J. W. F. Valle, Dirac neutrinos from Peccei-Quinn symmetry: a fresh look at the axion. (2019). [arXiv:1910.02961](#).
- [709] V. A. Kuzmin, M. E. Shaposhnikov, I. I. Tkachev, Strong CP violation, electroweak baryogenesis, and axionic dark matter, Phys. Rev. D45 (1992) 466–475. [doi:10.1103/PhysRevD.45.466](#).
- [710] G. Servant, Baryogenesis from Strong CP Violation and the QCD Axion, Phys. Rev. Lett. 113 (17) (2014) 171803. [arXiv:1407.0030](#), [doi:10.1103/PhysRevLett.113.171803](#).
- [711] J. Garcia-Bellido, M. Garcia-Perez, A. Gonzalez-Arroyo, Chern-Simons production during preheating in hybrid inflation models, Phys. Rev. D69 (2004) 023504. [arXiv:hep-ph/0304285](#), [doi:10.1103/PhysRevD.69.023504](#).
- [712] A. Tranberg, J. Smit, Baryon asymmetry from electroweak tachyonic preheating, JHEP 11 (2003) 016. [arXiv:hep-ph/0310342](#), [doi:10.1088/1126-6708/2003/11/016](#).
- [713] S. Ipek, T. M. P. Tait, Early Cosmological Period of QCD Confinement, Phys. Rev. Lett. 122 (11) (2019) 112001. [arXiv:1811.00559](#), [doi:10.1103/PhysRevLett.122.112001](#).
- [714] D. Croon, J. N. Howard, S. Ipek, T. M. Tait, QCD baryogenesis, Phys. Rev. D 101 (5) (2020) 055042. [arXiv:1911.01432](#), [doi:10.1103/PhysRevD.101.055042](#).
- [715] R. T. Co, K. Harigaya, Axionogenesis (2019). [arXiv:1910.02080](#).
- [716] A. A. Starobinsky, A New Type of Isotropic Cosmological Models Without Singularity, Phys. Lett. B91 (1980) 99–102, [771(1980)]. [doi:10.1016/0370-2693\(80\)90670-X](#).
- [717] A. H. Guth, The Inflationary Universe: A Possible Solution to the Horizon and Flatness Problems, Phys. Rev. D23 (1981) 347–356. [doi:10.1103/PhysRevD.23.347](#).
- [718] M. B. Einhorn, K. Sato, Monopole Production in the Very Early Universe in a First Order Phase Transition, Nucl. Phys. B180 (1981) 385–404. [doi:10.1016/0550-3213\(81\)90057-2](#).
- [719] K. Sato, Cosmological Baryon Number Domain Structure and the First Order Phase Transition of a Vacuum, Phys. Lett. 99B (1981) 66–70, [Adv. Ser. Astrophys. Cosmol.3,134(1987)]. [doi:10.1016/0370-2693\(81\)90805-4](#).
- [720] D. Kazanas, Dynamics of the Universe and Spontaneous Symmetry Breaking, Astrophys. J. 241 (1980) L59–L63. [doi:](#)

- 10.1086/183361.
- [721] J. Martin, C. Ringeval, R. Trotta, V. Vennin, The Best Inflationary Models After Planck, JCAP 1403 (2014) 039. [arXiv:1312.3529](#), [doi:10.1088/1475-7516/2014/03/039](#).
 - [722] M. Gerbino, K. Freese, S. Vagnozzi, M. Lattanzi, O. Mena, E. Giusarma, S. Ho, Impact of neutrino properties on the estimation of inflationary parameters from current and future observations, Phys.Rev.D 95 (4) (2017) 043512. [arXiv:1610.08830](#), [doi:10.1103/PhysRevD.95.043512](#).
 - [723] W. H. Kinney, S. Vagnozzi, L. Visinelli, The zoo plot meets the swampland: mutual (in)consistency of single-field inflation, string conjectures, and cosmological data, Class. Quant. Grav. 36 (11) (2019) 117001. [arXiv:1808.06424](#), [doi:10.1088/1361-6382/ab1d87](#).
 - [724] A. Linde, M. Noorbala, A. Westphal, Observational consequences of chaotic inflation with nonminimal coupling to gravity, JCAP 1103 (2011) 013. [arXiv:1101.2652](#), [doi:10.1088/1475-7516/2011/03/013](#).
 - [725] F. L. Bezrukov, M. Shaposhnikov, The Standard Model Higgs boson as the inflaton, Phys. Lett. B659 (2008) 703–706. [arXiv:0710.3755](#), [doi:10.1016/j.physletb.2007.11.072](#).
 - [726] C. P. Burgess, H. M. Lee, M. Trott, Power-counting and the Validity of the Classical Approximation During Inflation, JHEP 09 (2009) 103. [arXiv:0902.4465](#), [doi:10.1088/1126-6708/2009/09/103](#).
 - [727] J. L. F. Barbon, J. R. Espinosa, On the Naturalness of Higgs Inflation, Phys. Rev. D79 (2009) 081302. [arXiv:0903.0355](#), [doi:10.1103/PhysRevD.79.081302](#).
 - [728] P. Fox, A. Pierce, S. D. Thomas, Probing a QCD string axion with precision cosmological measurements, (2004). [arXiv:hep-th/0409059](#).
 - [729] M. P. Hertzberg, M. Tegmark, F. Wilczek, Axion Cosmology and the Energy Scale of Inflation, Phys. Rev. D78 (2008) 083507. [arXiv:0807.1726](#), [doi:10.1103/PhysRevD.78.083507](#).
 - [730] P. Gondolo, L. Visinelli, Axion cold dark matter in view of BICEP2 results, Phys. Rev. Lett. 113 (2014) 011802. [arXiv:1403.4594](#), [doi:10.1103/PhysRevLett.113.011802](#).
 - [731] D. J. E. Marsh, D. Grin, R. Hlozek, P. G. Ferreira, Tensor Interpretation of BICEP2 Results Severely Constrains Axion Dark Matter, Phys. Rev. Lett. 113 (1) (2014) 011801. [arXiv:1403.4216](#), [doi:10.1103/PhysRevLett.113.011801](#).
 - [732] F. Bauer, D. A. Demir, Inflation with Non-Minimal Coupling: Metric versus Palatini Formulations, Phys. Lett. B665 (2008) 222–226. [arXiv:0803.2664](#), [doi:10.1016/j.physletb.2008.06.014](#).
 - [733] K. Freese, D. Spolyar, Chain inflation: 'Bubble bubble toil and trouble', JCAP 0507 (2005) 007. [arXiv:hep-ph/0412145](#), [doi:10.1088/1475-7516/2005/07/007](#).
 - [734] K. Freese, J. T. Liu, D. Spolyar, Inflating with the QCD axion, Phys. Rev. D72 (2005) 123521. [arXiv:hep-ph/0502177](#), [doi:10.1103/PhysRevD.72.123521](#).
 - [735] D. Chialva, U. H. Danielsson, Chain inflation revisited, JCAP 0810 (2008) 012. [arXiv:0804.2846](#), [doi:10.1088/1475-7516/2008/10/012](#).
 - [736] D. Chialva, U. H. Danielsson, Chain inflation and the imprint of fundamental physics in the CMBR, JCAP 0903 (2009) 007. [arXiv:0809.2707](#), [doi:10.1088/1475-7516/2009/03/007](#).
 - [737] J. M. Cline, G. D. Moore, Y. Wang, Chain Inflation Reconsidered, JCAP 1108 (2011) 032. [arXiv:1106.2188](#), [doi:10.1088/1475-7516/2011/08/032](#).
 - [738] P. Svrcek, Cosmological Constant and Axions in String Theory. , Submitted to: JHEP (2006). [arXiv:hep-th/0607086](#).
 - [739] P. Svrcek, E. Witten, Axions In String Theory, JHEP 06 (2006) 051. [arXiv:hep-th/0605206](#), [doi:10.1088/1126-6708/2006/06/051](#).
 - [740] T. W. Grimm, Axion inflation in type II string theory, Phys. Rev. D77 (2008) 126007. [arXiv:0710.3883](#), [doi:10.1103/PhysRevD.77.126007](#).
 - [741] C. Long, L. McAllister, P. McGuirk, Aligned Natural Inflation in String Theory, Phys. Rev. D90 (2014) 023501. [arXiv:1404.7852](#), [doi:10.1103/PhysRevD.90.023501](#).
 - [742] E. Silverstein, A. Westphal, Monodromy in the CMB: Gravity Waves and String Inflation, Phys. Rev. D78 (2008) 106003. [arXiv:0803.3085](#), [doi:10.1103/PhysRevD.78.106003](#).
 - [743] L. McAllister, E. Silverstein, A. Westphal, Gravity Waves and Linear Inflation from Axion Monodromy, Phys. Rev. D82 (2010) 046003. [arXiv:0808.0706](#), [doi:10.1103/PhysRevD.82.046003](#).
 - [744] F. Marchesano, G. Shiu, A. M. Uranga, F-term Axion Monodromy Inflation, JHEP 09 (2014) 184. [arXiv:1404.3040](#), [doi:10.1007/JHEP09\(2014\)184](#).
 - [745] B. P. Abbott, et al., Observation of Gravitational Waves from a Binary Black Hole Merger, Phys. Rev. Lett. 116 (6) (2016) 061102. [arXiv:1602.03837](#), [doi:10.1103/PhysRevLett.116.061102](#).
 - [746] P. S. B. Dev, A. Mazumdar, Probing the Scale of New Physics by Advanced LIGO/VIRGO, Phys. Rev. D93 (10) (2016) 104001. [arXiv:1602.04203](#), [doi:10.1103/PhysRevD.93.104001](#).
 - [747] L. Delle Rose, G. Panico, M. Redi, A. Tesi, Gravitational Waves from Supercool Axions (2019). [arXiv:1912.06139](#).
 - [748] B. Von Harling, A. Pomarol, O. Pujolàs, F. Rompineve, Peccei-Quinn Phase Transition at LIGO (2019). [arXiv:1912.07587](#).
 - [749] D. Croon, R. Houtz, V. Sanz, Dynamical Axions and Gravitational Waves, JHEP 07 (2019) 146. [arXiv:1904.10967](#), [doi:10.1007/JHEP07\(2019\)146](#).
 - [750] C. S. Machado, W. Ratzinger, P. Schwaller, B. A. Stefanek, Gravitational wave probes of axion-like particles (2019). [arXiv:1912.01007](#).
 - [751] H. Georgi, M. B. Wise, Hiding the Invisible Axion, Phys. Lett. 116B (1982) 123–126. [doi:10.1016/0370-2693\(82\)90989-3](#).
 - [752] G. Lazarides, Q. Shafi, Axion Models with No Domain Wall Problem, Phys. Lett. 115B (1982) 21–25. [doi:10.1016/0370-2693\(82\)90506-8](#).

- [753] S. M. Barr, D. B. Reiss, A. Zee, Families, the Invisible Axion, and Domain Walls, Phys. Lett. 116B (1982) 227–230. [doi:10.1016/0370-2693\(82\)90331-8](#).
- [754] S. M. Barr, X. C. Gao, D. Reiss, Peccei-Quinn symmetries without domains, Phys. Rev. D26 (1982) 2176. [doi:10.1103/PhysRevD.26.2176](#).
- [755] A. Davidson, M. A. H. Vozmediano, Domain Walls: Horizontal Epilogue, Phys. Lett. 141B (1984) 177–180. [doi:10.1016/0370-2693\(84\)90198-9](#).
- [756] S. M. Barr, J. E. Kim, New Confining Force Solution of the QCD Axion Domain-Wall Problem, Phys. Rev. Lett. 113 (24) (2014) 241301. [arXiv:1407.4311](#), [doi:10.1103/PhysRevLett.113.241301](#).
- [757] M. Reig, On the high-scale instanton interference effect: axion models without domain wall problem, JHEP 08 (2019) 167. [arXiv:1901.00203](#), [doi:10.1007/JHEP08\(2019\)167](#).
- [758] A. Caputo, M. Reig, Cosmic implications of a low-scale solution to the axion domain wall problem, Phys. Rev. D100 (6) (2019) 063530. [arXiv:1905.13116](#), [doi:10.1103/PhysRevD.100.063530](#).
- [759] K. Harigaya, M. Kawasaki, QCD axion dark matter from long-lived domain walls during matter domination, Phys. Lett. B782 (2018) 1–5. [arXiv:1802.00579](#), [doi:10.1016/j.physletb.2018.04.056](#).
- [760] L. M. Krauss, F. Wilczek, Discrete Gauge Symmetry in Continuum Theories, Phys. Rev. Lett. 62 (1989) 1221. [doi:10.1103/PhysRevLett.62.1221](#).
- [761] E. Nardi, Naturally large yukawa hierarchies, Phys.Rev.D 84 (2011) 036008. [arXiv:1105.1770](#), [doi:10.1103/PhysRevD.84.036008](#).
- [762] L. Darmé, E. Nardi, K. Zhan, Origin and protection of the Peccei-Quinn symmetry from $SU(3)_L \times SU(2)_R$ quark flavour group. In preparation (2020).
- [763] D. Buttazzo, L. Di Luzio, P. Ghorbani, C. Gross, G. Landini, A. Strumia, D. Teresi, J.-W. Wang, Scalar gauge dynamics and Dark Matter, JHEP 01 (2020) 130. [arXiv:1911.04502](#), [doi:10.1007/JHEP01\(2020\)130](#).
- [764] M. B. Wise, H. Georgi, S. L. Glashow, $SU(5)$ and the Invisible Axion, Phys. Rev. Lett. 47 (1981) 402. [doi:10.1103/PhysRevLett.47.402](#).
- [765] G. Lazarides, $SO(10)$ and the Invisible Axion, Phys. Rev. D25 (1982) 2425. [doi:10.1103/PhysRevD.25.2425](#).
- [766] A. Ernst, A. Ringwald, C. Tamarit, Axion Predictions in $SO(10) \times U(1)_{PQ}$ Models, JHEP 02 (2018) 103. [arXiv:1801.04906](#), [doi:10.1007/JHEP02\(2018\)103](#).
- [767] L. Di Luzio, A. Ringwald, C. Tamarit, Axion mass prediction from minimal grand unification, Phys. Rev. D98 (9) (2018) 095011. [arXiv:1807.09769](#), [doi:10.1103/PhysRevD.98.095011](#).
- [768] A. Ernst, L. Di Luzio, A. Ringwald, C. Tamarit, Axion properties in GUTs, PoS CORFU2018 (2019) 054. [arXiv:1811.11860](#), [doi:10.22323/1.347.0054](#).
- [769] P. Fileviez Pérez, C. Murgui, A. D. Plascencia, The QCD Axion and Unification, JHEP 11 (2019) 093. [arXiv:1908.01772](#), [doi:10.1007/JHEP11\(2019\)093](#).
- [770] P. Fileviez Pérez, C. Murgui, A. D. Plascencia, Axion Dark Matter, Proton Decay and Unification, JHEP 01 (2020) 091. [arXiv:1911.05738](#), [doi:10.1007/JHEP01\(2020\)091](#).
- [771] H. Georgi, S. L. Glashow, Unity of All Elementary Particle Forces, Phys. Rev. Lett. 32 (1974) 438–441. [doi:10.1103/PhysRevLett.32.438](#).
- [772] B. Bajc, G. Senjanovic, Seesaw at LHC, JHEP 08 (2007) 014. [arXiv:hep-ph/0612029](#), [doi:10.1088/1126-6708/2007/08/014](#).
- [773] B. Bajc, M. Nemevsek, G. Senjanovic, Probing seesaw at LHC, Phys. Rev. D76 (2007) 055011. [arXiv:hep-ph/0703080](#), [doi:10.1103/PhysRevD.76.055011](#).
- [774] L. Di Luzio, L. Mihaila, Unification scale vs. electroweak-triplet mass in the $SU(5) + 24_F$ model at three loops, Phys. Rev. D87 (2013) 115025. [arXiv:1305.2850](#), [doi:10.1103/PhysRevD.87.115025](#).
- [775] R. Holman, G. Lazarides, Q. Shafi, Axions and the Dark Matter of the Universe, Phys. Rev. D27 (1983) 995. [doi:10.1103/PhysRevD.27.995](#).
- [776] B. Bajc, A. Melfo, G. Senjanovic, F. Vissani, Yukawa sector in non-supersymmetric renormalizable $SO(10)$, Phys. Rev. D73 (2006) 055001. [arXiv:hep-ph/0510139](#), [doi:10.1103/PhysRevD.73.055001](#).
- [777] S. Bertolini, L. Di Luzio, M. Malinsky, Light color octet scalars in the minimal $SO(10)$ grand unification, Phys. Rev. D87 (8) (2013) 085020. [arXiv:1302.3401](#), [doi:10.1103/PhysRevD.87.085020](#).
- [778] G. Altarelli, D. Meloni, A non supersymmetric $SO(10)$ grand unified model for all the physics below M_{GUT} , JHEP 08 (2013) 021. [arXiv:1305.1001](#), [doi:10.1007/JHEP08\(2013\)021](#).
- [779] E. Witten, Some properties of $O(32)$ superstrings, Physics Letters B 149 (4) (1984) 351 – 356. [doi:https://doi.org/10.1016/0370-2693\(84\)90422-2](#).
- [780] J. P. Conlon, The QCD axion and moduli stabilisation, JHEP 05 (2006) 078. [arXiv:hep-th/0602233](#), [doi:10.1088/1126-6708/2006/05/078](#).
- [781] J. E. Kim, 't Hooft mechanism, anomalous gauge $U(1)$, and "invisible" axion from string, in: 13th Patras Workshop on Axions, WIMPs and WISPs, 2018, pp. 216–222. [arXiv:1710.08454](#), [doi:10.3204/DESY-PROC-2017-02/kim_jihn](#).
- [782] J. E. Kim, S. Nam, Y. K. Semetizidis, Fate of global symmetries in the Universe: QCD axion, quintessential axion and trans-Planckian inflaton decay-constant, Int. J. Mod. Phys. A 33 (03) (2018) 1830002. [arXiv:1712.08648](#), [doi:10.1142/S0217751X18300028](#).
- [783] W. Taylor, On the Hodge structure of elliptically fibered Calabi-Yau threefolds, JHEP 08 (2012) 032. [arXiv:1205.0952](#), [doi:10.1007/JHEP08\(2012\)032](#).
- [784] A. Arvanitaki, S. Dimopoulos, S. Dubovsky, N. Kaloper, J. March-Russell, String Axiverse, Phys. Rev. D81 (2010) 123530. [arXiv:0905.4720](#), [doi:10.1103/PhysRevD.81.123530](#).
- [785] B. S. Acharya, K. Bobkov, P. Kumar, An M Theory Solution to the Strong CP Problem and Constraints on the Axiverse,

- JHEP 11 (2010) 105. [arXiv:1004.5138](#), [doi:10.1007/JHEP11\(2010\)105](#).
- [786] M. Cicoli, M. Goodsell, A. Ringwald, The type IIB string axiverse and its low-energy phenomenology, JHEP 10 (2012) 146. [arXiv:1206.0819](#), [doi:10.1007/JHEP10\(2012\)146](#).
 - [787] M. J. Stott, D. J. E. Marsh, C. Pongkitivanichkul, L. C. Price, B. S. Acharya, Spectrum of the axion dark sector, Phys. Rev. D96 (8) (2017) 083510. [arXiv:1706.03236](#), [doi:10.1103/PhysRevD.96.083510](#).
 - [788] L. Visinelli, S. Vagnozzi, Cosmological window onto the string axiverse and the supersymmetry breaking scale, Phys. Rev. D99 (6) (2019) 063517. [arXiv:1809.06382](#), [doi:10.1103/PhysRevD.99.063517](#).
 - [789] M. Dine, N. Seiberg, X. G. Wen, E. Witten, Nonperturbative Effects on the String World Sheet, Nucl. Phys. B278 (1986) 769–789. [doi:10.1016/0550-3213\(86\)90418-9](#).
 - [790] X. G. Wen, E. Witten, World Sheet Instantons and the Peccei-Quinn Symmetry, Phys. Lett. 166B (1986) 397–401. [doi:10.1016/0370-2693\(86\)91587-X](#).
 - [791] K. Becker, M. Becker, A. Strominger, Five-branes, membranes and nonperturbative string theory, Nucl. Phys. B456 (1995) 130–152. [arXiv:hep-th/9507158](#), [doi:10.1016/0550-3213\(95\)00487-1](#).
 - [792] A. Ringwald, Searching for axions and ALPs from string theory, J. Phys. Conf. Ser. 485 (2014) 012013. [arXiv:1209.2299](#), [doi:10.1088/1742-6596/485/1/012013](#).
 - [793] K. Choi, J. E. Kim, Harmful Axions in Superstring Models, Phys. Lett. 154B (1985) 393, [Erratum: Phys. Lett. 156B, 452 (1985)]. [doi:10.1016/0370-2693\(85\)90416-2](#).
 - [794] S. M. Barr, Harmless Axions in Superstring Theories, Phys. Lett. 158B (1985) 397–400. [doi:10.1016/0370-2693\(85\)90440-X](#).
 - [795] S. J. Asztalos, et al., An Improved RF cavity search for halo axions, Phys. Rev. D69 (2004) 011101. [arXiv:astro-ph/0310042](#), [doi:10.1103/PhysRevD.69.011101](#).
 - [796] R. Bähre, et al., Any light particle search II —Technical Design Report, JINST 8 (2013) T09001. [arXiv:1302.5647](#), [doi:10.1088/1748-0221/8/09/T09001](#).
 - [797] G. Aad, et al., The ATLAS Experiment at the CERN Large Hadron Collider, JINST 3 (2008) S08003. [doi:10.1088/1748-0221/3/08/S08003](#).
 - [798] S. Chatrchyan, et al., The CMS Experiment at the CERN LHC, JINST 3 (2008) S08004. [doi:10.1088/1748-0221/3/08/S08004](#).
 - [799] W. Chung, CULTASK, The Coldest Axion Experiment at CAPP/IBS in Korea, PoS CORFU2015 (2016) 047.
 - [800] J. Aalbers, et al., DARWIN: towards the ultimate dark matter detector, JCAP 1611 (2016) 017. [arXiv:1606.07001](#), [doi:10.1088/1475-7516/2016/11/017](#).
 - [801] W. L. Freedman, et al., Final results from the Hubble Space Telescope key project to measure the Hubble constant, Astrophys. J. 553 (2001) 47–72. [arXiv:astro-ph/0012376](#), [doi:10.1086/320638](#).
 - [802] E. Armengaud, et al., Conceptual Design of the International Axion Observatory (IAXO), JINST 9 (2014) T05002. [arXiv:1401.3233](#), [doi:10.1088/1748-0221/9/05/T05002](#).
 - [803] L. Evans, P. Bryant, LHC Machine, JINST 3 (2008) S08001. [doi:10.1088/1748-0221/3/08/S08001](#).
 - [804] B. C. Barish, R. Weiss, LIGO and the detection of gravitational waves, Phys. Today 52N10 (1999) 44–50. [doi:10.1063/1.882861](#).
 - [805] N. Rowell, N. Hambly, White Dwarfs in the SuperCOSMOS Sky Survey: the Thin Disk, Thick Disk and Spheroidal Luminosity Functions (2011). [arXiv:1102.3193](#).
 - [806] S. DeGennaro, T. von Hippel, D. E. Winget, S. O. Kepler, A. Nitta, D. Koester, L. Althaus, White Dwarf Luminosity and Mass Functions from Sloan Digital Sky Survey Spectra, Astron. J. 135 (2008) 1–9. [arXiv:0709.2190](#), [doi:10.1088/0004-6256/135/1/1](#).
 - [807] T. Accadia, et al., Virgo: a laser interferometer to detect gravitational waves, JINST 7 (2012) P03012. [doi:10.1088/1748-0221/7/03/P03012](#).
 - [808] C. L. Bennett, et al., The Microwave Anisotropy Probe (MAP) mission, Astrophys. J. 583 (2003) 1–23. [arXiv:astro-ph/0301158](#), [doi:10.1086/345346](#).